"CHARACTERIZATION AND REMOVAL OF NOM FROM RAW WATERS IN COASTAL ENVIRONMENTS"

A Thesis
Presented to
The Academic Faculty

by

Jason K. Check

In Partial Fulfillment
Of the Requirements for the Degree
Master of Science in Environmental Engineering

Georgia Institute of Technology
January 2005

“CHARACTERIZATION AND REMOVAL OF NOM FROM RAW WATERS IN COASTAL ENVIRONMENTS”

Approved by:

Dr. Michael Saunders, Advisor
School of Civil and Environmental Engineering
Georgia Institute of Technology, Atlanta

Dr. Jaehong Kim
School of Civil and Environmental Engineering
Georgia Institute of Technology, Atlanta

Dr. Paul Work
School of Civil and Environmental Engineering
Georgia Institute of Technology, Savannah

Approval Date: 1/28/2005

ACKNOWLEDGEMENT

I would like to thank the City of Savannah and Savannah Water I&D for their generosity and help in completing this research. I would also like to thank John Sawyer and Tony Tucker at Savannah Water I&D for all of their help along the way. Thanks to everyone in the lab for their help with sample analysis, this work would not have been possible without your assistance. Heath, I appreciate all of your help and support along the way. Lastly, I would like to thank Dr. Kim and Dr. Work for their participation and Dr. Saunders for providing the opportunity to become involved with this research.

Jamie, I hope you finally realize how coagulation affects your daily life. Lindsay, I hope your quest to be captain plant will one day come to fruition.

TABLE OF CONTENTS

LIST OF TABLES

LIST OF FIGURES

LIST OF SYMBOLS or ABBREVIATIONS

α	Weibull scale parameter
β	Weibull shape parameter
b	cell length (cm)
C_p	Permeate concentration (mg/L)
C_{r0}	PCM corrected initial concentration of sample (mg/L)
C_{ro}^*	Normalized permeate concentration (mg/L)
Da	Dalton
DBP	Disinfection by-product (µg/L)
DOC	Dissolved organic carbon (mg/L-C)
DOM	Dissolved organic matter
FA	Fulvic acid
FFF	Flow field fractionation
GC-MS	Gas chromatography-mass spectrometry
GPC	Gel permeation chromatography
HA	Humic acid
HAA	Haloacetic acid (µg/L)
HPSEC	High performance liquid chromatography
HR	Heavy rain period
kDa	Kilo Dalton
MF	Microfiltration
MW	Molecular weight (Daltons)
MWCO	Molecular weight cut off
NF	Nanofiltration
NOM	Natural organic matter
NR	No rain period
$\boldsymbol{p}$	permeate coefficient
POM	Particulate organic matter
PSS	Polystyrene sulphonate
RO	Reverse osmosis
^{2}	Variance
SEC	Size exclusion chromatography
SUVA	Specific ultraviolet absorbance (L/mg-M)
SWID	Savannah Water I&D
t time	(seconds, minutes)
t time	(days, hours, years)
THM	Trihalomethane (µg/L)
THM-FP	Trihalomethane formation potential (µg/mg-C)
TOC	Total organic carbon (mg/L-C)
UF	Ultrafiltration
UV	Ultraviolet
UV_{254}	Ultraviolet absorbance at 254 nm (m-1)
WTP	Water treatment plant

SUMMARY

An investigation into how NOM affects the coagulation process at Savannah Water I&D (SWID) was conducted. Current water treatment practice at SWID was investigated to determine the efficacy of NOM removal using existing coagulation methods. A robust assessment of alum and ferric sulfate for use as coagulants in the removal of disinfection byproduct (DBP) precursor material was conducted using composite water created from sample sites within the SWID watershed. Both coagulants were optimized for the removal of NOM.

Pragmatic methods of NOM size analysis and its reactivity with chlorine has been investigated. UF membranes were used in conjunction with a permeation coefficient model (PCM) to determine an apparent molecular weight distribution of NOM present in the SWID watershed. Individual size classes were assessed for their potential to form trihalomethanes (THMs) upon chlorination. Coagulation using alum and ferric sulfate was assessed to determine removal efficiency of individual NOM size classes under various coagulation scenarios.

Finally, UV_{254} absorbance (UVA) was assessed to determine its potential use as an indicator of DOC concentration in raw and treated water at SWID. Additionally, an investigation into the relationship between specific UVA (SUVA) and THM formation potential (THM-FP) was conducted.

CHAPTER 1 - INTRODUCTION

1.1 – Background

Aquatic natural organic matter (NOM) is ubiquitous in nature, arising from decomposition of plant and animal tissues. The size, structure, molecular weight, elemental composition, and the position and number of functional groups composing NOM vary both regionally and with time. Recent advances in analytical techniques (Croue 2004; Lee et al. 2003) have allowed scientists to better understand physical properties and chemical composition of humic and fulvic acids, which together compose approximately 50% of NOM in surface water. Other NOM constituents include hydrophobic and hydrophilic acids, bases, and neutrals. However, many important characterization properties associated with NOM are still unknown.

Although harmless itself, NOM reacts with chlorine to form undesirable disinfection by-products (DBPs) during the disinfection process (Krasner et al. 1989; Rook 1974). DBPs of significant consequence in the water treatment industry include trihalomethanes (THMs) and haloacetic acids (HAAs), both of which are suspected human carcinogens and are currently regulated by EPA Stage I statute for DPBs with maximum contaminant levels (MCLs) of 80 μg/L and 60 μg/L, respectively. Stage II limitations will lower the MCL for THMs and HAAs to 40 μg/L and 30 μg/L, respectively. This restriction will provide new challenges for conventional potable water treatment plants, which are often struggling to meet current EPA MCLs for both contaminants.

1.1.1 – Savannah Water I&D

Savannah Water I&D (SWID) plant is a conventional surface-water treatment plant servicing both industrial and domestic clientele with an average potable water supply of 30 million gallons per day (MGD). The raw water at SWID is subject to sporadic variation in raw water quality and treated water demand is also unpredictable due to a large portion of the demand arises from industrial clientele. Raw water is pumped from Abercorn Creek (near the Savannah River) approximately 10 miles (16 km) with an average residence time in the pipeline of 4 hr. The water quality observed at SWID varies as a function of tidal stage due to its close proximity to the Savannah River delta. In general, the raw water is of highest turbidity and color at low tide, improving in clarity and color as the tide begins to rise. In addition to variable raw water quality observed at SWID, industrial clients place heavy and variable-demand requirements. The coupling of these effects leads to varying chemical consumption throughout the treatment process and increased labor. Raw water characteristics may also change significantly in response to the season and directly after periods of heavy rainfall, which flush natural organics from the surrounding marsh and swamp land into the influent water at SWID.

1.2 – Motivation for study

It is clear that there is a pressing need for water utilities to understand the nature and composition of NOM present in their raw and treated water to minimize the formation of disinfection byproducts. Water treatment plants (WTPs) in the United States are experiencing difficulties in meeting THM limits (80 μg/L) in their finished drinking water. Given that color is effectively removed during the treatment process, it

appears that residual organics may be precursors to THMs. It is known that there are periods of the year where many water treatment plants (typically those with low alkalinity, highly colored waters) are observing periods of high organic loading associated with heavy rains or possibly melting snow. During these periods of elevated dissolved organic carbon (DOC) the conventional treatment process may exceed regulatory maximum contamination levels (MCLs) for THMs and other disinfection byproducts (DBPs).

The DOC concentration and color of water collectively provide insight to the concentration of naturally occurring organics in raw and treated water, however neither measurement reveals any information pertaining to the character, reactivity, or treatability of NOM. Simply measuring DOC and color in the bulk and treated water will not provide a dynamic assessment of NOM removal. To investigate the effectiveness of the coagulation process on the removal of NOM it was deemed necessary to separate NOM into its component parts and assess its character and reactivity.

CHAPTER 2 – LITERATURE REVIEW

A literature review has been conducted focusing on the characterization, removal, and fate of natural organic matter (NOM) in the conventional water treatment process. Each section is followed by a brief summary of the material provided and is designed to be read as a quick summary of the overall literature review.

2.1 – Aquatic natural organic matter (NOM)

Surface water and groundwater contain diverse types of aquatic natural organic matter (NOM) produced from a variety of sources. NOM can be leached from soils or peat bogs (pedogenic NOM), diffused from sediments that contain sorbed particles of NOM, or released by plankton and bacteria (aquagenic NOM) (Aiken et al. 1985). (McKnight et al. 2001) further described NOM to be (i) microbially derived (autochthonous), resulting from processes such as leachate and extracellular release of algae and bacteria and (ii) terrestrially derived (allochthonous), originating from decomposition and leaching of plant and soil organic matter.

NOM is responsible for a variety of other problems in water supplies, including color, taste and odor, and increased chemical disinfectant demand (Aiken et al. 1985). Understanding which particular species within this aquatic group of NOM are responsible for the creation of disinfection byproducts is necessary for a water treatment facility to maximize its efficiency of DBP precursor removal through the conventional treatment process while minimizing the cost of treatment. During potable water treatment, NOM can be removed through a variety of mechanisms. It may be removed via coagulation, granular activated carbon (GAC) adsorption, membrane filtration, or biological

degradation. NOM may also be partially transformed through oxidation during an advanced oxidation process.

Aquatic NOM is collectively referred to as the sum of humic (non-polar) and non-humic (polar) substances within a water source, generally derived from terrestrial and biological origin respectively (Hwang et al. 2001). Aquatic NOM can be categorized in a variety of ways, which include, but are not limited to; degree of aromaticity, fluorescence, C:N ratio, amino acid content, hydrophobicity, molecular weight (MW), and morphology observed by transmission electron microscopy (TEM). Chemically, natural organic matter consists of complex polysaccharides in variable proportions of pedogenic and aquagenic proteinaceous compounds (5-10 percent), polysaccharides (10-20 percent), aquagenic refractory matter (5-20 percent), and pedogenic refractory matter (PROM 50-80 percent). Operationally, humic and fulvic acids account for approximately 50% of the dissolved organic carbon (DOC) in a water source ranging in size from 500 to 10,000 daltons (Amy et al. 1992). The refractory components of NOM, largely dominated by phenols, quinones, amides, and esters, are recognized for their absence of carboxylate groups and their relatively low molecular weight. The carboxylate group (-COOH) within NOM allows the molecule to complex with metal species (e.g., dissolved aluminum & iron) and its absence from refractory organic matter explains why conventional treatment processes do not generally remove the refractory portion of NOM (Finch 1996). The variation associated with the composition of NOM within a natural water is due to the complex nature of the formation of aquatic humic substances and the origination of organic matter from which the NOM is derived, which can vary both regionally and seasonally.

Humic substances have been categorized into humic and fulvic acids (Deen 1987). In general, humic acids are more hydrophobic than fulvic acids, hence, they are more easily removed during the coagulation process. Humic acids compose the portion of humic substances that can be precipitated at pH = 1.0. At pH = 1.0, fulvic acids (Figure 2.1) remain in solution due to their carboxylic and hydroxyl (-OH) groups (Thurman 1985). Fulvic acids are less hydrophobic than humic acids and have relatively low molecular weights. Although both humic and fulvic acid exhibit a structural complexity that has yet to be fully understood, several unique features exist within this group. The general structure of a humic acid molecule is depicted in Figure 2.2. Various acidic functional groups are attached to the aromatic ring giving the polymer an overall net negative charge. For example, carboxylic acids are attached to the rings and can ionize as a function of pH to carboxylate ion, $-COO^-$ (Amy et al. 1992). The overall negative charge of the resulting humic acid facilitates its potential removal by colloidal destabilization (coagulation). Additionally, the overall negative charge of humic acid has proven to be closely linked to increased chemical coagulant demand in waters containing high concentrations of NOM (White et al. 1997).

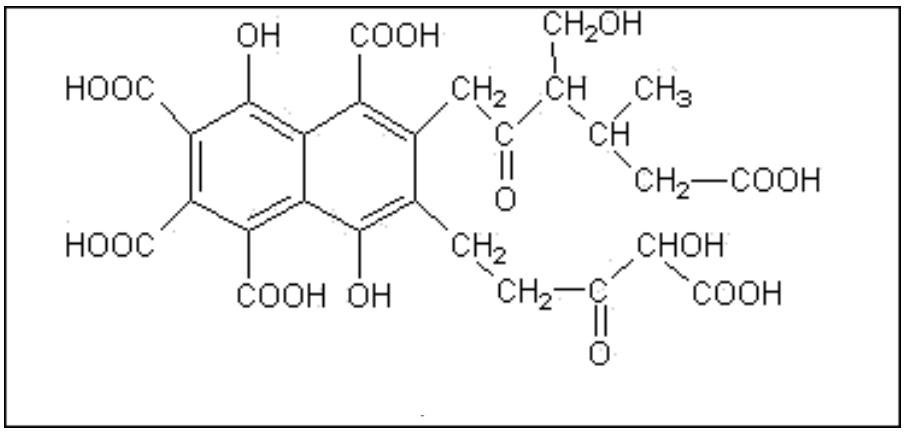

Figure 2.1 - Suggested structure of fulvic acid (adapted from Kubicki and Apitz 1999)

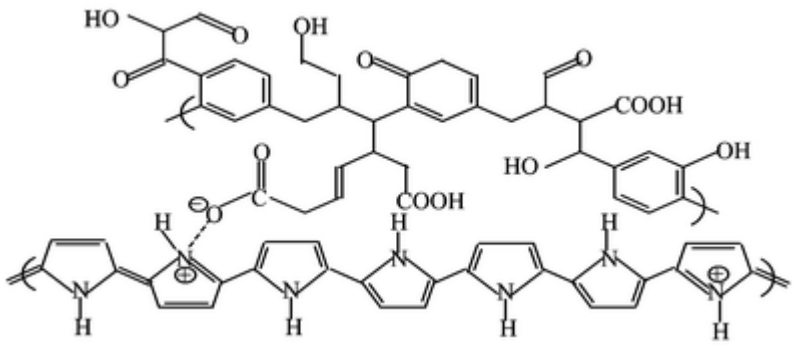

Figure 2.2 - Proposed chemical structure of humic acid (Aiken 1985)

2.2 – Bulk NOM characteristics

Bulk characterization of NOM can reveal important information about the interactions of humic substances with the environment in their unaltered state. The properties of humic substances play a pivotal role in their reduction through conventional water treatment processes. Humic substances react with chlorine during the drinking water treatment process to form disinfection byproducts (DPBs). In addition to the volatile fraction in DBPs such as THMs, non-volatile haloorganics such as haloacetic acids (HAAs), the second most prevalent group of known DBPs, are also formed by the chlorination of natural organic (humic and fulvic) matter. Fulvic acids are less aromatic than humic acids, hence, contributing less to color and THM formation (Wershaw et al. 1985). The formation of DBPs has shown to be a function of several factors including total organic carbon (TOC) concentration, type of organic precursor (i.e., humic or fulvic acid and its corresponding molecular weight), chlorination level, pH, temperature, bromide ion concentration, reaction time, and ultraviolet absorbance at 254 nm (UV_{254}) (Amy et al. 1987; Clark et al. 1998). To control DBPs resulting from the chlorination of drinking water an understanding of the key factors that influence their formation is required. Of the known factors influencing the formation of DBPs, NOM reactions with chlorine are regarded as the most important.

Many studies have revealed a strong correlation between DOC and the UV_{254} absorbance (Allgeier and Summers 1995; Amirtharajah and O'Melia 1990; Amy et al. 1987; Collins et al. 1986; Kitis et al. 2001; Nokes et al. 1999; Pomes et al. 2000; Singer et al. 1995; Vilge-Ritter et al. 1999; Volk et al. 2000; White et al. 1997). Many of these same studies reveal a second correlation between specific ultraviolet absorbance

(SUVA), defined as the ratio of UV absorbance to DOC (expressed as L/mg-M), and the formation of THMs. SUVA has been shown to be a good indicator of the composition of organic material (Edzwald and Tobiason 1999). SUVA has also proven to correlate well with the aromatic content of NOM (Croue et al. 1999; Krasner et al. 1996).

In general, the higher the DOC, the higher the UV_{254} absorbance (UVA) and concentration of THMs produced. Studies have demonstrated that the correlation between DOC and UVA was much stronger than the correlation between DOC and THMs produced. (Owen et al. 1993) determined that the poor correlation between DOC and THMs produced may be a consequence of the humic component in the water. Waters with a high MW humic component tend to form higher concentrations of THMs when compared to waters with equivalent DOC concentrations composed of a lower humic component (Owen et al. 1995). Watershed characteristics play a major role in the specific THM yield (μg of THMs formed/mg carbon) of a water source (Reckhow and Singer 1990).

Bulk characterization can provide good insight as to the nature of the NOM, but further studies relating to the structure, size, functional groups, and chemical behavior of the material requires further separation of the NOM, either chemical, physical, or both.

2.2.1 – Bulk NOM Variability

Decomposition of organic material can vary regionally according to climate and land use. In the northern United States, there has been a marked increase in the levels of color in surface water over the past 10 to 15 years (Skjelkvale et al. 2001). The increase in color has been greater than the increase in TOC content, which indicates that both the

quantity and quality of NOM have changed over the years. Climatic factors, such as temperature and precipitation, are major factors influencing the formation of NOM and carbon fluxes (Gjessing 2003). Intensity of precipitation has been closely linked to NOM concentration in the discharge from forested sites. Increased runoff intensities lead to higher levels of pedogenic NOM being flushed from the surface layer of soils into surrounding surface waters (Bishop et al. 2003).

2.3 –Fractionation of NOM

Fractionation of NOM focuses first on separation of particulate organic matter (POM) from a bulk water source. Operationally, this is achieved by separating POM from an aqueous solution through the use of a 0.45-μm pore filter. The resulting filtrate may be classified as the dissolved organic matter (DOM) portion of NOM. Once the DOM portion has been established, subsequent analysis may be conducted according to the objective of a study.

In general, DOM can be separated by molecular size through the use of membranes, field-flow fractionation (FFF), and chromatography or by molecular charge through the use of resin fractionation, mineral adsorption, and chromatography. Techniques used to determine approximate molecular weights of humic materials are also used to study biological macromolecules (Geoffrey and Elham 1999). Chromatography may be used to separate molecules based on size exclusion or can be used to separate organic matter based on polarity. Therefore, chromatography may be considered for either method of separation based on configuration of the experiment and available equipment.

A method for size-fractioning of DOM should be reproducible with minimal artifacts. Unfortunately, all methods used to isolate fractions of DOM based on molecular weight and/or charge are subject to operational limitations. Further study and analysis of the resulting chemistry and characteristics of the isolated humic and fulvic acids must incorporate the method(s) used to derive the material.

2.3.1 – Size Fractionation

The average molecular weight distribution of humic substances may be used to better understand the basic chemistry of unknown organic compounds. Size fractionation of NOM has been used successfully to provide an operational distribution of apparent molecular weights (Tadanier et al. 2000). Earlier methods employed to study molecular weight and size of NOM including gel chromatography, electrophoresis, scattering techniques, colligative property, ultracentrifugation, viscosity measurements, and electron microscopy (Hayes et al. 1989). Although these methods showed some promise, in more recent years, studies have focused on the use of membranes, flow field fractionation (FFF) and chromatographic methods due to their relative ease of use and reproducibility. Novel approaches to organic molecule size fractionation include dynamic adsorption experiments, multi-angle laser light scattering, and fluorescence correlation spectroscopy.

Given the wide variety of choices for NOM size fractionation, over the past decade, gel permeation chromatography and ultrafiltration have dominated as principal methods for NOM separation. This is primarily attributed to their ease and versatility of use, and to their ability to produce accurate results within a unique natural water source.

Each method provides an operational estimate of apparent molecular weight distribution of NOM.

GPC and UF harness different physicochemical principles to achieve solute separation. UF obtains separation of macromolecules through development of a concentration-dependent membrane balance with the solute. This equilibrium is subject to a number of operational parameters and solute-membrane interaction. GPC uses a porous gel matrix to achieve a size-dependent exclusion of solutes (i.e., larger constituents do not penetrate the gel matrix and move through the gel with the shortest retention time, while smaller constituents enter the gel matrix where their transport is hindered, leading to an overall longer retention time). This method of size exclusion provides an estimation of molecular weight (MW), however molecular configuration is dictated by secondary and tertiary structure, therefore molecular weight and size are not directly correlated.

2.3.1.1 – NOM standard

Research has focused on determining an ideal standard for representation of humic substances (Leenheer 1985; Perminova et al. 1998; Wershaw et al. 1985). Determining a proper standard requires a full chemical and physical understanding of the substance to which you wish to apply the standard. Unfortunately, this knowledge is not available for humic substances due to their undefined complex composition. Perminova et al. (1998) attempted a rigorous determination of "absolute size" by testing and modeling a variety of groups of humic substances based upon their structure rather than their hydrophobic-hydrophillic characteristics. The results of their research suggested

that sodium polystyrene sulfonates (PSS) were the ideal standard for modeling aquatic humic substances. In addition to PSS, many other well-defined macromolecules have been used as standards for NOM, including globular proteins, polyacrylic acids, polysaccarides, and low molecular weight organic acids (De Nobili and Chen 1999). Each of these standards deviates from the behavior of aquagenic NOM in their acidic functional group, pK_a, degree of crosslinking, or aromaticity. Lack of consensus on a proper standard for NOM and variation in methods used to determine solute apparent molecular weight distribution provides unique results to a particular solute or experiment.

2.3.1.2 – Ultrafiltration

Ultrafiltration is capable of separating particles across a wide range of nominal molecular weight cut-offs (MWCO) from 500 to 10^6 daltons (Da). The MWCOs are provided by the manufacturer and provide solute size exclusion based upon molecular weight. When considering ultrafiltration as a method in solute NOM molecular weight fractionation, several solute interactions must be considered. In addition to membrane-solute interactions, suspended solids retention may be affected by geometric properties of pores and their size distribution (Buffle and Deladoey 1978). For instance, the degree of overlapping of pores or flow dynamics between closely spaced pores may affect permeation behavior. Solute attenuation within membrane pores is a complex function of several physicochemical properties. Molecular size, charge, and hydrophobicity all play a role in the amount of solute rejection by a membrane surface (Hazlett et al. 1989). Furthermore, the level of solute rejection is dependent upon hydrodynamic characteristics of the membrane-solute interface. Experimental procedures must be structured to

effectively eliminate the formation of a solute layer at the membrane-solute interface. This enables the assumption that all solute molecules to have equal access to membrane pore openings; hence, all concentration dependent molecular sieving by a membrane is due to the membrane itself and is not a function of additional gel-layer sieving at the membrane-solute interface. Molecules that are closest to the average pore diameter are subject to the highest level of interaction with a membrane surface and within pores. These similarly-sized molecules may hinder or even prevent passage of smaller molecules that would otherwise pass through a membrane (Aiken et al. 1992).

Several materials have been used for construction of ultrafiltration membranes. Materials include regenerated cellulose, cellulose acetate, polyamide thin film composite (TFC), and polyethersulfone. Cellulosic ultrafiltration membranes are the least expensive and have low surface adsorption tendencies due to their hydrophilic nature. Polyehtersulfone ultrafiltration membranes are not hydrophilic and have high surface adsorption tendencies. However, these membranes are the most stable with respect to chemical, thermal, and mechanical implications arising during the filtration procedure. Polyamide ultrafiltration membranes demonstrate a high thermal, chemical, and mechanical stability and also have low surface adsorption due to their hydrophilic nature. However, surfaces of polyamide ultrafiltration membranes are highly reactive to chemical oxidants and the integrity of membrane is compromised by small quantities of chemical oxidants (i.e., chlorine, monochloramine, chlorine dioxide) (Cheryan 1998).

The composition of ultrafiltration membranes has been analyzed for membrane-solute interactions (Laine et al. 1989). Laine (1989) tested several materials including a hydrophilic regenerated cellulose membrane, a hydrophobic polysulfone membrane, and

a hydrophobic acrylic copolymer membrane. Their tests revealed that the extent of hydrophilicity of a membrane was the most important characteristic to consider when conducting ultrafiltration studies. Solute-surface interactions were minimized when using hydrophilic membranes with regard to separating aquatic NOM by molecular weight. Laine (1989) concluded that low MW fractions (MW<5000 Da) would be underestimated if the rejection properties of the membrane were not incorporated into experimental results.

In addition to the numerous physical properties that affect membrane attenuation, chemical properties may drastically reduce or increase the level of solute permeation through any of several forces including: van der Waals, hydrogen-bonding, electrostatic, and hydrophobic intermolecular forces. Hydrophobic intermolecular forces increase directly with ionic strength and their sign and magnitude are a function of the charge and polarity of the membrane and the solute. Electrostatic forces, experimentally determined to be the most prominent (Leenheer 1981), work in two ways to decrease solute permeation. Electrostatic repulsion between a molecule and the membrane surface can prevent the passage of an otherwise permeable molecule. Additionally, electrostatic attraction between solute particle and the membrane surface may increase sorption effects and ultimately decrease the effective hydraulic radius of the pore, thereby decreasing hydraulic permeation (Amy et al. 1987; Leenheer 1981).

Ionic strength and pH must be controlled and accounted for when analyzing results from NOM fractionation. Ionic strength is closely related to DOC rejection and can be attributed to the increased coiling of large organic molecules with increasing ionic strength. The functional groups within the NOM stretch to linear orientation at low ionic

strength. At high ionic strength, the groups become shielded and begin to curl up and eventually aggregate (Schaefer et al. 2002; Schaefer et al. 2000). This phenomenon may be attributed to increased membrane rejection. The pH of the solute also partially determines the overall shape and size of NOM. Research suggests that, for waters low in natural organic concentration, the effect of ionic strength is much greater than that of pH (Tadanier 1998). With increasing pH, NOM molecules develop an increasingly flexible linear shape and an increasingly negative charge. These two phenomena counteract one another with respect to solute-membrane interactions. Although the flexible linear shapes developed at high pH pass more readily through a UF membrane, their increased electrostatic interactions with the membrane pores serve to counteract these effects.

Dissolved calcium has proven to account for the majority of membrane-solute interactions with respect to ionic strength (Schaefer et al. 2002). Calcium concentration may significantly impact the level of organic rejection by ultrafiltration. At low to medium calcium concentration (< 0.5 mmol/L-Ca^{2+}) the average organic molecule size is reduced due to charge shielding and the formation of aggregates has been noted (Schaefer et al. 2000). (Schaefer et al. 2002) demonstrated that as calcium concentration increased, the organic retention increased when conducting batch ultrafiltration on chemically fractionated NOM created from a stock solution.

The overall physicochemical effects during batch membrane ultrafiltration may be accounted for by applying a two-parameter permeation coefficient model (PCM). A general outline of the PCM is provided in the next section.

*2.3.1.3 – **Membrane Separation***

In addition to ultrafiltration, microfiltration (Schaefer et al. 2000; Suzuki et al. 1998) and nanofiltration (Allgeier and Summers 1995; Bian et al. 1999; Cho et al. 1999; Fu et al. 1994; Nilson and DiGiano 1996; Schaefer et al. 2002; Siddiqui et al. 2000) membranes have been used for the removal, characterization, and/or concentration of NOM. Membrane separation has been considered for particulate removal for some time (Laine et al. 1989), but cost considerations have limited applicability until recent years. Problems with membrane fouling and flux decline have also slowed the transition from conventional mixed-media gravity filters to membrane technologies (Cho et al. 2000). Considerable research has revealed that UF, MF, and NF membranes may be used effectively to remove particulate organic matter given proper treatment up stream of a membrane application. High volume ultrafiltration techniques, such as hollow-fiber ultrafilter membranes, have been proposed for separation of humic materials in the water treatment industry (Gaffney et al. 1996). Membrane technology is often used in the characterization of NOM through the process of reverse osmosis (RO) concentration (Cho et al. 2000; Munster 1999). This process enables NOM to be concentrated for preservation or further analysis. However, all non-humic particles must be removed from concentrated material before further analysis is to be conducted. The desalting process that is required to remove non-humic materials is thought to transform the chemical and physical composition of the virgin humic material (Leenheer et al. 2000; Newcombe et al. 1997), thus, further analysis may reveal artifacts related to improper sample preparation.

A two parameter PCM has been used to correct raw batch UF data based on $\Delta C_p/\Delta t$, where C_p represents the instantaneous permeate concentration (Logan and Jiang 1990; Tadanier et al. 2003). The PCM is based on the assumption that mass transport between two homogenous phases is due to an arbitrary combination of convective and diffusive processes, each process driven by gradients in pressure, ΔP, solute mole fraction, $\Delta\chi_i$, and electrical potential, $\Delta\Psi$, on opposing sides of a semipermeable membrane. Each homogenous phase is a component of a larger heterogeneous system composed of *n* chemically, and in some cases, physically distinct solutes. Assuming mass transport does not allow the system to deviate significantly from equilibrium throughout the membrane and the system is operated under isothermal and isobaric conditions, the combined fluxes, J_i, of the *n* solutes in the systems may be described by the following equation:

$$J_i = \sum_{k=1}^{n} \alpha_{ik} X_k \qquad (i = 1,2,...,n) \qquad \text{(Eq. 2.1)}$$

Where X_k represents the driving forces and α_{ik} corresponds to the collective influences of solute-solute and solute-membrane interactions on mass transport through the membrane (Onsager 1931). X_k may be related to solute parameters by the relationship

$$X_k = V_k \Delta P + \sum_{j=1}^{n} \left(\frac{\partial \mu k}{\partial x j} \right)_{T,P} \Delta x_j + zkF\Delta\Psi \qquad (k = 1,2,...,n) \qquad \text{(Eq. 2.2)}$$

where parameters V_k, μ_k, and z_k are representative of partial molar velocity, chemical potential, and charge of species, respectively.

The PCM assumes that solution conditions are adequately controlled such that cross-coupling effects may be neglected. Based on Equation 2.1, flux (J_i) is dependent on both the conjugate driving force ($X_{k=i}$) and all nonconjugate driving forces ($X_{k\neq i}$). Thus, solute transport through a semipermeable membrane may be represented by a 'coupling' phenomenon. The amount of coupling is expressed by the magnitude of the phenomenological coefficient α_{ik} . When the solution remains well mixed and sufficiently dilute such that membrane fouling, gel-layer formation, and concentration polarization are minimized, Equation 2.1 may be simplified by neglecting cross-coupling phenomenological coefficients ($\alpha_{i\neq k}$) yielding:

$$J_i = \alpha_{ii} X_i \qquad i = (1,2,...,n) \qquad \text{(Eq. 2.3)}$$

Equation 2.3 demonstrates that membrane transport of each solute may be considered independent of all others and solute cross-coupling are effectively zero. The idea of neglecting cross-coupling effects in a simple heterogeneous solution has been evaluated with success in several studies (Logan and Jiang 1990; Simon et al. 1996; Tadanier et al. 2003). The effect of solute cross coupling on pressure driven membrane transport of dilute aqueous binary salt solutions was determined to be negligible for flat cast cellulose acetate membranes (Bennion and Rhee 1969). The assumptions of this method were later verified using compounds of known molecular weight such as sucrose (342 amu) and vitamin B-12 (1192 amu) and various MWCO UF membranes (Logan and Jiang 1990).

2.3.1.4 – Field Flow Fractionation (FFF)

Field-flow fractionation is similar to a chromatographic separation where an electromagnetic field is used to bring particles close to an accumulation wall in a very thin channel. Diffusive forces allow larger particles to move closer to the wall while smaller particles migrate farther away. Once the particles are given enough time to acclimate under the applied field the smallest particles are eluted using laminar flow in a thin channel. The mean thickness of the cloud of particles depends on the fluid velocity and the diffusion coefficient of the particle, which may be correlated to the MW of the particle. Subsequent elutions remove the larger particles and MW characteristics may be revealed from the resulting elution profile.

Membrane separation procedures have been used and compared to FFF to reveal that FFF can be used to determine the MW of NOM (Beckett et al. 1992). A comparison of FFF separation and ultrafiltration fractionation procedures revealed that the nominal MW fractions provided by UF did not produce fractions with the expected MW and size (Assemi et al. 2004). The results suggest that caution must be used upon analysis of UF fractionation results. Newcombe (1997) determined from a direct comparison of UF and FFF that the MW values measured by FFF were significantly lower than the nominal MWCOs for the three highest molecular weight membranes used in a study to determine the MW of local aquatic fulvic acid, humic acid, and standardized Aldrich humic acid. The difference in MW fractions observed may be attributed to charge rejection by the membrane and the variance in the globular protein standard chemical and physical characteristics used to calibrate the high MW membranes. Promising development of the FFF technique (Assemi et al. 2004; Thang et al. 2001; Zanardi-Lamardo et al. 2001) may

reveal a highly reproducible and reliable method for determining the physical characteristics of DOC.

2.3.2 – Size fractionation by adsorption

2.3.2.1 – Resin fractionation

Resin fractionation has been used for several decades to separate NOM based on chemical properties. Initially, Amberlite XAD non-ionic resins were used to adsorb organic solutes from water. The level of adsorption is dependent on the solution pH and the solubility of the solute (Cheng 1977). The polar functional groups (i.e., carboxyl, phenolic, hydroxyl, and ketone) govern the majority of the molecular behavior of NOM in water (Leenheer et al. 1989). At low pH, weak acids are protonated and can then be adsorbed onto the resin. Differences in chemical composition, pore size, and surface area of the resin account for differences in affinity for various fractions of NOM. These characteristics allow for use of resin materials to fractionate NOM based on varying chemical and physical characteristics.

A major study of XAD resin characteristics was conducted by (Aiken 1988) and later by (Leenheer et al. 2000). Aiken (1988) investigated several operational parameters to consider when conducting resin fractionation experiments, including initial filtration of a sample, sample preservation, and flow characteristics of a column. His studies revealed that, if correctly handled and stored, resin fractionation could provide quality results. Aiken (1988) showed that XAD-8 resin showed the highest sorptive capacity for the humic portion of NOM.

Many studies have focused on the use of XAD-8 and DAX-4 (previously supplied as XAD – 4) to isolate and concentrate various fractions of NOM (Aiken et al. 1992; Andrews and Huck 1993; Leenheer 1981; Malcolm and MacCarthy 1992; Thurman and Malcolm 1981) Both resins have a polymeric composition consisting of styrene divinylbenzene. The use of these two resins in series allows for the operationally defined humic fraction (i.e., hydrophobic acids) to be isolated by adsorption to XAD-8 resin. Non-humic acids (i.e., hydrophillic acids) may be subsequently isolated by adsorption to DAX-4 resin due to its small pore size and large surface area compared to XAD-8. A third resin may be used to further separate the hydrophillic portion eluted from the DAX-4 resin, however this step is often eliminated.

The hydrophobic acid fraction isolated by XAD-8 resin at pH 2 and eluted at pH 13 consists mainly of carboxylic acids and phenols. Fulvic acids, somewhat less defined, contain uronic and polyuronic acids in addition to single aliphatic acids and are considered to be hydrophillic acids . Several variations to this technique (Aiken et al. 1992; Thurman and Malcolm 1981)) have revealed similar results to fundamental studies conducted by Leenheer (1981) attempting to separate NOM using resin. Ion exchange resins may be used in conjunction with XAD resins to further separate and isolate NOM fractions. The isolated fractions can then be eluted and concentrated for further spectral and chemical characterization.

Both hydrophobic and hydrophillic acids contribute significantly to the formation of disinfection by-products (DBPs) upon chlorination, which is discussed further in section 2.5. It is necessary to explore the implications placed on the water treatment

process as a result from both fractions. However, absolute isolation of either fraction does not occur when using XAD resin.

*2.3.2.2 – **Mineral adsorption***

Mineral adsorption has been used with limited success to fractionate NOM based on molecular size and shape. Sorption of pollutants to humic material in soils and aquifers has been observed and often leads to retention of pollutants (Murphy et al. 1990). NOM has been shown to remobilize adsorbed pollutants and facilitate their transport in underground systems (Schmitt et al. 2003). Several studies have focused on the adsorption of NOM to metal hydroxides (Chandrakanth et al. 1996; Saito et al. 2004). These studies revealed that NOM adsorbed to alumina and iron particles and the electrophoteric mobility of the particles was attributed to the adsorbed NOM rather than the mineral composition. Fractionation of NOM based on MW by mineral adsorption was studied by (Meier et al. 1999) using kaolinite ($Al_2Si_2O_5(OH)_4$) and goethite (α-FeOOH) to fractionate NOM in aqueous solution. Results suggested that the MW of humic components in solution begins to decrease in the presence of absorbing clay minerals. These results suggest that the large NOM molecules demonstrate preferential adsorption to goethite and kaolinite. However, the study gave no indication as to the actual size of the NOM fractions. (Zhou et al. 2001) attempted to investigate the size of fulvic acid molecules sorbed onto goethite. Results suggest that high MW fractions are adsorbed at low pH and intermediate MW fractions were adsorbed at high pH.

2.3.3 – Chromatography

2.3.3.1 – Gel Permeation Chromatography

Gel permeation chromatography (GPC) has been applied to a great extent to determine the MW distribution of humic and fulvic acids. Sephadex gels are generally used to fractionate solutes based on retention time of particles within a porous column. GPC relies on molecular weight standards to calibrate a gel matrix and to determine a molecular weight composition of a solute. GPC also depends on the electrophoretic mobility of organics within the gel matrix, which may vary within each molecular weight group and alter their mobility through the gel when compared to a standard with alternate electrophoretic characteristics (Newcombe and Drikas 1996). Sorption interactions must be integrated into the AMW distribution results after GPC fractionation. In addition, analysis of GPC fractionation results must quantify the effects of electrostatic interactions at low ionic strength and hydrophobic interactions at high ionic strength. Due to the dilution of the solute in the mobile phase, solute detection in the gel column effluent relies on very sensitive online detection equipment. In the case of low intial DOC concentration (DOC < 10 mg/L), solute pre-concentration is necessary to obtain reasonable results.

The gel used in the GPC process interacts with weakly basic aromatic amines and weakly acidic polyphenols through hydrogen-bonding mechanisms to achieve MW fractionation of the materials. Sorption interactions account for the majority of fractionation that occurs in the absence of ion pair buffers (Leenheer 1985). Globular proteins have been used to calibrate GPC columns, which demonstrate a linear relationship between MW and hydrodynamic size (Kim et al. 1990). It is difficult to

understand and more importantly to quantify the gel-solute interactions that occur between Sephadex gel and NOM in solution. Artifacts arise when calibration solutes derived from a known MW standard behave differently from the unknown solute. Calibration curves are based on molecular size and hydrodynamic diameter, which are given as a function of the elution volume. Once the fractions have been established, further spectroscopic analysis may be conducted.

In addition to GPC, High Performance Liquid Chromatography (HPLC) and High Performance Size Exclusion Chromatography (HPSEC) may be used to separate NOM based on MW. HPLC methods have the advantage of basing solute separation on adsorption or partitioning, as well as ion exchange (Becher et al. 1985). Fundamentally, HPSEC utilizes the same principles of separation as GPC and is subject to the same constraints. During column elution, smaller molecules permeate the porous gel matrix where their transport is hindered, leading to an overall longer retention time when compared to larger molecules (Hongve et al. 1996).

2.3.4 – Fractionation Summary

In general, MW size distribution of dissolved organics is determined either as a continuous distribution using gel permeation or size exclusion chromatography, or as a discrete distribution using ultrafiltration. Each technique has its own set of limitations. In order to achieve an accurate MW distribution using chromatographic analysis, there must be no chemical interaction with the column packing material, the solvent (eluent), or the organic components. Additionally, a known MW calibration standard is required that is representative of the unknown solute. This is difficult given that the chemical

structure and composition of NOM remains unknown. Additionally, some components pass through the column more rapidly than calibration standards due to ion exclusion or complex formation, which may result in an overestimation of the solute component molecular weights. Alternatively, electrostatic forces or adsorption with the column packing material may delay some components in the solute leading to an underestimation of their concentration. Chromatographic analysis may also require concentration of organics (usually by freeze-drying) prior to sample analysis, which may inadvertently alter the size distribution of dissolved organic components.

Molecular weight distribution assessed through the use of UF membranes is obtained by calculating the difference in mass concentration between permeates from cells containing membranes with different nominal molecular weight cutoffs. Operationally, the UF procedure is less complex but may be more time consuming depending upon the type and MWCO of the membranes used in the procedure. An important advantage of ultrafiltration over chromatographic methods is that a large sample volume may be captured for further analysis. There are several factors that may influence the diffusive and advective transport of organics through UF membranes, including pore size distribution, cell pressure, membrane-solute interactions, solution pH, ionic strength, and cell pressure. Solute accumulation at the membrane surface (concentration polarization) may also decrease advective flux. However, all of these potential solute flux inhibitors may be minimized through the use of a rigorous UF protocol and accounted for using mathematical predictions to estimate membrane rejection.

2.4 - Coagulation

In most municipalities the treatment of surface water is focused on the removal of turbidity, however recently some plants have started to optimize their treatment process for the increased removal of NOM (Chow et al. 2000). Sharp (2004) demonstrated that NOM is almost always anionic due to the pH of natural water, therefore exhibiting a strong affinity to cationic additives such as metal coagulants and cationic polyelectrolytes. Coagulation has been defined as 'a process for combining small particles into larger aggregates' (Amirtharajah and O'Melia 1990) and more recently as 'a process for combining colloid materials and small particles into larger aggregates and for adsorbing dissolved organic matter on to these aggregates, thereby facilitating their removal in subsequent sedimentation/flotation and filtration stages' (Jiang and Graham 1998). These definitions will be investigated in the following sections.

2.4.1 – Coagulation Theory

Effective coagulation is the most critical aspect of the conventional water treatment process because it facilitates the removal of NOM in subsequent treatment processes. The conventional water treatment process incorporates several physicochemical processes including rapid mixing, slow mixing (flocculation), sedimentation, filtration, and disinfection. Coagulation reactions take place almost instantaneously in the rapid mix stage of the water treatment process and continue until the water is filtered. The effectiveness of coagulation affects the efficiency of the subsequent sedimentation and filtration processes.

Effective coagulation is achieved through addition of charged (or other destabilizing) species into a water source. This process may be accomplished using several coagulants, however the two most commonly used coagulants in practice are the hydrolyzing metal ions Al^{3+} and Fe^{3+}, which are typically supplied as aluminum sulfate (typical chemical formula - $Al_2(SO_4)_3 * 14H_2O$) and ferric chloride (typical chemical formula - $FeCl_3 * 6H_2O$), respectively. Aluminum sulfate, commonly referred to as alum, is the most widely used coagulant in the water treatment process today.

Water treatment plants primarily use chemical coagulants to remove dissolved organic matter (DOM) and particles, induce flocculation, and improve filtration. After coagulation occurs initially in the rapid mix stage it continues in the flocculation stage as particles continue to collide and begin to form larger aggregates. During sedimentation, aggregates or flocs, begin to settle and may collide with surrounding flocs to form even larger aggregates that may be effectively removed during sedimentation.

Organic polymers may be used as coagulant aids in water treatment. Polymers may be anionic, cationic, ampholytic, or neutral in charge. The most commonly used polymers are cationic polyelectrolytes that are able to increase the quality of floc achieved when used in conjunction with metal salts. (Edzwald et al. 1985) observed that the use of organic polymers alone may be effective in particle destabilization, but produce a poor quality floc. Additionally, the use of organic polymers have not exhibited increased DBP precursor removal (Hubel 1987)

2.4.2 – Mechanisms of coagulation

The work of (O'Melia 1972) and (Dempsey 1984) have identified four mechanisms through which coagulation may be achieved. These mechanisms include double layer compression, charge neutralization, sweep coagulation, and interparticle bridging. Amirtharajah (1982) conducted a survey of previous work performed with alum and ferric chloride coagulants on numerous water sources. Figure 2.3 shows a pC-pH diagram for alum coagulation, demonstrating the observed coagulation mechanisms at specified pH and coagulant doses (Amirtharajah and Mills 1982). This figure illustrates that operational coagulation mechanisms are a function of pH and coagulant concentration. A similar coagulation diagram for ferric chloride is presented in Figure 2.4.

Colloids are stable in aqueous systems due to the electrostatic charge and/or hydration on their surfaces. The chemical structure and composition of a particle at the water-solid interface determines the net charge and stability of the particle. In most natural systems, the net charge of a colloidal particle is negative due to the ionization of surface acidic functional groups and adsorption of ions. Solution pH determines the net charge of a particle to some degree. A negatively charged colloidal particle attracts ions of opposite charge (counterions) to its surface from the surrounding water. The layer formed from the abundance of counterions on the surface of the colloidal particle is known as the fixed layer. As the fixed layer becomes more concentrated, a diffusion layer will occur outside the fixed layer. An electrostatic potential exists at the boundary between and is known as the zeta potential. This electrostatic potential extends outward from the particle until there is a balance on ions with the bulk solution. The zeta potential

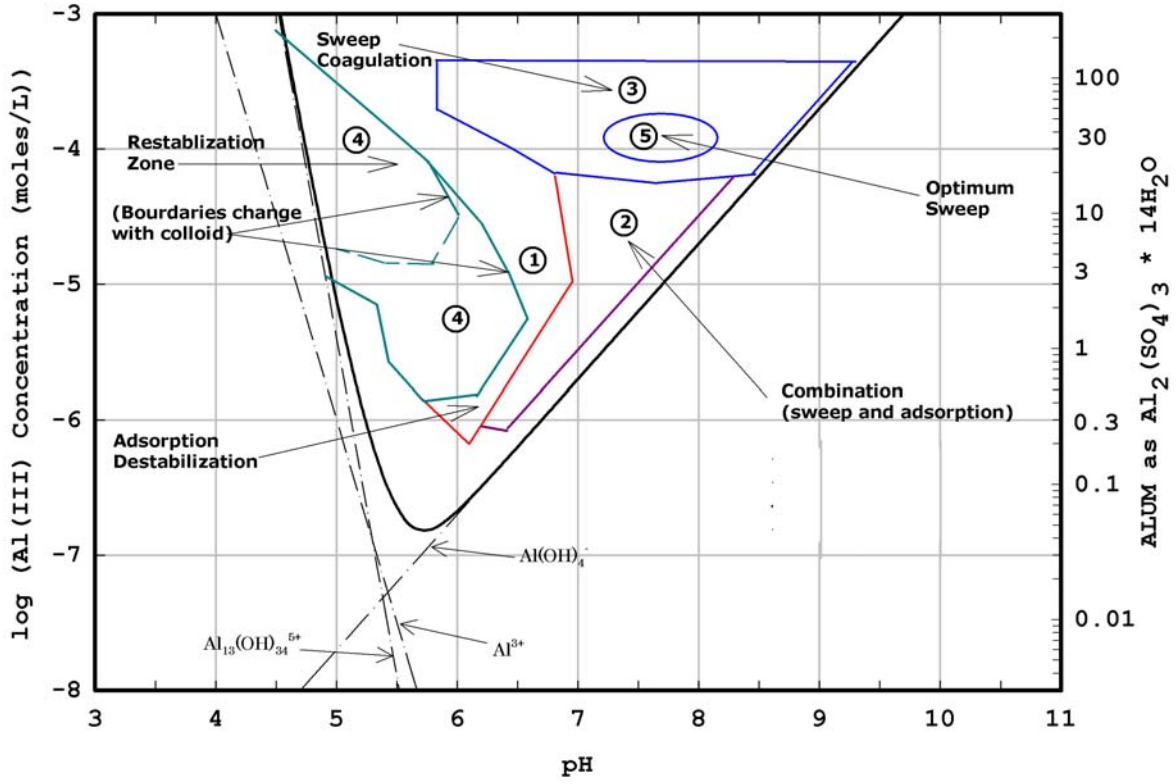

Figure 2.3 - Solubility diagram for aluminum showing predominate coagulation mechanisms (Amirtharajah 1982). Zone 1 – adsorption destabilization, zone 2 – Combination of sweep flocculation and adsorption, zone 3 – sweep coagulation, zone 4 – restabilization zone, zone 5 – optimum sweep floc

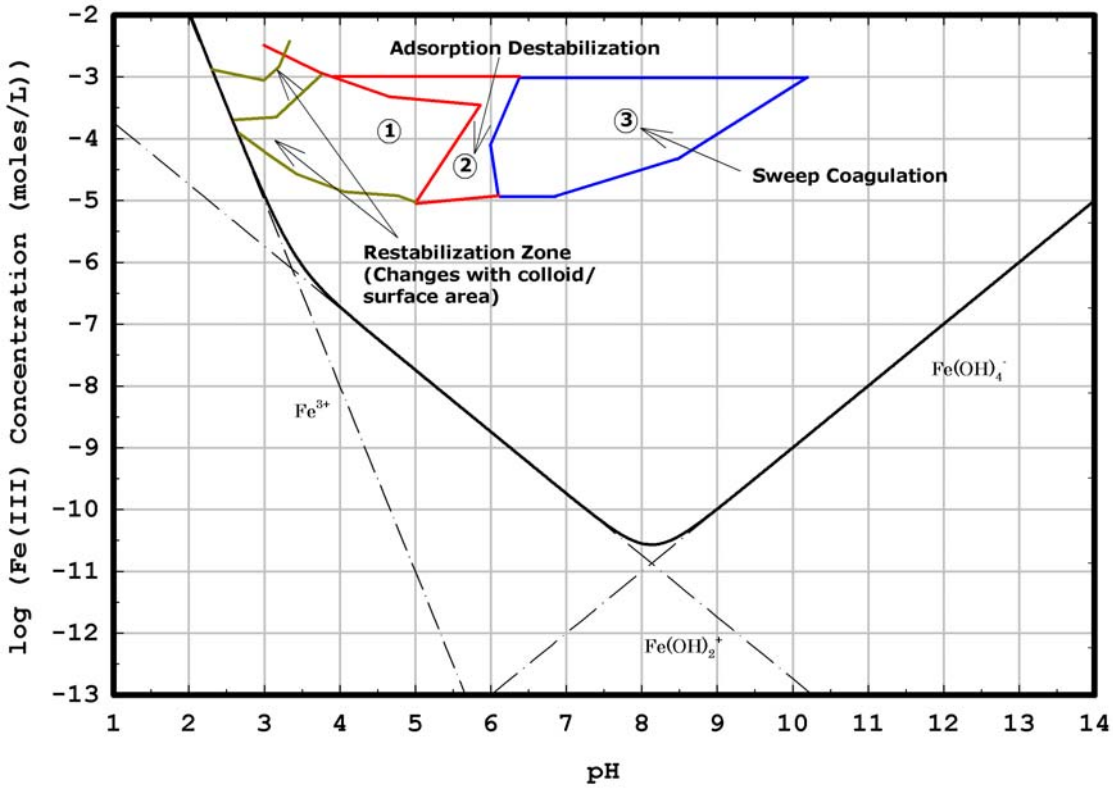

Figure 2.4 - Solubility diagram for iron showing predominate coagulation mechanisms (Johnson and Amirtharajah 1983). Zone 1 – restabilization zone, zone 2 – adsorption destabilization , zone 3 – sweep coagulation

may be used to determine the stability of the suspension. As zeta potential increases, repulsion forces between particles begin to increase and the colloidal suspension becomes more stable. The amount of bound water at the particle surface also effects stability by preventing particles from coming into close contact with one another (steamic hinderance).

Particle destabilization can occur through addition of polyvalent electrolytes through several mechanisms. The mechanisms that have been identified as the primary methods through which particle destabilization occurs are double layer compression, charge neutralization, interparticle bridging, and sweep floc (entrapment). These methods may take place individually or collectively to destabilize colloidal particles, facilitating their removal from suspension. Each mechanism is discussed briefly in the following sections.

2.4.2.1 – Double Layer Compression

Double layer compression is a classical method used to describe particle destabilization. The mechanism is achieved through addition of a simple electrolyte into a suspension of colloids. Ions possessing a net charge opposite to the net charge of the colloid material are attracted to the area surrounding the outside of the particle, referred to as the diffuse layer. As more counter-ions are added to the suspension they are attracted towards the suspended particles causing the diffuse layer to become compressed. This in turn reduces the amount of energy required to move the two colloidal particles of like surface charge together. Double layer compression has proven

to be an important destabilization mechanism, particularly in estuarine systems (O'Melia et al. 1999).

2.4.2.2 – Surface charge neutralization

Surface charge neutralization harnesses the principles involved in double layer compression and occurs in two processes. The first process involves the addition of a coagulating agent with a net charge opposite to that of the net surface charge of the suspended particles. Many of these coagulants are natural organic polyelectrolytes or hydrolysis products formed from the addition of hydrolyzing metal salts, such as alum or ferric chloride. In solution, these ions may sorb to, or react with, particle surfaces to the extent where the net surface charge of the particle is reduced or reversed. In some cases when excessive coagulating agent is added, the particle may become restabilized with a net surface charge opposite to that of the original net surface charge. The reduced surface charge of the particle will lower the energy necessary for two particles to come into contact with one another, similar to double layer compression. (Amirtharajah and Mills 1982)examined the influence of hydrolysis time on particle destabilization during alum coagulation. They found that aluminum hydroxo-complex species of maximum destabilization capacity formed within 0.1s after coagulant addition.

2.4.2.3 – Interparticle bridging and sweep floc

Interparticle bridging occurs when high-molecular-weight polymers branch out and adsorb to multiple particles. This process may also occur when polymers chemically react with other polymers or share ions directly to form ionic bridges. The resulting

aggregated particles may have reactive polymer branches extending into the aqueous suspension. The process of interparticle bridging occurs when particles combine with other particles through this manner. The branched polymer that facilitates this process must extend past the diffuse layer to avoid repulsion tendencies of similarly charged particles. The creation of polymer branches causes particle destabilization and may cause restabilization.

During interparticle bridging, particles come together to form a mesh-like matrix consisting of destabilized colloids and polymer branches. As the floc begins to settle, it may entrain smaller particles. This process is referred to as sweep floc, which includes other coagulation mechanisms to form the initial floc. Most conventional surface water treatment plants operate in the region where sweep floc is the predominate mechanism of coagulation (Amirtharajah and O'Melia 1990).

2.4.3 – Coagulation chemistry

The chemistry of multivalent hydrolyzing metal coagulants in solution is rather complex. Metal coagulants in solution complex with water to from aqua-metal complexes ($M\text{-}(H_2O)_6^{-3}$). The initial metal hydrolysis is followed by a series of hydrolytic reactions, where hydroxide ions present from the disassociation of H_2O molecules replace water molecules bound to the metals. The reduction in net charge occurring from these reactions initially leads to the formation of monomeric and then polymeric species. Insoluble metal hydroxide precipitates may form and be removed from solution.

Several factors influence the formation of metal hydroxides. These factors include pH, alkalinity, temperature, NOM concentration and composition, coagulant dosage, and type of coagulant used. The rapid-mix method used to distribute coagulants has also proven to partially determine the ultimate hydration species formed (Amirtharajah and Mills 1982). An understanding of the reactions that occur upon coagulant addition is necessary to comprehend organo-metal interactions.

2.4.3.1 – Aluminum Hydrolysis

The reactions occurring during aluminum hydrolysis have been studied for several decades. Scientists have not been able to discern all of the individual species formed during coagulant addition and a comprehensive assessment of previous studies conducted on the hydrolysis of metal salts (Amirtharajah and Mills 1980; Amirtharajah and Mills 1982; O'Melia 1972; Spengler et al. 1983; Stumm and O'Melia 1968) reveals minor variations in hydrolysis kinetics associated with aluminum and iron.

Monomeric aluminum species occur when only one aluminum ion is involved in metal-ligand exchange and are referred to as a 'mononuclear species' (Nordstrum 1996). These species form instantaneously, within milli-seconds, in aqueous solution and influence solution pH due to rapid hydrolysis and de-protonation. The hydrolyzed monomeric species formed have a strong tendency to complex with anionic compounds such as carbonate, sulfate, fluoride, and phosphate. In addition, they will complex with various functional groups composing NOM.

Polynucleation of monomeric aluminum species can occur to form polymeric species. Although many polymeric species are soluble, some are considered colloidal

species. The ability for these colloidal polymeric species to coagulate depends on several factors. Solution chemistry, including mixing conditions, aluminum concentration, presence or absence of complexing anions, and temperature are all factors contributing to the coagulation of polymeric species (Chow et al. 2000). The sequence in which chemicals are added to solution may also affect polynucleation. Anion addition prior to coagulant addition may cause the nucleation and/or precipitation of polymeric species not to occur (Parthasarathy and Buffle 1985). However, anion addition later in the coagulation process may cause aggregation to occur and produce precipitates. An early study by (Knocke et al. 1986) indicated that increased temperature causes reaction kinetics to favor polynucleation.

Dominate reactions for the hydrolysis of alum are described by the following series of equations (Benjamin 2002):

$$Al^{3+} + H_2O = Al(OH)^{2+} + H^+ \qquad \log K = -5.03$$

$$2Al^{3+} + 2H_2O = Al_2(OH)_2^{4+} + 2H^+ \qquad \log K = -6.27$$

$$Al^{3+} + 3H_2O = Al(OH)_3(s) + 3H^+ \qquad \log K = -9.1$$

$$Al(OH)_3(s) + H_2O = Al(OH)_4^- + H^+ \qquad \log K = -12.47$$

$$6Al^{3+} + 15H_2O = Al_6(OH)_{15}^{3+} + 15H^+ \qquad \log K = -47$$

$$7Al^{3+} + 17H_2O = Al_7(OH)_{17} + 17H^+ \qquad \log K = -48.8$$

$$13Al^{3+} + 34H_2O = Al_{13}(OH)_{34}^{5+} + 34H^+ \qquad \log K = -97.6$$

Aluminum hydroxide is the common precipitate formed upon alum addition. A high concentration of dissolved aluminum ions is often required for the precipitate to form. This can be seen by referring to the pC-pH diagram for aluminum in Figure 2.4. Any combination of pH and aluminum concentration corresponding to a point above the V-

shaped solubility boundary results in the formation of aluminum hydroxide. In the absence of colloids, this concentration was shown to occur at approximately 30 mg/l, as alum (Amirtharajah and O'Melia 1990). The majority of precipitates formed during coagulation at water utilities is in the form of "aluminum hydroxide". Ultimately, aluminum hydroxide will convert to gibbsite, the more thermodynamically stable form of the solid exhibiting the same chemical formula ($Al(OH)_3$).

2.4.3.2 – Iron Hydrolysis

Iron hydrolysis occurs in a very similar form when compared to aluminum hydrolysis (Amirtharajah and O'Melia 1990). Iron hydrolyzes in water and undergoes hydrolytic reactions, forming monomeric and polymeric species similar to that of aluminum. The precipitate formed under favorable conditions is iron hydroxide ($Fe(OH)_3$). Dominate hydrolysis reactions for Fe(III) in aqueous solution have been reported in several studies and may be summarized by the following hydrolysis reactions (Benjamin 2002):

$$Fe^{3+} + H_2O = Fe(OH)^{2+} + H^+ \qquad \log K = -2.17$$

$$Fe^{3+} + 2H_2O = Fe(OH)_2^{+} + 2H^+ \qquad \log K = -6.75$$

$$Fe^{3+} + 3H_2O = Fe(OH)_3(s) + 3H^+ \qquad \log K = -31.1$$

$$Fe(OH)_3(s) + H_2O = Fe(OH)_4^{-} + H^+ \qquad \log K = -38$$

$$Fe(OH)_3(s) + 3H_2O = Fe(OH)_6^{-3} + 3H^+ \qquad \log K = (\text{Not known})$$

$$2Fe^{3+} + 2H_2O = Fe_2(OH)_2^{4+} + 2H^+ \qquad \log K = -2.85$$

2.4.4 – Factors affecting coagulation

Several factors influence the efficiency and effectiveness of coagulation by metal salts. These factors include, but are not limited to, coagulant dose, pH, alkalinity, temperature, and ions present in solution. Each of these factors is described in more detail in the following sections.

2.4.4.1 – Coagulant Dose

The amount of coagulant addition is an important factor in determining the final metal-hydroxide species formed. The effectiveness of colloidal destabilization is also directly proportional to the amount of coagulant added. For every coagulant there exists an 'optimal dose' for a specific water chemistry and particle composition at which the coagulation of particles is optimized. Too little coagulant may provide insufficient destabilization to promote particle aggregation or destabilization. Too much coagulant and the particles themselves may become restabilized as the concentration of counterions increases. Coagulation is conceptually optimized when just enough coagulant is added to enable the highest level of particle removal possible. As the precipitates settle, sweep coagulation may occur and some organics may absorb to the solid metal hydroxide. Most water utilities operate in the region where 'sweep floc' occurs (Amirtharajah and Mills 1982). Although this area of operation requires more coagulant, hence a higher capital cost, it is easier to maintain coagulation in this region with fluctuating raw water conditions. Figure 2.6 demonstrates the regions where the previously discussed coagulation mechanisms occur with respect to pH and alum dose.

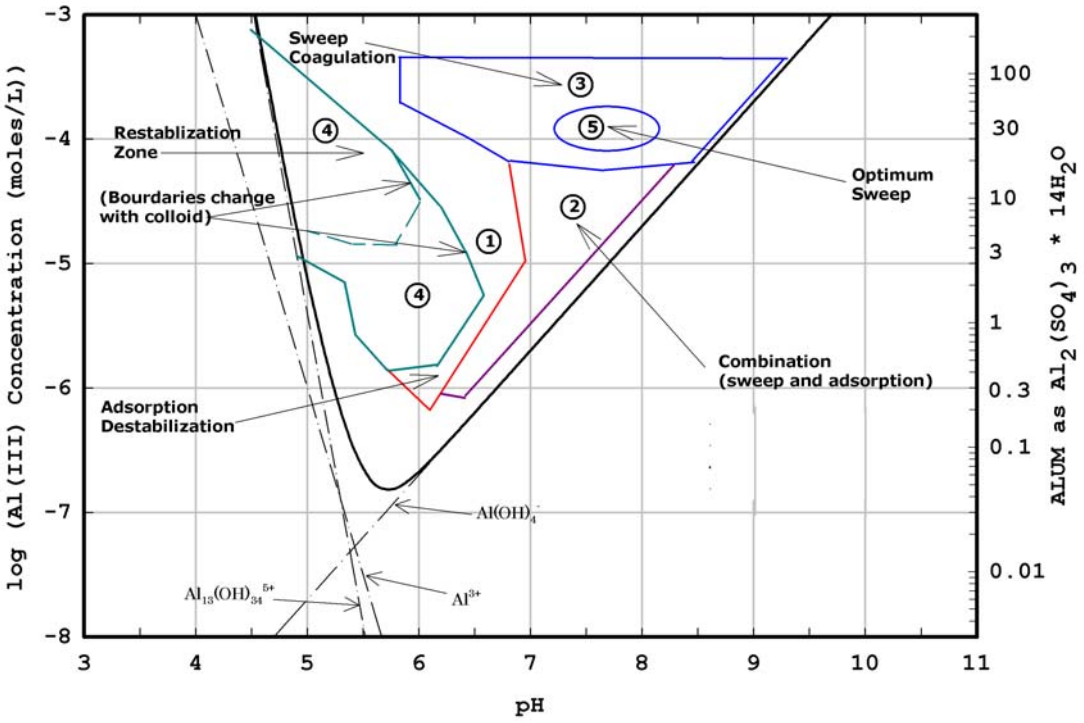

Figure 2.6 - Solubility diagram for aluminum and respective coagulation mechanisms (Amirtharajah 1990). Zone 1 – adsorption destabilization, zone 2 – Combination of sweep flocculation and adsorption, zone 3 – sweep coagulation, zone 4 – restabilization zone, zone 5 – optimum sweep floc

2.4.4.2 – Alkalinity

Alkalinity in raw water can limit the pH reduction observed after metal coagulant addition. Waters with high alkalinity often prevent water utilities from operating at an optimum pH for precursor removal (pH 4-5 for iron, pH 5-6 for alum). On the average, each mg/L of alum ($Al_2(SO_4)_3 \cdot 14\ H_2O$) and iron ($FeCl_3$) addition consume 0.5 mg/L and 0.62 mg/L of alkalinity respectively. Acid addition may be used to adjust the pH of waters high in alkalinity; however this process may be difficult for some water utilities that must deal with influent variations in both coagulant dose and alkalinity (as $CaCO_3$).

Waters containing very little alkalinity may be adjusted to an optimum pH through addition of Al^{3+} or Fe^{3+}. In situations where the pH is suppressed to very low conditions (pH < 4.5), the hydrogen ion may out compete metal hydrolysis products for ligand sites, therefore poor turbidity and NOM removal would result. In these situations, additional buffering capacity must be provided to enable the proper amount of coagulant addition for particle destabilization.

A study conducted on the relationship between alkalinity and coagulation effectiveness revealed that metal hydrolysis alone was sufficient in achieving the optimum coagulation pH for both alum and ferric chloride (Chadik and Amy 1983). Destabilization of humic material by charge neutralization was also achieved in low alkalinity waters. High alkalinity waters were resistant to pH depression and coagulation occurred at nearly neutral pH (6<pH<7).

*2.4.4.3 – **Solution pH***

The solution pH prior to and after coagulant addition is crucial in determining the effectiveness of colloidal destabilization. The initial pH determines the character of NOM in solution, as well as the propensity for NOM to react with metal polymers. The instantaneous polymeric metal-hydroxide species formed upon on coagulant addition are also affected by initial pH (Amirtharajah and O'Melia 1990). The solubility of metal hydroxide species is drastically affected by solution pH. This is evident by referring to Figure 2.6, notice how the soluble species present changes as pH increases from 4 to 8. When adjusting pH during the coagulation process, pH adjustment prior to coagulant addition is necessary to influence initial reactions that occur.

2.4.4.4 – Temperature

Temperature affects reaction rates, viscosity, and structural characteristics in the floc formed (Knocke et al. 1986). Lower temperatures have been found to cause lower turbidity removal. Floc settling velocity is also decreased at lower temperatures due to an increase in water viscosity. Alum was determined to be less sensitive to changes in temperature when compared to ferric sulfate (Knocke et al. 1986).

2.4.4.5 –Ionic effects

The activity of a solution can affect the hydrolysis of metal coagulants. (Hundt and O'Melia 1988) observed the removal of fulvic acid by aluminum coagulants. Hundt and O'Melia (1988) revealed that the presence of sulfate in solution can affect the formation of aluminum species. In low pH regions (pH<4.5), where soluble polymeric aluminum species exist, the presence of sulfate may form precipitates. Sulfate increases the likelihood of precipitates due to the formation of polymers with aqueous aluminum monomers. Aluminum-sulfate precipitates in addition to aluminum hydroxide precipitates provided additional adsorption sites for the removal of NOM.

2.4.5 – NOM removal by coagulation

Sources of organic matter in water supplies come from NOM, industrial organic matter, storm waters and runoff, and domestic wastewaters. The removal of organic matter is a critical process in the reduction of disinfection by-products. The coagulation-sedimentation process has the potential to remove the vast majority of DBP precursors if the process is optimized for their removal.

Coagulation of NOM has been widely investigated by (Hall and Packham 1965) and in more recent years by (Goslan 2004; Huang and Shiu 1996; O'Melia et al. 1999; Sharp et al. 2004; Singer 1999; Van Benschoten and Edzwald 1990; White et al. 1997). Humic and fulvic acid removal from water by iron and aluminum coagulants may be regarded as a chemical precipitation process forming insoluble basic aluminum/iron humates rather than coagulation (Hall and Packham 1965). The solubility and variety of metal-humate precipitates is dependent on the coagulant dose (Edzwald and Glaser 1979). There exists a stoichiometry between an optimum coagulant dose and humic concentration (Edzwald and Glaser 1979; Narkis and Rebhum 1977).

NOM removal may be achieved through charge neutralization and adsorption by coagulant addition (Dempsey 1984). This method occurs when dissociable hydrogen within the NOM is replaced by positively charged metal ions. The magnitude of this process is regulated by the solution pH. Under acidic and neutral conditions (pH<7), protonation of the carboxylic group (R-COOH) and deprotanation (R-COO) provide competition for free metal ions and metal polymers. Under alkaline conditions (pH>8) the hydrogen of the phenolic group provides competition for metal species (Chow et al. 2000). When NOM acts as a chelating agent, metal ions create strong bonds with organic molecules through electron transfer with potential to form a ring structure around the metal ion. Non-humic fractions of NOM are generally less reactive with metal coagulants when compared to humic fractions.

(Van Benschoten and Edzwald 1990) found that the role of complexation of aluminum polymers and fulvic acid is significant with regards to coagulation. If metal concentrations are greater than the reaction capacity of functional groups of the organic

matter surface complexation may occur (Evanko and Dzombak 1998). Ambient pH determines the net charge as well as the surface charge of the metal hydroxide, thus governing the magnitude of the reaction. The point of zero charge (PZC), where the net surface charge is zero, is drastically effected by the pH. As the pH increases above the PZC, the surface develops a net negative charge. As the pH falls below the PZC, net surface charge becomes positive, translating to increased anionic particle sorption (Dzombak and Morel 1990).

Ambient pH is critical in maximinzing the effectiveness of NOM removal. Although maximum adsorption of both humic and fulvic acids occurs under acidic conditions, studies have revealed that adsorption is the key mechanism involved in the removal of humic and fulvic acids over the entire pH range (Dempsey 1984). NOM removal by mineral adsorption occurs primarily due to Van der Walls forces or polarization arising from the rearrangement of macromolecules (Matilainen et al. 2002). Through this mechanism, polar moments in two adjacent molecules will cause a net attractive force. Hydrophobic humic molecules, the most easily removed by coagulation, are strongly influenced by physical absorption (Matilainen et al. 2002). (Hundt and O'Melia 1988) suggested that a co-precipitation of aluminum hydroxide and aluminum-humates is the primary mechanism for humic compound removal. However, there is a general concensus that higher MW natural organic compounds are more easily removed than their low MW counterparts.

2.4.6 – Aluminum and iron coagulant comparison

A direct comparison between coagulants is often necessary to determine the effectiveness of a particular coagulant on a water source. In most cases, proper coagulant dose and effectiveness is monitored by performing *in-situ* jar test experiments. Selecting a proper coagulant is dependent on several factors including availability, coagulant cost, and sludge disposal costs. There is no clear consensus among researchers or practitioners indicating the most effective coagulant for water treatment. In many cases a coagulant that performs particularly well with one water source may not produce the same results with a different water source. (Chadik and Amy 1983) compared ferric chloride and alum in organic precursor removal and concluded that ferric chloride was more effective than alum. However, many other studies (Crozes et al. 1995; Edwards 1997) suggest ferric based coagulants are superior for organic precursor removal, demonstrating that NOM removal is a function of regional water chemistry. Over the past few years some research has focused on the use of iron salts as coagulants due their potential benefits in the increased removal of DBP precursors (Baltpurvins et al. 1996). It is clear there is a need to identify the behavior of a metal coagulant based on water quality parameters including the type of NOM present. This knowledge will allow water utilities to select appropriate coagulant(s) based on scientific knowledge, rather than performing jar-test experimentation.

The solubility, acidity, and the extent of hydrolysis determine the coagulation characteristics of trivalent metal coagulants. It is important to understand the interactions of both aluminum and iron based coagulants with various NOM fractions to maximize

removal efficacy. The key differences between aluminum and iron based coagulants are described as follows:

(1) Based on dry weight of coagulant, Ferric chloride (34.4 % Fe^{3+}) presents approximately two times more active metal species than aluminum sulfate (15.7% Al^{3+})

(2) It has been reported that the specific surface are of ferric hydroxide and aluminum hydroxide flocs are similar, however due to the lower concentration of active metal in Aluminum (III) sulfate solution and the lower MW of aluminum, similar doses of aluminum produce approximately less metal hydroxide when compared to a similar dose of iron. This translates to the surface area available for adsorption being considerably lower for aluminum than iron.

(3) For Al, there is a minimum solubility (about 2 μM) in the region of pH 6. Ferric species show a much lower solubility (around 20 nM) over a rather broad pH range (5.5 – 8.0). The minimum solubility of iron ($Fe_2(SO_4)_3$ & $FeCl_3$) is much lower than aluminum ($Al_2(SO_4)_3$) at normal coagulation pH values ($5 < pH < 7$) which enables the formation of iron hydroxide at a lower coagulant dose.

Several studies (Helfrich et al. 1992; Knocke et al. 1992; Lovins III et al. 2003) have concluded that iron based coagulants are more effective than alum for the removal of DOC leading to an overall lower DBP formation potential. However, optimizing the

coagulation pH for alum has been found to increase DOC removal up to 65% (Helfrich et al. 1992).

2.4.7 – Coagulation Summary

The practice of coagulation for the removal of colloidal material from surface waters is source specific and highly variable depending on water chemistry, character of suspended particles and NOM, and coagulant type. The coagulation process is used to destabilize suspended particles and react with dissolved organic matter in influent raw water. Proper coagulation is essential to remove sufficient quantities these elements to promote good filtration performance and disinfection byproduct (DBP) control. Many water treatment municipalities are not fully utilizing the capabilities of the coagulation mechanisms put into place. A deeper understanding of the coagulation process specific to the raw water observed at an individual water treatment plant is instrumental in the reduction of disinfection byproducts and removal of DBP precursors.

2.5 – Disinfection

Historically, chlorine has been the primary disinfectant used in water treatment for more than 100 years. However, pioneering work conducted by (Rook 1974) uncovered carcinogenic byproducts formed due to the chlorination of organic particles. Three years after these compounds were discovered, the EPA began regulating the by-products class known as trihalomethanes (THMs). Alternative disinfectants such as ozone, UV irradiation, and chlorine dioxide are subject to their own set of related disinfection by-products (DBPs) and may also have adverse health effects. Although

other methods of disinfection exist, chlorine is likely to be used in the future for some time due to its economic sensibility, commercial availability, and ability to provide residual disinfection (required in the United States).

2.5.1 – NOM and Chlorine

Disinfection is necessary to prevent acute outbreaks of potentially deadly diseases and other deleterious health effects; however chlorine disinfection may be the cause chronic health problems in the future. Chlorine reacts with organic humic materials in solution (DBP precursors) to produce THMs in finished drinking water. THMs account for approximately 30 - 60% of all known DBPs (Singer et al. 1995). The maximum contaminate level (MCLs), set in 1979 by the D/DBP rule, for total THMs (TTHMs) was initially 100 μg/L, but was soon changed under Stage I DBP rules to 80 μg/L where it stands today (2004). Stage II DBP regulations are expected to lower the MCL for TTHMs to 40 μg/L. Other halogenated-by-products include haloacetic acids (HAAs), haloacetonitriles (HANs), haloketone (HKs), chloropicrin (CHP), and chloral hydrate (CH) (Krasner et al. 1989). Hydrophobic fractions of humic materials are readily removed during coagulation, prior to chlorine addition. However, removal of the hydrophilic (polar) fraction of humic substances by coagulation is inefficient and subsequent reactions with chlorine generally involve the hydrophilic humic fraction (Hwang et al. 2001).

The humic fraction of aquatic NOM is responsible for the majority of disinfection by-products formed upon chlorination. Previous research has focused on the removal of this fraction by various methods, primarily coagulation. (Oliver and Lawrence 1979)

witnessed a dramatic decrease in the formation of haloform in several Great Lakes waters by alum coagulation. In one study, THM-FP reduction by alum ranged from 36-66 percent and the reduction by iron ranged from 33-77 percent (Chadik and Amy 1983). (Jodellah and Weber 1985) found that a greater reduction in TOC through coagulation did not always translate to a decreased formation of DBPs. (Croue et al. 1993) observed that humic acids are the most amenable fraction of NOM to removal by coagulation. It may be concluded that the reduction of THM-FP is a function of the physical nature and characteristics of NOM rather than the amount removed through coagulation. Therefore, a full understanding of both the physical and chemical characteristics of the NOM comprising a water source is necessary to optimize and evaluate removal strategies.

Chlorine is a powerful oxidant capable of reacting with both inorganic and organic species (i.e., NOM, proteinaceous compounds. etc.). Increased presence of inorganic and organic compounds requires higher doses of chlorine to overcome the initial chlorine demand of the water and provide an adequate level of residual chlorine for disinfection. Chlorine may be applied as a gas or liquid to produce HOCl and OCL^- ions in solution. HOCl and OCl^- are the predominate forms of aqueous chlorine under normal operating conditions with a pK_a of 7.53. HOCl provides superior disinfection capacity, as measured through *E. coli* inactivation, when compared to OCl^- in solution. Aqueous chlorine species may combine with ammonia to form chloramines. The combined chlorine species provide residual disinfection capacity while limiting the formation of DBPs.

Haloacetic acids account for the majority of DBPs formed that are not associated with THMs. The Stage I MCL for HAAs is currently set at 60 μg/L for the sum of five

species (HAA_5) and will be lowered to 30 μg/L once Stage II MCLs are enacted for the sum on six species (HAA_6). HAA_5 includes mono-, di-, and tri-chloroacetic acids (MCAA, DCAA, TCAA) and mono- and di-bromoacetic acids (MBAA and DBAA), while HAA_6 also includes bromochloroacetic acid (BCAA).

The exact mechanism of THM and HAA formation is not clearly understood. Slavinskaya (1991) described the formation of THMs occurring through destruction of conjugate bonds and fragmentation of humic substances. Due to the complex nature and structure of natural aquatic humic materials, the study of (Slavinskaya 1991) and others (e.g., (Norwood et al. 1980; Rebenne et al. 1996; Rook 1974) were conducted using simple models of humic substances (i.e., m-dihydroxybenzene). There is little evidence to support the idea that these simple models are representative of naturally occurring aquatic humic substances.

The three major types of reactions that occur in the presence of Cl^- and Br^- ions are oxidation, substitution, and addition. Oxidation agents include HOCl and HOBr, which are capable of transforming a chemical by decreasing the hydrogen content of the species. Substitution reactions occur when the hydrogen atom of the transforming chemical is replaced by oncoming halogen. In addition, a reaction between two reactants results in a single product such as halogenated alkane.

In the case of aromatic compounds, such as NOM, chlorine reacts by activating the aromatic ring. Chlorine reacts strongly with electron donating groups (i.e., -OH, -OR, $-NH_2$, -R) and is incorporated more easily when compared to electron-withdrawing groups (i.e., -COOR, -COOH, $-NO_2$, -X) (Rook 1974). The reactivity of chlorine with electron-donating groups (e.g., phenol, anisole) and electron withdrawing groups (e.g.,

nitrobenzene, chlorobenzene, benzonitriles) was investigated by (Carlson and Lin 1975). Their results suggested that electron donating groups had a higher reactivity with chlorine due to the ability of electron-donating groups to direct the halogen to both the para and ortho positions, while electron-withdrawing groups where limited in their halogen placement to the meta position.

(Rook 1977) suggested that humic material was the primary cause of THM formation and attributed byproduct formation to dihydroxybenzene moieties existing in humic material. Later studies revealed that the initial reactivity of chlorine with NOM is attributed to the successive electrophilic chlorination of resorcinol (Rebenne et al. 1996). Higher levels of resorcinol are linked to increased reactivity of NOM with chlorine. As pH increases (i.e., pH > 6), a phenol constituent is formed upon chlorination of phenolic compounds, which is more reactive than unionized phenol (Rebenne et al. 1996). Determination of THM reaction kinetics in acidic solution (pH < 6) has not been extensively investigated.

Aliphatic structure accounts for a significant portion of naturally occurring NOM. The structure is also a major contributor to the formation of THM species upon chlorination of NOM. Chloroform formation has been documented as early as 1931 through halogen reactions with methyl-ketone (Berliner 1931). Chlorination of the aromatic compound resorcinol has been shown to produce various chlorinated intermediates, such as the aliphatic compound methyl ketone through its reaction pathways, followed by base-catalyzed hydrolysis to form chloroform (Norwood et al. 1980). The presence of additional oxidizable precursors has been shown to contribute significantly to THM formation (Rook 1977).

2.5.2 - **Factors that influence DBP formation**

There are several factors that can influence the concentration and amount of time it takes for DBPs to form. These factors include, but may not be limited to pH, temperature, disinfectant contact time, chlorine dose, and bromide ion concentration. In general, THMs account for the majority of recognized DBPs and are often more abundant than HAAs in chlorinated waters. (Singer et al. 1995) observed that in some waters HAAs were more abundant than THMs. His work suggested that both physical and chemical parameters may influence the type and concentration of DBP formed. Changes in the nature and chemical composition of NOM have also proven to elicit different types of DBPs (Goslan 2004). Influence of physical characteristics with regards to THM formation has been extensively studied, however limited information exists on HAAs.

2.5.2.1 – Physical parameters

Temperature may be responsible for disparities observed between levels of THMs produced in different climatic regions under similar chlorination characteristics (Koukouraki and Diamadopoulos 2003). An earlier study (Knocke et al. 1986) demonstrated that the rate of THM formation at 22°C was 60-70% higher than that observed at 2°C. The 7-day THM-FP revealed THM yields to be 40% less for samples incubated at 2°C when compared to samples incubated at 22°C. Intermediary studies have revealed similar trends for THM formation with respect to variations in temperature (Koukouraki and Diamadopoulos 2003). Throughout the studies water temperature was generally positively correlated with formation or DBPs.

The level of hydrogen-ion concentration (pH) has a measurable effect on the formation of both THMs and HAAs. Unlike temperature variance, a change in pH affects speciation of both the oxidant (disinfectant) and organic matter present in solution. pH shifts may alter the mechanisms through which chlorine is capable of reacting with aquatic organic matter by facilitating the protonation and deprotonation of its various functional groups. Resorcinol, a key intermediary for the formation of THMs, exhibits phenolic functional group deprotonation ($Ar\text{-}O^-$) at a higher pH ($pH > 6$). This enables the compound to react faster with chlorine through multiple substitution reactions. At a lower pH, this same functional group undergoes protonation (Ar-OH), eliciting a much slower oxidation reaction, albeit in a stronger oxidizing environment due to shift from OCl^- to HOCl as pH is decreased (Reckhow and Singer 1990).

The effect of pH on the formation of HAAs has be found to be opposite to that of THMs (Reckhow and Singer 1990). Although the exact mechanism through which HAA formation occurs is unknown, a decrease in pH will generally increase the formation of HAAs. Reckhow and Singer (1990) analyzed isolated heterogeneous humic substances to reveal decreased TCAA (a dominant HAA_5 species) at a higher pH ($7 < pH < 12$), while THM formation increased.

Stability and coaguability of NOM is largely dependent on ambient pH conditions. The application of any oxidant (primarily chlorine) at various stages in a treatment process will produce varying results with respect to DBP formation. If chlorine is added at a higher pH (i.e., after lime addition), or at a lower pH (i.e., after coagulation) it can affect the amount of THMs and HAAs formed, as well as other DBPs. If THM

formation is a primary concern for THMs, chlorine addition at a lower pH may be advisable. The opposite is true if HAA reduction is a primary concern.

Ionic strength has the ability to alter the chemical morphology and reaction kinetics of aquatic NOM. Waters with low ionic strength evoke an elongated NOM structure, whereas waters with high ionic strength cause the NOM to form a coiled shape thereby reducing the reactivity of some stymied functional groups (Staub et al. 1984). Therefore, waters exhibiting high ionic strength typically produce fewer THMs.

The amount of time NOM is exposed to a particular oxidant is also a matter of concern for water utilities due to the relationship between contact time and DBP formation. An earlier study by (Oliver and Lawrence 1979) revealed rapid chloroform formation during the initial 24 hours after chlorination followed by a steady increase in overall concentration. Rates were shown to be dependent on the type of precursor material present and the type of reaction which may occur.

2.5.3 – Disinfection summary

The amount of disinfection byproducts formed relies heavily on the concentration of dissolved organic matter present in water. The reactions that are occurring between chlorine and NOM are very complex and not fully understood. It is known, however, that optimization of the coagulation process for removal of NOM can greatly reduce the amount of DBPs formed. Furthermore, formation of DBPs does not only depend on the quantity of NOM, but also its physical and chemical structure. Ambient water chemistry and imposed coagulation chemistry can drastically change the amount of DBPs formed. Relationships relating to the formation of DBPs may be better understood and controlled

by first gaining a better understanding of the naturally occurring precursors (NOM) that are the cause of their formation.

CHAPTER 3 - OBJECTIVES

The aim of this project was to investigate the change in character of influent raw water at Savannah Water I&D (SWID) containing elevated levels of NOM. This overall goal was achieved by the following objectives:

(1) Assess SWID coagulation practice for the concurrent removal of turbidity and color (NOM) using iron (ferric) and aluminum based coagulants under varying dose and coagulation pH.

(2) Characterize SWID natural organic matter using ultrafiltration to determine a molecular size distribution and assess NOM fractional removal by coagulation with alum and ferric sulfate.

(3) Investigate the relationship between NOM character and chlorine reactivity with respect to THM formation and assess relationship between SUVA and THM formation potential.

CHAPTER 4 – MATERIALS AND METHODS

The objectives listed in chapter three were accomplished using the following methods and experimental procedures. The procedures and methods described here are referenced in following chapters and any variations or changes to the basic procedure is described prior to discussing experimental results.

4.1 – NOM Isolaiton

Three waters were used throughout the coarse of experiments. Raw water located at SWID was used to determine coagulation efficacy during jar test studies. Isolated source water was measured for color, turbidity, pH, and alkalinity from discrete points within the SWID watershed. Finally, a raw composite water was created using isolated source water from within the SWID watershed.

In an effort to obtain adequate levels of DOC for fractionation purposes, working solutions of NOM were taken from the SWID watershed. Raw water composite was created using equal volumes of water from within the SWID watershed (reconstituted TOC = 10.7 – 12.2 mg/L & UV_{254} Absorbance = 0.933 - 1.001 cm^{-1}). 100-mL aliquots were processed through 0.45–μm Teflon filters then stored collectively at 4°C.

4.2 – Characterization of NOM

4.2.1 – UV_{254} absorbance

UV_{254} absorbance (UVA) in a natural water sample generally increases as NOM concentration increases. Additionally, valuable information about the character and size of NOM may be obtained through the use of UVA. UV_{254} absorbance was measured

using a Hach DR-4000 UV/VIS Spectrophotometer operated at a wavelength of 253.4 nm and a 1-cm quartz cell (8 mL sample volume). The instrument was calibrated using reagent grade water as a blank.

4.2.2 – TOC (DOC)

Dissolved organic carbon was measured using a Pheonix 8000 Total Organic Carbon (TOC) analyzer (Tekmar-Dohrmann Cincinnati, OH) operated in TOC mode. A five-point calibration curve was created using reagent grade water for a zero point and TOC standards at 2.5, 5, 10, and 15 mg/L made from dilutions of potassium biphthalate (1000 mg C/L). The instrument was calibrated regularly and calibration was verified before each sample set. The analyzer was recalibrated if the value of the standards were not within 2% of the expected value. The analyzer took up to five replicates and reported the average of the last three trials given that the coefficient of variance was not greater than 2%.

4.2.3 – THM formation potential (THM-FP)

Trihalomethane formation potential was carried out using an adaptation of procedure 5710 in 'Standard Methods for the Examination of Water and Wastewater' (American Public Health Association) and is described in the following sections (Harriet, 2003). The adapted procedure and reagents used in THM-FP studies are listed in the following section.

4.2.3.1 – THM-FP Reagents

Determination of strength of hypochlorite solution - sodium hypochlorite (15%, 0.5 mL) solution was diluted to 25 mL in a volumetric flask with reagent grade water and thoroughly mixed. The diluted solution was placed in a conical flask containing acetic acid (5 mL) and potassium iodide (~ 1g). The contents of the flask were mixed and titrated with aqueous sodium thiosulfate (0.1M) prepared with reagent grade water until the faint yellow color of the liberated iodine was almost discharged. Iodine indicator powder (~ 1g) was added and the titration continued until the blue/black color was discharged. The volume was recorded and used in Equation 4.1 to calculate the hypochlorite concentration.

$$\text{Hypochlorite concentration (mg mL}^{-1}\ \text{Cl}_2) = \left(\frac{\text{M} * 33.45 * \text{titrant volume (mL)}}{\text{hypochlorite added (mL)}} \right) \qquad \text{Eq. 4.1}$$

Where M is the molarity of the titrant (sodium thiosulfate). The titration should require at least 10 mL titrant. If the titration required less titrant then 0.8 mL of the hypochlorite solution should be used. The strength of the sodium hypochlorite solution was measured each time a new dosing solution was made. The solution was discarded when the concentration fell below 30 mg/L Cl_2.

Chlorine dosing solution (1000 mg/L Cl_2) – The volume of hypochlorite solution required was calculated using Equation 4.2 (Standard Methods).

$$\text{Hypochlorite required (mL)} = \left(\frac{1250}{\text{Hypochlorite concentration (mg mL}^{-1}\ \text{Cl}_2)} \right) \div 5 \qquad \text{Eq. 4.2}$$

The calculated volume was diluted to 250 ml in a volumetric flask to mark with reagent grade water. The concentrate was then placed in an amber bottle and refrigerated at 4 ºC. The free chlorine was measured by diluting the dosing solution to < 2.0 mg/L Cl_2 and using a DPD powder pillow photometric method measured using a HACH DR 4000 spectrophotometer. The solution was discarded after 1 week.

Phosphate buffer – 68.1 g potassium dihydrogen phosphate (KH_2PO_4) and 11.7 g sodium hydroxide (NaOH) were dissolved in 1 L reagent grade water (pH~7.0). The buffer was refrigerated and discarded after 1.5 weeks.

Sodium sulfite solution – 10 g sodium sulfite was dissolved in 100 ml reagent grade water. The solution was used for dechlorination with the assumption that 0.1 mL destroyed 5 mg residual chlorine. The solution was discarded after 1.5 weeks.

Reagent grade water – treated water was deionized and distilled and stored in autoclaved glassware. Freshly distilled reagent grade water was used to make all solutions and for instrument calibration.

4.2.3.2 – THM-FP Method

Sample chlorination – The appropriate volume of chlorine dosing solution was put in a 60 mL amber bottle with 1 mL phosphate buffer and filled completely with sample. The bottle was stored in an incubator at 25 ±2 ºC for seven days.

Reagent blank – 1 mL chlorine dosing solution was placed in a 50 mL volumetric flask and filled to the mark with phosphate buffer. A 40 mL PTFE – lined screw cap vial was completely filled with the mixture and stored with the sample at 25 ±2 ºC for seven days.

Sample Analysis – after the seven day incubation period 0.40 mL sodium sulfite solution was placed in a 40 mL vial and gently and completely filled with sample. If the sample was not being analyzed immediately, the pH was reduced to <2 by adding 3 drops of concentrated ascorbic acid. The vial was sealed with a PTFE-lined screw cap. The sample was refrigerated but brought to room temperature before analysis by Gas Chromatography. The total THM (trichloromethane ($CHCl_3$), dichlorobromomethane ($CHBrCl_2$), dibromochloromethane ($CHClBr_2$), and bromoform ($CHBr_3$)) concentration was measured at Spectrum Laboratories (Fort Lauderdale, Fl) using an HP 5890 Gas Chromatograph.

Blank Analysis – after the seven day incubation period 0.25 mL of sulfite reducing solution was added to a 250 mL bottle and 5 mL of the reagent mixture added without mixing. The bottle was immediately and completely filled with reagent grade water and capped with a PTFE-lined screw cap. A portion was analyzed for THMs using the same method described previously. The sum of all THMs should be < 5 μg/L.

4.2.4 – <u>Jar test procedure</u>

Standard jar-tests were conducted in 1-L glass jars (Phipps and Byrd 1985) using alum and ferric sulfate. During each jar test, coagulant dose was fixed and pH was

adjusted to achieve desired pH through the addition of 0.1 M HCl or filtered slaked lime ($Ca(OH)_2$) saturated solution. The lime solution was mixed thoroughly to ensure all lime was in solution prior to use.

A jar-test sequence was established to accurately reproduce the current process employed at SWID. The sequence consisted of 1-min rapid mix at 100 RPM, followed by flocculation for 5 min at 60 RPM, 5 min at 40 RPM, and 5 min at 20 RPM. The flocculation sequence was followed by a 30-min settling period. Settled water samples were extracted after the 30 min settling period from the center of the 1-L glass beaker using a 600 cc syringe. 40-mL, settled-water aliquots were filtered using pre-washed 0.45-μm glass fiber filters prior to further analysis.

*4.2.4.1 –**Reagents***

Lime Solution – A fully saturated lime solution was prepared using quick lime ($Ca(OH)_2$) and reagent grade water. The solution was filtered using a 0.45-μm Teflon filter and stored at 4˚C until use.

Coagulants - Solutions of alum and ferric sulfate were prepared using de-ionized/distilled water to a bulk concentration of 10 g/L. Alum was collected in its concentrated liquid form from SWID and diluted to the appropriate concentration. Ferric sulfate solution was created using dry ferric sulfate supplied by Chemron (Savannah, GA) and reagent grade water. Solutions were stored at 4˚C, brought to room temperature (23˚C ±0.2) before use and discarded after 2 weeks.

4.3 – NOM Ultrafiltration

Ultrafiltration was conducted using an Amicon model 8200 ultrafiltration stirred-cell (200 mL process volume). Amicon cellulose acetate membranes YM30, YM10, YM3, and YM1 with MWCOs of 30,000 Da, 10,000 Da, 3000 Da, and 1000 Da, respectively, were used. In addition, Amicon regenerated cellulose membrane YC05 (MWCO 500) was used. Aliquots of each working solution were passed through several ultrafiltration membranes operated in parallel. Figure 4.1 illustrates an outline of this procedure. Raw composite NOM samples were filtered using 0.45-μm Teflon filters. NOM (DOC) was subsequently filtered using each of the individual ultrafiltration membranes in parallel. Permeate samples from each of the membranes were measured for specified water quality parameters and apparent molecular weight distribution was determined using data provide.

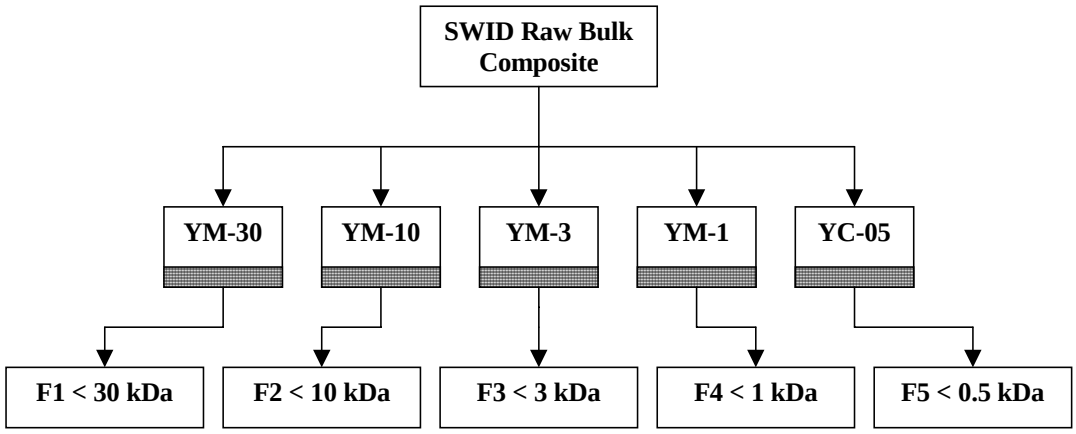

Figure 4.1 – Parallel UF process schematic

4.3.1 – Membrane preparation

Initial membrane preparation was necessary to remove the storage materials (glycerin and sodium azide) used to package membranes for shipping. Membranes were rinsed for 30 min with 0.5% NaCl solution to remove UV_{254} absorbing material. The membranes were then rinsed using de-ionized / distilled (ultrapure) water for 1 hour changing the rinse water every 15 min. Membranes were then equilibrated in ultrapure water over-night. Before use, each membrane was placed into individual Amicon® 8200 series stirred cells and ultra-pure water passed through each at the nominal nitrogen operating pressure 3.79 bar (55 psig) for 15 min.

4.3.2 – Ultrafiltration procedure

Clean-water flux values were measured before each trial and compared with manufacturers values in Table 4.1. Initial sample volume was 200 mL, of which 140 mL was processed leaving a final volume of 60 mL which was continuously stirred for 10 min before retentate concentrations were sampled. During each trial, stir bar speed was maintained at 210 ±10 RPM using an optical tachometer to ensure constant speed. The chosen mixing speed allowed for complete utilization of the membrane surface while maintaining adequate tangential scouring velocity (Tadanier et al. 2003). During each filtration cycle eight 10-mL aliquots were collected at periodic intervals to account for cumulative effects of membrane rejection, using the PCM model (discussed in section 5.3). The efficiency of solute recovery was evaluated by conducting a mass balance on DOC and/or UV_{254} absorbance.

Table 4.1 – Clean water flux range for YM/YC Amicon® UF membranes at 6.35 cm diameter.

Membrane	Clean Water Flux @ 55 psig ($mL/ hr\text{-}cm^2$)
YM30	42 - 66
YM10	6 - 12
YM3	3.6 – 4.8
YM1	1.2 – 2.4
YC05	1.8 – 2.4

CHAPTER 5 – RESULTS AND DISCUSSION

The focus of this chapter is to provide results to experiments conducted in this study. Additionally, a background of the water treatment plant (Savannah Water I&D) used to conduct these studies has been provided to better familiarize the reader with the treatment processes employed.

5.1 – Savannah Water I&D (SWID)

5.1.1 – Water Plant Operation

The SWID water plant is a conventional surface water treatment plant employing coagulation, gravity sedimentation, pre-filtration chlorination, filtration, and post-filtration chlorination. SWID was originally designed in 1946 to treat approximately 35 million gallons per day (MGD) and expanded to 62.5 MGD (75 MGD maximum capacity) in 1997. Over the past 56 years, water demands have increased to an average of 45 MGD. Demand reaches 50 MGD on a regular basis with relatively long demand periods (24 to 48 hr) of approximately 55 MGD and short demand periods (2 to 4 hr) of up to 60 MGD. Potable water is provided to major industrial facilities on the Savannah River corridor, as well as small, but expanding, commercial and residential users.

Currently, liquid alum ($Al_2(SO_4)_3 * 14H_2O$) is used as a primary coagulant and high molecular weight cationic polymer is used to supplement coagulation. Lime is presently fed for raw and finished water pH and alkalinity adjustment. Raw-water lime addition promotes optimized coagulation whereas finished water lime addition buffers the water such that it will maintain a relatively stable pH and chlorine residual in the distribution system. Raw water lime addition only occurs during poor raw water quality

episodes in which the alkalinity is low or color is high and alum demand is high. Finished-water lime feed is continuous with plant operation.

Coagulation pH, with or without lime addition, is $5 \leq pH \leq 7$ and is primarily adjusted through addition of alum prior to the rapid-mix basin. Table 5.1 displays rapid

Table 5.1 – Rapid mix design criteria for SWID.

Rapid Mix Basins			
Dimensions of Each Basin (m)			
1st/3rd Stage	3.05 W x 3.05 L x 4.42 D		
2nd Stage	3.05 W x 1.83 L x 4.42 D		
Volume of Each Basin (cubic meters)			
1st/3rd Stage	41.1 (1450 ft^3)		
2nd Stage	24.7 (870 ft^3)		
Mixer Type	Axial Flow Turbine - Type		
Drive Type	Variable Speed		
Motor Size (hp)	45		
	Max. Flow	Avg. Flow	Min. Flow
Flowrate (MGD)	75	50	35
Detention Time per Mix Basin (sec)	13	19	27
Total Detention Time (sec)	33	49	70
Maximum G-value	1000	1000	1000
Minimum G-value	700	700	700

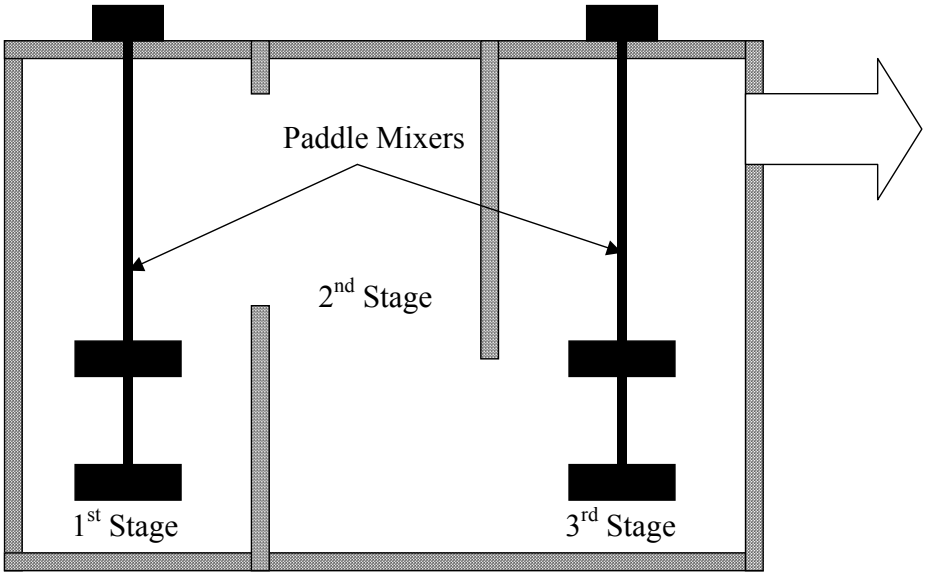

Figure 5.1 – Example of 3 stage rapid mix design used at SWID (side view)

mix design criteria for SWID. Figure 5.1 shows a flow schematic of the 3 stage rapid mix employed at SWID. Alum is applied to the influent water at a point that is 4.6 meters (≅ 15 feet) upstream of the rapid mix basins following the raw water venturi meter. Rapid mix detention time is approximately 50 sec at 50 MGD. The rapid mix structure is located off-center relative to the flocculation/sedimentation basins. As a result, flow to sedimentation basins 1 and 2 flows through a 48-inch pipe connecting the inlet channels. The rapid mix offset may result in disproportionate flow to both sides of the plant.

Flocculation is achieved through the use of 6 parallel treatment trains, each train containing 3 separate flocculation chambers in series with rotating paddle mixers. Each flocculator (stage) mixer is equipped with its own variable speed drive unit which allows

for tapered flocculation over a G-value from 10 sec^{-1} to 75 sec^{-1}. The hydraulic residence time (HRT) in the flocculation basins is approximately 30 min at 50 MGD, which is considered acceptable for adequate flocculation. Design criteria associated with the flocculator basins is provided in Table 5.2

Following flocculation, flow is dispersed and sent to sedimentation basins (6 total), each having an HRT of approximately 3.8 hr at 50 MGD. The flocculation basins and sedimentation basins share a common head and are separated by a common wall with approximately 35% void space. Waste sludge is collected in the sedimentation basins using an automated sludge vacuum (Trac Vac) and sent to sludge thickeners where it is chemically conditioned, dewatered with a centrifuge, and disposed of in a sanitary landfill.

Table 5.2 – Flocculator design criteria for SWID

Flocculator Basin Design Criteria				
Dimesions of Each Basin (m)	19.81 W x 4.11 L x 3.96 D			
Total Volume (cubic meters)	322.4 (34,800 ft3)			
Mixer Type	Horizontal Turbine-Type			
Drive Type	Variable Speed			
Motor Size (hp)	7.5, 3.0, 2.0			
Detention Time per Basin at 47,500 m3/d (12.5 MGD) (min)	10			
Total Detention Time at 47,500 m3/d (12.5 MGD) (min)	30			
	Stage 1	Stage 2	Stage 3	Total
Typical Operating G-Value (1/sec)	75	50	42	~
Typical Operating GT-Values at 12.5 MGD	45,000	30,000	25,200	100,200

Minor differences exist between the newly constructed rapid mix basin, flocculator basins, and sedimentation basins compared to the original design. Notable differences are the serpentine flow path used in the two (2) newly constructed flocculator basins and the design of the flow dispersions walls separating the final flocculation basin from the sedimentation basin. Figure 5.2 and 5.3 show a representation of the common wall between the flocculator and sedimentation basins for SWID upgraded design (1998) and original design (1946). The open cross-sectional area of the two walls is equivalent however; different flow characteristics are visible through the two walls. The smaller voids in the new design appear to project newly formed floc at a high velocity through the circular openings causing a visible stream of floc in the first 1-2 m of the sedimentation basin. This increases the time required for floc to settle as the first 1-2 m of the sedimentation basin are effectively lost due to high horizontal flow velocities through the circular openings. This phenomenon is not visibly evident in the original

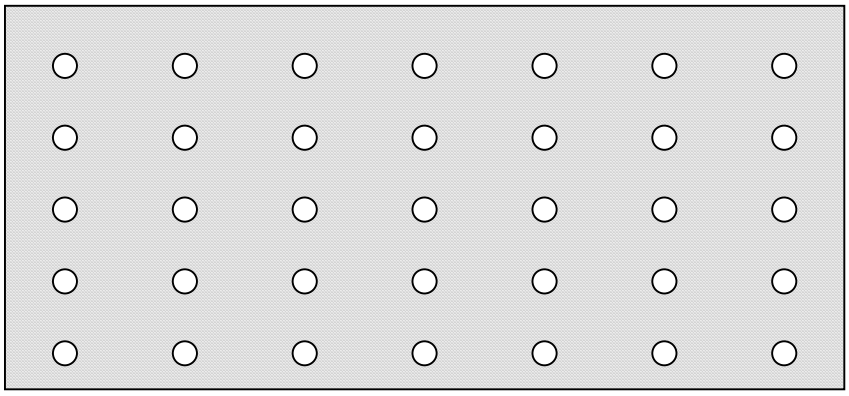

Figure 5.2 – Common wall between third flocculation basin and sedimentation basin (New Design (1998))

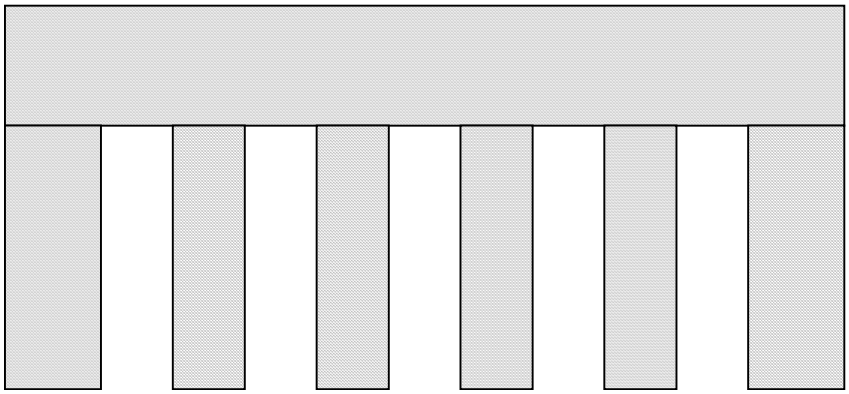

Figure 5.3 – Common wall between third flocculation basin and sedimentation basin (Original Design (1946))

design. The original sedimentation basins also contain a cedar slatted fence spanning the entire width and depth to promote plug flow through the basins. This additional flow dispersion device was determined to be unnecessary in the design of the additional (2) sedimentation basins. Table 5.3 displays the design criteria for SWID sedimentation basins. Chlorine is added to launders located at the end of the sedimentation basins to

Table 5.3 – Design criteria for individual sedimentation basins at SWID.

Sedimentation Basin Design Criteria	
Design Capacity of Basin (m^3/d)	47,500 (12.5 MGD)
Suface Area of Each Basin (m^2)	1,151 (12,395 ft^2)
Length x Width (m)	53.3 x 21.6 (175' x 71')
Average Sidewater Depth (m)	4.57 (15')
Tank Volume (m^3)	5,261(1,390,000 gal)
Detention Time at 47,500 m^3/d (12.5 MGD) (min)	160
Sludge Removal System	Trac Vac
Collection Launder Type	Underflow
Total Launder Length (m)	190.5 (625 ft)

prevent biological growth in the filters. Pre- and post-filter chlorine doses are set based on a 0.5 mg/L Cl_2 required residual both through the filter and at the tap of customers. SWID has ten (10) dual media (sand and anthracite coal) filters, each equipped with a Wheeler filter bottom over an open plenum. The plant is generally operated with the effluent valve set to achieve a flow rate of approximately 100 L/min-m^2 (2.5 gpm/sf). Filtration flow rate is initially set to the specified flow rate and is not adjusted during the filter run 100 hr filtration run (i.e., declining flow filtration). After a 100 hr filtration cycle, the filter is taken out of service and backwashed prior to starting another filtration run. Filtered water is diverted to a clearwell prior to distribution pumping. The clearwell serves to buffer demand variations that would otherwise severely impact filter operation. Additionally, the clearwell serves to increase disinfectant contact time and as finished water storage.

The protocol for monitoring coagulant dose at SWID consists of periodic *jar tests* conducted at a minimum of 1-hr intervals to monitor changes in raw water quality and adjust coagulant dose accordingly to achieve minimum settled turbidity. When a jar test is conducted, coagulant dose is varied until an optimal dose is established based on the criteria of minimizing both settled water turbidity and amount of coagulant required. The settled water in the jar containing the 'optimum' coagulant dose is measured for settled water pH and alkalinity in addition to turbidity. Once the optimal coagulant dose has been established, an additional 10 mg/L of alum is added to provide 'enhanced' coagulation during periods of sufficient raw water alkalinity. If the optimum coagulant dose causes the settled water alkalinity to drop below approximately 4.5 mg/L as $CaCO_3$,

pre-lime addition is used to ensure proper coagulation and maintain adequate buffering capacity throughout the treatment process.

5.1.1.1 – SWID pilot plant

The SWID pilot plant was built to provide a water treatment facility capable of testing alternative treatment options and evaluating process adjustments. The pilot plant is set up with two identical side-by-side treatment trains each scaled down from the original SWID plant dimensions. Each train is capable of processing 94,500 L/day (24,964 gal/day), approximately 0.05 % SWID capacity. Pre-treatment may be accomplished through the use of two plug-flow (PF) reactors located ahead of the rapid mix basins, providing an additional 30 min of retention time at 65 L/min (≅18 gpm). The approximate HRTs for the rapid-mix basin, flocculator, and sedimentation basin are 20 sec, 30 min, and 4 hr, respectively, at 56 L/min (14.79 gpm). Filtration is accomplished through the use of dual media (sand and anthracite coal) filters operated under declining flow (i.e., initial flow rate is set and allowed to decline throughout a filter run). Critical pilot plant dimensions are listed in Table 5.4. Rapid mix and flocculator G-values are similar to those exhibited in the production scale facility and may be adjusted using variable speed drives to simulate a variety of mixing scenarios.

Table 5.4 – SWID pilot plant dimensions

Pilot Plant Dimensions			
Flowrate (L/min)	53 – 68 (14 gpm - 18 gpm)		
Rapid Mix Basins	Stage 1	Stage 2	Stage 3
Volume (ft^3)	0.428	0.428	0.428
Volume (m^3)	0.01	0.01	0.01
Flocculators	Stage 1	Stage 2	Stage 3
Volume (ft^3)	29.3	29.3	29.3
Volume (m^3)	0.83	0.83	0.83
Sedimentation Basin			
Total Volume (m^3)	10.35 (366 ft^3)		

5.1.2– Historical Watershed Data

The watershed for SWID is affected by significant tidal variation due to its close physical proximity to the Savannah River delta. The location of SWID leads to large variations in raw water quality, observed daily as changes in raw water turbidity, alkalinity, color, and pH. During high tide, saltwater flows up gradient in the Savannah River, which leads to higher water levels in the creeks surrounding, and interior to, the SWID watershed. During low tide, water is flushed from the surrounding vegetation and brought downstream to Savannah Waterworks, the raw water pump station for SWID. During low tide, SWID raw water generally exhibits increased TOC concentration and color, compared to that experienced during high tide. This may be attributed to the high level of natural organics flushed from surrounding bogs and swamps during low tide. This same effect may also be seen during periods of heavy rain or changes in flow conditions due to runoff amendments upriver.

Figure 5.4 displays the sampling locations used to monitor watershed parameters in this study of raw-water properties and characteristics. Locations were chosen to encompass the SWID watershed and incorporate major influent flows into the region. The SWID pump station (site 1) is located down gradient of all other sites. Sites 3, 4, and 5 were chosen due to their location and proximity to the town of Rincon, GA. Rincon is located approximately 2 miles directly west of sites 3 and 4 and collectively represent the main points of entry into the western and northwestern side of the SWID watershed. Site 6 is located directly on the Savannah River just north of the intersection of Mill Creek and the Savannah River. This site incorporates any upstream influences in the northern Savannah River watershed. Sites 2 and 7 are located on the interior of the SWID watershed and subject to any interior influence present between Abercorn Creek, Mill Creek, and the Savannah River. The region outlined by the Savannah River and sites 1, 3, 4, and 5 is protected by the federal government and serves as a natural preserve. The area is heavily wooded with dense undergrowth which explains the high levels of organic concentration in runoff observed during heavy rainfall.

Figures 5.5, 5.6, 5.7, and 5.8 display pH, alkalinity, color, and turbidity measured at each location throughout the year, respectively. Sampling dates were selected to incorporate seasonal variations in water quality parameters and were tested on days without rainfall throughout 2003 and early 2004 calendar years. pH values were consistently lowest at sites 4 and 5. Low alkalinity detected at sites 4 and 5 correspond to the low pH values observed. Site 3 displayed relatively high alkalinity when compared to other sampling sites. Color appeared to be highest where alkalinity and pH were lowest, with the exception of site 3. High levels of decaying plant matter observed at these

locations suggest increased concentrations of humic and fulvic acid, accounting for pH and alkalinity effects. Turbidity varied both seasonally and regionally displaying no observable trends at individual sites or between sites.

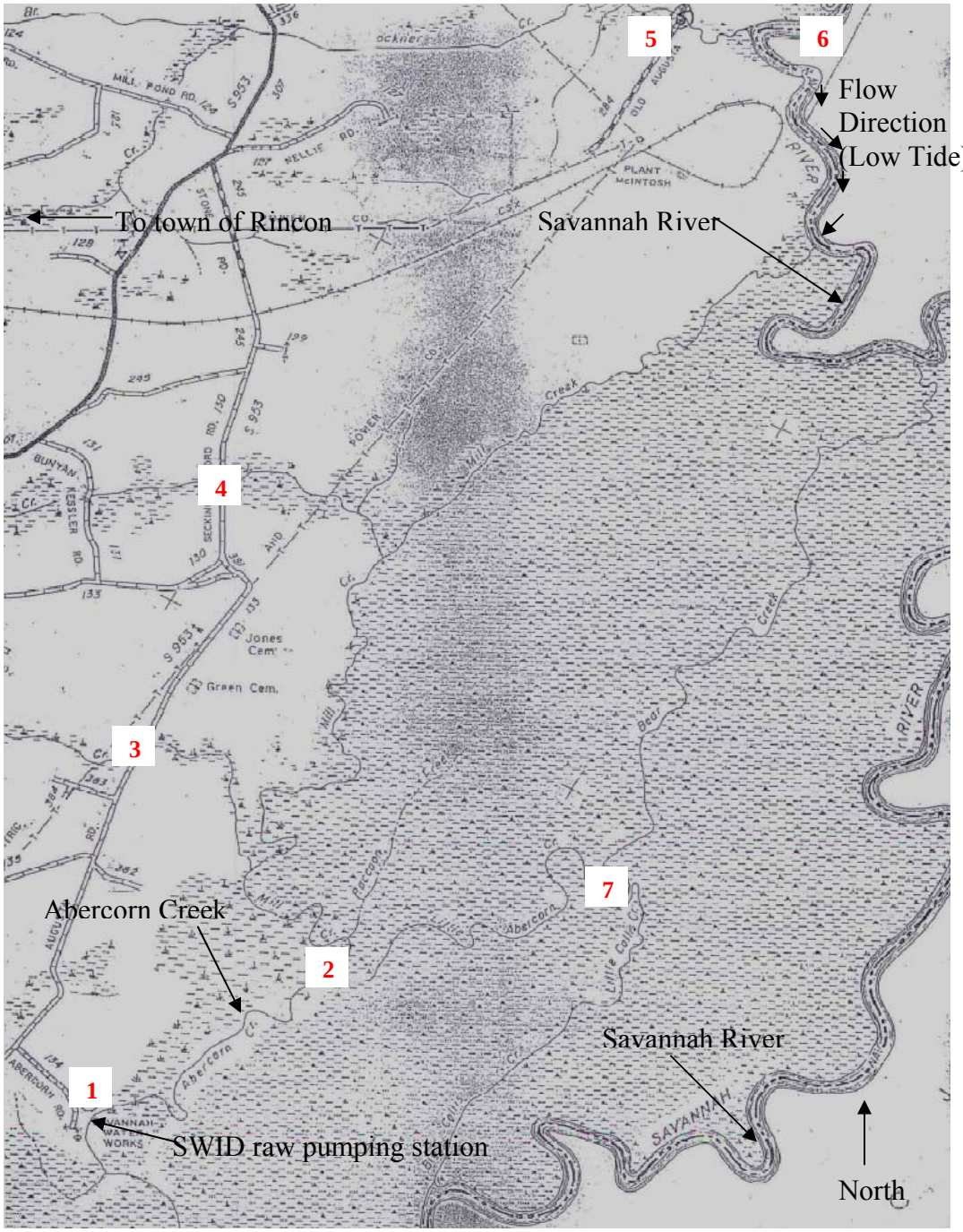

Figure 5.4 - SWID watershed and sampling locations. Savannah Waterworks pump station (site 1). Interior watershed sampling sites with limited accessibility (sites 2 & 7). Sampling sites located at major influent creeks (sites 3, 4, and 5). Sampling site on the Savannah river up-gradient of Savannah Waterworks (site 6).

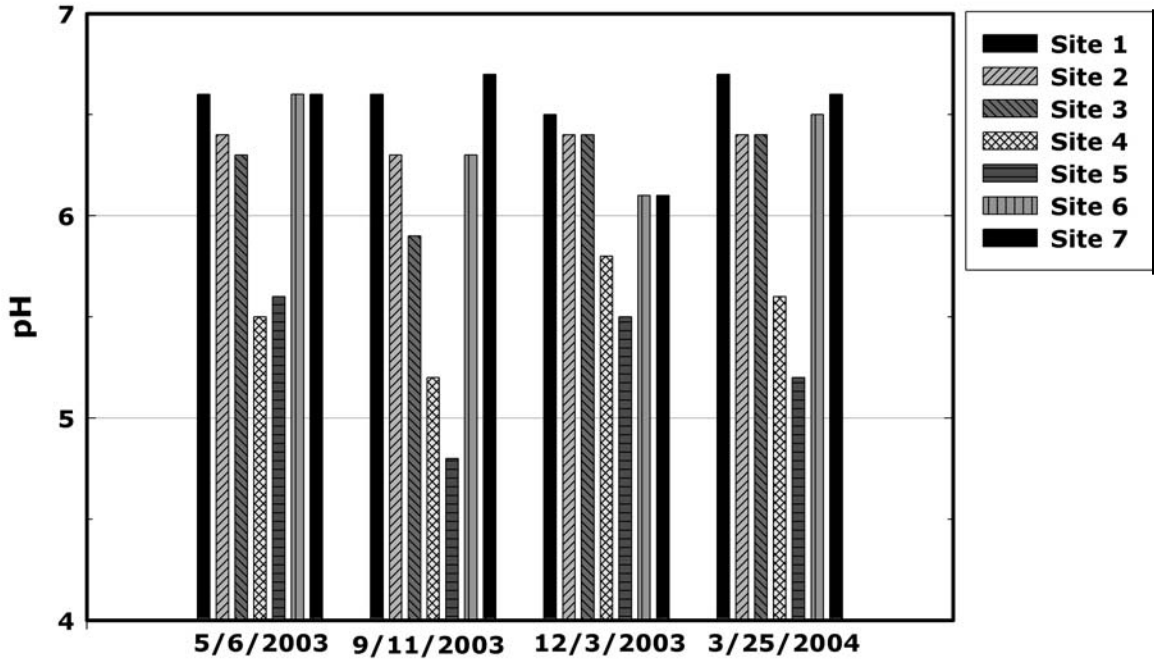

Figure 5.5– Variation of pH observed at each sampling location

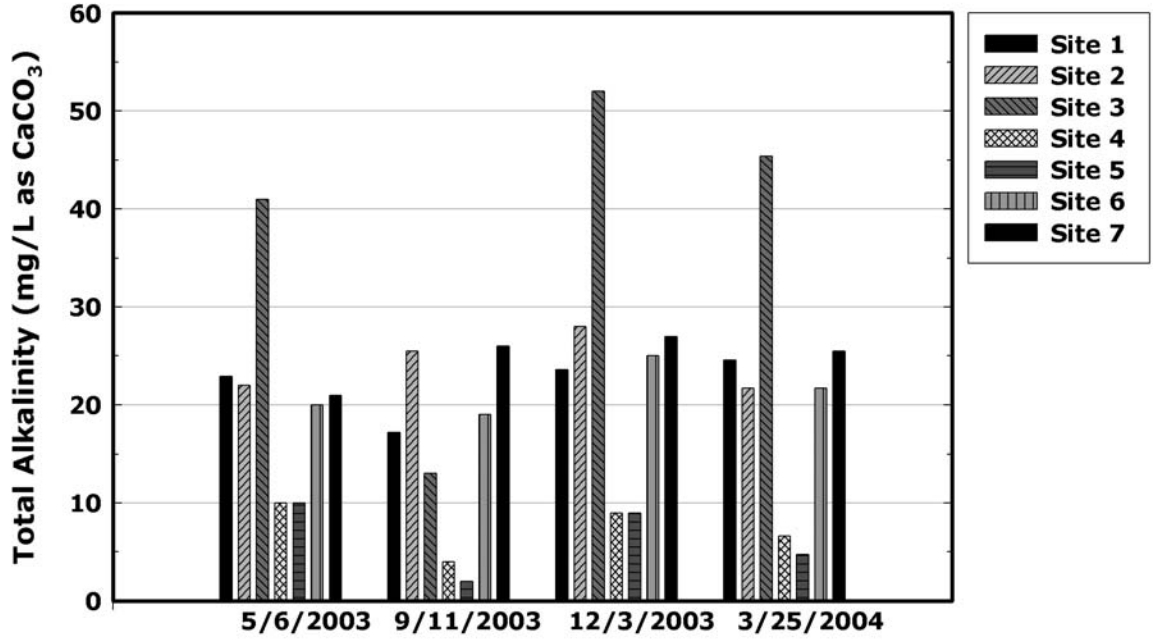

Figure 5.6 – Variation of alkalinity observed at each sampling location

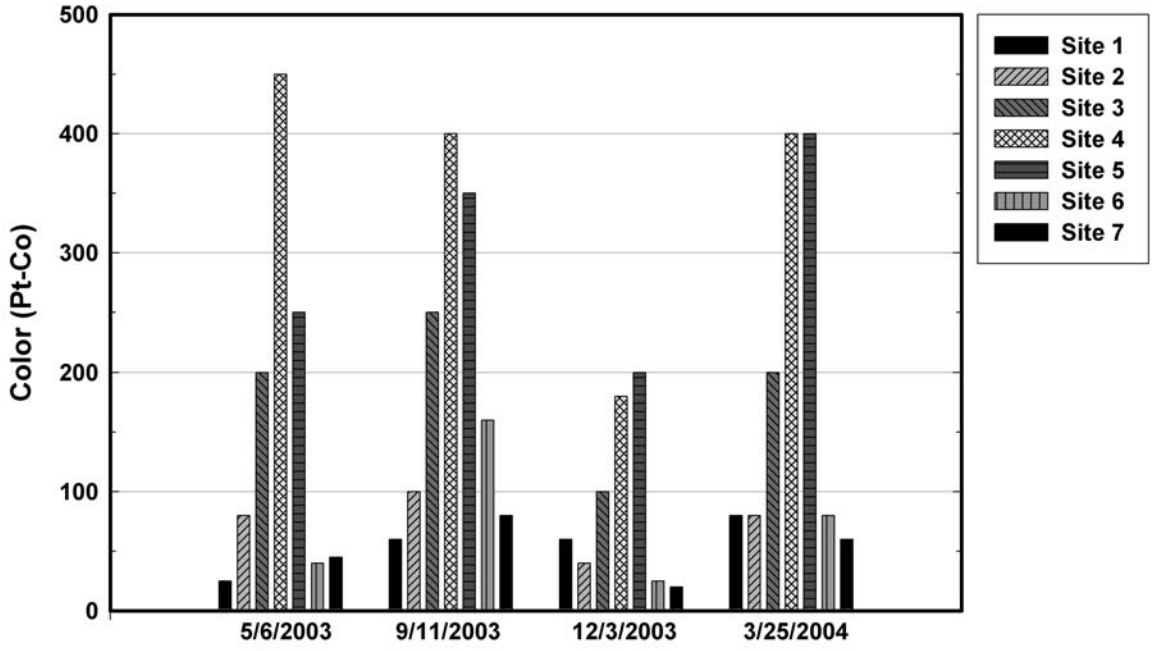

Figure 5.7 – Variation of color observed at each sampling location

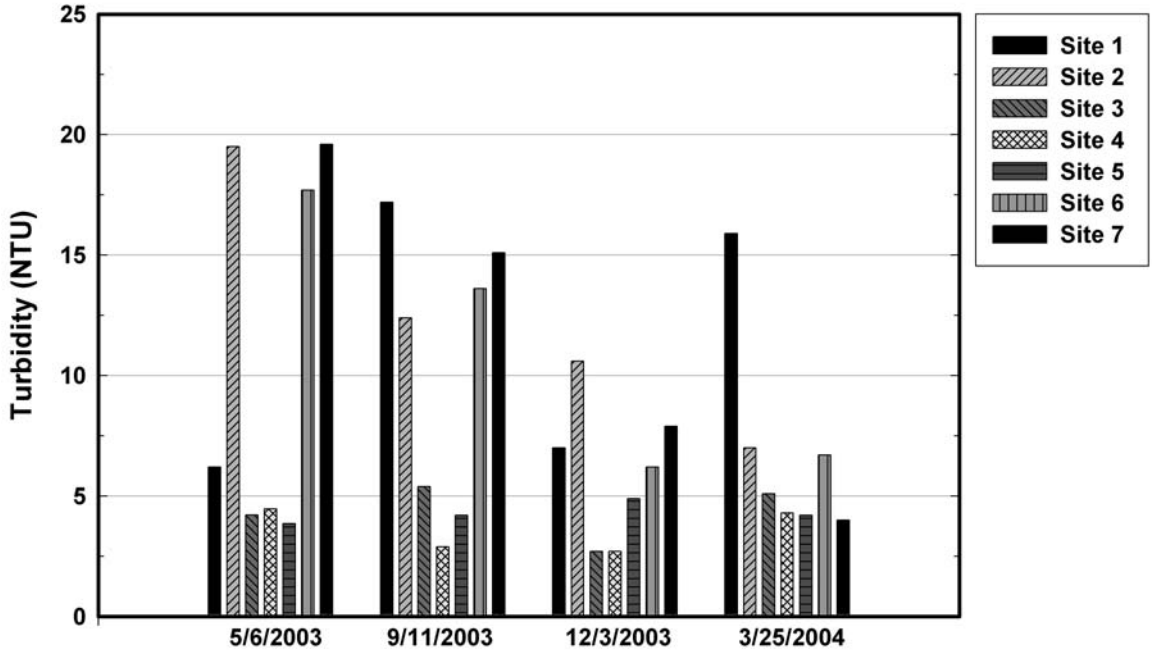

Figure 5.8 – Variation of turbidity observed at each sampling location

5.1.3 – Watershed Assessment

A watershed assessment was conducted to determine the relation between dissolved organic carbon (DOC) and ultraviolet absorbance at 254 nm (UV_{254}). Previous studies have demonstrated a positive linear relationship between DOC and UV_{254}, however some waters have not shown this correlation (Symons et al. 1975). Excellent correlations have also been established between DOC and trihalomethane formation potential (THM-FP), although water sources tend to vary in specific THM yield, as determined by characteristics of an individual watershed (Reckhow and Singer 1990).

The specific ultraviolet absorbance (SUVA) can be a useful indicator of NOM character and composition. SUVA is defined as the normalized UV absorbance of a given sample determined at 254 nm and divided by the DOC concentration of the solution. A study conducted on the nature and composition of NOM (Edzwald and Tobiason 1999) has shown a good correlation between the nature of organic material and the SUVA absorbance. Table 5.5 summarizes the findings of their study.

Table 5.5 – Guidelines for the nature of NOM and observed DOC removal by coagulation with aluminum and iron based salts (Edzwald and Tobiason 1999).

SUVA (L/mg-M)	Composition	Coagulation	DOC Removal
> 4	Mostly aquatic humics. High MW, high hydrophobicity	NOM Controls Good DOC removal	>50% for Alum >50% for Ferric
2-4	Mixture of aquatic humics and other NOM. Both hydrophilic and hydrophobic organics	NOM influences. DOC removal OK	25 – 50% for Alum. Slightly more for Ferric
< 2	Mostly non-humics. Low MW, low hydrophobicity	NOM has little influence. Little DOC removed	<25% for Alum. Slightly more for Ferric

Water samples were collected from locations throughout the local SWID watershed at five sites. These sites were selected based on accessibility and potential influence on SWID raw water quality. The location of each site in relation to the watershed for SWID has been provided in Figure 5.4. Sites 3, 4, and 5 encompass the southwestern side of the SWID watershed. Site 6 is located on the Savannah River upriver of sites 2 and 7. Samples from this site are assumed to incorporate any upstream influence that may be observed in the interior of the watershed, observable at sites 2 and 7. Samples from sites 2 and 7 were not included in this study.

Grab samples of SWID watershed water from sites 3, 4, 5, and 6 were collected on a falling tide in an effort to observe the nature of the TOC contributed to the raw water from each of these sites. The samples were taken during a period after 5 consecutive days without rainfall to ensure that any organics present were a function of natural tidal cycles without the influence of additional organics contributed by rainfall runoff. Savannah River stage data from Port Wentworth, located approximately 14.5 kilometers (≅ 9 miles) downstream of site 1, were used to determine the proper sampling time. The sampling time with respect to river stage can be seen in Figure 5.9. A raw water sample was taken at SWID 4 hrs after samples 3, 4, 5, and 6 were collected. This was done to ensure the sample obtained was as close as possible to the raw water observed at SWID by accounting for the HRT between the pump station on Abercorn Creek and SWID, i.e., approximately 4 hr.

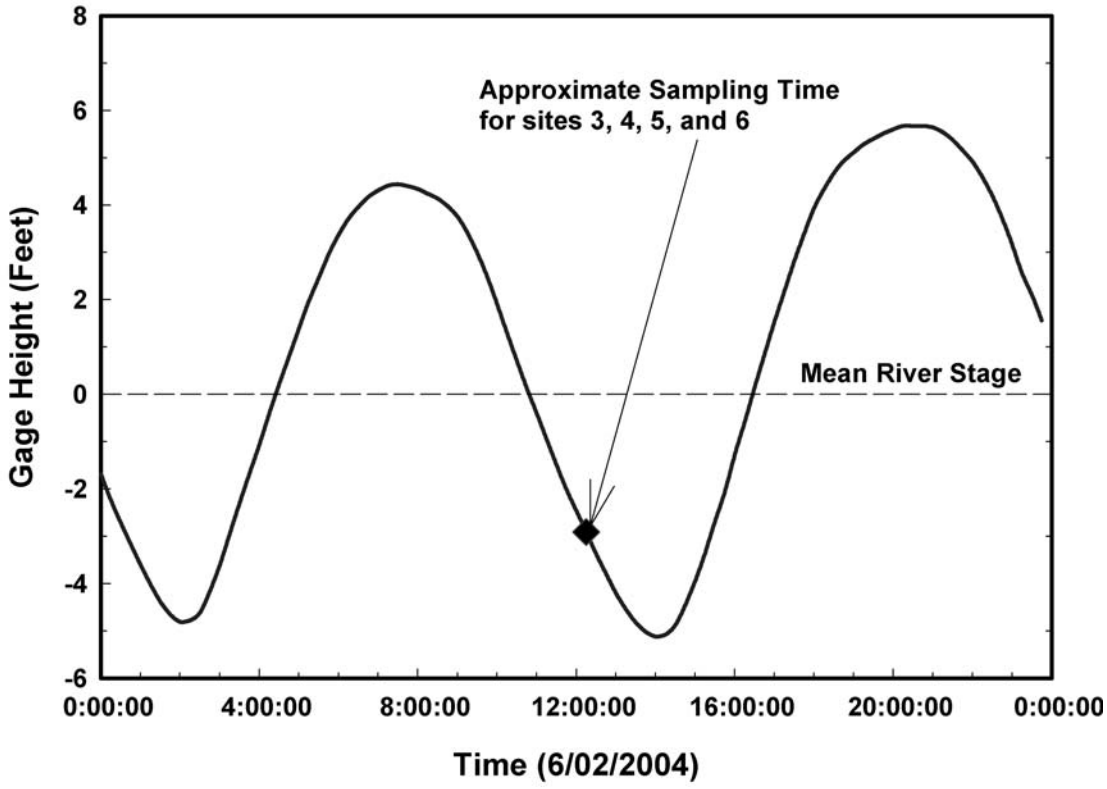

Figure 5.9 – Approximate sampling time in relation to Savannah river stage data from Port Wentworth (USGS 2004)

Samples were filtered with a 0.45-μm Teflon filter and analyzed for initial values of DOC, UV_{254} absorbance, and specific UV absorbance (SUVA) calculated using EPA method 415.3 (Standard Methods 2003). UVA of the sample, normalized to the cell path length, in cm^{-1} is divided by the DOC of the sample, multiplied by 100 cm/m and either reported in units of L/mg-M or as "SUVA". The SUVA is calculated as follows:

$$SUVA\ (L/mg\text{-}M) = UVA(cm^{-1}) / DOC\ (mg/L) * 100\ cm/m$$

UVA Calculation: UVA = A /b

where: UVA = Calculated UV absorbance of the sample in absorbance units (cm^{-1}).

A = Measured UV absorbance at 254 nm of the sample that is filtered through a 0.45-µm filter media (dimensionless).

b = Quartz cell path length in cm.

Initial DOC, UV_{254} absorbance values, and average SUVA values are listed in Table 5.6. The SUVA data indicate that NOM from sites 1, 3, 4, and 5 is of the same general character (Edzwald and Tobiason 1999) and composed of high molecular weight hydrophobic aquatic humic substances. SUVA data from site 6 indicate that NOM may be composed of slightly less hydrophobic, lower MW compounds. This is to be expected as sample site 6 is located on a large section of the Savannah River compared to all other sampling sites, which are located on relatively small tributaries where a large amount of decaying plant matter exists. The samples from each site were subjected to serial dilutions whereupon the UV_{254} absorbance (UVA) and DOC concentrations were measured after each dilution. DOC was measured after samples from each site were processed using a pre-rinsed glass fiber filter rated at 0.45-µm.

Table 5.6 – Initial DOC, UV_{254}, and SUVA measurements for sites surveyed in SWID watershed assessment

Site #	DOC (mg/L)	UV_{254} (cm^{-1})	SUVA (L/mg-M)
1	2.14	0.133	6.98
3	12.92	0.716	5.57
4	17.73	1.163	6.45
5	15.01	.971	6.27
6	2.09	0.119	3.87

The separation was used to define the dissolved portion of organic carbon from the suspended (particulate) portion. It is recognized that the filtrate is only an operational

definition of DOC and relevant size data related to the separation may not be considered reliable. The resulting linear relation between DOC and UVA from the five sites surveyed is demonstrated in Figure 5.10. These data suggest that despite significant changes in DOC concentration measured at each site, the nature and composition of NOM based on SUVA is similar, leading to a characteristic NOM present in the raw water for SWID.

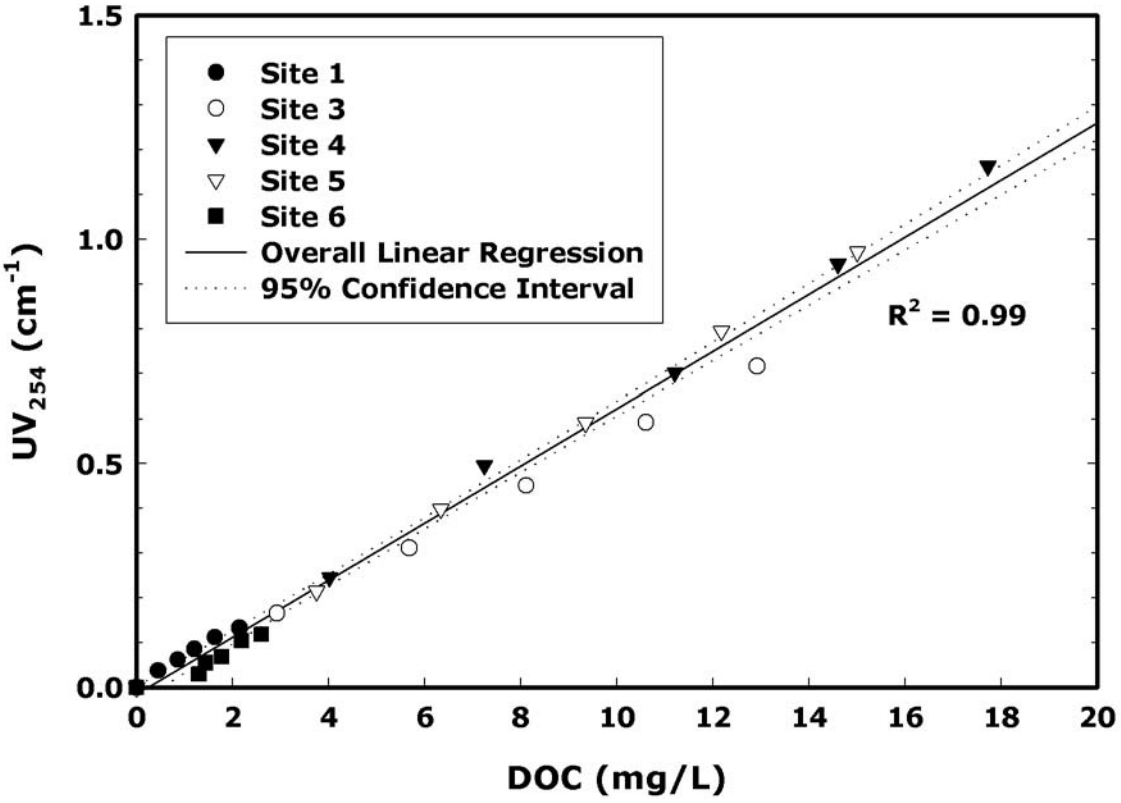

Figure 5.10 – UV_{254} absorbance versus DOC for serial dilutions of SWID watershed samples

5.1.4 - Watershed Runoff Effects

Raw water samples were collected from sites 3, 4, 5, and 6 during a period of heavy rainfall to observe any measurable changes in SWID raw water characteristics affected by runoff. Table 5.7 shows the average daily rainfall recorded at Port Wentworth on the days prior to, and during, the time when samples were captured for the specified sampling dates (USGS, 2004).

In an effort to observe the influence of organic matter present at sites 3, 4, 5, and 6 on raw water during a period of heavy rainfall, samples were again captured on a falling tide. The raw water characteristics observed at each site are listed in Table 5.8

Table 5.7 – Average daily total rainfall at Port Wentworth (USGS).

Date	Total Daily Rainfall (Inches)
6/10/2004	0.01
6/11/2004	0
6/12/2004	0
6/13/2004	2.49
***6/14/2004**	1.63

* Grab samples from SWID watershed sampling locations were secured 3:00 – 4:00 P.M. on 6/14/2004

Table 5.8 – Measured parameters at sites 1 and 3-6 on 28 May 2004 after a 5-day period of no rainfall

Parameter Measured	Site 1	Site 3	Site 4	Site 5	Site 6
pH	6.72	6.44	6.43	5.61	5.52
Alkalinity	19.6	45.4	6.62	4.73	19.7
DOC	1.63	10.61	14.6	12.17	2.18
UV_{254}	0.112	0.592	0.944	0.795	0.104

*DOC was measured as carbonaceous organic material present after 0.45 – µm glass fiber filtration. Alkalinity (mg/L as $CaCO_3$), DOC (mg C/L), and UV_{254} (cm^{-1})

and Table 5.9 for a period of no rainfall (NR), and for a period of heavy rainfall (HR). HR pH at each site was consistently lower than the observed pH for the NR period. Raw water alkalinity was also lower during heavy rainfall when compared to a period of no rain. Elevated DOC concentration and UVA values during heavy rainfall may be attributed to increased organic loading due to storm water runoff.

Samples were analyzed for SUVA and compared with values observed during the NR period. These results are displayed in Table 5.10. Site 6 demonstrated the most significant change in SUVA concentration. This change suggests the general composition of NOM present during HR shifts to slightly higher MW aquatic humics, however this change is only represented as a function of SUVA variation

Table 5.9 – Measured parameters at sites 1 and 3-6 on 14 June 2004 during heavy rainfall

Parameter Measured	Site 1	Site 3	Site 4	Site 5	Site 6
pH	6.48	5.84	5.58	5.41	5.20
Alkalinity	15.0	6.7	6.0	6.5	14.0
DOC	6.82	14.27	15.82	12.03	8.24
UV_{254}	0.370	0.793	0.824	0.617	0.407

*DOC was measured as carbonaceous organic material present after 0.45 – µm glass fiber filtration. Alkalinity (mg/L as $CaCO_3$), DOC (mg C/L), and UV_{254} (cm^{-1})

Table 5.10 – SUVA comparison for periods of heavy rainfall and no rainfall at sites 1, 3, 4, 5, and 6.

	SUVA (L/mg-M)				
	Site 1	Site 3	Site 4	Site 5	Site 6
No Rainfall	6.98	5.57	6.45	6.27	3.87
Heavy Rainfall	5.43	5.56	5.21	5.13	4.94

(Edzwald and Tobiason 1999). Figure 5.11 demonstrates the relation between DOC and UV_{254} absorbance exhibited during HR. These data reveal no significant deviation from the linear relation observed between DOC and UVA during the NR period indicating that NOM was similar in both cases even though there was considerable variation in DOC concentrations observed during the two periods.

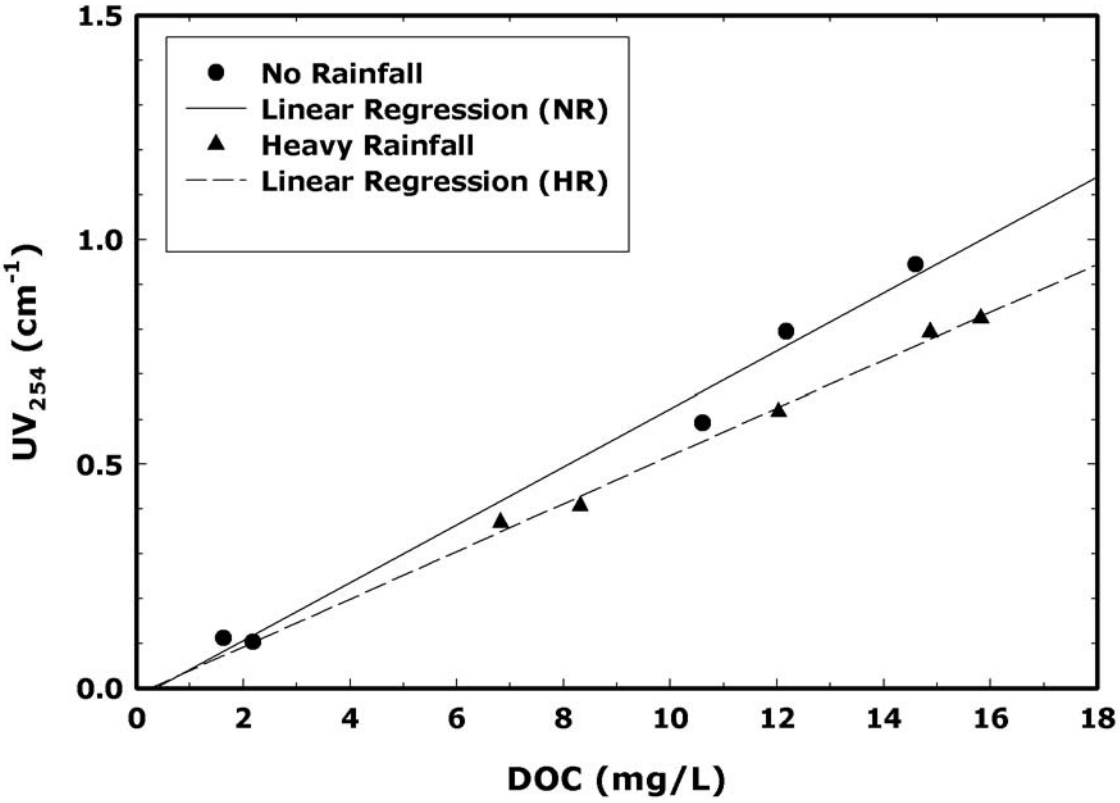

Figure 5.11 – UV_{254}/DOC relationship for periods of heavy and no rainfall demonstrating strong linear correlation between monitoring sites.

Section 5.1.5 – Water treatment

SWID raw water turbidity, alkalinity, and pH were monitored over the time period when samples were taken for periods of no rain (NR) and heavy rainfall (HR) from early morning to early evening. In addition, alum dose was recorded to demonstrate the impact of water quality on chemical consumption with respect to rainfall and tidal variation. A direct comparison of pH, alkalinity, turbidity, and alum dose between NR and HR periods is shown in Figures 5.12 through 5.15. The pH range of HR samples is slightly lower ($6.05 < pH < 6.62$) than the pH observed during NR ($6.43 < pH < 6.78$). This is to be expected considering the average pH of rainwater in Georgia is mildly acidic, generally somewhere between

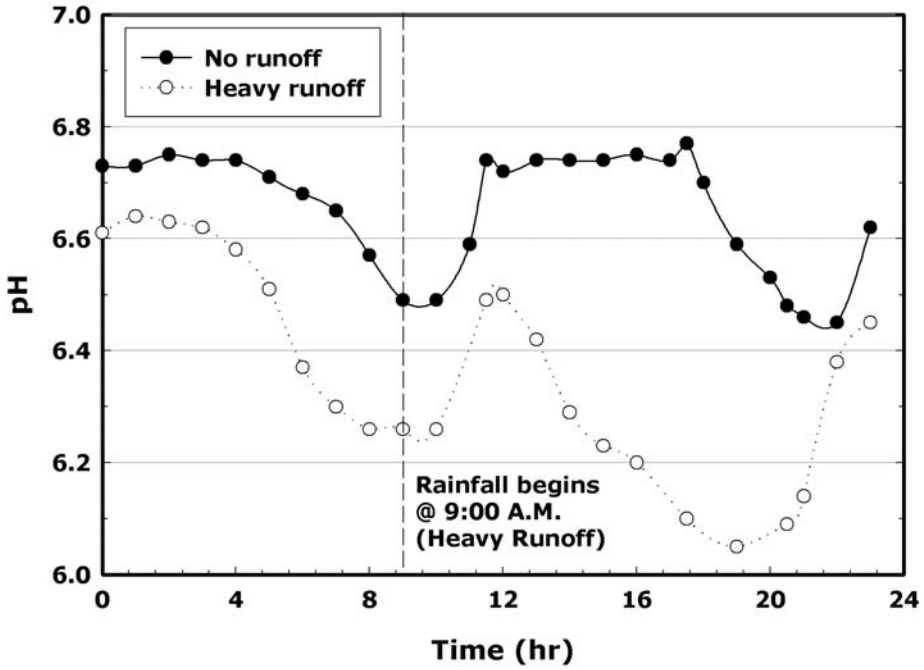

Figure 5.12 - Comparison of raw water pH during HR (14 June 2004) and NR (28 May 2004) periods

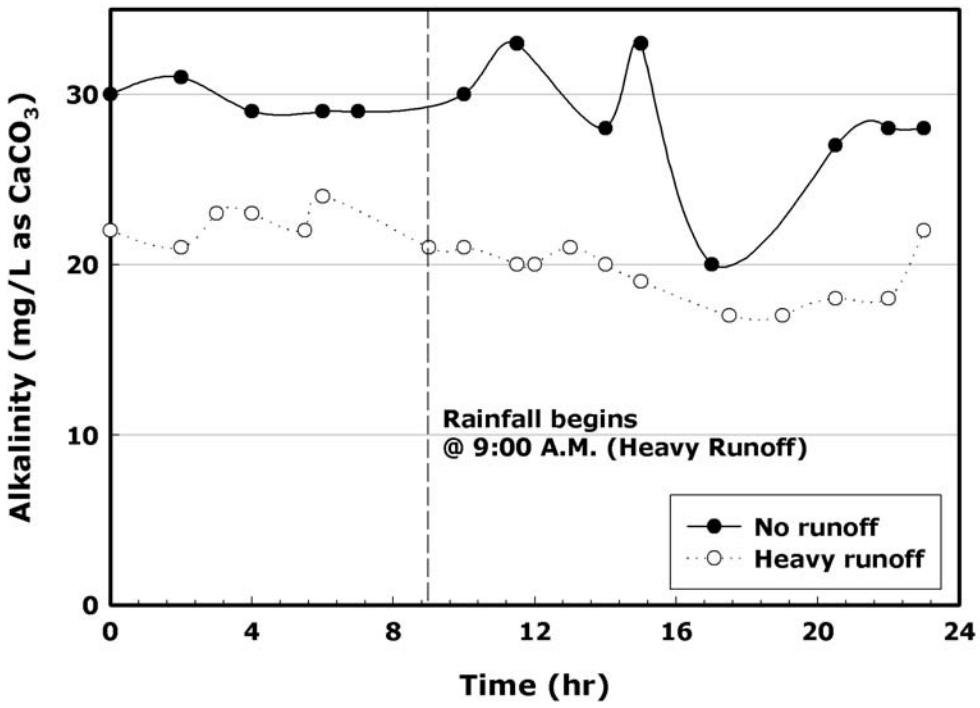

Figure 5.13 - Comparison of raw water alkalinity during during HR (14 June 2004) and NR (28 May 2004) periods

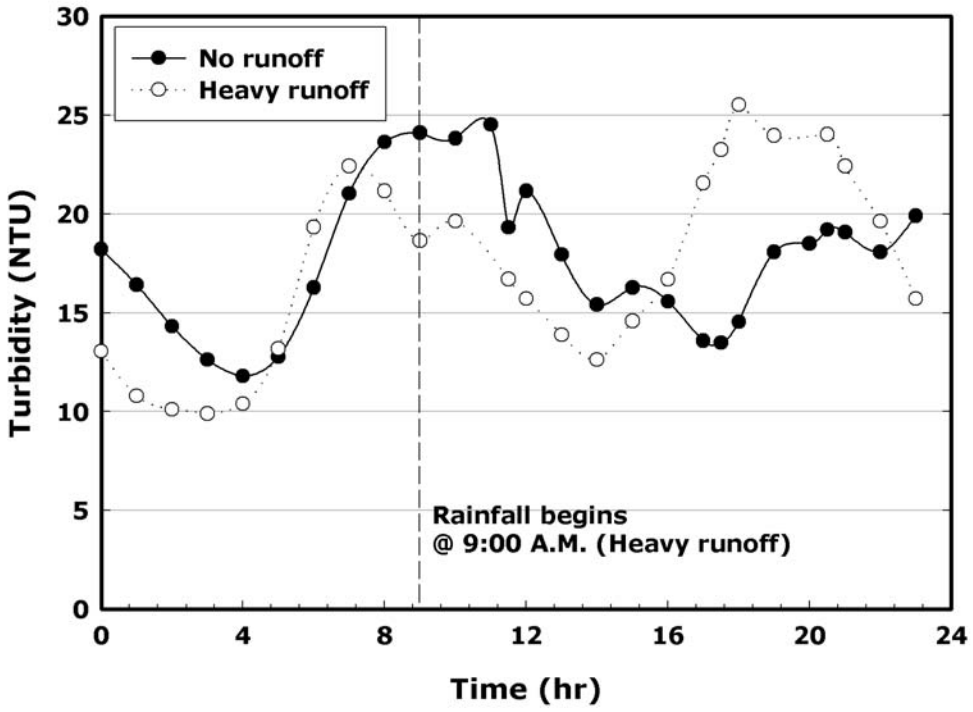

Figure 5.14 - Comparison of raw water turbidity during HR (14 June 2004) and NR (28 May 2004) periods

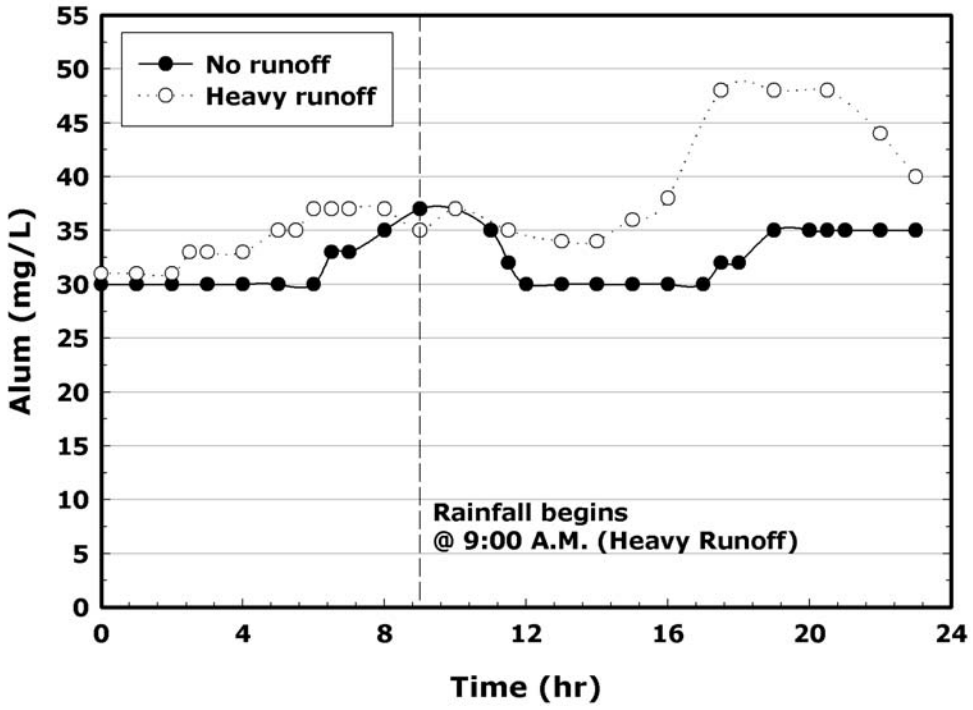

Figure 5.15 - Comparison of alum feed during HR (14 June 2004) and NR (28 May 2004) periods

pH=5-6.5. HR alkalinity values were generally less than values associated with the equivalent NR period. Low levels of alkalinity corresponded directly with low pH values observed during the HR period. Turbidity levels in NR and HR water correlated very well prior to observed rainfall during the HR period. Turbidity observed during HR reaches a second peak approximately 4 hrs after rainfall begins. The 4 hr lapse may be attributed to the raw water HRT between Savannah Water Works (SWID pump station) and SWID treatment plant. These data suggest that rainfall within the SWID watershed increases the turbidity of raw water observed at SWID. Alum feed increased by approximately 15 mg/L (1.35 mg Al^{3+}/L) during the HR period. This is directly attributed to the increased turbidity observed during the HR period and the method employed by SWID to determine the level of coagulant addition, which relies on minimizing the settled water turbidity. In general, an increased level of alum is required to destabilize additional particles associated with increased turbidity (HR period). In some cases where low alkalinity exists with high turbidity, treatment becomes difficult due to insufficient alkalinity for the complete hydrolysis of alum. During these time periods, pre-lime addition is used to improve coagulant efficacy.

5.1.6 – SWID summary

Preliminary watershed studies and historical plant data reveal trends in water treatment practices at SWID. Immediate observations show a strong correlation between SWID raw water quality and diurnal river stage fluctuations. SWID raw water associated with high tide generally requires less coagulant and exhibits higher alkalinity when compared to slightly more turbid low tide water.

A watershed assessment of DOC concentration with respect to SUVA revealed no significant changes in associated character of NOM between NR and HR periods. These data suggest that changes in DOC concentration associated with rainfall and tidal variation in the SWID watershed do not result in significant changes to the overall character and composition of NOM with respect to SUVA. SWID NOM appears to contain mostly hydrophobic aquatic humics of high molecular weight based on SUVA data (Edzwald and Tobiason 1999).

Preliminary findings demonstrate the overall impact of rain and tidal variation on raw water quality. The general composition and character of NOM present in the SWID watershed does not appear to vary drastically with respect to either of these variables. Further analysis of NOM removal by conventional coagulation may provide beneficial insight into proper treatment techniques for maximizing NOM removal prior to chlorination.

5.2 – Analysis of bulk NOM

Currently, SWID uses conventional jar testing to define coagulant (alum) dose in the treatment process. Alum dose and pH at SWID were recorded during three months selected from the 2003 calendar year (February, April, and November) to incorporate seasonal effects into coagulation behavior. The results from this analysis are presented on a pC/pH diagram for aluminum in Figure 5.16. Dashed lines represent the solubility of hydrated aluminum species (Amirtharajah 1982). The figure shows pH on the x-axis, log concentration of Al^{3+} ions on the left y-axis, and log concentration of alum on the right y-axis. The numbered regions in the figure represent results used by Amirthrajah

(1982) to describe regions where destabilization mechanisms dominate the coagulation process. In general, this figure shows the very specific areas where coagulation would occur and also the major mechanism causing coagulation. Minor changes should only be expected on the restabilization zone, which will change with the type of colloid, according to Amirtharajah and Mills (1982). Historical jar test data from SWID show that the plant operates predominately in the sweep coagulation zone with some degree of adsorption destabilization. A description of the various coagulation mechanisms has been provided in section 2.4.2.

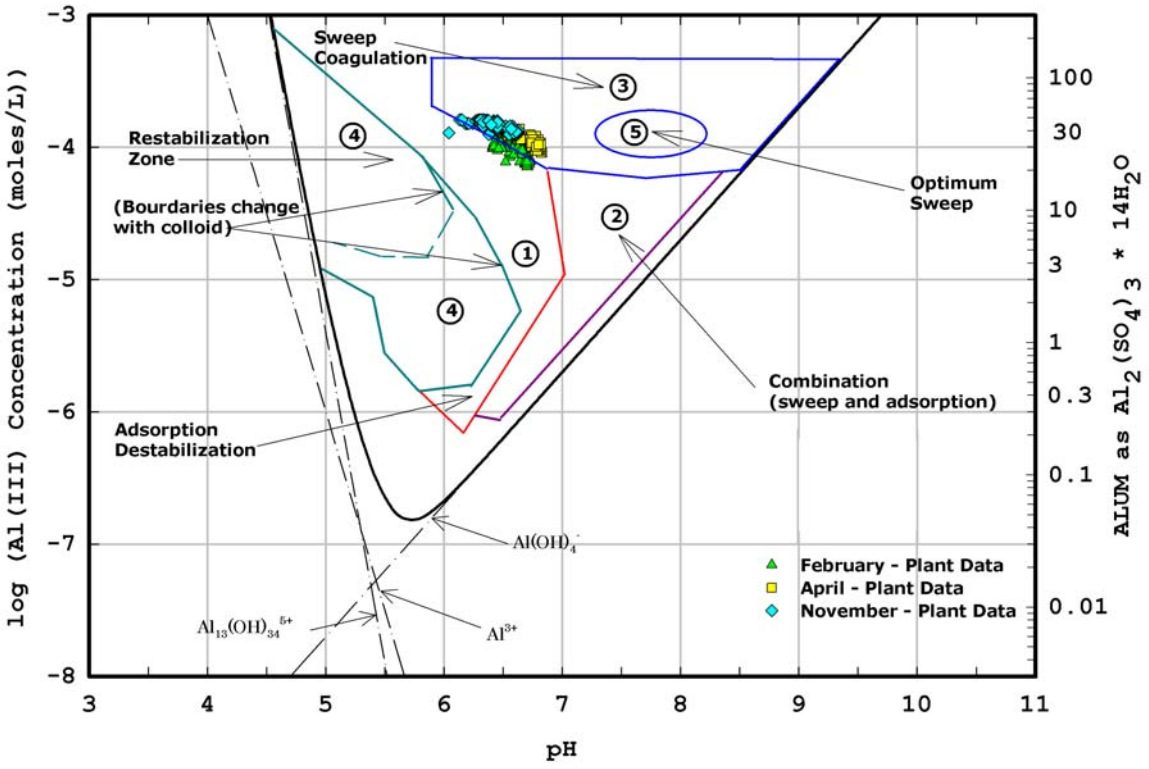

Figure 5.16 – Design and operation diagram for alum coagulation showing SWID jar test data in relation to predominate coagulation mechanisms as described by (Amirtharajah and Mills 1982). Zone 1 – Adsorption/Destabilization, zone 2 – Combination of sweep floc and adsorption, zone 3 – Sweep floc, zone 4 – Restabilization zone, and zone 5 – optimum sweep floc.

5.2.1 – Preliminary Jar Testing

Currently, SWID does not adjust rapid-mix pH during the coagulation process for optimizing DOC removal. As a part of this research project, a study was conducted to determine color and turbidity removal with respect to coagulant dose, coagulation pH, and coagulant type (alum and ferric sulfate). Studies were conducted using the jar test method described in section 4.3. Initial parameters describing the raw water quality observed throughout preliminary jar test experiments are listed in Table 5.11. A pH range of 4 to 9 was used with coagulant doses ranging from 3.0 to 75 mg/L (as alum). pH was adjusted to the desired value with 0.2 M HCL or filtered, saturated solution, of $Ca(OH)_2$ prior to coagulant addition. The decrease in pH due to the required coagulant addition was determined prior to analysis and incorporated into the required acid or base addition. Therefore, any subsequent pH value represents the instantaneous coagulation pH incorporating the additional acidity attributed to the coagulant itself.

Settled water was analyzed for percent removal of color and turbidity based on initial raw water values. Results from these experiments are displayed in Figure 5.17 and Figure 5.18 for color removal and turbidity removal, respectively. The two graphs are very similar with respect to optimum pH for maximum coagulation efficacy, which occurs around pH = 5.5 and an alum dose near 20 mg/L. The data in Figure 5.16 suggest that SWID currently operates in a sub-optimal region with respect to color and turbidity removal. These data reveal that the optimum pH and minimum alum dose for greater than 60 percent color removal and 90 percent turbidity removal occurs very near the restabilization boundary with adsorption / destabilization as the main coagulation

Table 5.11 – Initial raw water range of SWID raw water parameters

	Initial Values		
	Min	Max	Units
pH	6.35	6.75	~
Temperature	23.4	25.3	°C
Turbidity	7	12	NTU
TOC	3.35	5.4	mg/L
Color	17	26	Pt-Co
Nitrate-N	0.52	0.72	mg/L
Sulfate	13.89	14.26	mg/L
Iron	0.499	0.508	mg/L
Manganese	0.033	0.034	mg/L
Phosphate	0.252	0.545	mg/L
Aluminum Res.	0.019	0.049	mg/L

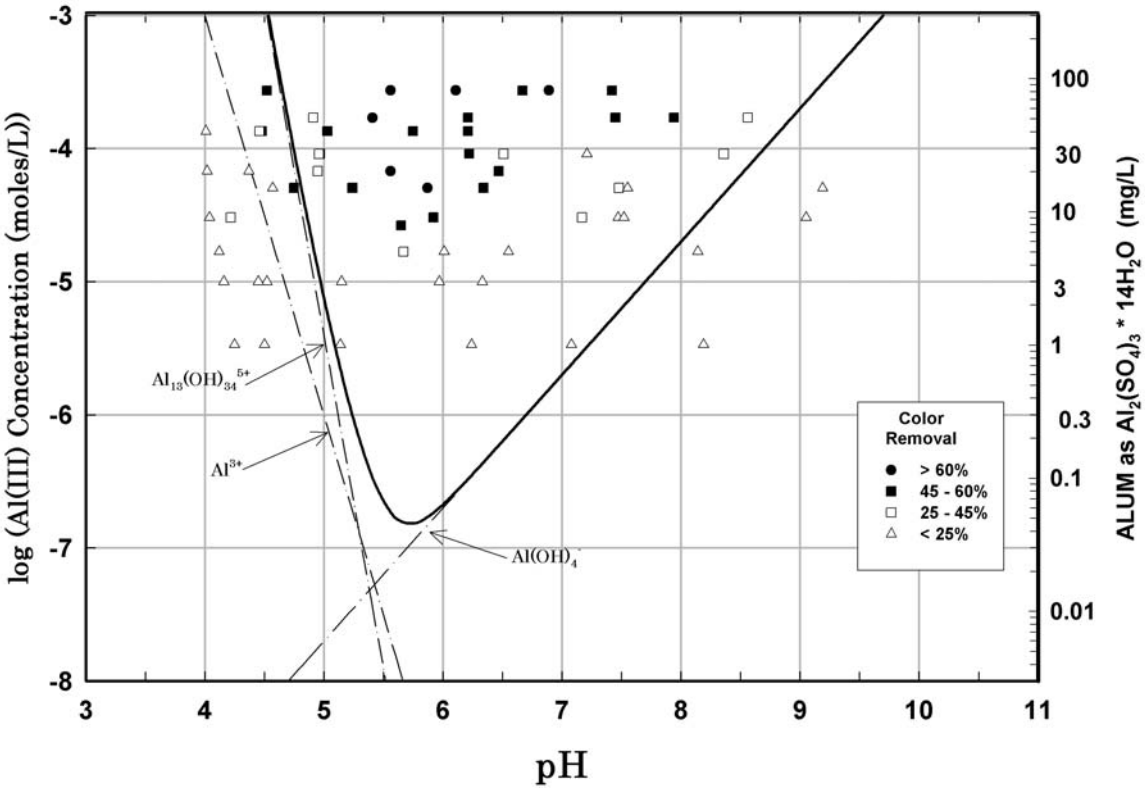

Figure 5.17 – Residual color concentration after jar mixing, flocculation, settling, and 0.45 – μm filtration as a function of pH and alum dose. Original color = 17 ADMI – 26 ADMI

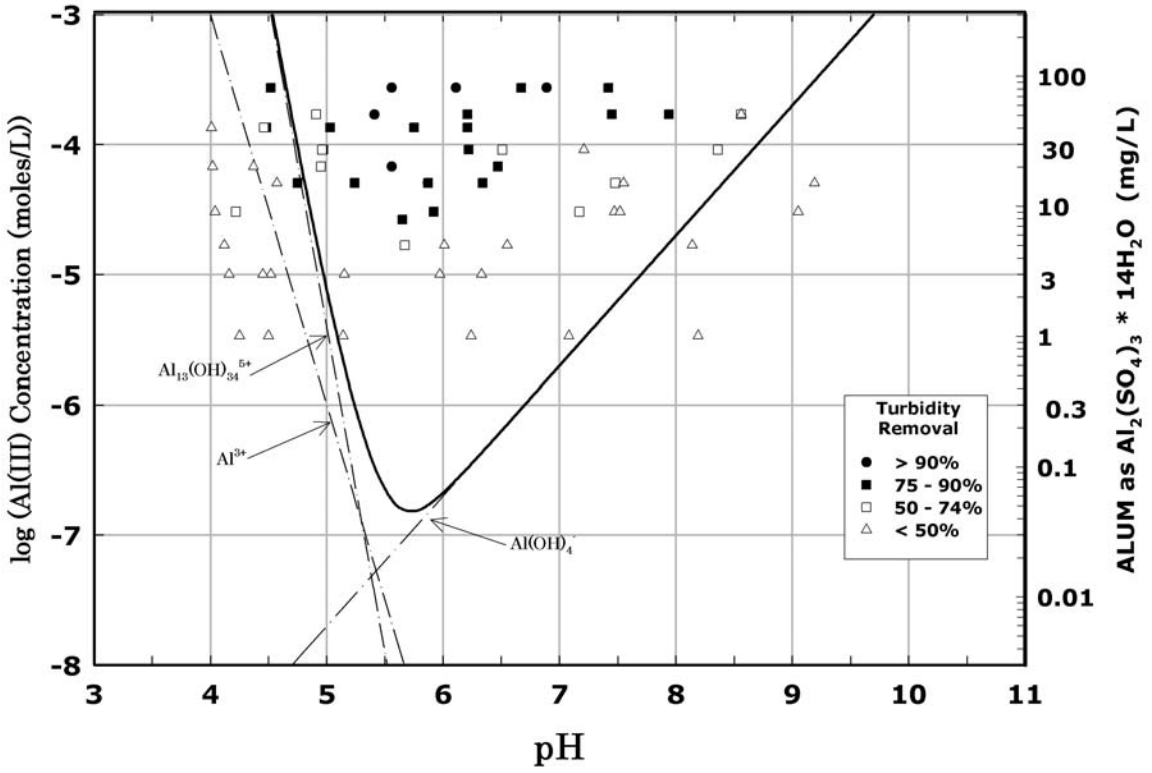

Figure 5.18 – Residual turbidity after jar mixing, flocculation, and settling as a function of pH and alum dose. Original turbidity = 7 NTU – 12 NTU

mechanism. In general, the highest removal of color and turbidity occurred at a lower pH (5.5) than current SWID practice (i.e., pH = 6-7). The most effective coagulation pH for alum, with respect to color and turbidity removal, was observed near a pH of 5.5 and a minimum coagulant dose of 1.5 mg/L as Al(III) (16.5 mg/L alum). Optimizing coagulant dosing demonstrated effective color removal over all measured pH values ($4.0 < pH < 9.0$) for alum concentrations in excess of 4.55 mg/L as Al(III) (50 mg/L alum).

Ferric sulfate was tested as a coagulant at SWID using the procedure outlined previously for alum. The results for these experiments are illustrated on a pC/pH

diagram for aqueous hydrolyzed iron species in Figure 5.19 and Figure 5.20 for percent color removal and percent turbidity removal, respectively.

Optimum coagulation pH for ferric sulfate (supplied hereafter as $Fe_2(SO_4)_3 \cdot 9H_2O$), with respect to color, occurred near a pH of 4.0 and a minimum coagulant dose of 3.98 mg/L as Fe(III) (20 mg/L as ferric sulfate). Optimum dosing for ferric sulfate occurred at coagulant concentrations in excess of 9.94 mg/L as Fe(III) (50 mg/L ferric sulfate). The two coagulants behaved similarly with respect to overall percent removals, however ferric sulfate was most effective at a relatively low pH when compared to alum (pH = 4.0 for ferric sulfate versus pH = 5.5 for alum).

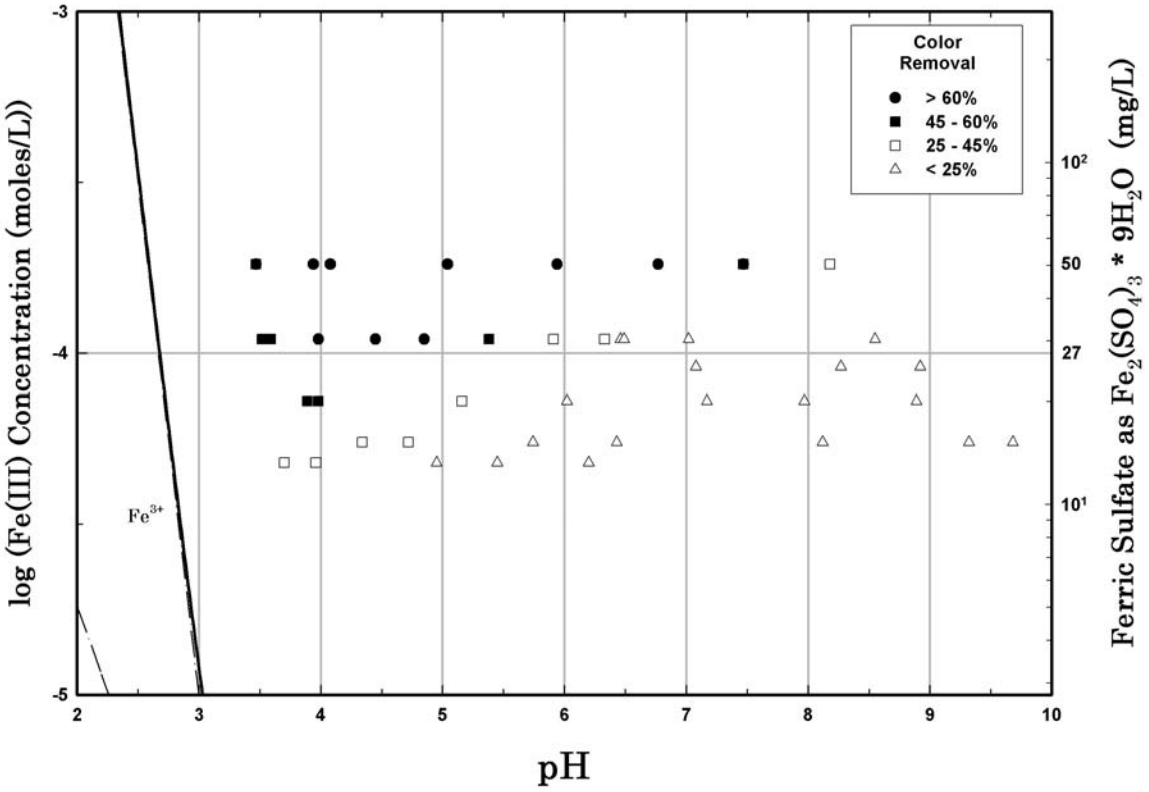

Figure 5.19 – Residual color concentration after jar mixing, flocculation, settling, and 0.45 – μm filtration as a function of pH and ferric sulfate dose. Original color = 17 ADMI – 26 ADMI

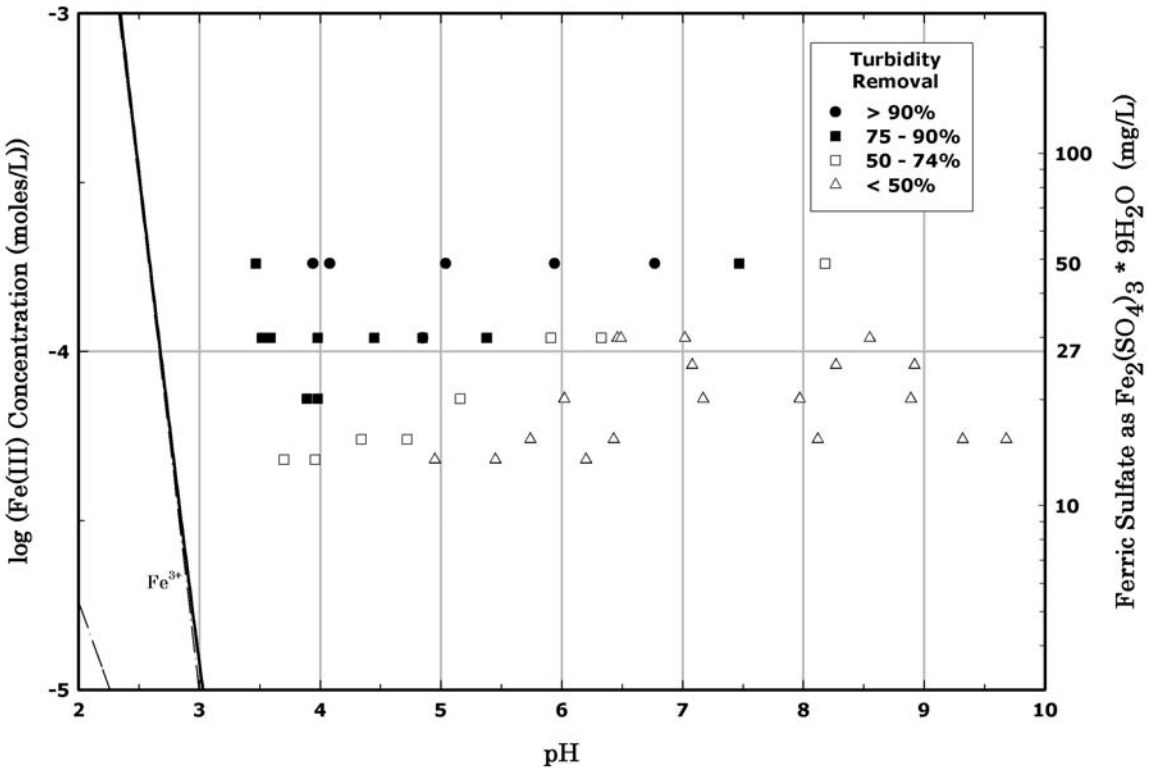

Figure 5.20 – Residual turbidity concentration after jar mixing, flocculation, settling as a function of pH and ferric sulfate dose. Original turbidity = 7 NTU – 12 NTU

5.2.2 –<u>Defining optimum coagulant dose</u>

The removal of bulk NOM by coagulation was assessed to determine optimum coagulant doses for both alum and ferric sulfate. The objective of the initial tests focused on establishing relationships between raw water parameters and the coagulant dose used to treat the water. Optimum dose has been defined by a variety of definitions based on both economic and physicochemical characteristics of water. These definitions include but are not limited to:

1.) The minimum coagulant dose may be defined by meeting the target values for a set number of parameters.

2.) Achieving a water quality where further coagulant addition does not result in any significant improvement in water quality. However, the parameters used to determine 'no significant improvement' should be documented. The resulting water quality should also satisfy any guidelines or regulations.

3.) Monitoring physical and chemical characteristics of the raw and treated water to determine proper coagulant dose (i.e., determination of point zero charge, PZC) (Bernhardt and Schell 1995)]).

For this study the idea of 'optimum' coagulant dose was applied on the following basis: Figure 5.21 (a) illustrates the results of adding alum to move from conventional coagulation to coagulation optimized for the removal of TOC. Conventional coagulation refers to the dose range most frequently observed at SWID (i.e., alum dose between 10 mg/L and 55 mg/L). Observing coagulant doses from the 2003 calendar year at SWID and defining a general range of coagulant addition determined the conventional alum dose range described. The region described as 'optimized coagulation' refers to the coagulant dose required to meet Stage I disinfection by-product rule (DBPR) under the prevailing conditions surrounding a particular jar test experiment and also refers to the region where increasing coagulant dose does not result in a significant increase in TOC removal. Relatively large alum doses achieved optimized removal of TOC and ranged from 50 to 120 mg/L as indicated by the optimum zone in Figure 5.21. The figure represents jar testing of water randomly sampled from SWID throughout the winter of 2003 and the spring and summer of 2004. Alum doses to control turbidity using the current SWID jar test procedure for determining coagulant dose ranged from as low as 10 mg/L to as high as 55 mg/L, as indicated by the conventional zone in the figure. Control

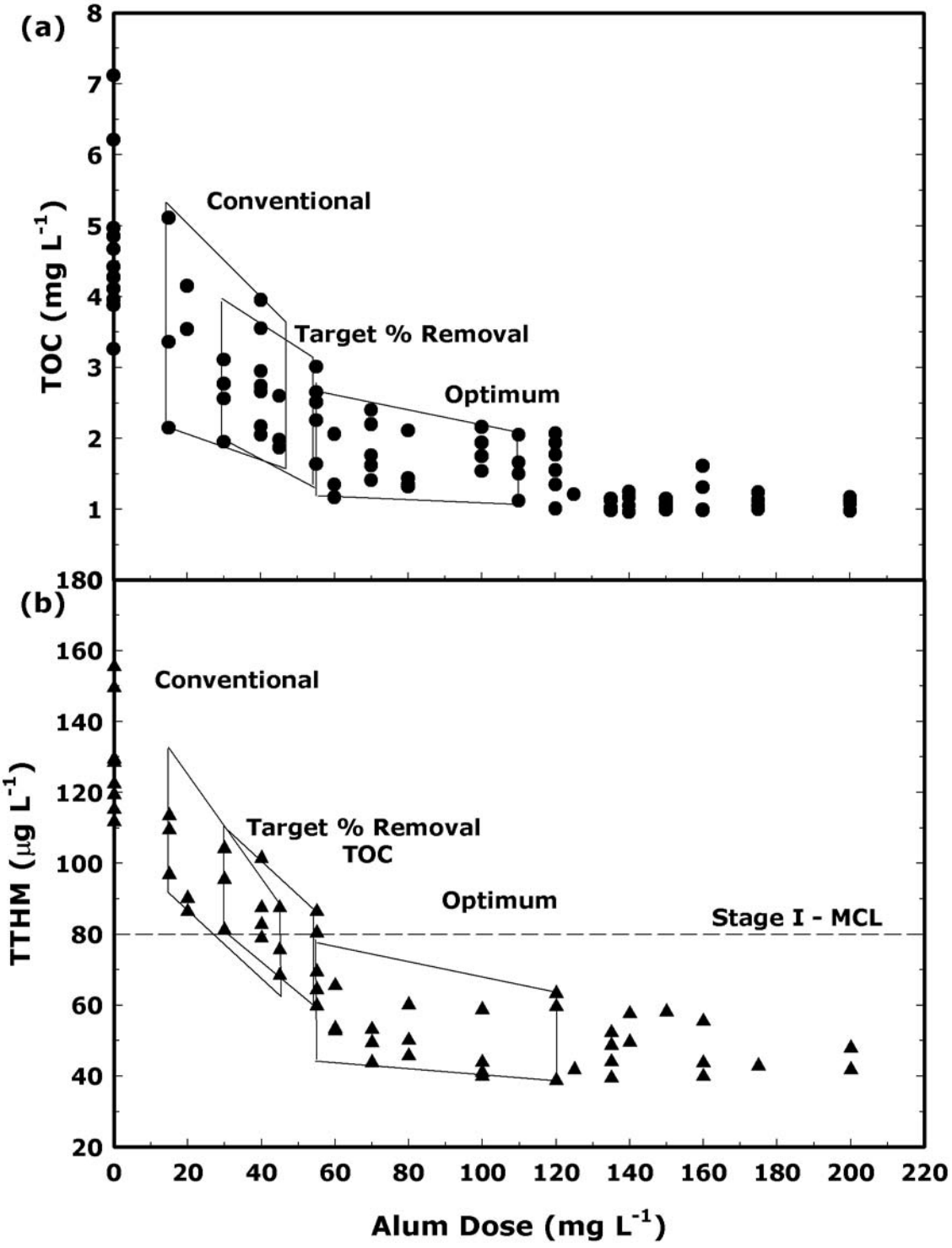

Figure 5.21 - DOC (a) and TTHM (b) removal as a function of increasing alum dose

of turbidity during jar testing was defined as achieving less than 2.0 nephelometric turbidity units (NTU) in settled waters. These criteria were selected based on current SWID coagulation practice, under which a settled water turbidity of less than 2.0 NTU is consistently met and is often well below this value.

The USEPA 1998 Stage I DBPR requires use of an alternative or additional NOM removal strategy called "enhanced coagulation" to limit disinfection by-product (DBP) formation. The effective alum dose to meet the requirements of enhanced coagulation ranged from 25 to 50 mg/L as indicated by the target percent removal TOC zone in Figure 5.21 (a). Enhanced coagulation ties the TOC removal requirement to the raw water alkalinity to avoid forcing a utility to add enough coagulant to reduce pH to between 5 and 6, the range where most hydrolyzing metal coagulants are most efficient. A summary of the coagulation zones described here is provided in Table 5.12. SWID raw water generally contains low alkalinity (< 60 mg/L as $CaCO_3$) and a TOC between 2.0 mg/L and 8.0 mg/L, resulting in a required 35% to 45% TOC removal by coagulation as defined by the Stage I DBPR.

Table 5.12 – Description of coagulation zones to describe SWID coagulation practice.

Zone	Description
Conventional	Zone used to describe current baseline SWID coagulant dose range
Target % Removal	Coagulant dose required to meet requirements for enhanced coagulation
Optimum	Point at which further coagulant addition provides little additional DOC removal

Guidelines for percent removal of TOC based on influent water TOC and alkalinity are summarized in Table 5.13. Any overlapping of 'optimized' and 'target percent removal' treatment zones suggests that enhanced coagulation may be achieved at doses lower than those required to optimize TOC removal and at doses not significantly greater than the alum concentration necessary to control turbidity. The overlapping of the 'conventional' and 'target % Removal TOC' zones suggests that, in various cases, conventional treatment was sufficient to meet the guidelines of enhanced coagulation.

Table 5.13 - Required Percent Removal of TOC by Enhanced Coagulation (Federal Register 1998)

Source Water TOC (mg/L)	Source Water Alkalinity (mg $CaCO_3$/L)		
	0 to 60	>60 to 120	>120
>2.0 to 4.0	35	25	15
>4.0 to 8.0	45	35	25
>8.0	50	40	30

Figure 5.21 (b) shows THM precursor removal as a function of alum dose. THM-FP samples were prepared for this study using the THM-FP test described previously (section 4.2.3) with the following exceptions. Settled water (250 mL) was captured and prepared with chlorine dosing solution (section 3.3.3.1) such that the residual chlorine after 24 hrs was 1.0 ±0.15 mg/L measured as free chlorine. In addition the 24-hr THM-FP was assessed under uniform formation conditions (UFCs) at pH 7 and 20 ºC (Summers et al. 1996). Under these conditions, conventional coagulation rarely produced TTHM concentrations below the D/DBP Rule Stage I maximum contaminant level (MCL) of 80 µg/L. Increasing alum dose to enhanced coagulation standards resulted in a

larger portion of samples meeting the Stage I MCL for TTHM. Optimizing coagulation for TOC removal always resulted in Stage I MCL compliance.

5.2.3 – Impact of NOM (DOC) on water treatment

The removal of humic substances by coagulation in SWID water has been investigated. Conventional jar tests were performed (section 4.3) using alum and ferric sulfate as coagulants for the removal of NOM. Previously, the two coagulants have been compared on a variety of influent raw waters; however these data provide only a general estimation of TOC removal based on color and turbidity for a given coagulant at a specified coagulant dose and pH. A direct comparison of the two coagulants is necessary to determine potential benefits or drawbacks of either coagulant with respect to TOC removal.

The two coagulants were compared directly on identical raw water samples to determine relative TOC reductions based on UV_{254} absorbance (UVA). Experimental results from section 5.1.3 describe a linear relationship between DOC and UVA in SWID raw water. The raw water characteristics for this experiment and the respective optimum coagulant doses are provided in Table 5.14. The optimum coagulant dose was established for both alum and ferric sulfate using the same raw water. Coagulant dose was fixed at the minimum dose required to meet Stage I DBPR criteria (target % removal) and residual organic concentration, measured by UVA, after jar settling is shown in Figure 5.22 as a function of pH at the 'target % removal' coagulant dose. The curves in Figure 5.22 (a) and (b), represent normalized UV_{254} absorbance over various pH values for unfiltered and filtered (0.45-μm Teflon filter), respectively. The pH value

where the largest removal of UV_{254} absorbing material (DOC) occurred at a pH of 5.5 and 4.0 for alum and ferric sulfate, respectively. Values for coagulation pH were selected based on interpretation of the data provided in Figure 5.17 and Figure 5.19 for alum and ferric sulfate, respectively, and determined to be the optimum pH for color and turbidity removal. In all experiments the coagulant dose for each coagulant was fixed and pH varied. Empirical results indicate optimal pH values for DOC removal with alum and ferric sulfate at respective optimum coagulant concentrations are different, approximately 5.5 and 4.5, respectively.

Table 5.14 – Initial SWID raw water parameters and optimum coagulant dose for DOC removal studies

Initial Parameter	Value	Units
pH	6.61	~
Temperature	25.1	°C
Turbidity	8.2	NTU
TOC	4.1	mg/L
UV254	1.001	cm^{-1}
Color	18	Pt-Co
Optimum Alum Dose	30	mg/L
Optimum Ferric Sulfate Dose	25	mg/L

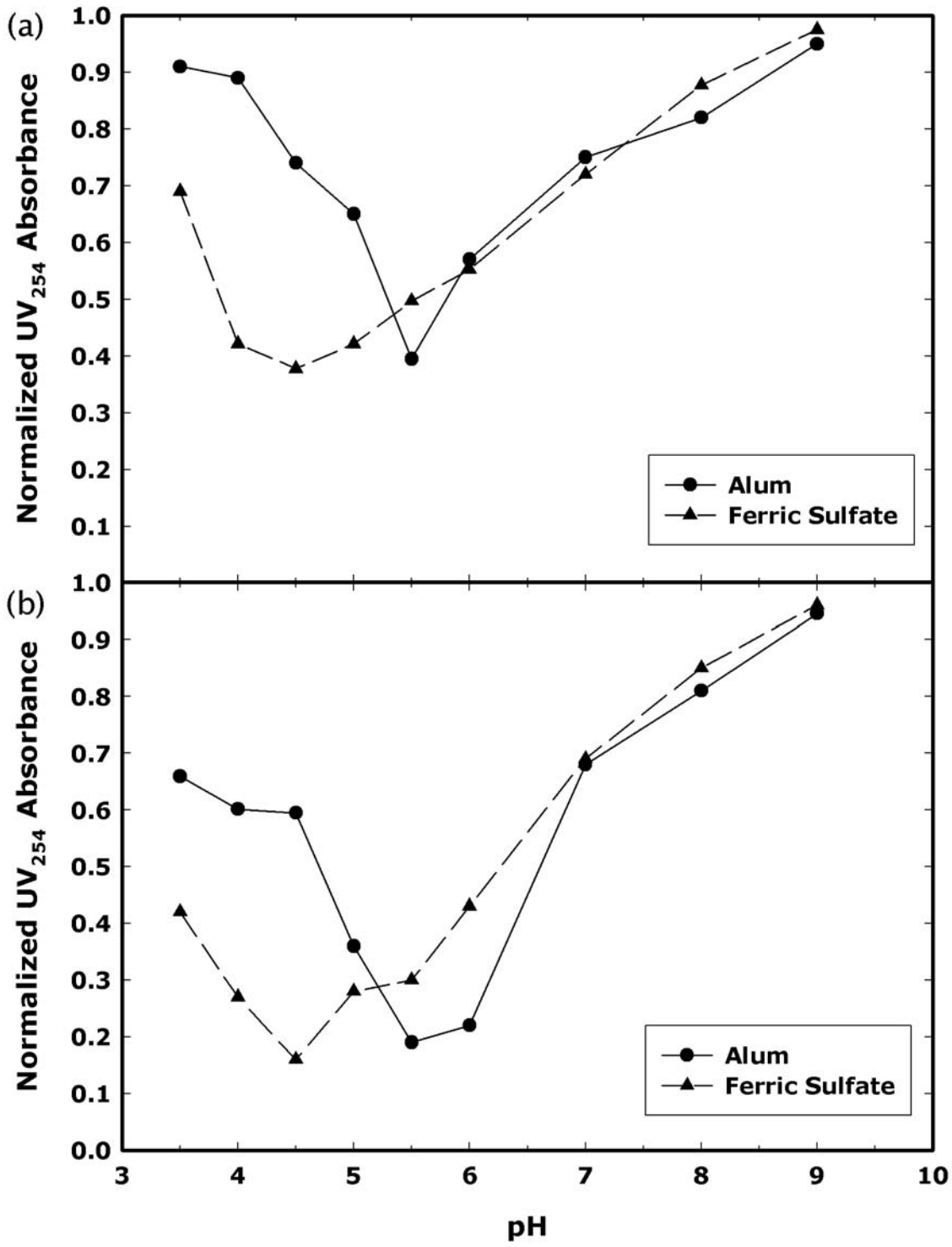

Figure 5.22 - UV254 Absorbance as a function of pH at optimum coagulant dose for unfiltered settled water (a) and filtered settled water (b).

Using the same raw water and jar test procedure described earlier, pH values were fixed at the previously determined optimum pH values for alum and ferric sulfate (pH=5.5 and pH=4.5, respectively) using 0.1 M HCl or filtered saturated lime, $Ca(OH)_2$, solution to provide a constant coagulation pH with increasing coagulant concentration. The influence of increased alum and ferric sulfate concentrations on the removal of UV_{254} absorbing organic materials is illustrated in Figure 5.23 (a) and (b) for unfiltered and filtered waters respectively. It is evident from the figure that the coagulant dose yielding optimal removal of UV_{254} absorbing organic material occurs at approximately 2.5 mg/L and 4.0 mg/L as aluminum, Al^{3+}, and iron, Fe^{3+}, respectively, which both correspond to approximately 80% removal of UV_{254} absorbing material.

Generally, ionization of carboxyl groups, namely carboxylic acids ($pKa \cong 4.5 – 5.0$), leads to humic acids possessing a negative charge. This may place an added coagulant demand on the amount of coagulant required to achieve optimum coagulation, by enhancing the availability of active binding sites for aqueous iron and aluminum complexes. All interpretation of these results must consider the molecular weight of the metal species (iron [MW = 55.85] or aluminum [MW = 26.98]) involved in the coagulation experiments given that coagulant doses were measured on the basis of metal ion concentration. One (1) equivalent of aqueous aluminum is equal to 2.04 equivalents or 1 meq/L of aluminum or iron is equal to 9 mg Al^{3+}/L or 18.6 mg Fe^{3+}/L, respectively. Figure 5.23 has been redisplayed in Figure 5.24 to show UVA of treated water at fixed optimum pH and increasing coagulant dose based on equivalents.

Based on equivalents, ferric sulfate provides increased DOC removal (with respect to UVA) at lower coagulant concentrations. Again, each jar test at the respective

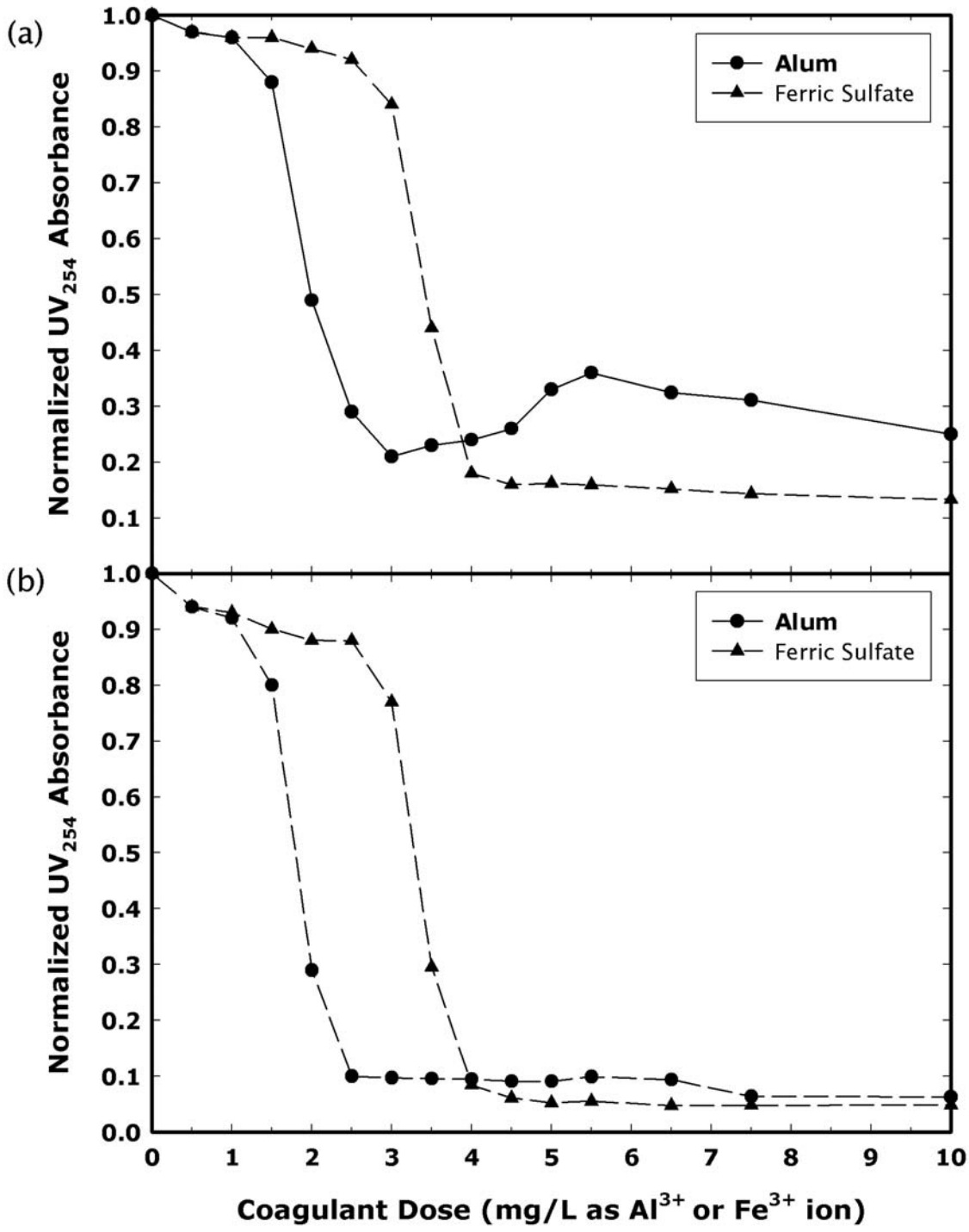

Figure 5.23 -UV_{254} Absorbance as a function of increasing coagulant dose (based on mg metal ion per liter) for (a) unfiltered settled water and (b) filtered settled water.

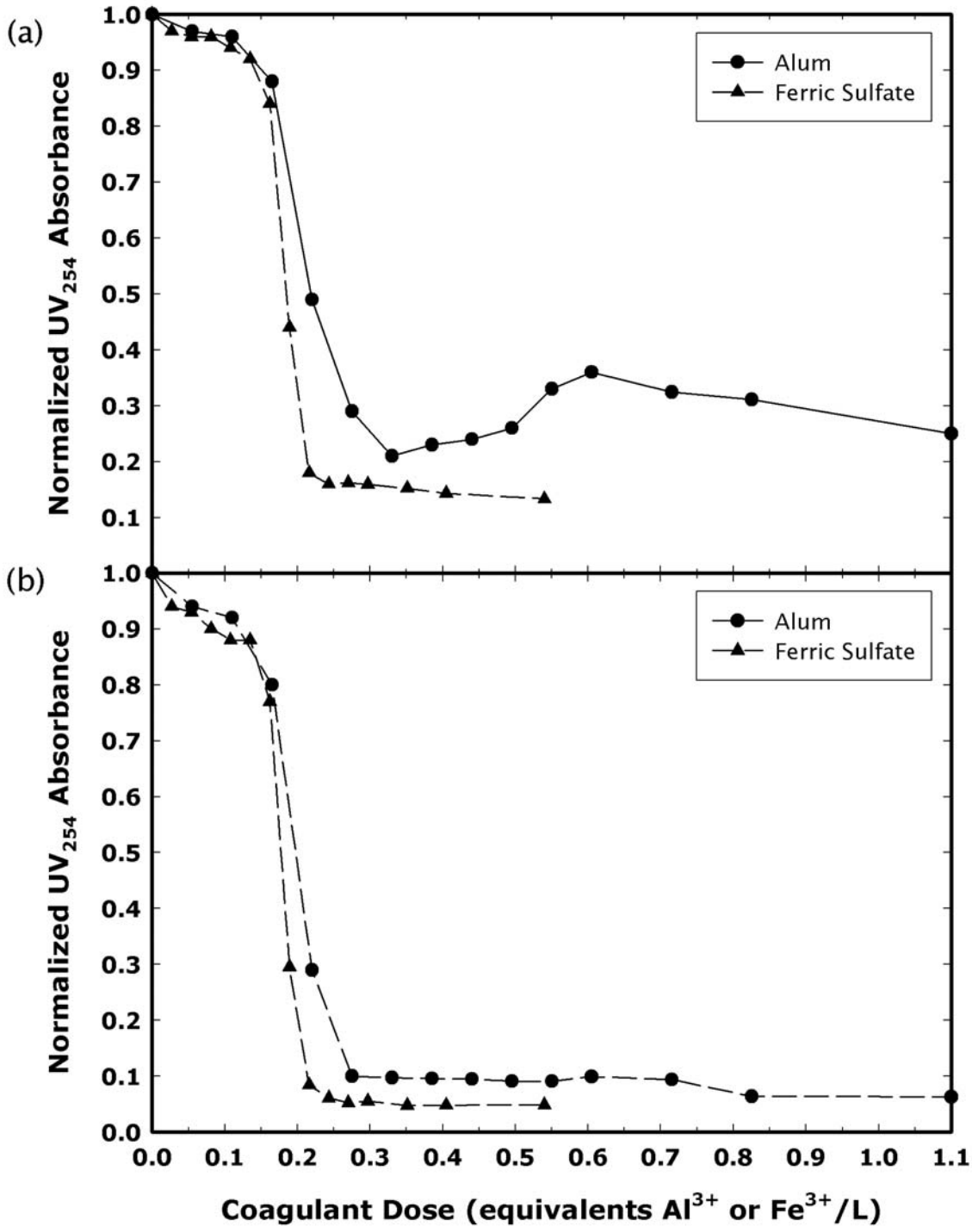

Figure 5.24 -UV_{254} Absorbance as a function of increasing coagulant dose (based on equivalents) for (a) unfiltered settled water and (b) filtered settled water.

coagulant concentration was fixed at the previously established optimum pH for DOC removal based on UVA (pH=5.5 and pH=4.5 for alum and ferric sulfate, respectively). The aluminum and iron complexes formed with organic material (metal-humates) may be soluble or insoluble depending on the molecular size of the polymer formed from the interaction of aluminum and humic material. As the amount of aluminum hydroxide and ferric hydroxide precipitated as hydrolyzed Al (III) and Fe (III) species increases, additional surface area is created. This allows for smaller organics and metal-humates to adsorb to larger amorphous precipitates, increasing their removal by settling or filtration. After a significant amount of metal hydroxide forms, the major mechanism of organic removal by coagulation can be expected to shift from metal-humate complexation and aggregation due to charge neutralization to adsorption onto metal hydroxide precipitates (Hur 2003). These collective processes may be described as 'sweep floc'.

5.2.4 – Bulk analysis summary

Current coagulation practice at SWID suggests that the mechanism controlling coagulation is a combination of both adsorption / destabilization and sweep-floc coagulation. Preliminary jar tests revealed that the current SWID coagulation practice is sub-optimal with respect to DOC removal, operating at a coagulation pH slightly higher ($6 < \text{SWID coagulation pH} < 7$) than the optimal coagulation pH determined for alum ($\text{pH} \cong 5.5$).

In addition to alum, ferric sulfate was tested as a coagulant under similar coagulation conditions. Ferric sulfate appeared to have slightly better overall DOC removal while requiring less coagulant (based on equivalents), however the optimal pH

occurred at 4.5 versus 5.5 for alum. Additional DOC removal at this low pH may be associated with increased protonation of NOM reactive groups, which lower the overall negative charge of the NOM molecule promoting destabilization at relatively low coagulant doses. However, the optimum pH for DOC removal by alum coagulation was determined to occur near pH=5.5, therefore additional DOC removal associated with ferric sulfate must be linked to iron-humate interactions and subsequent formation of insoluble iron-humate complexes and sorption of soluble NOM to ferric hydroxide precipitate.

Coagulation experiments have demonstrated SWID bulk NOM (DOC) response to various changes in pH, coagulant type, and coagulant concentration. Further study is required to determine the specific characteristics of NOM enabling a better assessment of potential removal techniques using conventional treatment processes.

5.3 – Analysis of fractionated NOM

5.3.1 - Ultrafiltration

An operationally-defined experimental protocol was designed to fractionate dissolved organic matter (DOM) at SWID to determine an apparent molecular weight distribution based on molecular weight cut-off (MWCO) values established by the membrane manufacturer. Amicon YC-05, YM-1, YM-3, YM-10, and YM-30 membranes were chosen for the low specific binding and associated high solute recovery observed in their use for the fractionation of globular proteins (Amicon 1995). Each membrane is designed with an apparent molecular weight cutoff (MWCO) of 0.5, 1, 3,

10, and 30 kDa, respectively. These membrane MWCOs were selected to encompass the general size range of NOM present in U.S. surface waters (Amy et al. 1992).

Membranes were prepared as described in section 4.5.1 and clean water solute flux was verified based on manufacturer's guidelines. The operational protocol consisted of parallel ultrafiltration cycles conducted on reconstituted SWID raw water and the use of a two parameter permeation coefficient model (PCM) (Logan and Jiang 1990; Tadanier et al. 2000). The ultrafiltration procedure described in the following sections was designed to minimize variation in membrane permeability caused by uncontrolled filtration conditions. Each parameter associated with an ultrafiltration cycle was monitored carefully to ensure reproducible results.

The shape and character of aquatic NOM is primarily influenced by solution pH and ionic strength (see section 2.2). The pH was adjusted to 6.5±0.05 with 2N solutions of HCL or NaOH depending on pre-filtration ambient pH. The specific conductance was measured and adjusted using reagent grade NaCl to achieve an ionic strength of 0.01 or a specific conductance of 625 μmho/cm. These values were selected to represent the average coagulation pH and ionic strength at SWID. Membranes were used a maximum of 5 filtration cycles, then discarded to avoid any loss in flux rate due to pore blockage or potential contamination of membranes by bacterial growth. Membranes were regenerated using 0.1N NaOH following each use and the clean water flux was verified to meet manufacturer guidelines prior to use.

Prior to UF, samples were filtered using a 0.45-μm Teflon filter. The pH and ionic strength of each sample was adjusted and the sample was stored at 4°C in glass amber bottles in the dark. Aliquot samples were brought to ambient temperature (23

±1°C) prior to ultrafiltration and maintained in this temperature range throughout the UF cycle. Filtration volume was set at 140 mL of a possible 200 mL. A portion of the concentrated solute (60 mL) was not processed to reduce the effects of concentration polarization and allow for accurate mass balances to be conducted. Stir speed was maintained at 210 ±10 rpm throughout each filtration run by periodic monitoring with an optical strobe tachometer. During each individual ultrafiltration cycle, eight 10 mL aliquots were collected to allow the effect of membrane rejection to be accounted for using the permeation coefficient model (PCM) to calculate the expected permeate concentration based on change in the instantaneous permeate concentration over time (Logan and Jiang, 1990). A detailed description of the PCM is discussed in section 5.3.2.

5.3.1.1 – Permeation Coefficient Model justification

The UF procedure outlined in the previous section was followed using SWID raw composite water created from equal portions of samples collected from sites 1, 3, 4, 5, and 6 in the SWID watershed (section 4.2.2). Individual samples from each site were prepared as described in section 4.1 and combined in equal proportions to form the bulk raw composite water. The initial SWID raw composite water characteristics are presented in Table 5.15. Aliquot samples from the bulk raw composite water were processed using each of the specified UF membranes (YC-05, YM-1, YM-3, YM-10, and YM-30). Filtrates produced using each of the listed membranes yielded the size classes listed in Table 5.16. Note in the table that 'F' and 'R' are used to denote size fractions

Table 5.15 – Initial bulk raw composite water parameters for UF procedure

Initial Parameter	Value	Units
pH	6.61	~
Temperature	25.1	°C
Turbidity	8.2	NTU
TOC	4.1	mg/L
UV_{254} Absorbance	1.001	cm^{-1}
Color	18	Pt-Co
Optimum Alum Dose	30	mg/L
Optimum Ferric Sulfate Dose	25	mg/L

Table 5.16 – MW size fractions determined by UF separation

Size Fraction	MW Range (Daltons)
F1	F1> 30,000
R2	30,000 > R2 > 10,000
R3	10,000 > R3 > 3000
R4	3,000 > R4 > 1,000
R5	1,000 > R5 > 500
F6	F6 < 500

found by measurement of permeate concentration directly and determining the difference in permeate concentrations, respectively. A photograph of the process setup and a bulk raw composite water sample are displayed in Figure 5.25. A photograph of samples captured from permeate and retentate volumes is displayed in Figure 5.26. Visually it is clear that a large fraction of the NOM is retained on the YM-10 membrane due to the dark color observed in this sample. Using the same raw composite water the UF parallel size fractionation process was repeated eight (8) times to assess variability of measured permeate concentration using the specified UF protocol. The final permeate DOC

Figure 5.25 – Raw composite DOM sample and Amicon® 8200 series ultrafiltration cells.

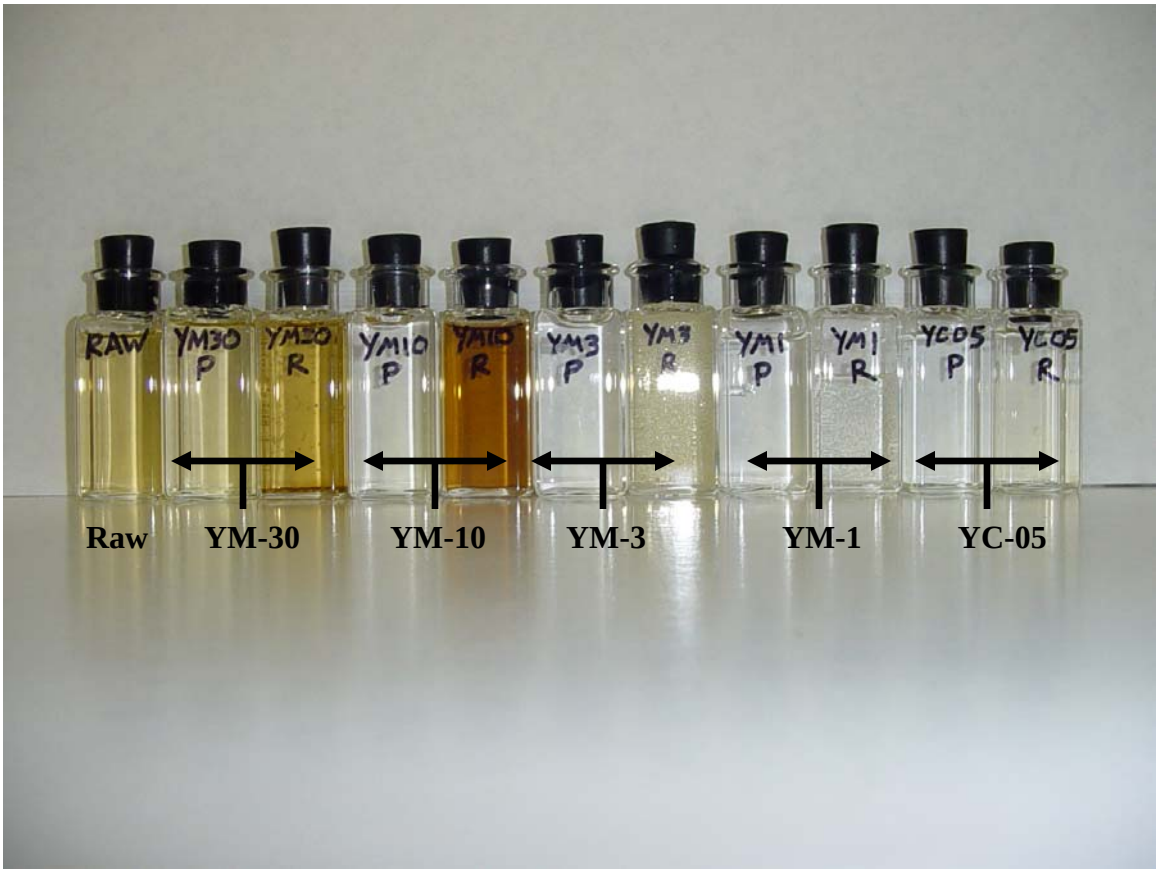

Figure 5.26 – Raw water and Permeate (P) and Retentate (R) samples (left and right, respectively, for each pair) from each UF membrane

concentration and UVA were measured and recorded. The results from the UF trials are presented in Table 5.17. The table displays average final permeate DOC concentration and UVA for eight consecutive trails and the respective standard deviation. Intermediate size fractions (i.e., 30 kDa > R2 > 10 kDa, 10 kDa > R3 > 3 kDa, etc…) were calculated by determining the difference in permeate DOC concentration and UVA between size fractions. The MW distribution based on these two parameters with respect to MW size fractions is presented in Figure 5.27. The figure displays a similar general size distribution for SWID DOM based on DOC and UVA. These data suggest the following:

Table 5.17 – Final permeate DOC concentration and UVA for specified fractions for 8 repeat UF trials on SWID bulk raw composite water. **F1** > 30 kDa, 30 kDa > **R2** > 10 kDa, 10 kDa > **R3** > 3 kDa, 3 kDa> **R4** > 1 kDa, 1 kDa > **R5** > 0.5 kDa, 0.5 kDa > **F6**

Fraction	DOC (mg/L)	Std. Dev	UVA (cm^{-1})	Std. Dev
<30 kda	11.00	0.35	0.745	0.042
<10 kDa	4.62	0.30	0.289	0.014
<3 kDa	2.03	0.15	0.094	0.009
<1 kDa	1.27	0.09	0.069	0.004
<0.5 kDa	0.76	0.05	0.042	0.001
F1	1.19	0.35	0.231	0.027
R2	6.38	0.59	0.404	0.035
R3	2.59	0.31	0.162	0.016
R4	0.76	0.16	0.065	0.065
R5	0.50	0.09	0.028	0.028
F6	0.76	0.05	0.047	0.046

* Initial Values: DOC = 12.2 mg/L UVA = 1.001 cm^{-1}

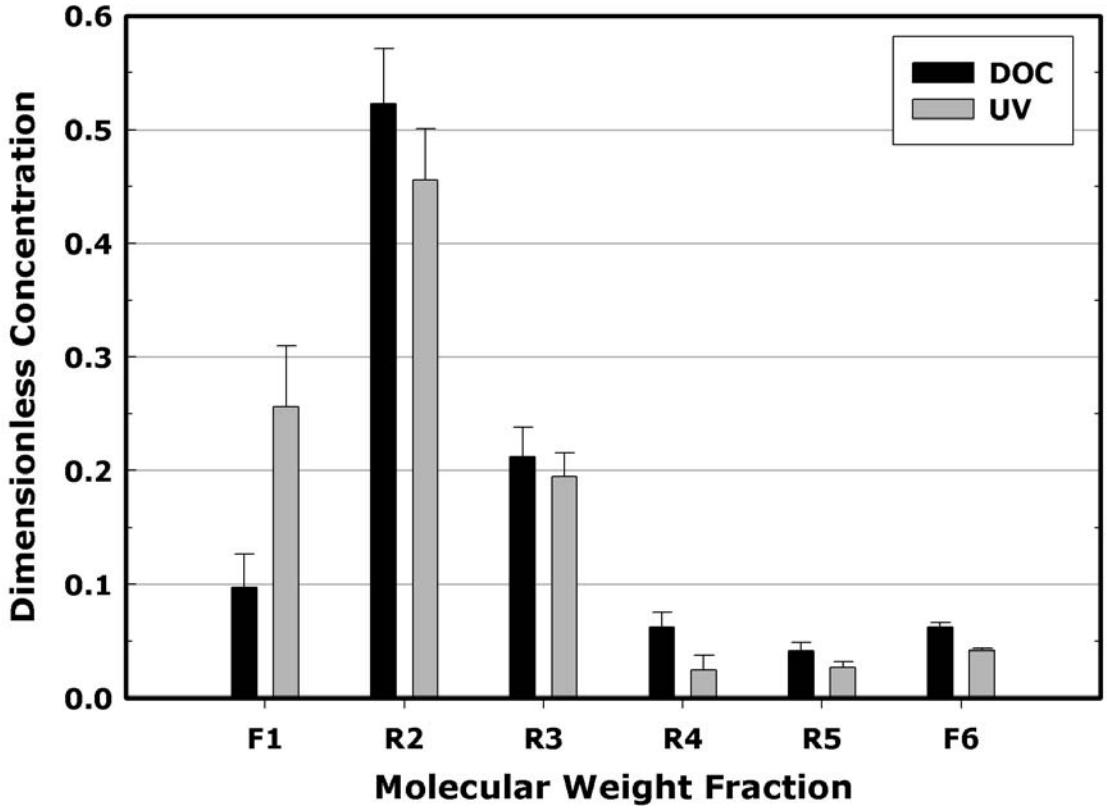

Figure 5.27 – Range of MW distributions for SWID DOM based on DOC and UVA values from final permeate values.

(1) The majority of SWID NOM resides in the R2 size fraction (30 kDa > MW > 10 kDa)

(2) Over 80% present of SWID NOM resides in the first three (3) size classes representing NOM with MW values of 3,000 to > 30,000 Da.

(3) The F1 size fraction (> 30,000 Da) exhibits the highest UVA/DOC ratio indicating that the degree of unsaturation is highest in this size fraction.

(4) The F6 size fraction (< 500 Da) exhibits the lowest UVA/DOC ratio indicating that the amount of unsaturated carbon will be relatively high.

These data indicate that the degree of unsaturation is highest in the largest (F1) size fraction. The amount of carbon double or triple bonds will be higher in this size fraction and lowest in the smallest (F6) size fraction.

It must be noted that these data were obtained by measuring DOC and UVA in the final permeate. This approach uses the average permeate concentration over the entire filtration cycle. In order to determine the validity of this assumption the permeate flux was measured with respect to the volume filtered. The results from these analyses are presented in Figure 5.28.

It is clear from these data that instantaneous permeate concentration (C_p) changes as a function of filtrate volume. C_p increases nonlinearly as the filtration cycle progresses, which will ultimately affect any estimation of molecular size based on measuring final permeate and retentate concentrations. NOM molecules nominally sized to pass through a specific MWCO may be underestimated if samples are collected early in the filtration cycle. The opposite may be true if DOC and UVA are measured in the latter half of any given filtration cycle. The data from Figure 5.29 have been redisplayed in Figure 5.30 to illustrate this point. Notice the change in size fractions as the filtration progresses from 20 mL to 120 mL of filtered solute. F1 and R2 appear to decrease as the remaining size fractions (R3, R4, R5, and F6) increase.

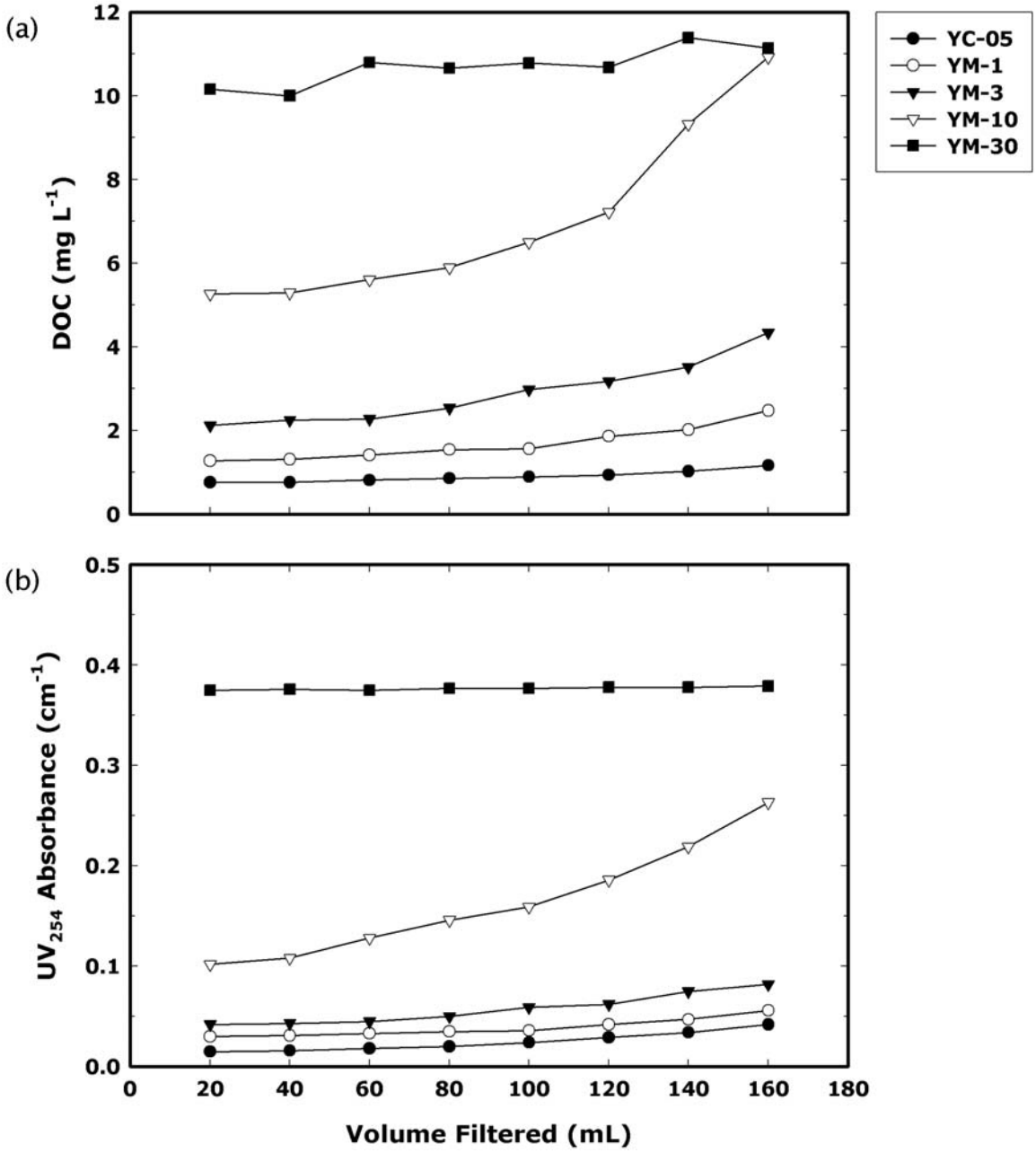

Figure 5.28 - Instantaneous permeate concentration (C_p) for (a) DOC and (b) UVA as a function of volume filtered.

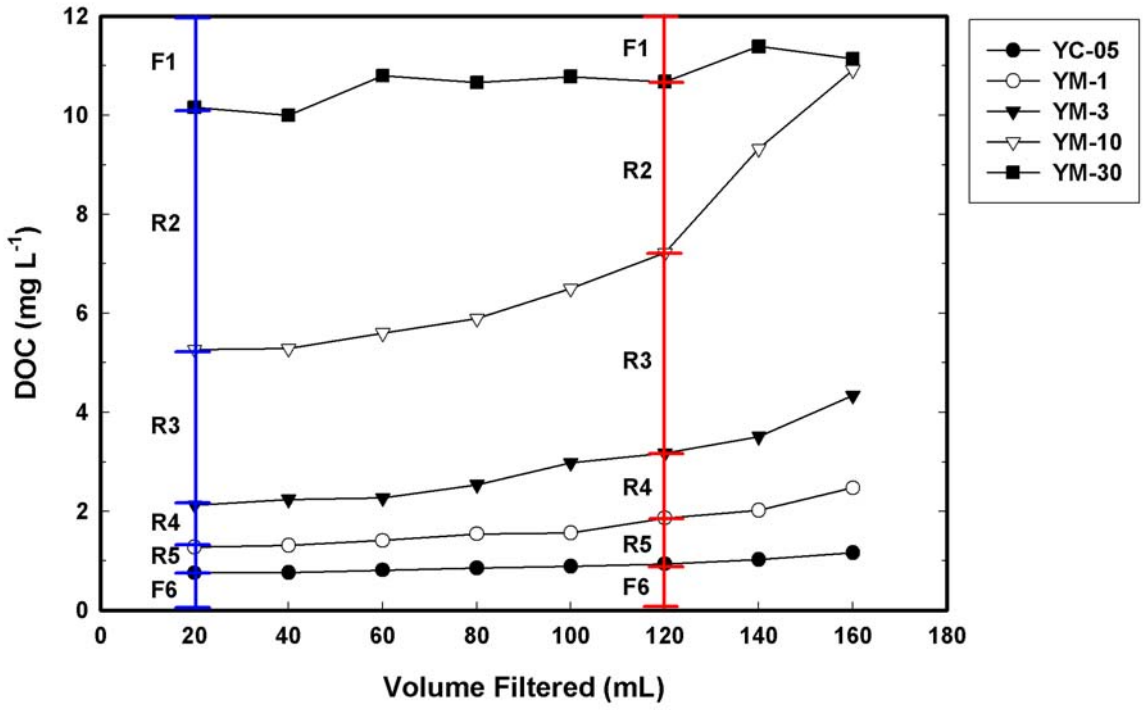

Figure 5.29 - Instantaneous permeate concentration (C_p) measured as DOC. MW size fractions at filtered volumes of 20 mL (blue) and 120 mL (red).

The change in MW size fractions with respect to volume filtered is further illustrated in Figure 5.30 for all points in the filtration cycle. This figure shows a clear increase in the R3, R4, R5, and R6 size fractions and decrease in F1 and R2 fractions over the filtration cycle. Based on these data, it is clear that a method must be employed to account for the variability in permeate concentration over time. The variability can be directly associated with the cumulative membrane rejection occurring during the ultrafiltration. The results obtained from this experiment and future experiments will be used to determine a permeation coefficient that will in turn used to correct size distributions of dissolved organic matter (DOM) determined using batch ultrafiltration

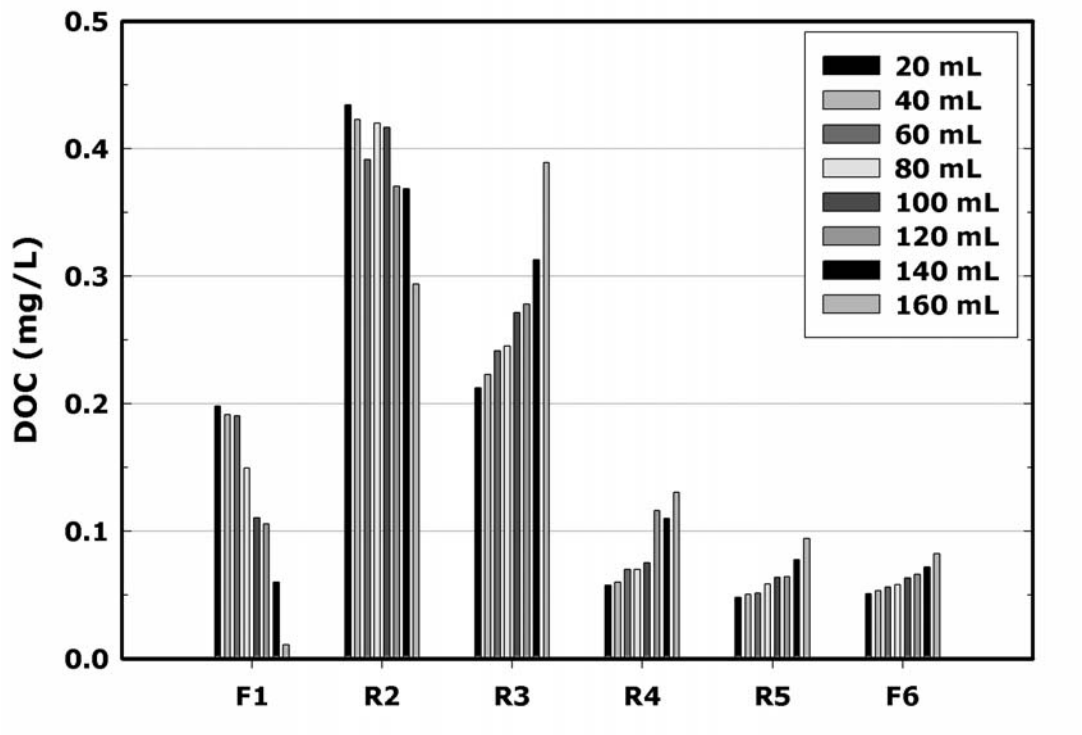

Figure 5.30 - MW size fractions as a function of increasing filtered volume over a single filtration cycle.

cells. A detailed description of the method used (permeation coefficient model) to correct for membrane rejection follows.

5.3.2 – <u>Permeation coefficient model (PCM)</u>

Several models exist that account for flux reductions through ultrafiltration membranes during continuous flow systems (Fane et al. 1990; Porter 1972; Probstein et al. 1978). A two parameter PCM (Logan and Jiang 1990; Tadanier et al. 2003) was used to correct raw batch UF data based on $\Delta C_p/\Delta t$, where C_p represents the instantaneous permeate concentration. The PCM is based on the assumption that mass transport between two homogenous phases is due to an arbitrary combination of convective and

diffusive processes, each process driven by gradients in pressure ΔP, solute mole fraction $\Delta\chi_i$, and electrical potential $\Delta\Psi$ on opposing sides of a semipermeable membrane. Each homogenous phase is a component of a larger heterogeneous system composed of both chemically and, in some cases, physically distinct solutes.

The rejection associated with each membrane is a function of solute concentration at the membrane surface, which cannot be easily measured. Membrane rejection was measured as an observed rejection coefficient, defined (Fane 1986) as

$$R = 1 - \left(\frac{C_p}{C_b} \right) \qquad \text{(Eq 5.1)}$$

where C_p and C_b are defined as the permeate and bulk concentrations, respectively. The objective of the initial bulk water analysis was to determine the initial concentration of material in a water sample with an apparent molecular weight smaller than the nominal membrane molecular weight cutoff, defined (Logan and Jiang 1990) as C_{ro}.

If the permeation behavior of the membrane is assumed to remain constant throughout the ultrafiltration cycle, the permeation coefficient *p* may be described as,

$$p = \frac{C_p}{C_r} \qquad \text{(Eq 5.2)}$$

where C_p and C_r are defined as the instantaneous permeate and retentate concentrations, respectively. A linear differential equation may be used to describe a mass balance conducted on the pressurized filtration cell. The equation developed takes the form,

$$\frac{d(VC_r)}{dt} = -pC_rQ \qquad \text{(Eq 5.3)}$$

where Q is the filtration flow rate. The change in the volume is related to Q by the relationship $Q = -dV/dt$. The equation above may be expanded to the following differential mass balance.

$$\frac{1}{C_r}\frac{dC_r}{dt} = (p-1)\frac{1}{V}\frac{dV}{dt} \qquad \text{(Eq 5.4)}$$

Eliminating dt from both sides of Equation 5.4, the integration of the resulting mass balance between the initial condition $(C_r)_{Vo}=C_{r0}$ and any discrete point during an ultrafiltration cycle where $(C_r)_{Vt} = C_r$ yields,

$$C_r = C_{r0}\left(\frac{V_r}{V_{r0}}\right)^{p-1} \qquad \text{(Eq 5.5)}$$

Substitution of Equation 5.2 into Equation 5.5, and expressing retentate volume as $V_r = V_{r0} - V_p$ yields an integrated equation relying on two experimentally-determined parameters, p (permeation coefficient) and C_p (instantaneous permeate concentration). V_r is eliminated due to difficulty in accurate measurement of retentate volume under mixing conditions. The membrane permeation during batch ultrafiltration is now illustrated using the single nonlinear equation:

$$C_p = pC_{ro}F^{p-1} \qquad \text{(Eq 5.6)}$$

Where $F = 1 - (V_f / V_o)$ and corresponds to the fractional reduction in retentate volume at time t. The permeation coefficient, p, is defined as the instantaneous ratio of permeate and retentate solute concentrations. The equation for C_p above may be linearized to yield the following equation.

$$\ln C_p = \ln(pC_{ro}) + (p-1)\ln F \qquad \text{(Eq 5.7)}$$

From Equation 5.7, p and C_{ro} may be determined by the slope (p-1) and y-intercept [ln(pC_{ro})], respectively, of the linearized equation. In order to help with curve fitting and graphical representation of empirical UF data, the actual concentration of DOM (C_{ro}) nominally sized to pass through the pores of the membrane in use was nondimensionalized (Tadanier 2003) as,

$$C_{ro}^{*} = \frac{C_{ro}}{C_o} \qquad \text{(Eq 5.8)}$$

where C_o is defined as the total concentration of DOM in the given sample during an individual UF cycle.

5.3.2.1 – Application of the PCM

The molecular size distribution of SWID bulk raw composite water was determined by parallel processing of samples through five ultrafiltration cells. A repeatability test was conducted on UF membranes to determine variability of experimentally-derived parameters p and C_{ro} using the PCM. An example of the permeate concentration change during a filtration cycle for 8 separate trials has been provided for the YM-1 membrane in Figure 5.31. The data in the figure were linearized using Equation 5.7 yielding the permeation coefficient p and the PCM adjusted concentration C_{ro} for the YM-1 membrane. The linearized data for this series are provided in Figure 5.32.

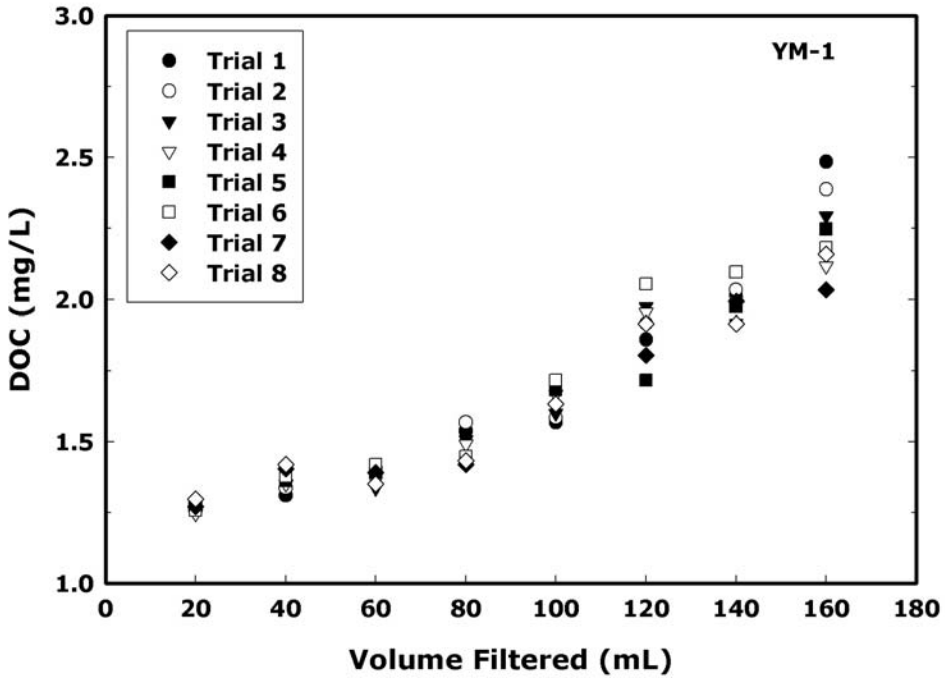

Figure 5.31 – Change in YM-1 permeate DOC concentration as a function of volume filtered for eight UF trails using SWID bulk raw composite water

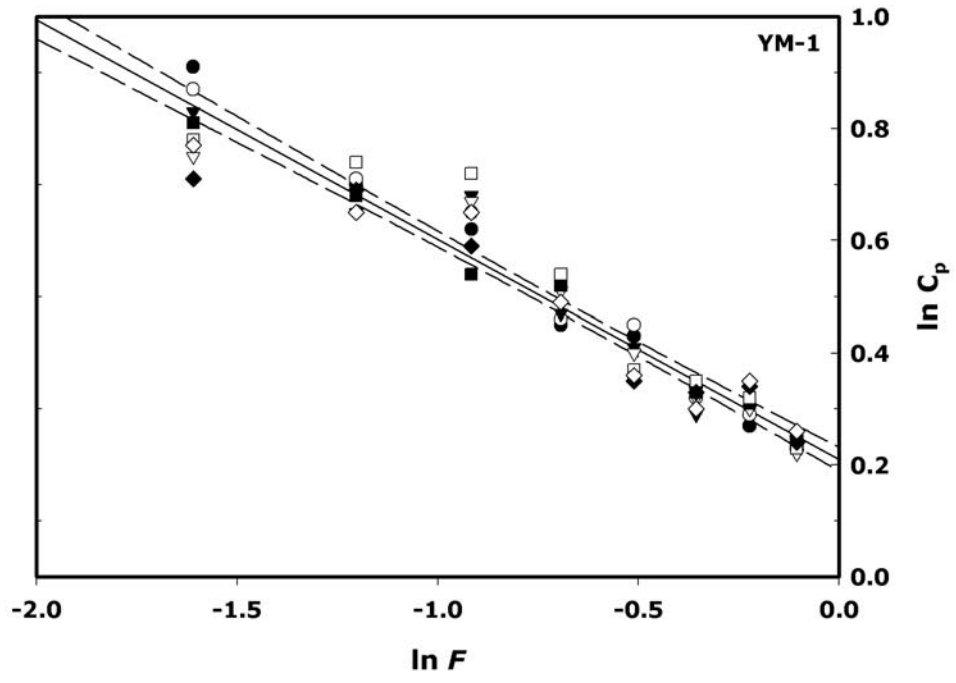

Figure 5.32 – YM-1 linearized permeate (DOC) concentration for eight trials using SWID bulk raw composite water

Similar data sets were created for each of the remaining membranes and the linearized results are provided in Figure 5.33. Goodness of fit data for the linearization of each data set is provided in Table 5.18. These data suggest that cumulative membrane rejection effects are consistent throughout each filtration supporting the use of the PCM to correct observed ultrafiltration data. The cumulative effects of small errors in sample volume and DOC measurement as well as minor variations in the previously defined UF protocol (i.e., applied pressure, temperature, and mixing intensity) are manifested as variability in the PCM parameter estimates. Any recurring error or uncertainty in the MW distribution acquired by the PCM was incorporated in the repeatability study discussed previously.

The permeation coefficient (p) and PCM adjusted concentrations (C_{ro}) from this study are displayed in Table 5.19. Based on the results of the repeatability study, no significant decline in membrane flux was observed due to any inconsistencies in membrane structure or filtration protocol. Average sample fluxes were generally slightly lower than clean water fluxes values, but were again within the nominal range for solute flux specified by the manufacturer. Table 5.20 displays clean water flux and solute flux values for each membrane. In all cases solute flux exhibited less than a 3 percent deviation from clean water flux. Thus, flux decline associated with membrane-solute interactions was considered negligible. No systematic trends in flux behavior were observed either between or within individual filtration cycles. Under the specified experimental structure and results, the permeation coefficient model assumption of constant membrane solvent flux was considered to be satisfied by the structure of the experimental procedure used in this research.

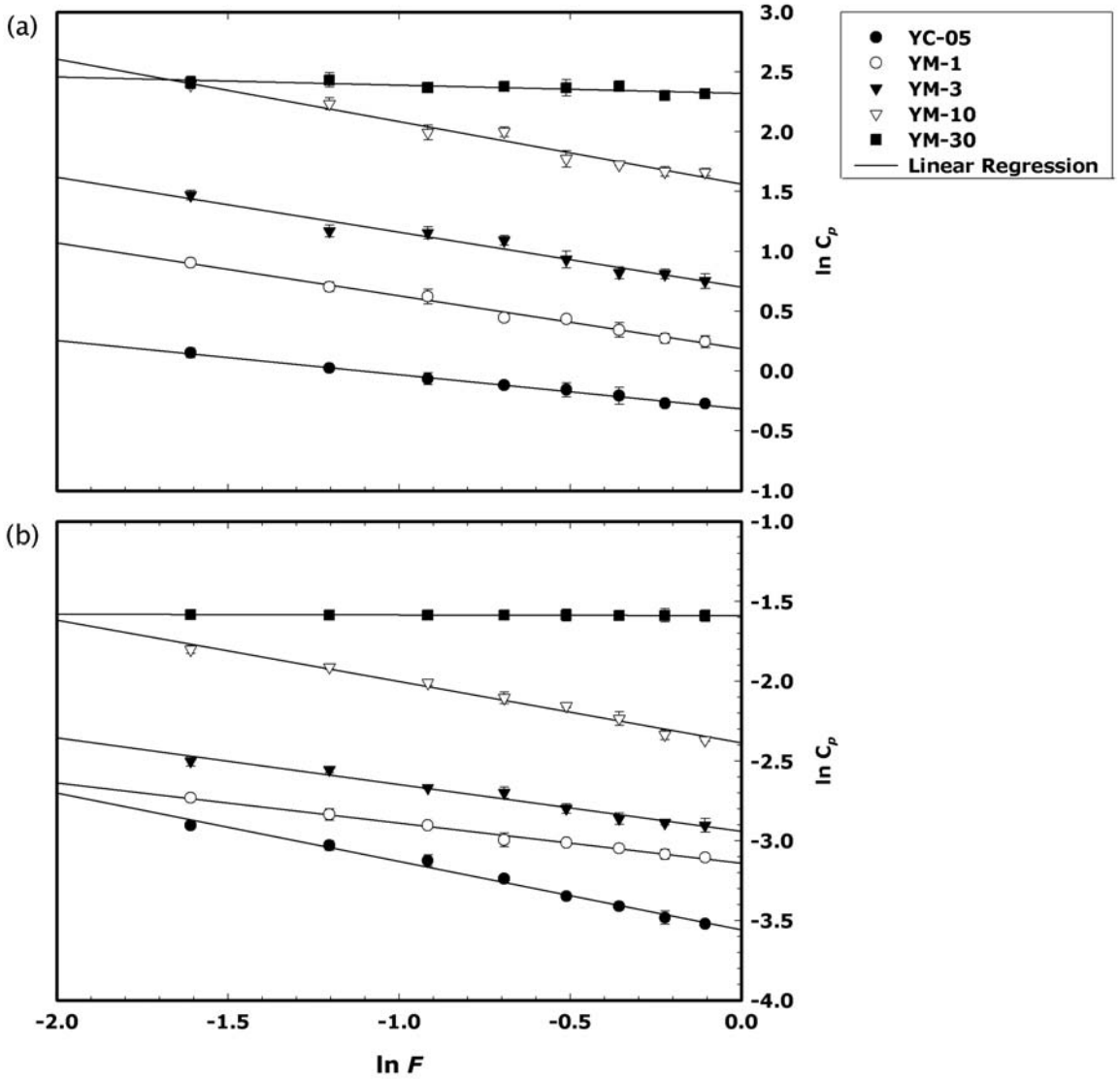

Figure 5.33 – Linearized permeate (a) DOC concentration and (b) UVA for UF membranes for eight (8) trials with SWID raw bulk composite water

Table 5.18 – Coefficient of determination for linearized permeate concentration

Membrane	Coefficient of Determination (r^2)	
	DOC	UV_{254} Absorbance
YC-05	0.984	0.994
YM-1	0.991	0.992
YM-3	0.986	0.988
YM-10	0.993	0.987
YM-30	0.996	0.994

Table 5.19 – Repeatability study results for permeation coefficient (p) and PCM adjusted permeate concentration (C_{ro})

Membrane	Based on DOC		Based on UVA	
	p	C_{r0} (mg/L)	p	C_{r0} (cm^{-1})
YC-05	0.72 ±0.02	1.021 ±0.006	0.28 ±0.05	0.05 ±0.006
YM-1	0.57 ±0.03	2.16 ±0.148	0.58 ±0.03	0.049 ±0.01
YM-3	0.51 ±0.03	3.73 ±0.408	0.51 ±0.03	0.078 ±0.012
YM-10	0.48 ±0.04	10.11 ±1.87	0.36 ±0.04	0.278 ±0.010
YM-30	0.93 ±0.005	11.04 ±1.84	0.99 ±0.001	0.380 ±0.025

Table 5.20 – Clean water and solute flux as a function of instantaneous fractional reduction in retentate volume (F)

F	Clean Water and Solute Flux ($mL/hr\text{-}cm^2$)									
	YC05		YM1		YM3		YM10		YM30	
	Ref.	SWID	Ref.	SWID	Ref.	SWID	Ref.	SWID	Ref.	SWID
0.9	1.8	1.8	2.4	2.4	4.2	4.2	8.4	8.6	63.0	63.0
0.8	1.8	1.7	2.4	2.4	4.2	4.1	8.4	8.4	63.6	61.8
0.7	1.8	1.8	2.4	2.2	4.2	4.2	9.0	8.7	63.6	63.6
0.6	1.8	1.7	2.4	1.8	4.2	4.2	9.0	8.9	64.2	63.0
0.5	1.8	1.8	2.4	1.9	4.2	3.8	8.4	8.4	63.6	62.4
0.4	1.8	1.8	2.4	1.8	4.2	3.8	8.4	8.9	63.6	61.8
0.3	1.8	1.7	2.4	2.0	4.2	4.2	9.0	9.0	64.2	64.8
0.2	1.8	1.8	2.4	1.8	4.2	4.2	9.0	9.0	63.6	63.0

The PCM adjusted values from Table 5.20 have been plotted against the unadjusted final permeate concentration in Figure 5.34 for both DOC and UVA. The unadjusted size distribution was based on final filtrate concentration after an individual UF cycle. PCM adjusted size distributions were determined using C_{ro} values calculated from the instantaneous permeate concentration (C_p) and Equation 4.7. To avoid scaling confusion, C_{ro} values are normalized to initial bulk concentrations and displayed as C_{ro}^* values. The most significant difference between unadjusted UF data and data resulting from the implementation of the PCM occurs in the 10 kDa to 3 kDa size range. The unadjusted molecular weight distribution contains a larger percentage of material having a nominal molecular weight larger than 3 kDa. Another significant change occurs in the R2 size fraction. Without accounting for membrane rejection, 47% of the UV absorbing material and 55% DOC were calculated to be in the R2 size fraction. Alternatively, only 27% of the UV absorbing material and 32% of the DOC was calculated to be within the same size fraction after correction using the PCM.

5.3.3 – Continuous MW distribution

The molecular weight range of natural organic matter spans several orders of magnitude. Due to this large DOM range, a logarithmic scale has been used to analyze DOM molecular weight distribution. (Beyer 1991) used this approach coupled with a normal distribution to describe ultrafiltration data. The Weibull distribution has also been used to describe the observed distribution of DOM molecular weight. This approach has a high level of flexibility in fitting SWID data due to its two parameters

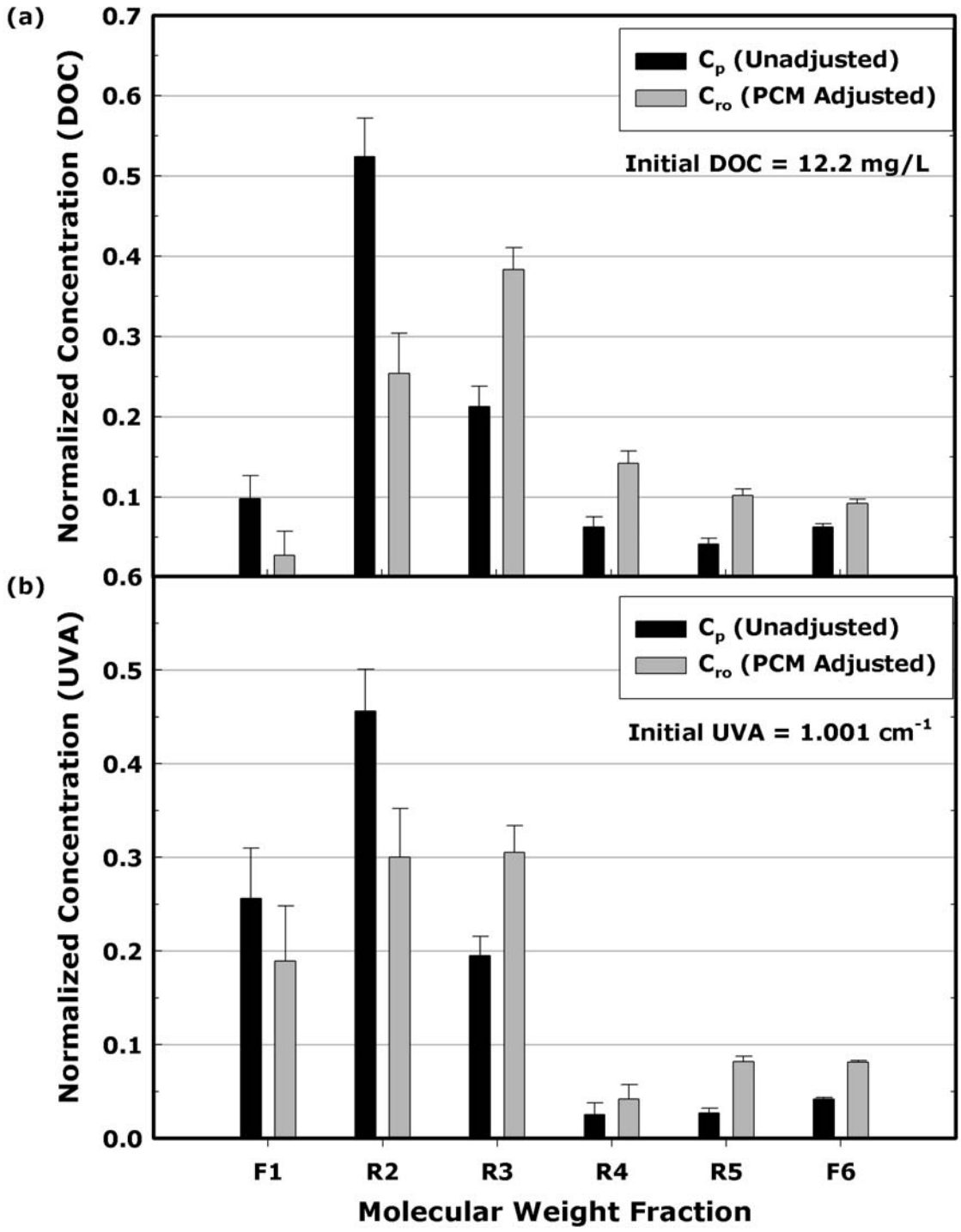

Figure 5.34 – PCM adjusted and unadjusted MW distribution of SWID bulk raw composite water based on (a) DOC and (b) UVA.

α and β (Kottegoda and Rosso 1997; Milton and Arnold 1995). The Weibull distribution has been used in these studies to estimate the MW distribution of DOM at SWID.

The two-parameter Weibull distribution is fit to PCM corrected permeate concentrations, C_{ro}^{*}, from each of the membranes used in the following experiments. Using the Weibull distribution, a number average molecular weight for SWID raw water UF data from section 5.3.2 was determined. The Weibull probability density function, *pdf*, and its associated cumulative distribution function, *cdf*, are presented in Equation 5.9 and Equation 5.10 respectively,

$$f(x) = \alpha\beta x^{\beta-1} e^{-\alpha x^{\beta}} \qquad \text{(Eq.5.9)}$$

$$F(x) = 1 - e^{-\alpha x^{\beta}} \qquad \text{(Eq.5.10)}$$

where alpha, α, and beta, β, are scale and shape parameters, respectively, and *x* equals log average molecular weight (AMW). Alpha and beta for each DOM fraction were determined by fitting the cumulative distribution function (Equation 5.10) to C_{ro}^{*} ultrafiltration data. A non-linear regression analysis based on the Levenberg-Marquardt algorithm was used to perform all curve fitting of Equation 5.10 to ultrafiltration data (Origin 7.5). Initial values for alpha and beta were determined by minimizing the sum of squares of deviations (χ^2) between the Weibull *cdf* and C_{r0}^{*} data points. The mean and variance of the Weibull distribution are described using the Gamma function (Γ) in the following equations (Milton and Arnold 1995):

$$\mu = \alpha^{-\frac{1}{\beta}} \Gamma\left(1 + 1/\beta\right) \qquad \text{(Eq.5.11)}$$

$$\sigma^2 = \alpha^{-\frac{2}{\beta}} \Gamma\left(1 + 2/\beta\right) - \mu^2 \qquad \text{(Eq.5.12)}$$

The Weibull *pdf* was assumed to describe the concentration of DOC as a function of molecular weight. Equation 5.11 describes the mean of the Weibull *pdf* and is mathematically considered to be equivalent to the number average molecular weight (AMW) of the continuous distribution (Beyer 1991). Average molecular weight based on mass (weight) may be determined separately from the AMW. The calculation of weight average molecular weight requires knowledge of the *Weight Fraction*, W_i, of each type of molecule (or the fraction of the total weight represented by each type of molecule). Weight fractions may be calculated from experimental data by determining the mass of an individual fraction of interest divided by the total mass in the system. It must be noted that 'number average' and 'weight average' are generally not the same. Distribution of molecular weights in a NOM sample is often described by the ratio of the weight average molecular weight to the number average molecular weight, which is defined as the Polydispersity Index (PDI).

The Weibull distribution was fit to PCM adjusted permeate data for both DOC and UVA. The results from section 5.3.2 were used to determine AMW distribution and the resulting average aggregate C_{ro}^* values for the eight trials are displayed in Figure 5.35 for both DOC and UVA. Dimensionless C_{ro}^* values derived from either DOC or UVA displayed similar MW distribution (95% correlation coefficient = 0.72 ±0.016) suggesting that UVA may be used to determine MW distribution without the need for DOC testing. However, DOC provides a better estimate of DOM concentration because it accounts for both UV absorbing material and non-UV absorbing material.

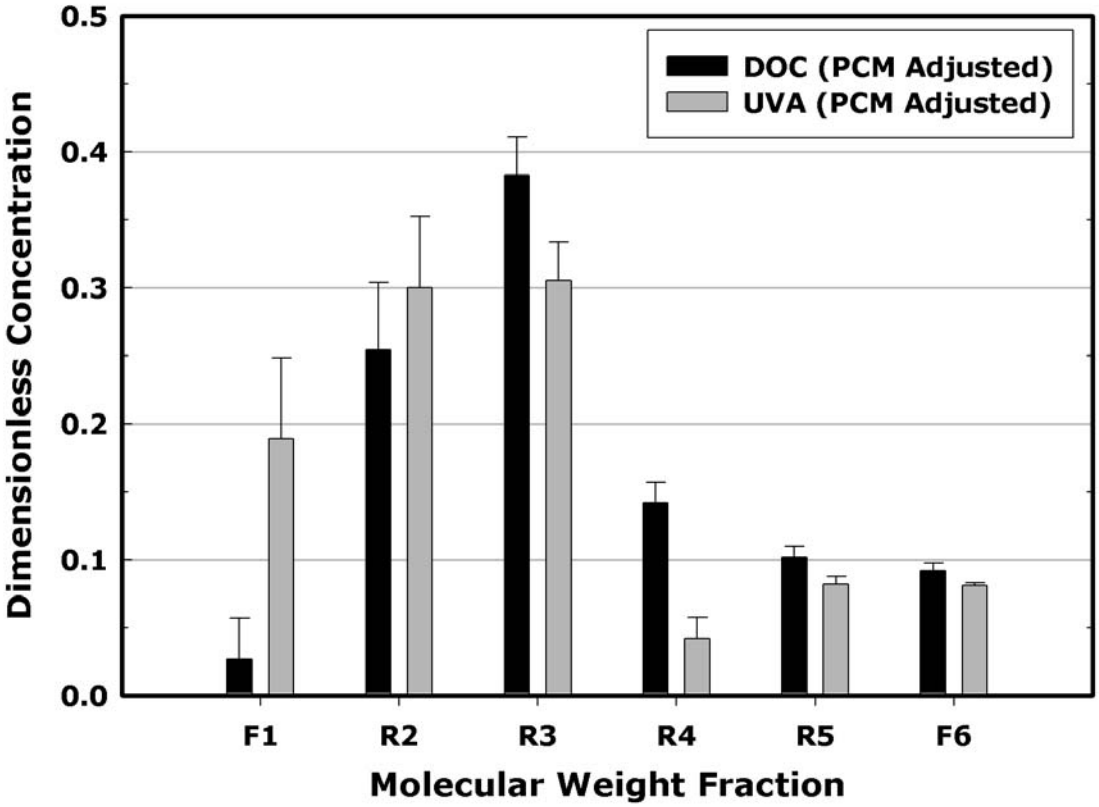

Figure 5.35 – PCM adjusted DOC and UVA data for eight (8) individual UF cycles using SWID raw composite water. Initial DOC concentration (DOC_i = 12.2 mg/L) and intial UVA (UVA_i = 1.001 cm^{-1}). (F1 > 30 kDa, 30 kDa > R2 > 10 kDa, 10 kDa > R3 > 3 kDa, 3 kDa> R4 > 1 kDa, 1 kDa > R5 > 0.5 kDa, 0.5 kDa > F6)

Figure 5.36 shows PCM adjusted DOC and UVA permeate values (C_{ro}*) for each UF membrane plotted on a logarithmic scale. The sigmoidal shape demonstrated by these points was fit using the Weibull cumulative distribution function (Equation 5.10). The Weibull *pdf* was subsequently plotted using Equation 5.9. Both curves are plotted in Figure 5.37. The Weibull *pdf* provides a clear visual representation of continuous DOM molecular weight distribution, showing the predominant size fraction as a single peak in the curve.

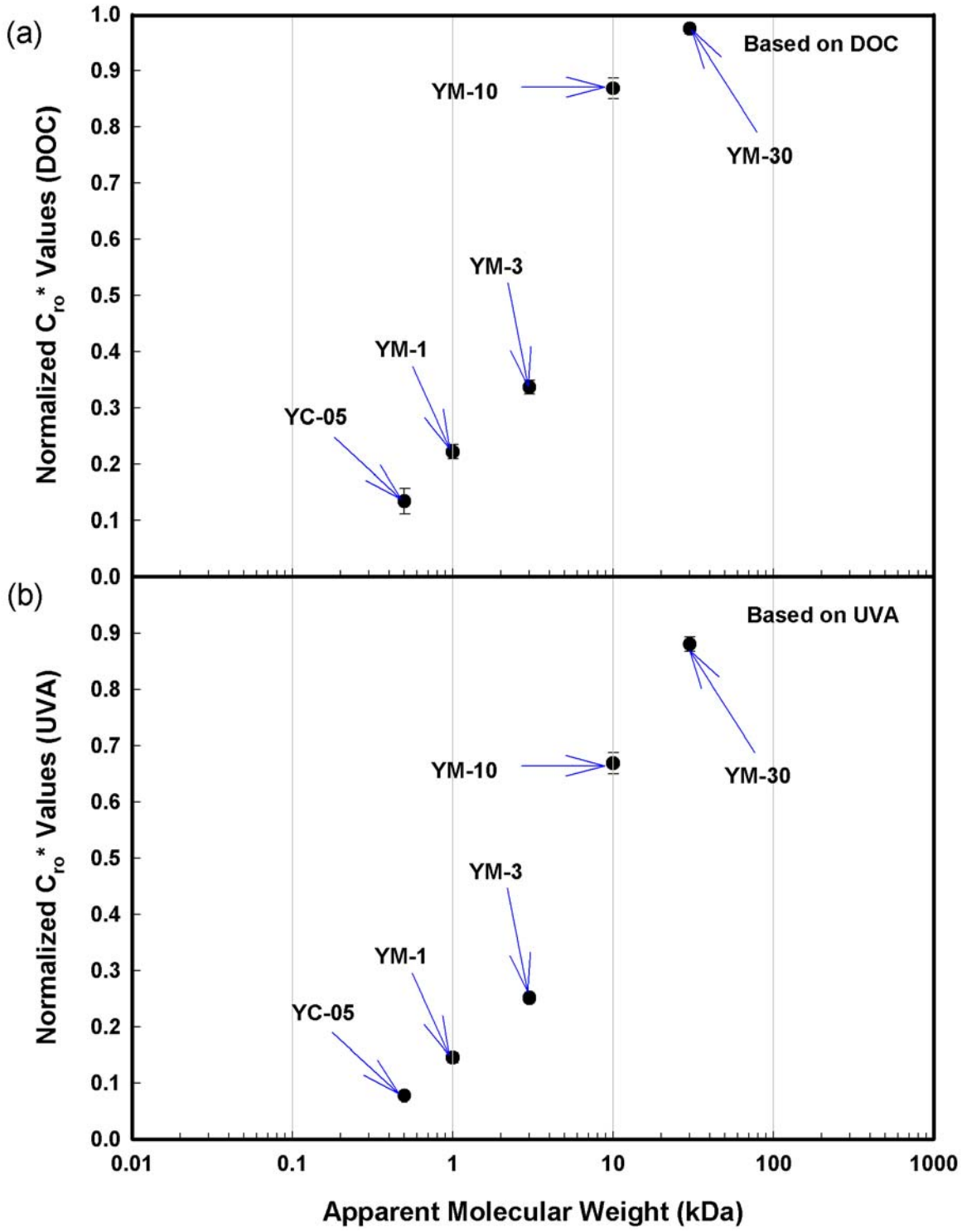

Figure 5.36 – PCM adjusted UF data plotted on a logarithmic scale based on (a) DOC and (b) UVA

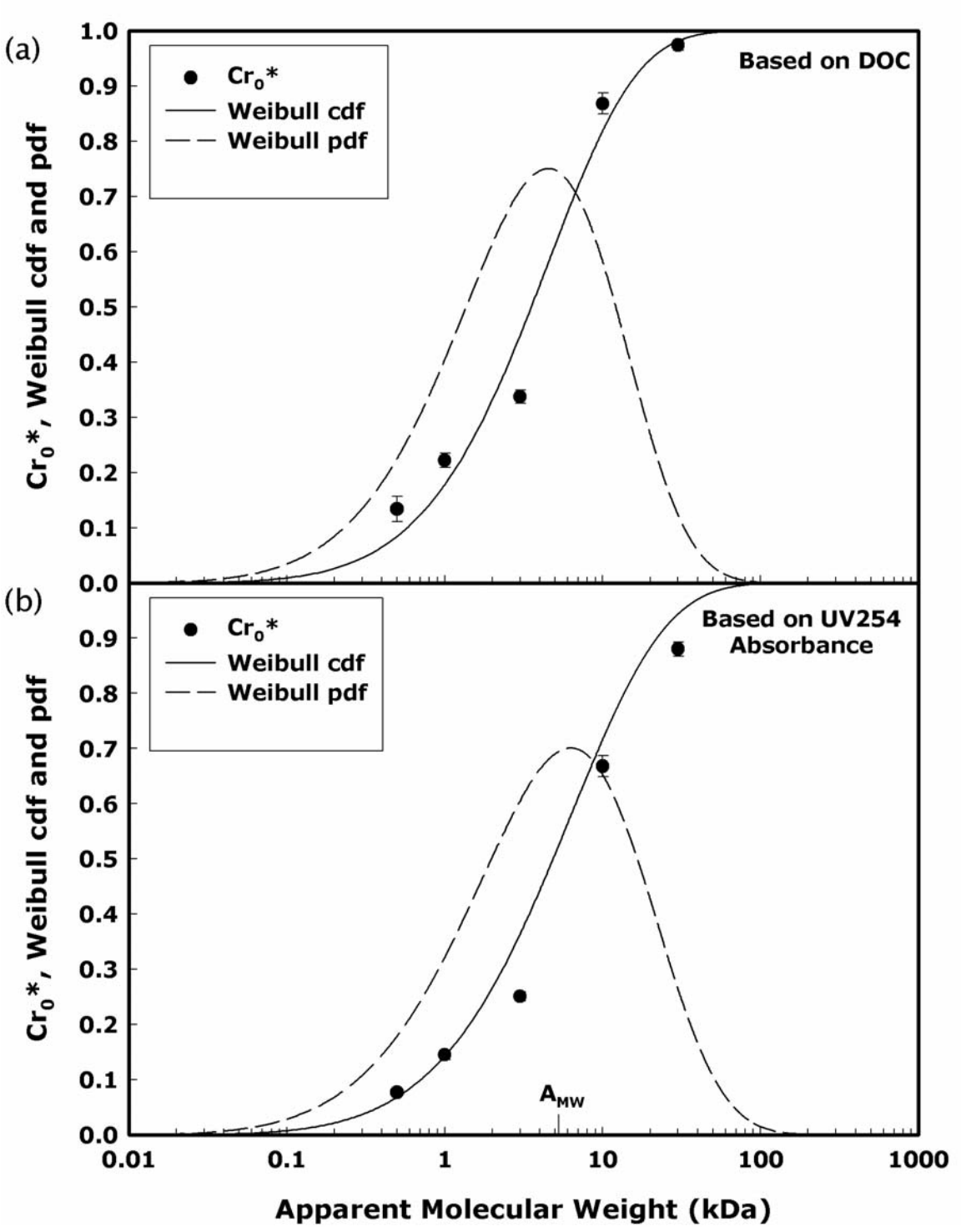

Figure 5.37 - Weibull *cdf* and *pdf* fit to PCM adjusted data for SWID raw water concentrations of (a) DOC and (b) UV254

5.3.4 – Number Average Molecular Weight Distribution

The PCM was used in conjunction with the Weibull distribution to determine number average molecular weight for reconstituted water collected from the SWID watershed. The overall compliance of the ultrafiltration data with the applied PCM model was verified by performing a repeatability study consisting of 8 ultrafiltration cycles using all membranes. Figure 5.37 illustrates the Weibull *cdf* and *pdf* fit to all data provided from the 8 UF trials with associated curve-fitting and statistical data provided in Table 5.21. The polydispersivity index (PDI) was calculated to demonstrate the ratio of mass average MW to number average MW. Number average molecular weight, based on DOC and UVA, was determined to be 3145 Da and 4172 Da, respectively. Due to the use of the logarithmic scale, the mean (μ) is represented as log (3145) or approximately 3.50 with standard deviations (σ) equal to ± 0.55. These values translate to an average MW between 11,220 Da and 891 Da, within 1 standard deviation. The change in molecular weight (Δ AMW $\pm\sigma_{AMW}$) has a value of 10,329 Da.

Although the range appears large for experimentally determined AMW values, statistical analysis must consider the MWCO of membranes used to perform serial separations of SWID DOM. Figure 5.38 illustrates this point by depicting the AMW and standard deviation of SWID DOM with respect to membranes used for experimental MW separations. Reproducibility studies revealed consistent observed AMW values and MW distributions as demonstrated in Table 5.22. The consistency of observed experimental AMW values is very high and standard deviations are relatively low with respect to the MWCO values used to distinguish MW fractions. Table 5.23 displays number average molecular weight (AMW) values for SWID raw water provided from each of the eight (8)

Table 5.21 – Curve fitting data for Weibull *cdf* based on both DOC and UVA for all data associated with eight (8) UF trials conducted using SWID bulk raw composite water

Overall Fit	Alpha α	Beta β	Chi Squared χ^2	Mean log (AMW)	PDI	Std. Dev. σ	Variance σ^2
Based on DOC	5.00E-05	7.53	0.0677	3.55	1.26	0.55	0.30
Based on UVA	6.30E-05	7.15	0.0361	3.62	1.48	0.60	0.36

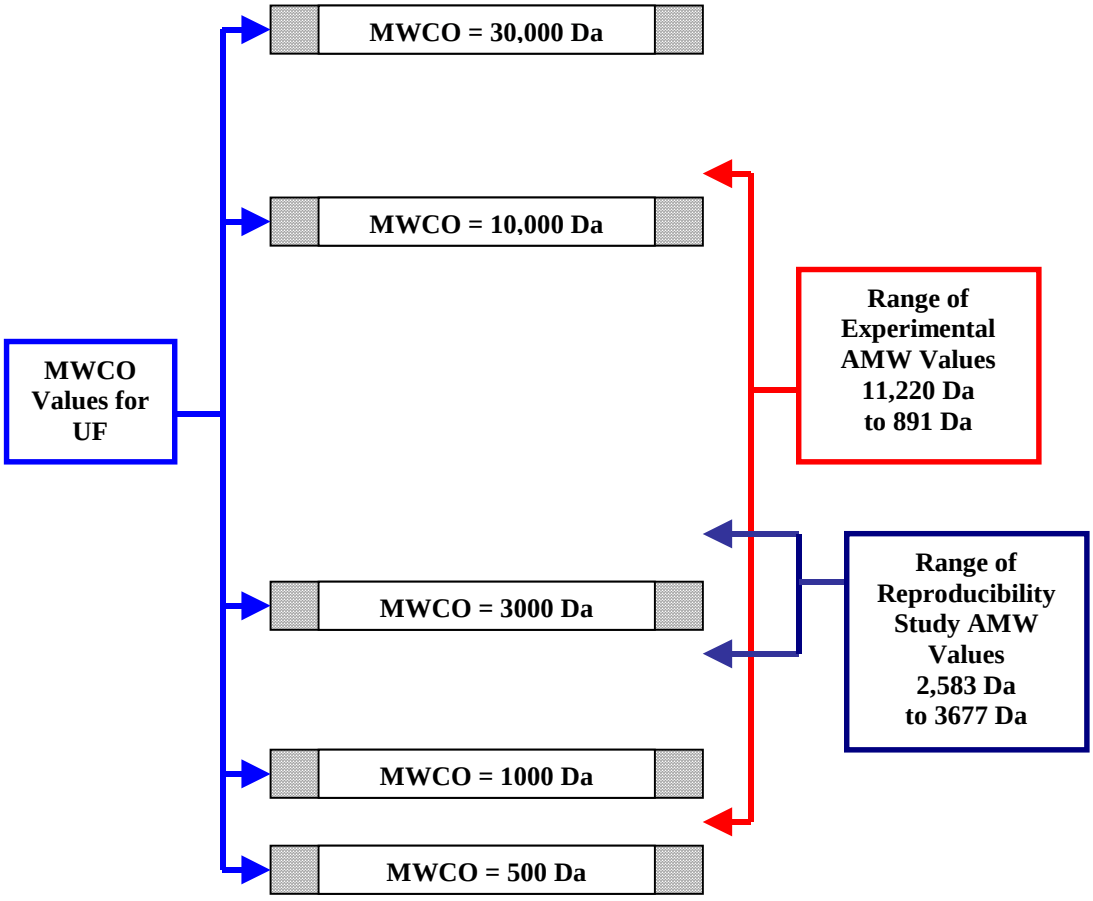

Figure 5.38 – Range of SWID raw composite AMW values with respect to MWCO values for UF membranes

Table 5.22 -Average molecular weight values for eight trials and overall AMW based on DOC and UV_{254} absorbance

Based on DOC			Based on UVA		
Trial #	A_{MW} (kDa)	Chi Squared (χ^2)	Trail #	A_{MW} (kDa)	Chi squared (χ^2)
1	3145	0.0394	1	4296	0.0248
2	2381	0.0278	2	3644	0.0395
3	3784	0.0714	3	4485	0.0647
4	3097	0.0652	4	4662	0.0541
5	2538	0.0497	5	4678	0.0834
6	3945	0.0554	6	3885	0.0642
7	3284	0.0521	7	4106	0.0445
8	2867	0.0297	8	4023	0.0374
Average			Average		
3130.13	±547.41		4222.38	±373.57	

individual UF cycles. C_{ro}^* ultrafiltration data and associated curve-fit Weibull *cdf*s and *pdf*s for SWID were used to determine the average MW distribution over the eight cycles. The AMW based on DOC and UVA, 3130 ±547 kDa and 4222 ±373 kDa, respectively, was determined using Equation 5.11 and C_{ro}^* values. Chi squared values describe the goodness of fit of the Weibull cumulative distribution function (Equation 5.10) for C_{ro}^* values. The associated overall probability density function for each data set was symmetrical about its mean, as expected for shape parameter values (β) of 4 and greater (Kottegoda and Rosso 1997). The symmetrical distribution associated with the high β values observed throughout the UF trials translates to a normal distribution for SWID DOM.

5.3.5 – Fractionated NOM analysis summary

These studies investigated molecular weight distribution of SWID DOM using parallel batch ultrafiltration. Initial results demonstrated the observed variation in permeate concentration over the course of an ultrafiltration cycle. A permeation coefficient model (PCM) was use to correct UF permeate data with respect to the fraction of volume filtered (Logan and Jiang, 1990). The Weibull distribution was used to fit discrete PCM corrected permeate data, yielding a continuous distribution and associated average molecular weight for individual UF trials. The average molecular weight (AMW) for SWID raw composite DOM was determined to be 3145 Da and 4172 Da based on DOC concentration and UVA, respectively. The polydispersivity coefficients, 1.26 and 1.48 measured with respect to DOC and UVA, respectively; suggest that the mass average molecular weight is 26% to 48% higher than the number average molecular weight in SWID raw composite samples.

A reproducibility study was conducted to determine the variability associated with observed SWID MW distribution and associated AMWs. Eight (8) individual UF trials conducted using SWID bulk raw composite water demonstrated a narrow range for both SWID bulk DOM distribution and AMW. The AMW based on DOC and UVA was determined to be 3130 ±547 kDa and 4222 ±373 kDa, respectively. These values are consistent with previously observed MW ranges for surface water NOM in the United States (Aiken et al. 1985; Amy et al. 1992; Assemi et al. 2004; Collins et al. 1986).

The response of SWID DOM to current and anticipated coagulation practices will be studied in the following section. Percent removal of each size class will be assessed

providing better insight as to which DOM size fractions are best removed by coagulation and coagulant doses effective in their removal.

5.4 – Coagulation and molecular weight distribution

Coagulation studies for removal of NOM have historically been conducted using bulk water characteristics to determine the efficacy of different coagulants. Recently due to the need for water utilities to meet tightening legislation more studies focusing on the major cause of THMs have been conducted. As discussed in the literature review chapter (chapter 2), the composition of water in terms of isolated size and chemical fractions can help determine which targeted removal methods are most effective for a particular source water. In this study, raw and treated SWID water have been isolated into MW fractions to determine which fractions are most amenable to removal by coagulation.

5.4.1 – <u>Coagulant dose</u>

SWID raw water was subjected to coagulation using alum ($Al_2(SO_4)_3 * 14H_2O$) and ferric sulfate ($Fe_2(SO_4)_3 * 9H_2O$) to observe effects of coagulant addition on MW distribution. Optimum pH values of 5.5 and 4.5 for alum and ferric sulfate (see section 5.2.2), respectively, were fixed for varying coagulant doses. Coagulant doses of 3, 10, 30, and 50 mg/L of alum or ferric sulfate were used to cover conventional, target percent removal, and optimum dose ranges established in section 5.2.1. The rapid mix procedure outlined in section 4.3 was applied to 1 L SWID bulk raw composite isolates. Coagulant doses of 3, 10, 30, and 50 mg/L of alum and ferric sulfate are hereafter referred to as alum 3, alum 10, alum 30, and alum 50 for alum and ferric 3, ferric 10, ferric 30, and

ferric 50 for ferric sulfate, respectively. The resulting settled water was filtered using a 0.45-μm Teflon filter and brought to standard pre-ultrafiltration conditions (pH 6.5, T=23 ºC, and ionic strength = 0.01 mM). C_{ro} data sets for each UF trial were fit using Equation 5.10 the resulting scale and shape parameters, as well as AMW values for individual coagulation trials, are presented in Table 5.23.

Table 5.23 - AMW values and scale/shape parameters for coagulated waters

	Scale Parameter (α)	Shape Parameter (β)	AMW (Da)	PDI	Standard Deviation -σ	Standard Deviation +σ
Alum 50	2.70E-04	6.57	1810	1.21	474	6864
Alum 30	8.00E-05	7.41	2256	1.21	656	7673
Alum 10	3.00E-05	8.06	2677	1.24	839	8607
Alum 3	2.00E-05	8.43	2549	1.24	843	7741
Ferric 50	5.80E-04	6.23	1191	1.14	315	4470
Ferric 30	2.20E-04	6.7	1916	1.21	508	7151
Ferric 10	4.00E-05	7.79	2836	1.23	843	9457
Ferric 3	2.00E-05	8.38	2694	1.24	881	8324

Discrete C_{ro}* values (based on DOC) for SWID raw bulk composite water are plotted with similar values for SWID raw bulk composite water treated with 3 mg/L and 50 mg/L of alum in Figure 5.39 (a). These data were fit using equation 5.10 to determine the Weibull *cdf* after coagulation with respective alum doses. These results are displayed in Figure 5.39 (b). It is clear from the data in Figure 5.39 that marginal differences occur between SWID raw composite water and that which is treated with 3 mg/L of alum. Additionally, large differences in C_{ro}* data are apparent between water treated with 50 mg/L alum and 3 mg/L alum however; the overall sigmodial shape of the data remains

the same. All curve fittings displayed chi-squared values less than 0.1, therefore representing an accurate fit to SWID C_{ro}* data (Tadanier, 2003). Therefore, all future data analysis will be conducted using the Weibull *cdf* and *pdf* fit to discrete data series. For the remaining coagulant doses, Weibull *cdfs* and *pdfs* were plotted using the data provided in Table 5.23 and Equations 5.9 and 5.10, respectively. These data are displayed for both alum and ferric sulfate in Figure 5.40 (Weibull *cdfs*) and Figure 5.41 (Weibull *pdfs*). Note again that all Weibull continuous distributions were fit to discrete filtrate PCM adjusted data.

Direct comparisons were conducted between SWID raw composite AMW distributions for coagulation with alum and ferric sulfate at doses of 3, 10, 30, and 50 mg/L. Low coagulant doses (Alum 3 and Ferric 3) demonstrated an initial increase in mid-range ($1000 < MW < 3000$) solute MW compounds. These results are displayed in Figure 5.42. The initial increase in mid-range DOM may be attributed to metal-humate complexes formed with low MW NOM molecules to form larger insoluble complexes followed by a continuous decrease in AMW with increasing coagulant dose. The low concentration of hydrolyzed metal species in solution may not provide sufficient binding capacity to aid in the complete removal of low MW active NOM. In addition, low concentrations of aluminum hydroxide decrease the potential for low to mid-range MW species to be removed during sedimentation through particle adsorption.

Figure 5.43 and Figure 5.44 display data for SWID raw composite water treated with 10 mg/L and 30 mg/L of coagulant, respectively. Notice in both figures that the area under the Weibull *pdf* curve for ferric sulfate is less than the area under the Weibull *pdf*

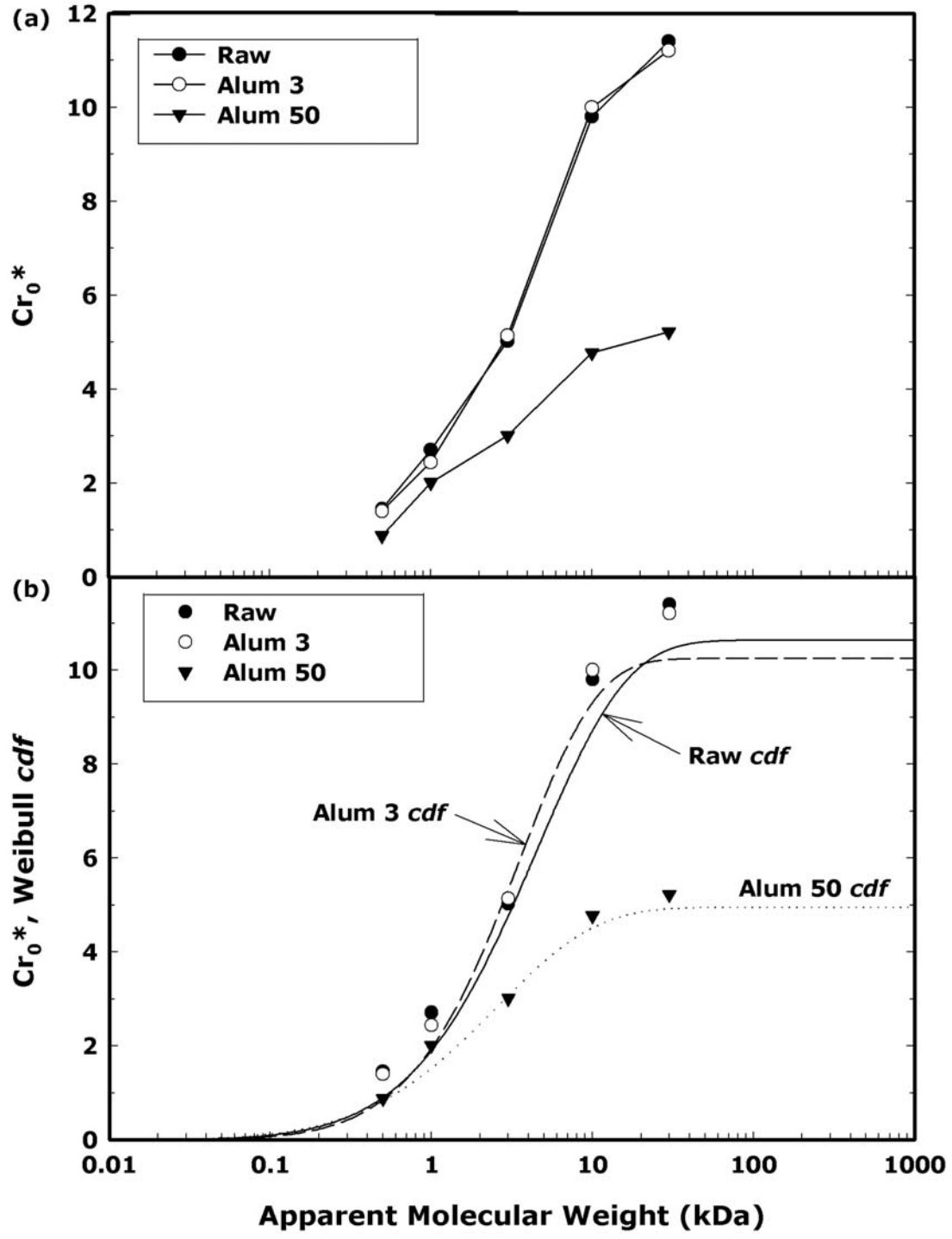

Figure 5.39 – (a) C_{ro}* data (based on DOC) plotted on a logarithmic scale for SWID bulk raw composite water and the same water after coagulation with 3 mg/L and 50 mg/L of alum. (b) Weibull *cdf* fit to C_{ro}^{*} data

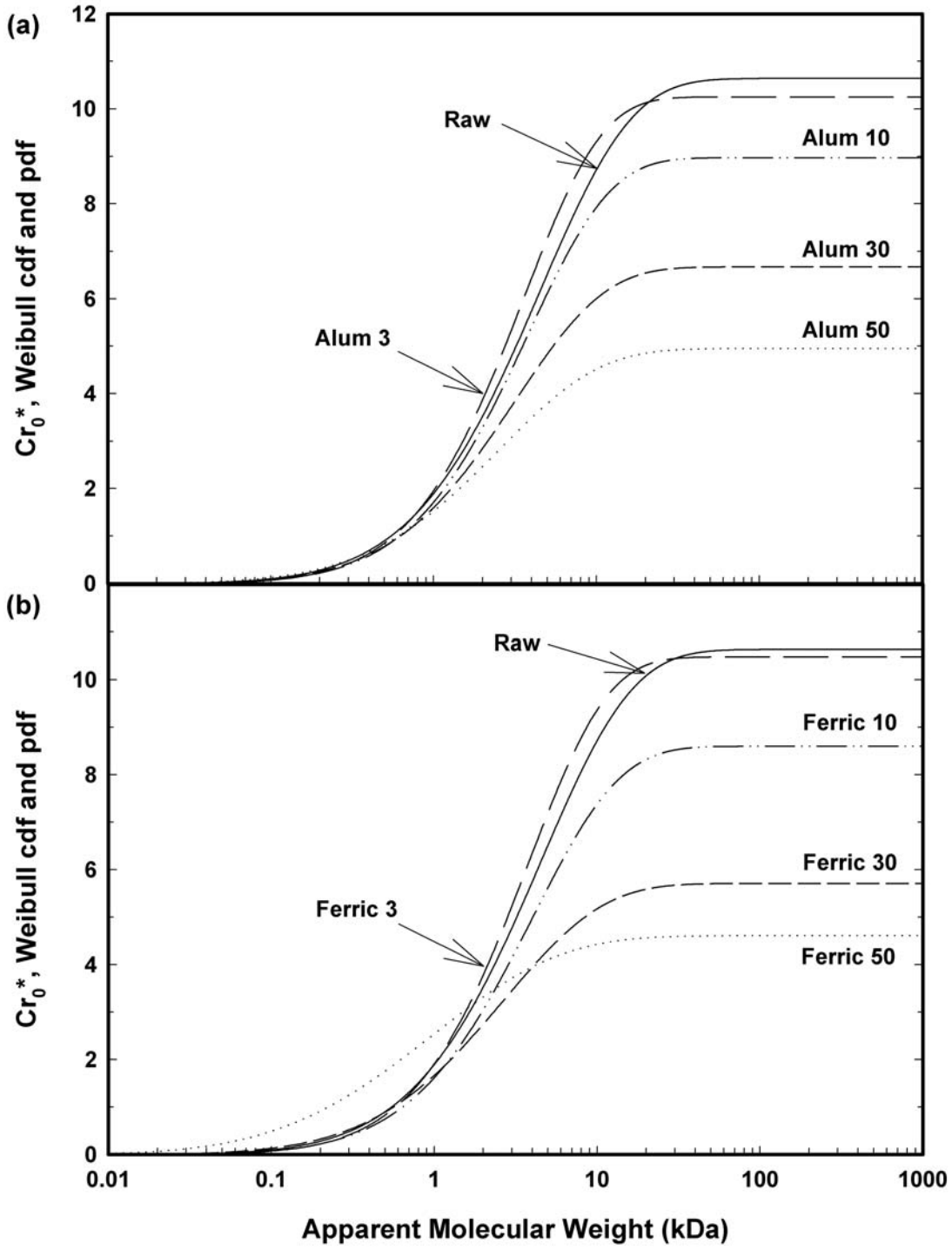

Figure 5.40 - Overall *cdf* comparison for treatment with varying doses of (a) alum and (b) ferric sulfate

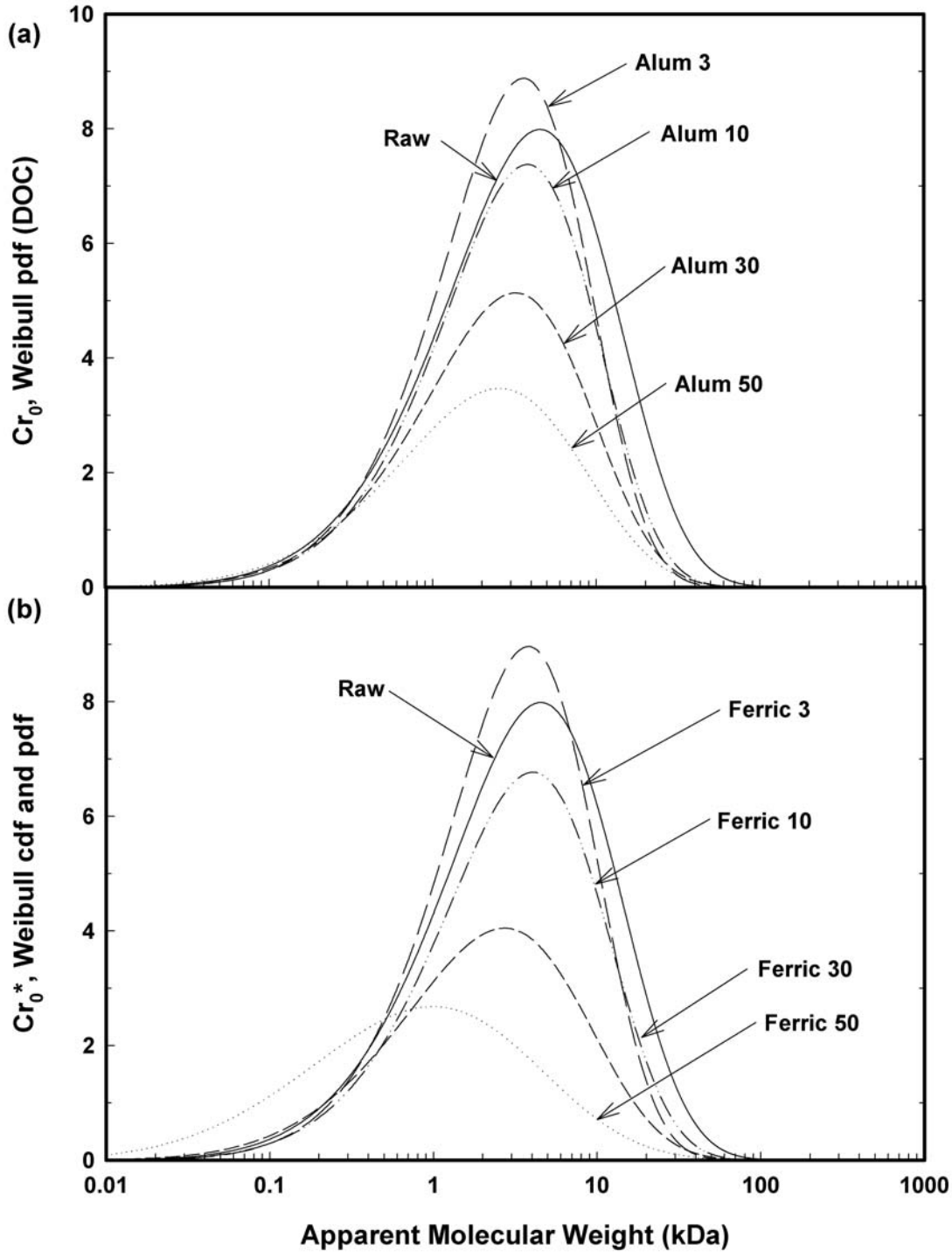

Figure 5.41 - Overall *pdf* comparison for treatment with varying doses of (a) alum and (b) ferric sulfate

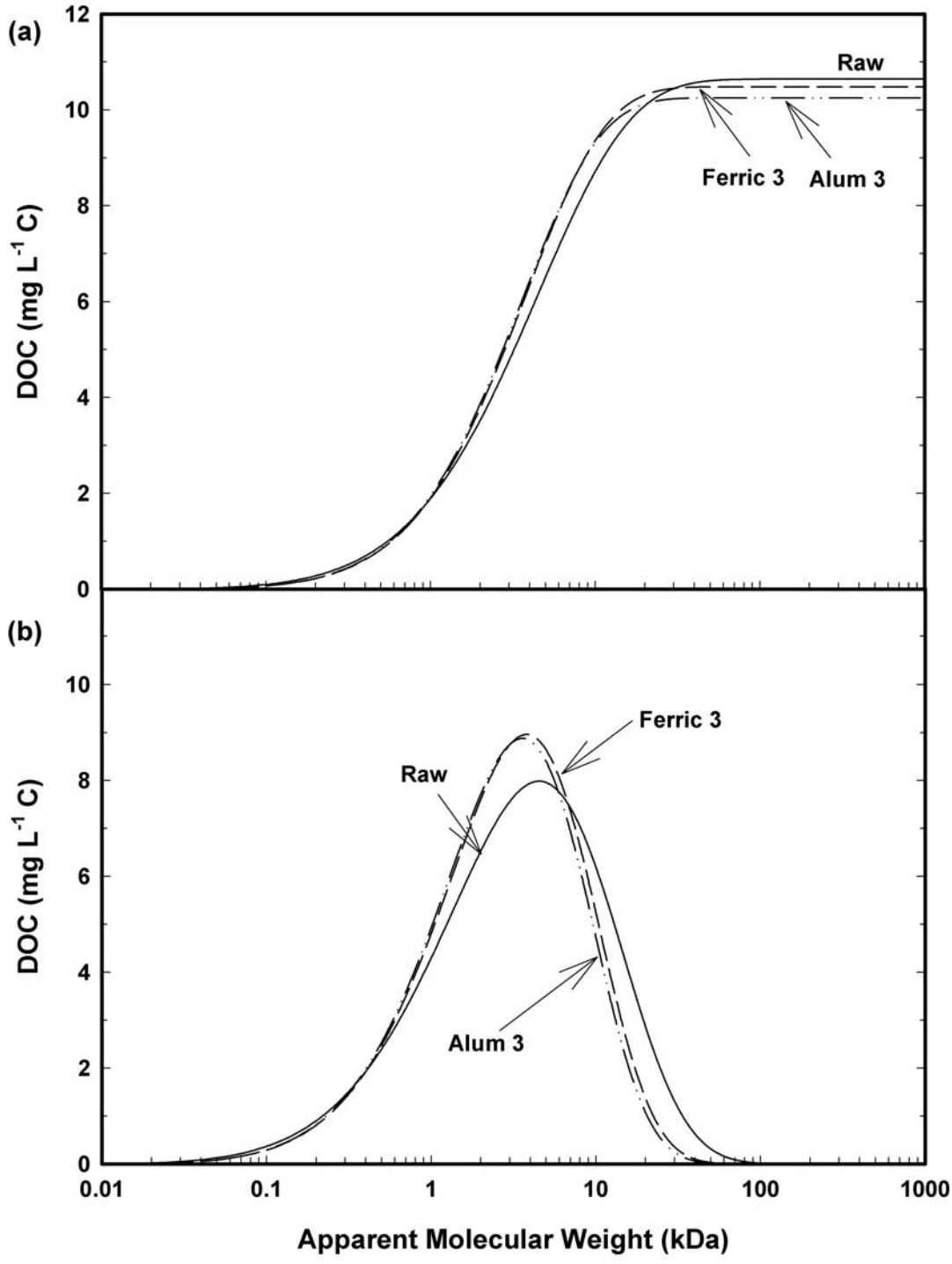

Figure 5.42 - Weibull (a) *cdf* and (b) *pdf* comparison for SWID treated water at coagulant concentrations of 3 mg/L

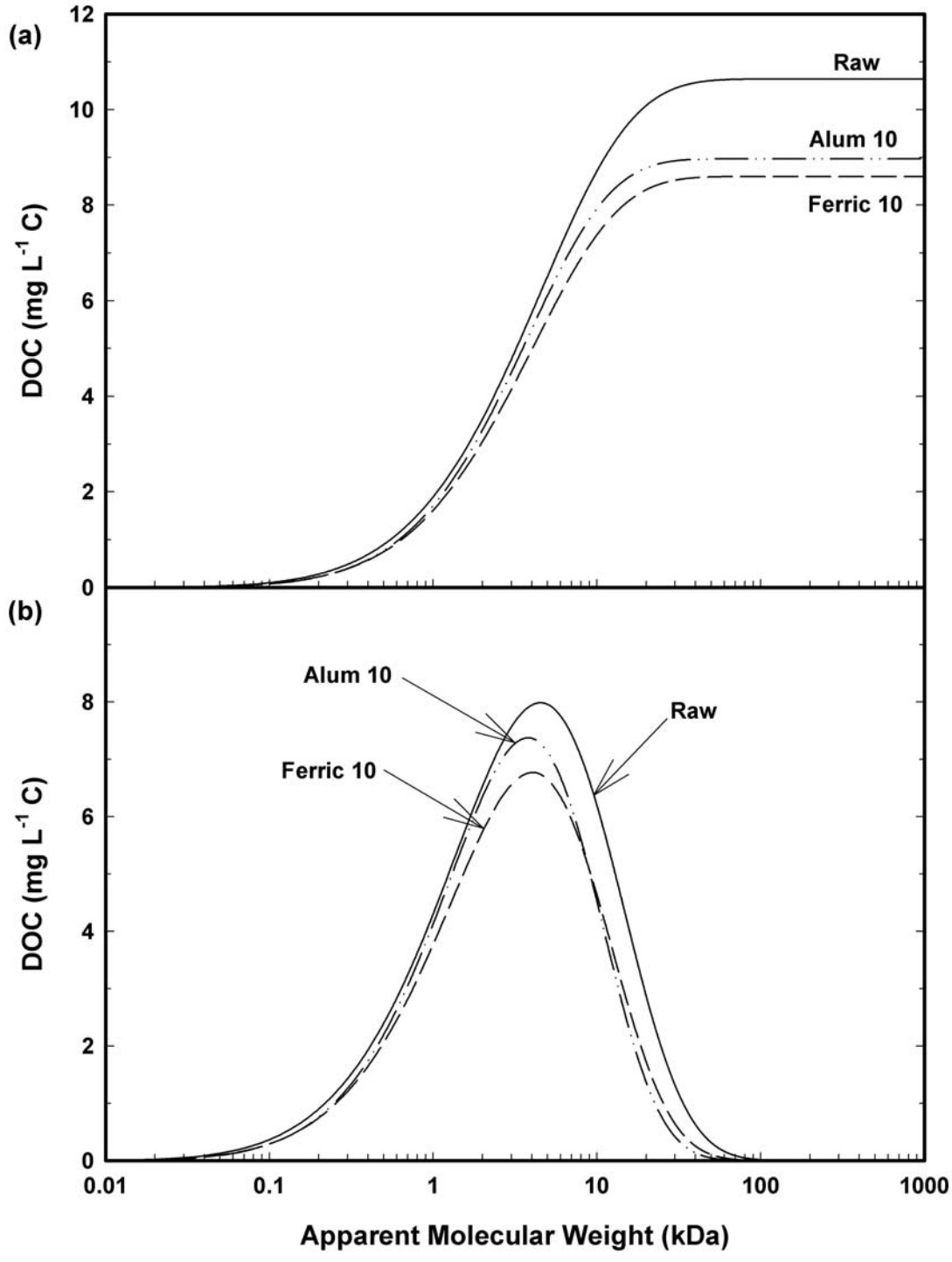

Figure 5.43 - Weibull (a) *cdf* and (b) *pdf* comparison for SWID treated water at coagulant concentrations of 10 mg/L

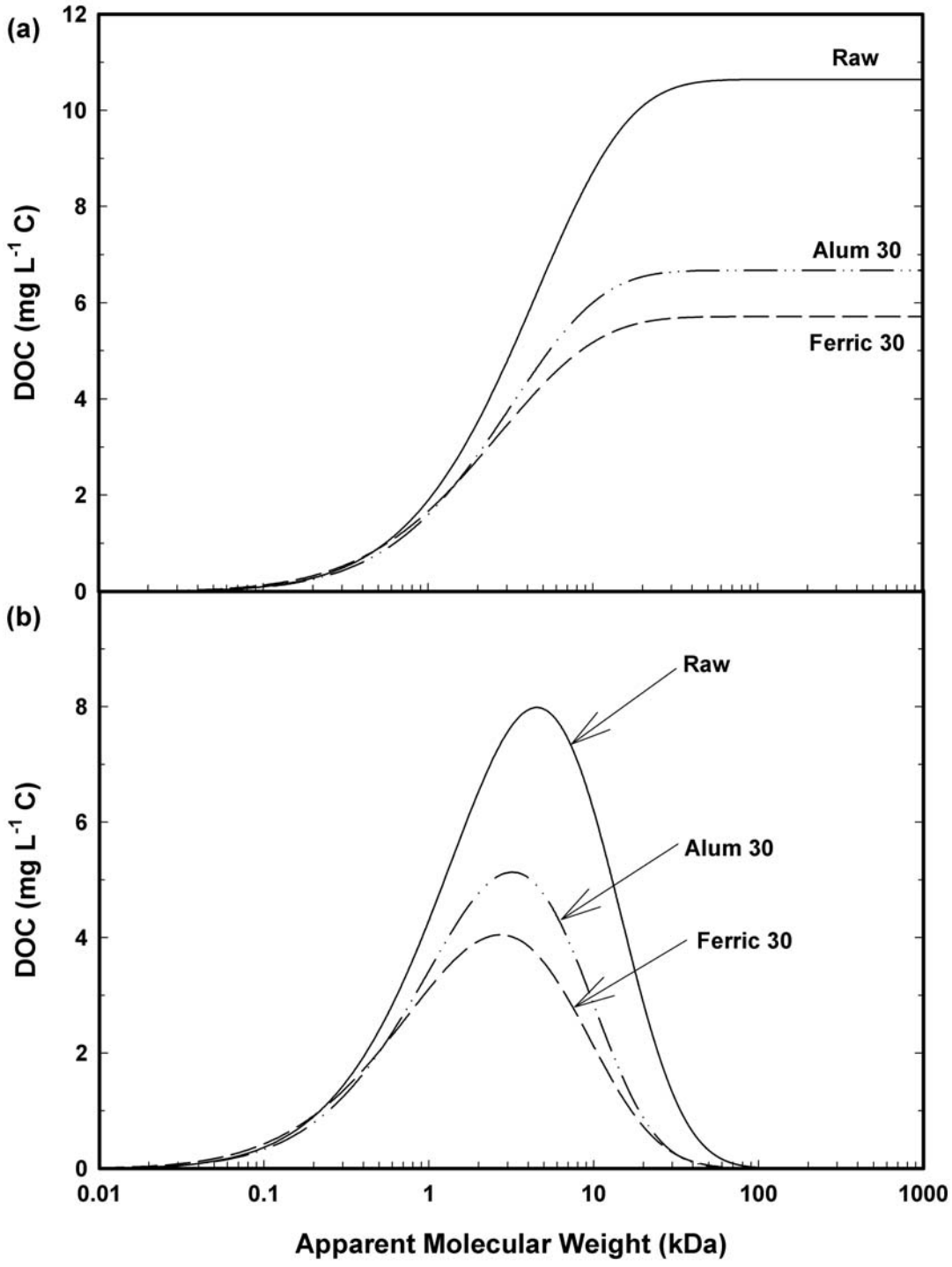

Figure 5.44 - Weibull (a) *cdf* and (b) *pdf* comparison for SWID treated water at coagulant concentrations of 30 mg/L

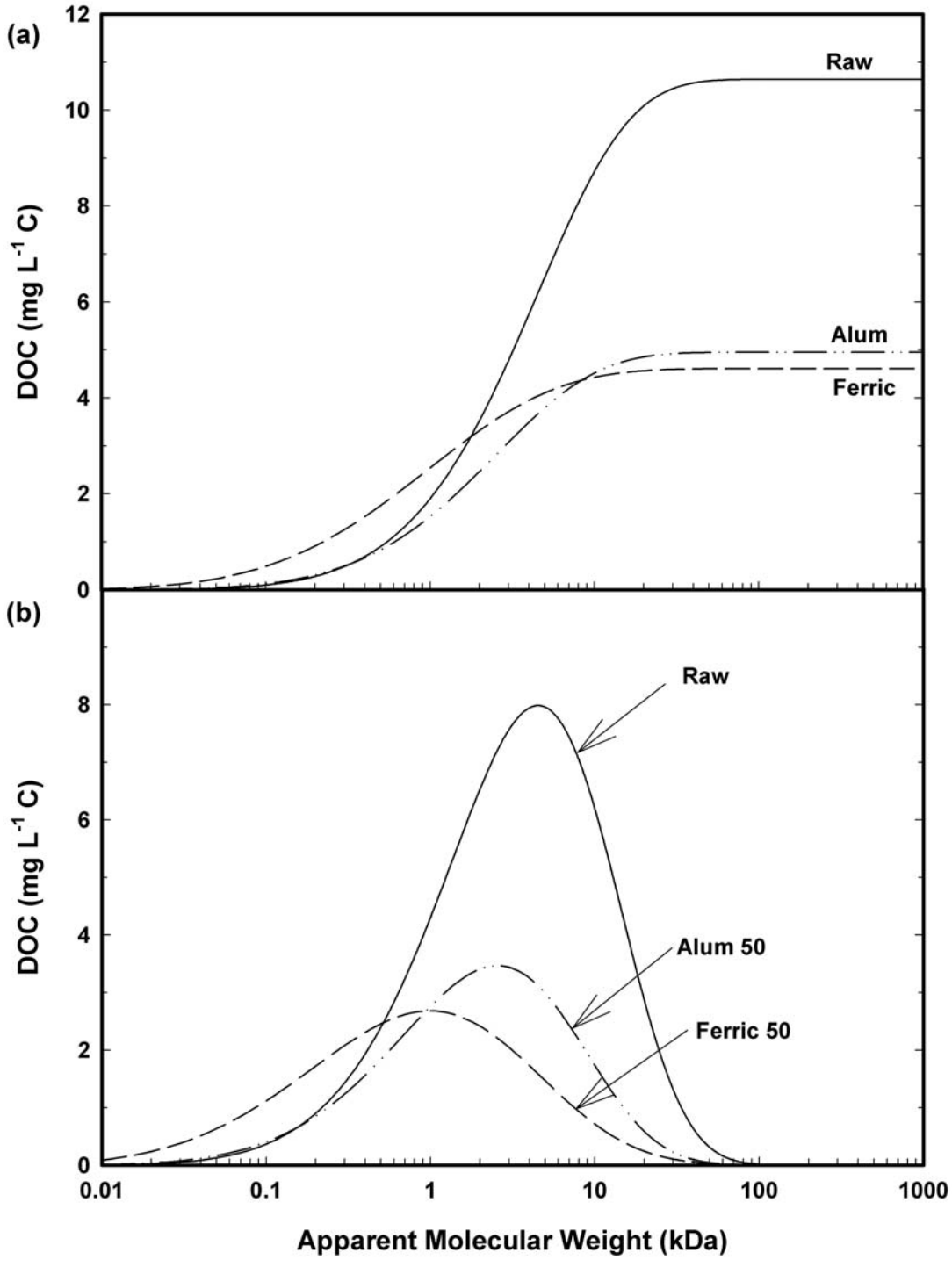

Figure 5.45 - Weibull (a) *cdf* and (b) *pdf* comparison for SWID treated water at coagulant concentrations of 50 mg/L

for alum at equivalent coagulant doses, indicating that ferric sulfate removes slightly more DOC overall. In both figures the MW distribution of alum and ferric sulfate treated water appears to be similar. Figure 5.45 displays SWID raw composite water treated with alum and ferric sulfate at 50 mg/L. The difference between AMW values associated with the Weibull *pdf* for each coagulant is the greatest at this coagulant dose. Figure 5.45 demonstrates that larger portions of DOM have a MW < 1000 Da after treatment with 50 mg/L of ferric sulfate compared to alum.

The concentration of DOC present in each MW fraction and SWID raw composite water after coagulation at specified coagulation doses is presented in Table 5.24 and Table 5.25 for alum and ferric sulfate, respectively. Figure 5.46 and Figure 5.47 display the information in the tables graphically for alum and ferric sulfate, respectively. The largest portion of DOC occurred in the 3,000 Da to 10,000 Da, R3, size class. However, a high percent removal of the 10,000 Da and greater, F1 and R2, size fraction was also observed. Percent reduction of each MW fraction with respect to coagulant dose is displayed in Table 5.26 and Table 5.27 for alum and ferric sulfate, respectively. The 500 – 1000 MW fraction, R5, displayed the lowest percent removal of any size fraction for both alum and ferric sulfate. The 3000 to 30,000 Da MW fraction, F1, R2, and R3 fractions, was most amenable to removal by coagulation. This is consistent with previous experiments conducted on NOM coagulation (Dryfuse 1995; Dryfuse et al. 1995; Goslan 2004) which all displayed significant removal of NOM with MW greater than 3 kDa.

Ferric sulfate generally removed a larger percentage of NOM with respect to DOC over all MW fractions with the exception of low MW (< 1.0 kDa) fractions. Alum demonstrated higher removal of the R5 and F6 fraction at optimum coagulant dose.

However, ferric sulfate demonstrated better overall removal of DOC at every coagulant dose with the exception of the lowest coagulant dose tested (3 mg/L). This may be attributed to increased reactivity of iron in the natural environment, where more active binding sites are available for dissolved iron complexes.

Table 5.24 – DOC concentration for SWID raw composite water and UF separated MW fractions for varying alum dose.

	DOC (mg/L)						
	Total	**F1**	**R2**	**R3**	**R4**	**R5**	**F6**
SWID Raw	12.2	1.26	0.96	6.24	1.58	1.14	1.02
Alum 3	11.75	1.02	0.80	5.99	1.52	1.19	1.08
Alum 10	10.28	0.35	0.66	5.09	1.47	1.14	1.03
Alum 30	7.65	0.06	0.37	3.26	1.48	1.07	0.86
Alum 50	5.68	0.04	0.26	1.92	1.21	1.05	0.78

Table 5.25 – DOC concentration for SWID raw composite water and UF separated MW fractions for varying ferric sulfate dose.

	DOC (mg/L)						
	Total	**F1**	**R2**	**R3**	**R4**	**R5**	**F6**
SWID Raw	12.2	1.26	0.96	6.24	1.58	1.14	1.02
Ferric 3	12.02	0.95	0.89	6.14	1.47	1.24	1.11
Ferric 10	9.86	0.41	0.58	4.67	1.55	1.18	1.02
Ferric 30	6.55	0.07	0.34	2.20	1.51	1.06	0.91
Ferric 50	4.60	0.03	0.08	1.09	1.06	1.10	0.89

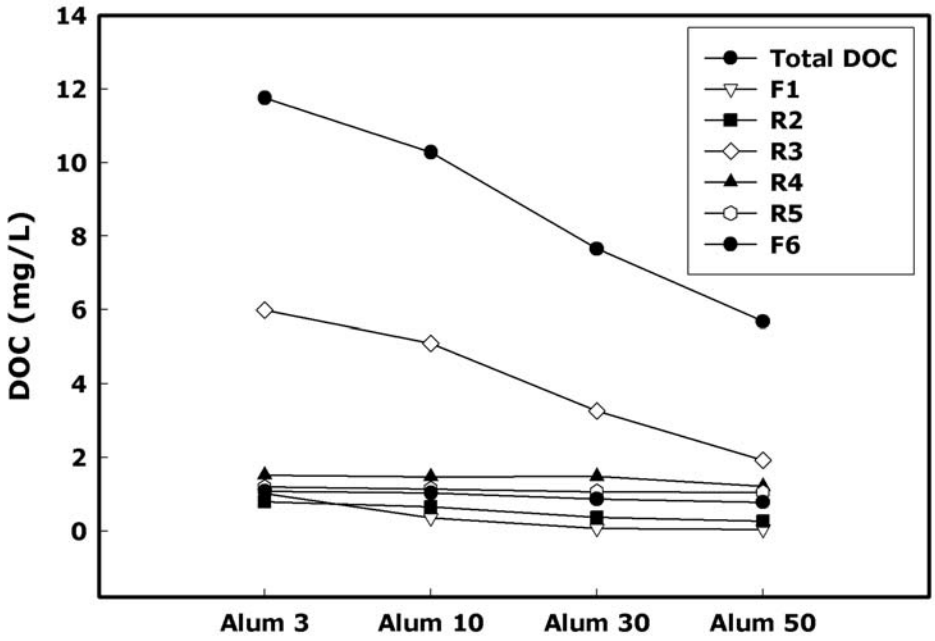

Figure 5.46 – DOC removal with respect to alum dose for MW fractions and SWID raw composite water.

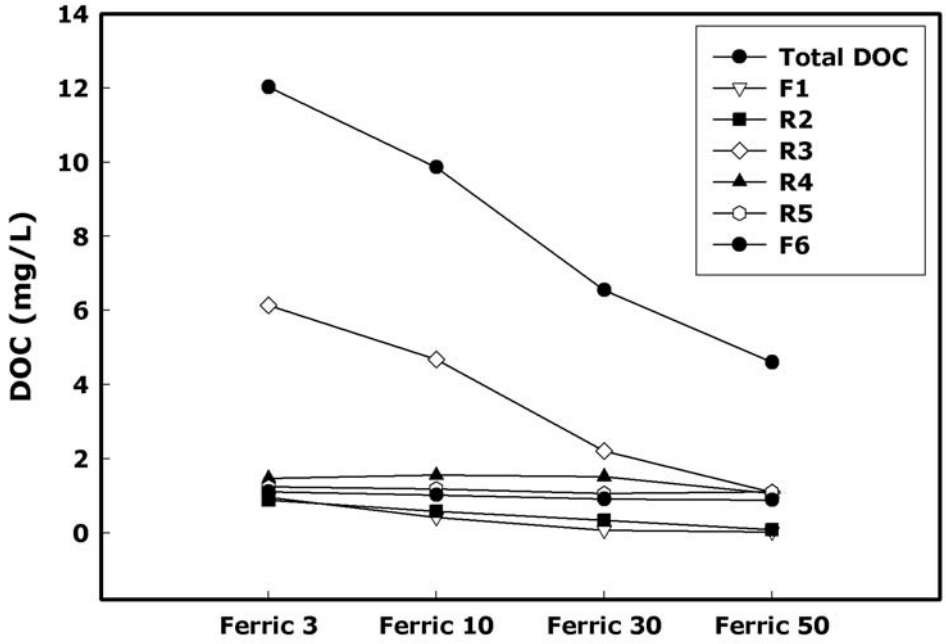

Figure 5.47 – DOC removal with respect to ferric sulfate dose for MW fractions and SWID raw composite water.

Table 5.26 - Percent reduction of DOC MW fractions by alum coagulation

Fraction	Nominal Size (Daltons)	Alum 50	Alum 30	Alum 10	Alum 3
		% Reduction			
Total	N/A	53.48	37.31	15.70	3.67
F1	> 30K	96.61	95.44	72.38	19.33
R2	10K-30K	72.80	61.88	30.99	16.63
R3	3K-10K	69.32	47.82	18.44	4.03
R4	1K-3K	23.28	6.02	6.71	3.72
R5	0.5K-1K	7.50	5.75	-0.07	-4.82
F6	<0.5K	23.12	15.74	-1.23	-6.13

Table 5.27 - Percent reduction of solute MW fractions by alum

Fraction	Nominal Size (Daltons)	Ferric 50	Ferric 30	Ferric 10	Ferric 3
		% Reduction			
Total	N/A	62.31	46.33	19.17	1.50
F1	> 30K	97.26	94.14	67.63	24.69
R2	10K-30K	91.19	64.23	39.51	7.85
R3	3K-10K	82.48	64.71	25.30	1.70
R4	1K-3K	32.74	4.22	1.90	6.48
R5	0.5K-1K	3.07	7.10	-3.94	-9.12
F6	<0.5K	12.81	11.32	0.27	-8.51

5.4.2 – Coagulation and pH

Coagulation pH is a critical factor in maximizing DOC removal, affecting the charge density of humic substances and determining the type of hydrolyzed and polymeric metal species present after coagulant addition. Natural organic matter maintains a predominately negative charge at the pH of natural water (Sharp et al. 2004), hence, cationic additives such as metal coagulants and cationic polyelectrolytes have a strong affinity for NOM. This characteristic gives rise to the importance of coagulation as a vital unit process when treating a water source for the removal of organic matter (e.g., (Lind 1995; Volk et al. 2000).

SWID raw composite water was treated with varying coagulant doses over a predetermined pH range established for optimum DOC removal (see section 5.2.2). The pH range for alum and ferric sulfate coagulation was set at $5.0 \leq pH \leq 6.0$ and $4.0 \leq pH \leq 5.0$, respectively (see section 5.2.1). Aliquot volumes of settled water were prepared and fractionated as described in section 5.3. The procedure used to fit the Weibull distribution to PCM corrected filtrate DOC concentration values, C_{ro}^{*}, were identical to the procedure described previously in section 5.3.3. In these trials, coagulation pH was varied and various coagulant doses were used to determine the effect of coagulation pH on MW size removal. Average MW values and respective shape and scale parameters at various coagulant concentrations and pH values are displayed in Table 5.28 for alum and Table 5.29 for ferric sulfate. Alum and ferric sulfate generally demonstrated the lowest average molecular weight of each fraction at pH values of 4.5 and 5.5 for ferric sulfate and alum respectively and high coagulant dose (alum 50 and ferric 50). This point is

Table 5.28 - Scale and shape parameters for the Weibull distribution and AMW values for variable alum concentrations and pH

	Scale Parameter (α)	Shape Parameter (β)	AMW (Da)	PDI	Standard Deviation - σ	Standard Deviation + σ
pH = 6.0						
Alum 50	1.98E-04	6.72	2091	1.22	550	7937
Alum 30	7.64E-05	7.18	3197	1.29	854	12101
Alum 10	1.89E-05	8.26	3302	1.24	1029	10618
Alum 3	5.01E-05	7.36	3991	1.35	1055	15073
pH = 5.5						
Alum 50	2.70E-04	6.57	1810	1.20	474	6864
Alum 30	8.00E-05	7.41	2256	1.21	656	7673
Alum 10	3.00E-05	8.06	2677	1.23	839	8607
Alum 3	2.00E-05	8.43	2549	1.23	843	7741
pH = 5.0						
Alum 50	2.86E-04	6.61	1605	1.18	433	5925
Alum 30	1.04E-04	7.18	2269	1.22	643	8150
Alum 10	1.78E-05	8.26	3507	1.25	1082	11360
Alum 3	4.97E-05	7.26	4673	1.46	1184	18434

Table 5.29 - Scale and shape parameters and AMW values for variable ferric sulfate concentrations and pH

	Shape Parameter (α)	Shape Parameter (β)	AMW (Da)	PDI	Standard Deviation - σ	Standard Deviation + σ
pH = 5.0						
Ferric 50	3.11E-04	6.55	1579	1.18	423	5889
Ferric 30	9.72E-05	7.03	3035	1.29	793	11614
Ferric 10	5.31E-05	7.5	3073	1.25	867	10895
Ferric 3	2.63E-05	8.15	2740	1.23	864	8693
pH = 4.5						
Ferric 50	5.80E-04	6.23	1188	1.15	315	4470
Ferric 30	2.20E-04	6.7	1907	1.21	508	7151
Ferric 10	4.00E-05	7.79	2824	1.23	843	9457
Ferric 3	2.00E-05	8.38	2708	1.24	881	8324
pH = 4.0						
Ferric 50	4.92E-04	6.36	1209	1.14	328	4454
Ferric 30	1.78E-04	6.62	2733	1.33	673	11086
Ferric 10	2.94E-05	7.94	3188	1.24	955	10642
Ferric 3	2.69E-05	8.07	2957	1.24	912	9587

further illustrated in Figure 5.48 and Figure 5.49 for the AMW of treated SWID raw composite water at each coagulant dose and coagulation pH. Increasing coagulant addition reduced the average molecular weight of NOM in treated waters. This may be attributed to the deposition of large NOM fractions, which are most amenable to removal by coagulation (Crozes et al. 1995) and (Amy et al. 1992), suggest that at lower pH values (e.g., pH < 5.5), humic molecules become highly protonated and coagulating species become more positively charged, increasing the likelihood of NOM removal by adsorption onto, or ion exchange with, metal hydroxides. Coagulation at pH = 4.0 and 50 mg/L ferric sulfate yielded the lowest average molecular weight observed throughout the coagulation studies. However, both coagulants demonstrated the least effective removal of the < 500 Da (F6) size fraction. These data are consistent with previous studies conducted by Pierce (2004) and (Jiang and Graham 1998), which both demonstrated that lower NOM MW fractions are recalcitrant to removal by coagulation. The increased removal of mid to high MW fractions (e.g., 3,000 to 10,000 Da) by coagulation with ferric sulfate may be attributed to the overall lower minimum solubility of Fe(III) compared to Al(III), 20 nM and 2.0 μM, respectively (Gregory and Jinming 2001). The low solubility of Fe(III) promotes the formation of ferric hydroxide at low dissolved metal concentrations, thereby increasing the number of potential reactive adsorption sites for NOM molecules which is the primary method of NOM removal for mid to high MW humic molecules during coagulation (Gregory and Jinming 2001).

Figures 5.50 thru 5.53 display Weibull *cdfs* and *pdfs* based on PCM adjusted filtrate values, C_{ro}^{*}, for alum treated water with coagulant concentration varying from 3mg/L to 50 mg/L at three different pH values. Weibull *pdf*s demonstrated similar MW

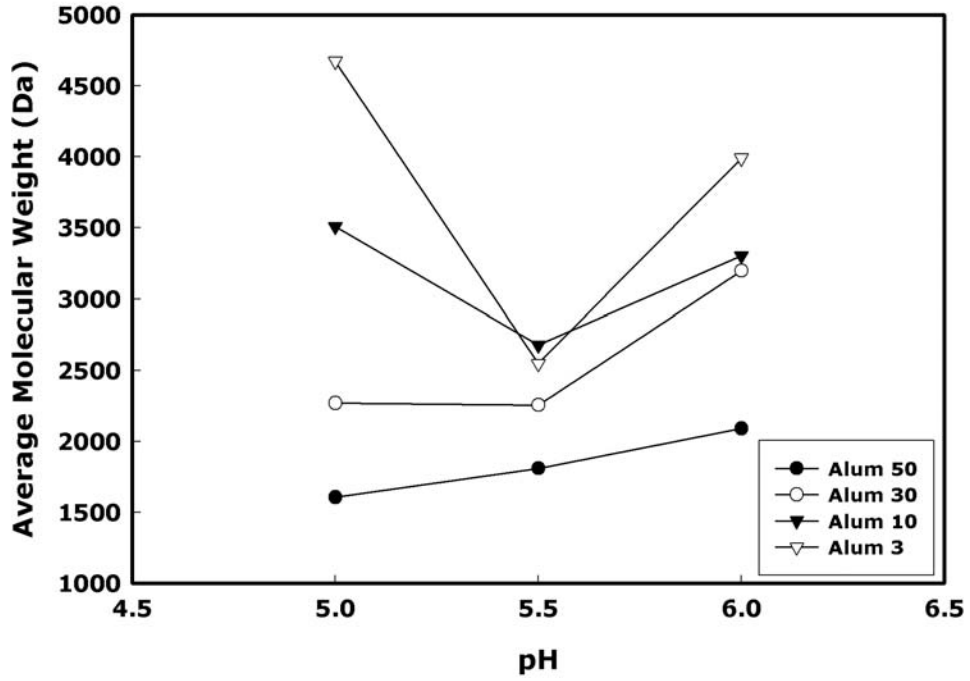

Figure 5.48 – Number average molecular weight as a function of pH and alum dose

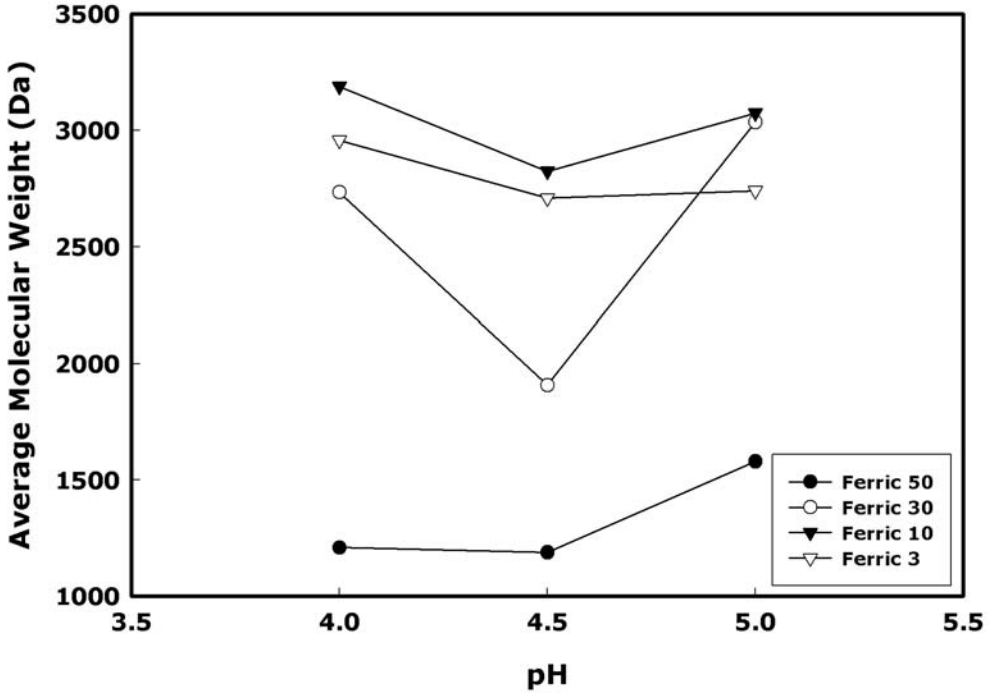

Figure 5.49 – Number average molecular weight as a function of pH and alum dose

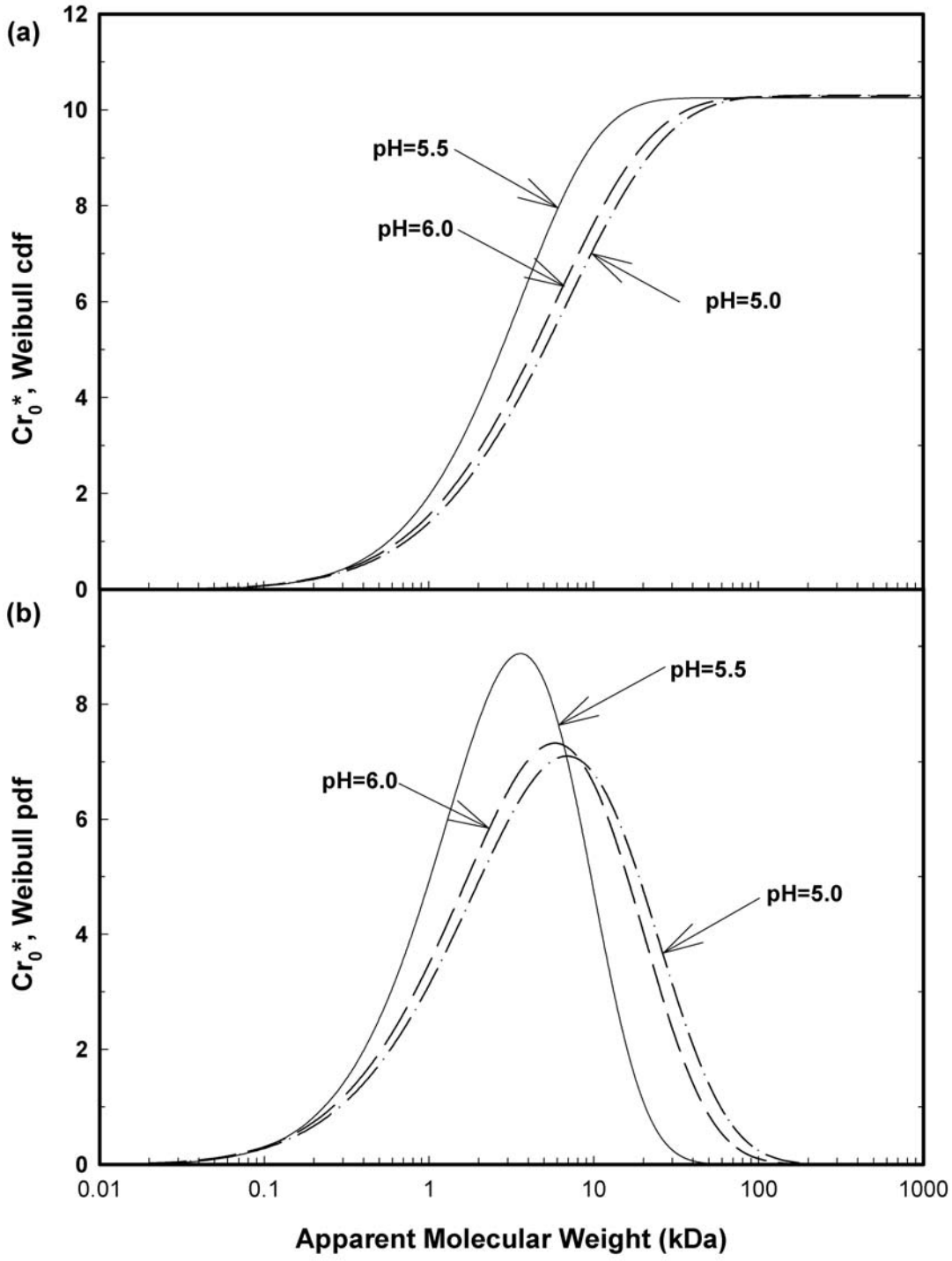

Figure 5.50 - Weibull (a) *cdf* and (b) *pdf* comparison for alum 3 treated water at pH 5.0, 5.5, and 6.0.

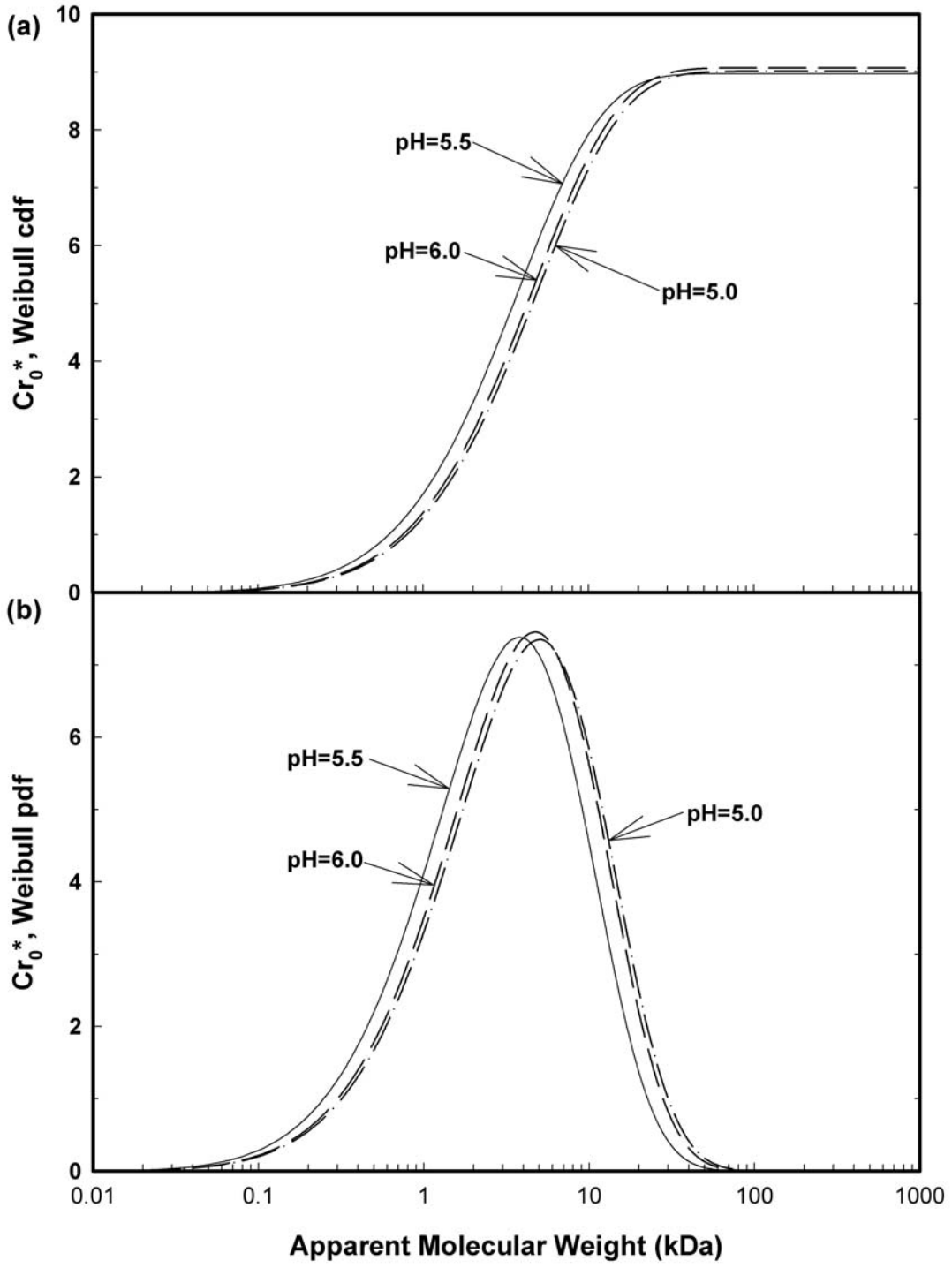

Figure 5.51 - Weibull (a) *cdf* and (b) *pdf* comparison for alum 10 treated water at pH 5.0, 5.5, and 6.0.

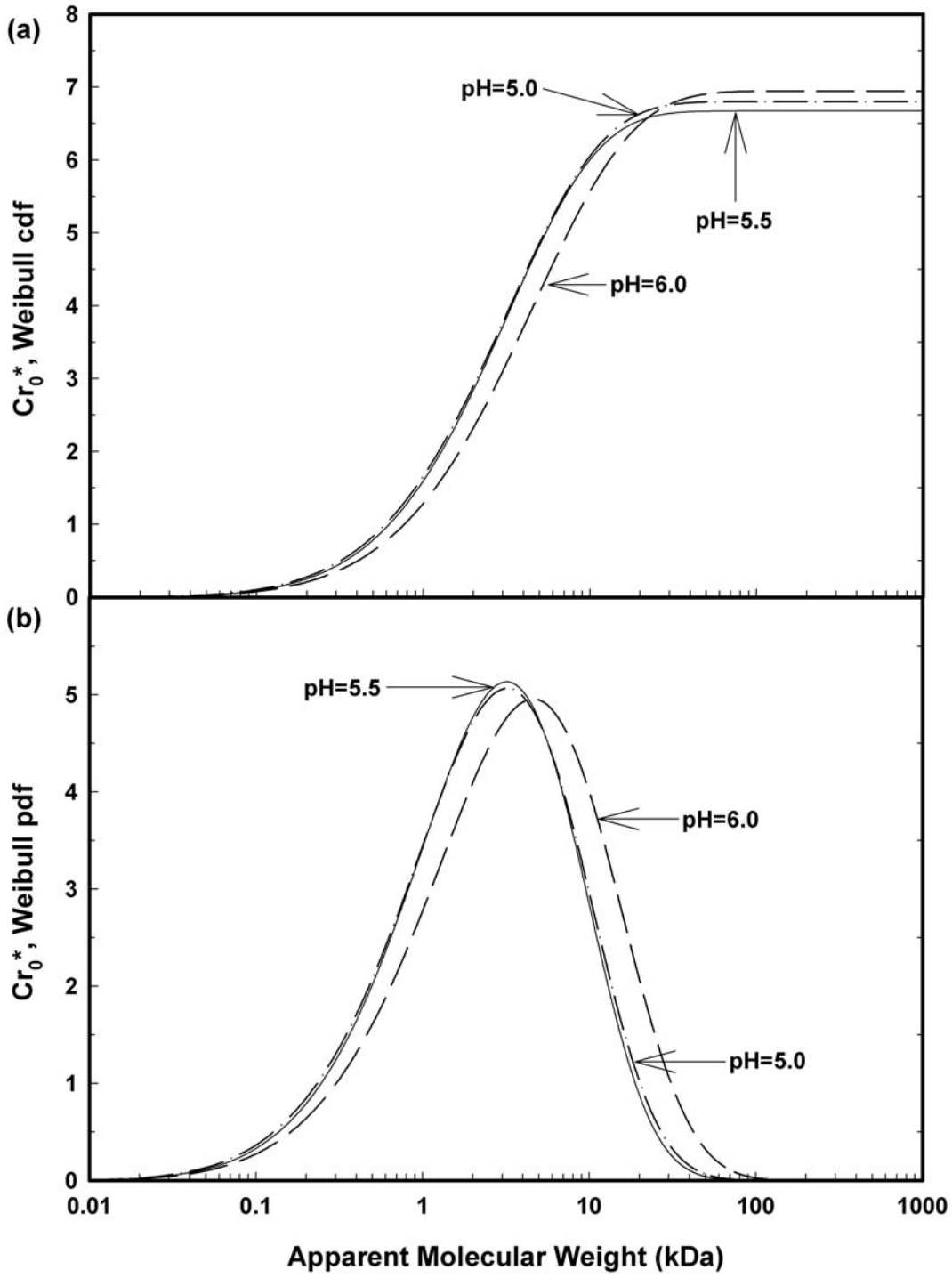

Figure 5.52 - Weibull (a) *cdf* and (b) *pdf* comparison for alum 30 treated water at pH 5.0, 5.5, and 6.0.

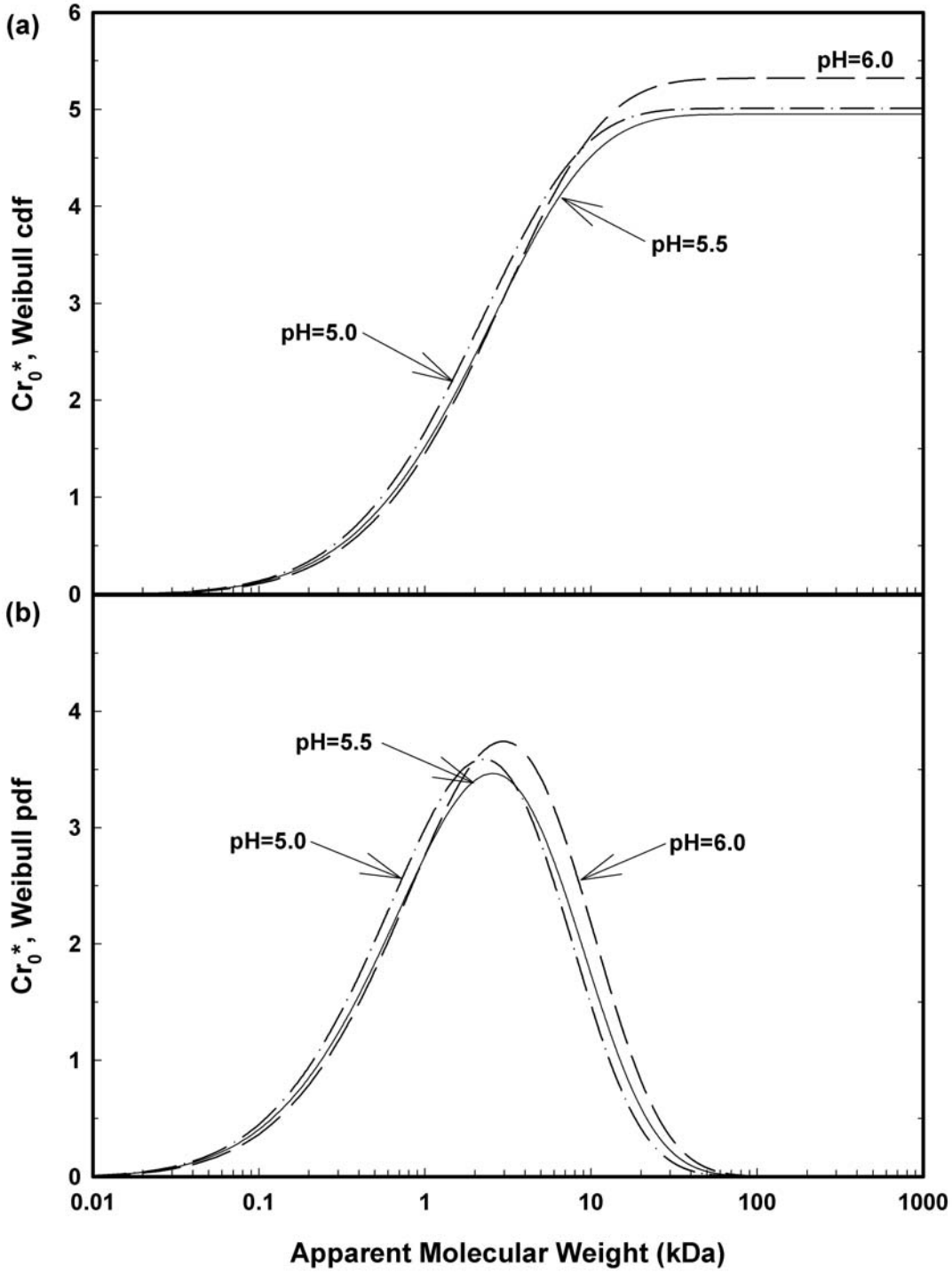

Figure 5.53 - Weibull (a) *cdf* and (b) *pdf* comparison for alum 50 treated water at pH 5.0, 5.5, and 6.0.

distributions for each pH value tested at coagulant doses of 10, 30, and 50 mg/L alum. Only the lowest coagulant dose tested (3 mg/L alum) displayed a significant variation in overall shape and scale of the Weibull distribution curve. Alum treated water at pH=5.5 (optimum pH for alum) displayed a statistically significant decrease in average MW when compared to similar values observed during coagulation at higher and lower pH values. However, no significant increase in DOC removal was observed at this pH.

Figures 5.54 thru 5.57 display Weibull *cdf*s and *pdf*s for fractionated water after treatment with ferric sulfate at doses ranging from 3mg/L to 50 mg/L at three pH values. No significant variation in AMW values is apparent after treatment with 3, 10, and 30 mg/L ferric sulfate. Unlike alum-treated water, ferric-sulfate-treated water displayed statistically significant deviations between Weibull *cdf* and *pdf* curves at a coagulant dose of 50 mg/L. Coagulation at this concentration and pH=4.5 demonstrated the lowest average molecular weight, however coagulation at pH=4.0 demonstrated the highest removal of DOC.

5.4.3 – Coagulation and MW distribution summary

The effectiveness of coagulation for the removal of DOM has been evaluated with two coagulants (alum and ferric sulfate) at various coagulant doses and pH values. Overall, ferric sulfate generally demonstrated the highest removal of DOC. At coagulant doses of 10 mg/L, 30 mg/L, and 50 mg/L ferric sulfate demonstrated approximately 4%, 14%, and 19% better total DOC removal in SWID raw composite water. However, at the lowest coagulant dose (3 mg/L coagulant) alum demonstrated

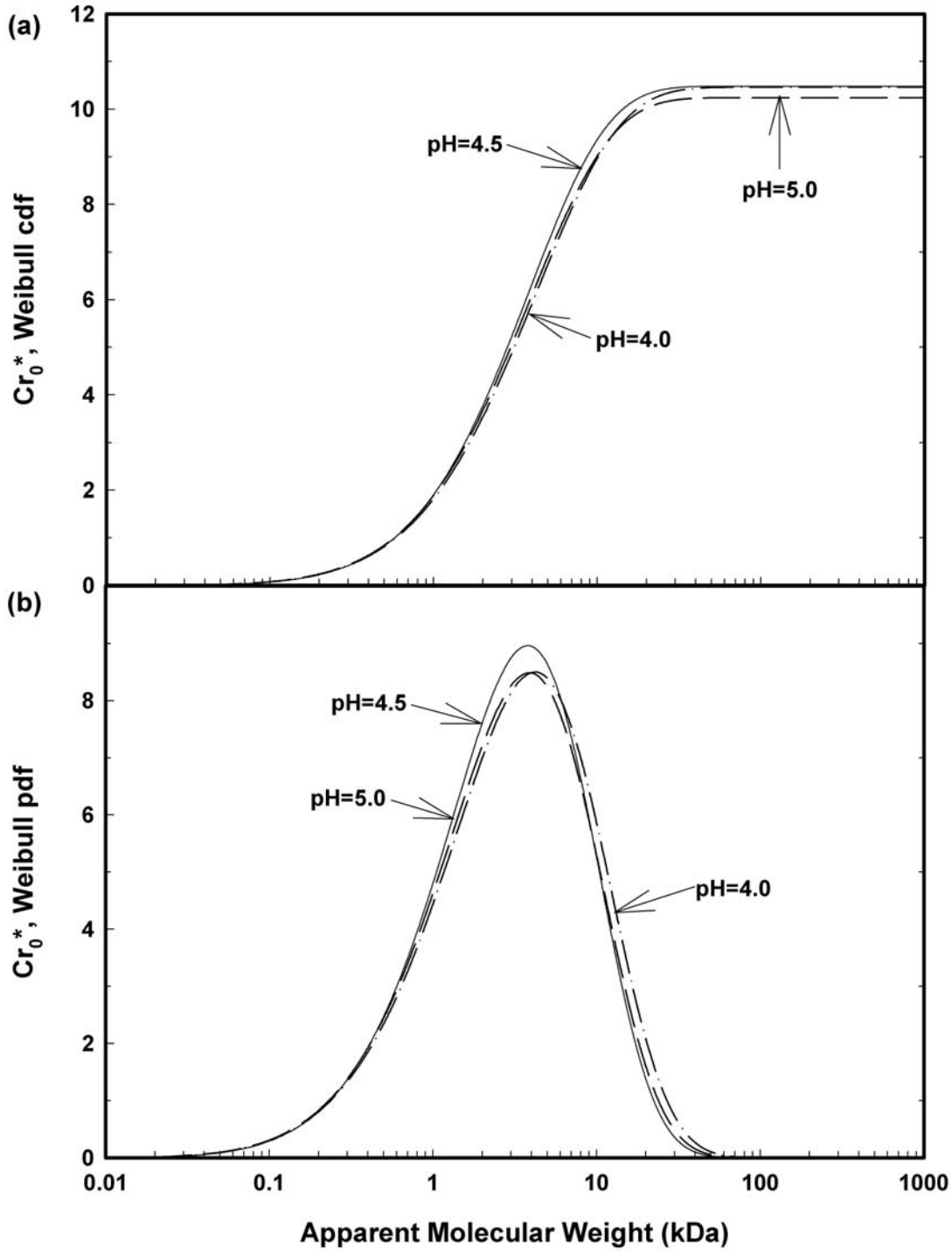

Figure 5.54 - Weibull (a) *cdf* and (b) *pdf* comparison for ferric 3 treated water at pH 4.0, 4.5, and 5.0.

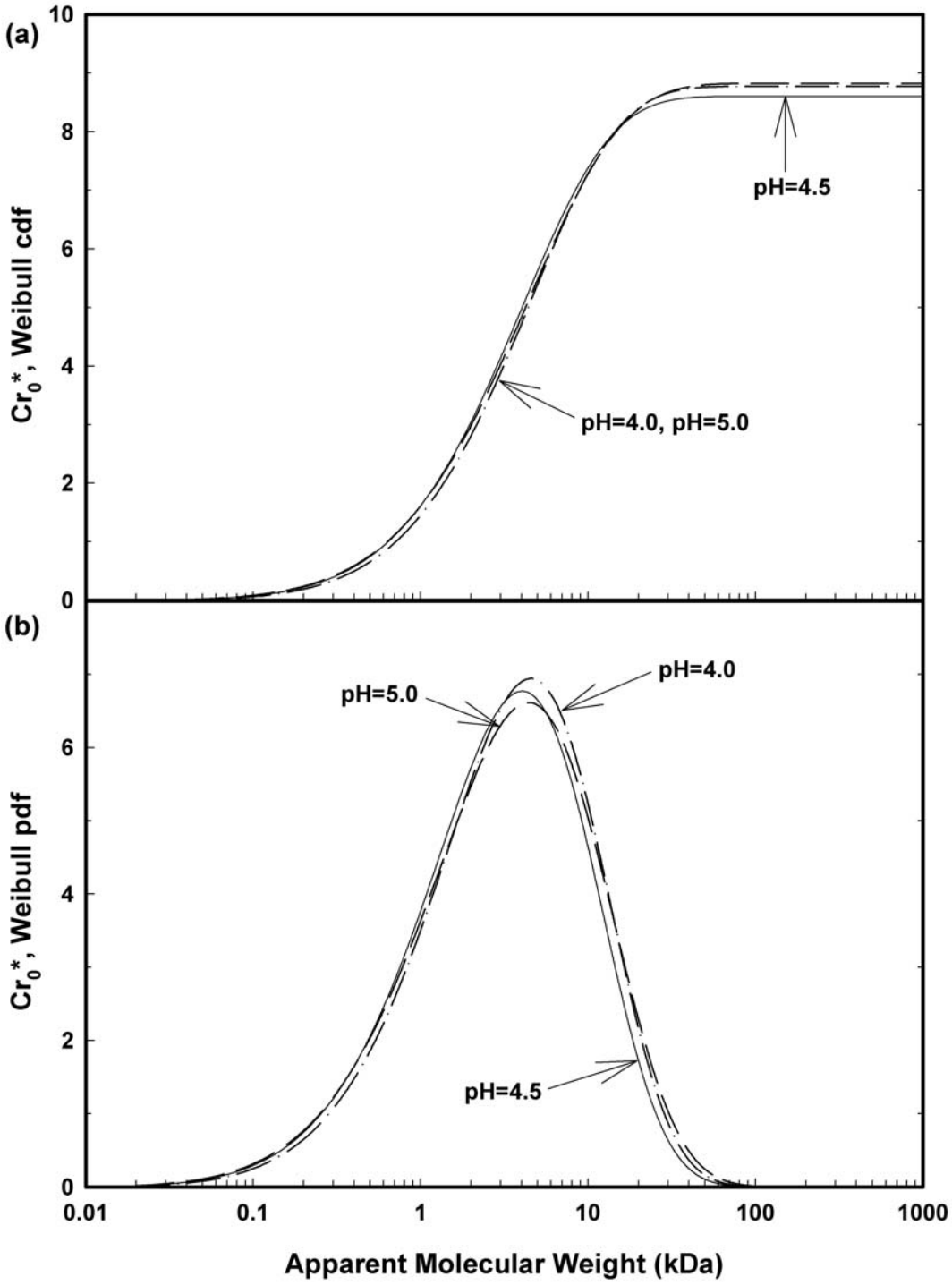

Figure 5.55 - Weibull (a) *cdf* and (b) *pdf* comparison for ferric 10 treated water at pH 4.0, 4.5, and 5.0.

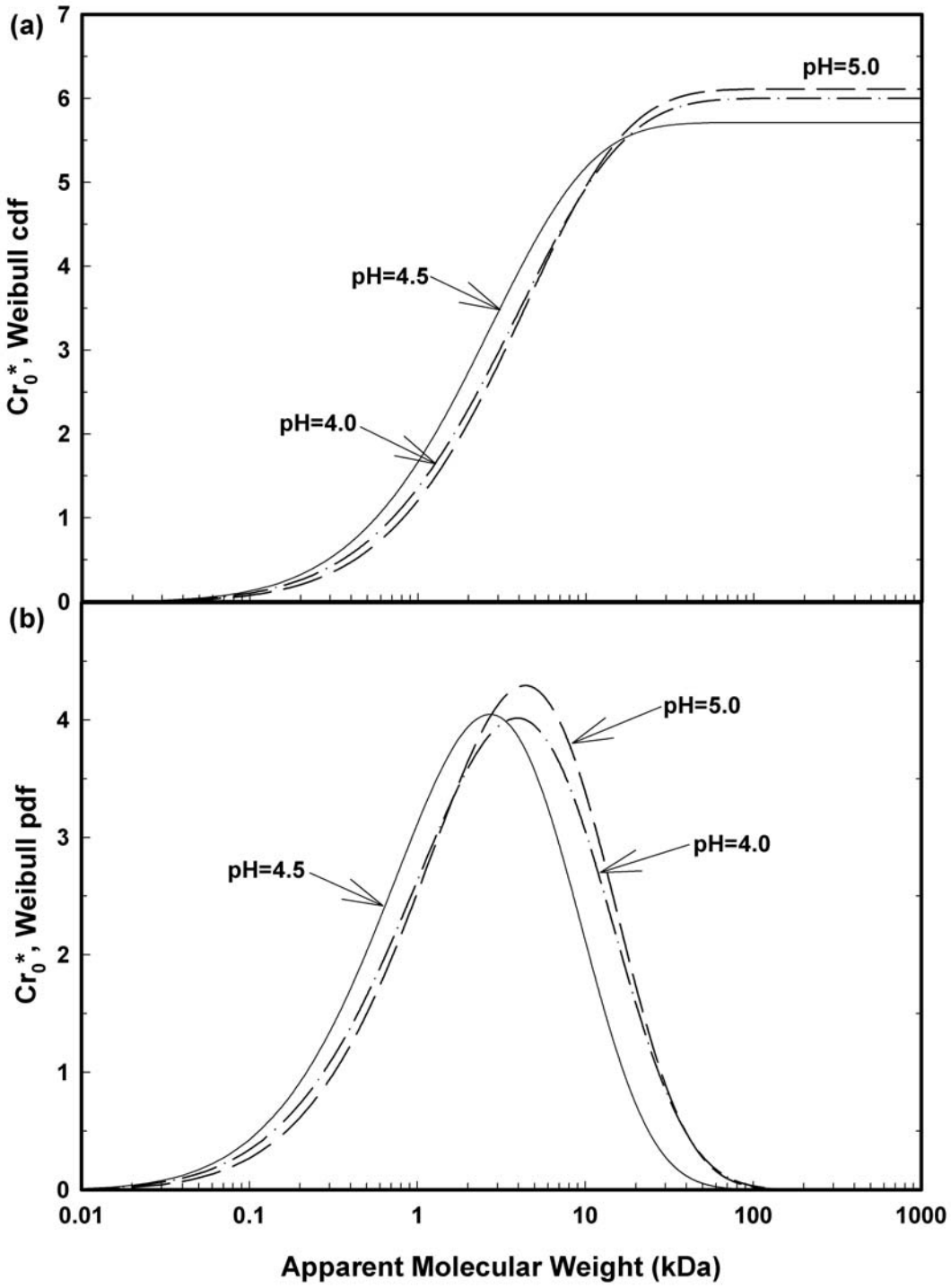

Figure 5.56 - Weibull (a) *cdf* and (b) *pdf* comparison for ferric 30 treated water at pH 4.0, 4.5, and 5.0.

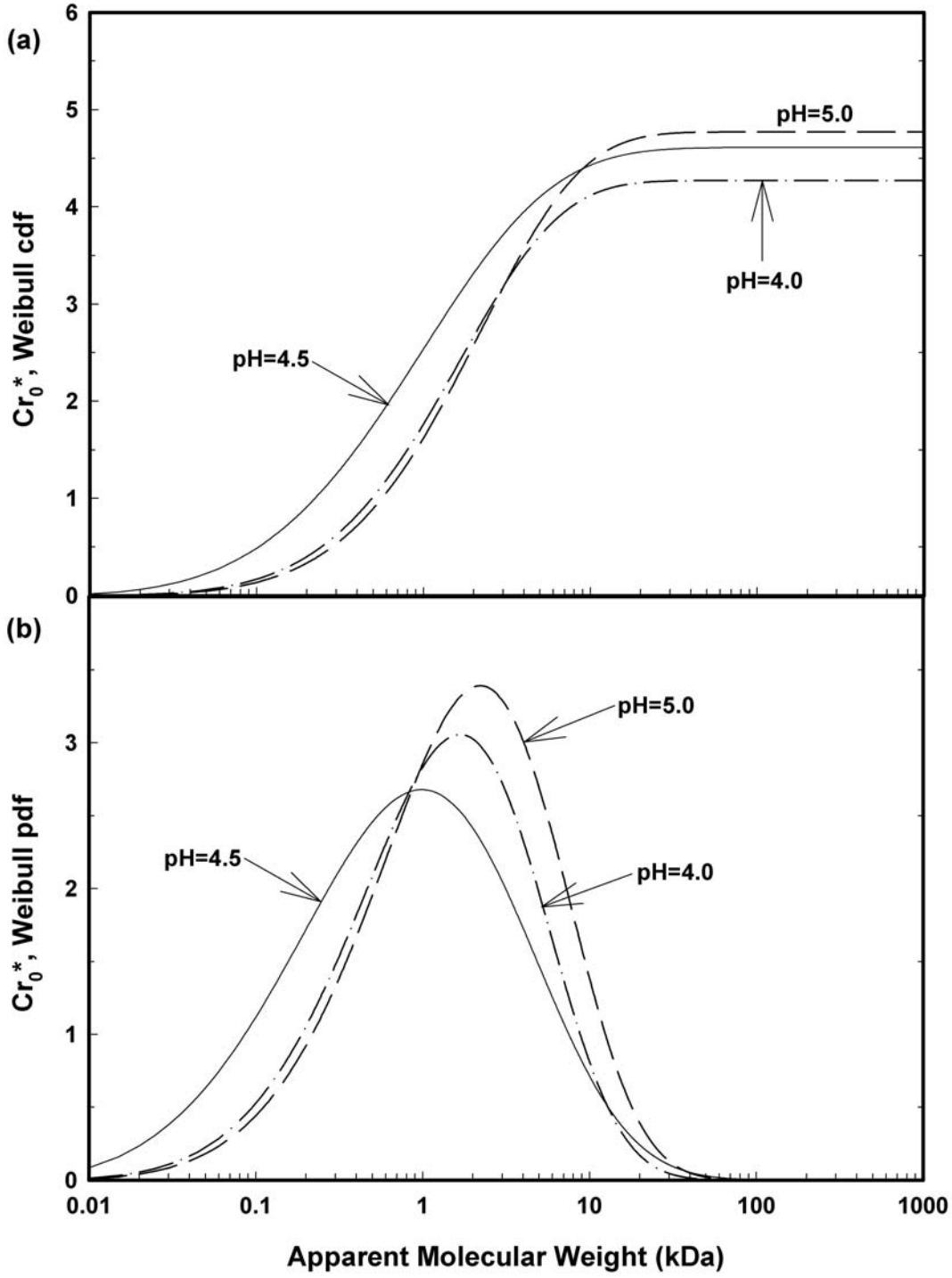

Figure 5.57 - Weibull (a) *cdf* and (b) *pdf* comparison for ferric 50 treated water at pH 4.0, 4.5, and 5.0.

approximately 2.5% better total DOC removal. Percentages are based on coagulation at the optimum pH for both alum and ferric sulfate (5.5 and 4.5, respectively).

The greatest percent removal was observed in the 3000 to 30,000 Da and greater size range (F1, R2, and R3). The smallest size fractions (R5 and F6) demonstrated the lowest percent removal of DOC. This may be partially due to competition reactions between the size fractions. As coagulant dose increased the percent removal of each size class also increased. At the highest coagulant dose < 1,000 Da, R5 and F6, size fractions comprised approximately 30% of the DOC for alum treated water and 50% of the DOC for ferric sulfate treated water.

The optimum pH for alum and ferric sulfate coagulation with respect to DOC removal occurred at 5.5 and 4.5, respectively. In both cases, deviation from the optimum pH resulted in an increase in DOC concentration and, in most cases, AMW. However, at the lowest pH tested for alum coagulation, pH = 5.0, the AMW was the lowest.

Although ferric sulfate removed more DOC overall, the consequence of 50% DOC existing in the < 1000 Da (R5 and F6) size class with respect to potential disinfection byproducts needs further investigation. Disinfection byproduct precursor removal will be assessed to determine any benefits associated with increased DOC removal when using ferric sulfate at SWID.

5.5-THM-FP and MW distribution

Coagulation studies have historically been conducted using bulk water characteristics to determine treatment efficacy. This focus is shifting due to tightening legislation to determine the acute cause of THMs. As discussed in section 2.3, the

composition of NOM in terms of isolated fractions provides better insight as to which removal methods are most effective in eliminating prominent DBP precursors. In this study, SWID raw and treated water have been isolated into 5 size classes to determine DBP (THM) formation with respect to MW fractions. Filtrate samples from each of the 5 membranes used in the study (YC-05, YM-1, YM-3, YM-10, and YM-30) were measured and size classes (< 500 Da, < 1000 Da, < 3000 Da, < 10,000 Da, and < 30,000 Da) were isolated for THM-FP tests. Note that size classes used in the THM-FP studies are not equivalent to previously determined size fractions (F1, R2, R3, R4, R5, and F6).

SWID raw water was separated using the UF procedure described in section 4.4. Alum and ferric sulfate treated SWID bulk raw composite isolates (see section 5.4) were also separated using the same procedure. Individual UF fractions were subjected to chlorination by the procedure described in section 4.2.3 to achieve a Cl_2 to DOC ratio of 3:1 by mass (Cl_2 to C) or 0.507 mmol Cl_2/mmol C. This ratio was determined by selecting a sufficiently high ratio to maintain a measurable residual chlorine concentration in each size fraction after the 7-day incubation period. PCM adjusted filtrate DOC concentrations are listed for SWID raw composite water and alum and ferric sulfate treated water in Table 5.30 and Table 5.31, respectively. THM-FP tests were conducted on UF separated fractions using a 3:1 Cl_2 to DOC mass ratio. The amount of chlorine added to each size class is presented in Table 5.32 and 5.33 for alum and ferric sulfate treated water, respectively. THM formation (μg THMs/mg C) by each UF size fraction in SWID raw and treated water is presented in Table 5.34 for alum and Table 5.35 for ferric sulfate.

Table 5.30 – PCM adjusted filtrate DOC concentration for SWID raw composite water and alum treated water.

	DOC (mg/L)					
	Composite	**<30,000**	**< 10,000**	**< 3,000**	**< 1,000**	**< 500**
SWID Raw	12.2	10.9	10.0	3.7	2.2	1.0
Alum 3	11.8	10.6	9.8	3.8	2.3	1.1
Alum 10	10.3	9.4	8.7	3.6	2.2	1.0
Alum 30	7.6	7.0	6.7	3.4	1.9	0.9
Alum 50	5.7	5.2	5.0	3.0	1.8	0.8

Table 5.31 – PCM adjusted filtrate DOC concentration for SWID raw composite water and alum treated water.

	DOC (mg/L)					
	Composite	**<30,000**	**< 10,000**	**< 3,000**	**< 1,000**	**< 500**
SWID Raw	12.2	10.9	10.0	3.7	2.2	1.0
Ferric 3	12.0	10.8	10.0	3.8	2.3	1.1
Ferric 10	9.9	9.0	8.4	3.7	2.2	1.0
Ferric 30	6.5	6.0	5.7	3.5	2.0	0.9
Ferric 50	4.6	4.2	4.1	3.1	2.0	0.9

Table 5.32 – Chlorine dose for THM-FP tests based on 3:1 Cl2 to DOC ratio (mmol Cl_2/mmol C) for alum treated SWID raw composite water

	Cl_2 Dose (mg/L)					
	Composite	**<30,000**	**< 10,000**	**< 3,000**	**< 1,000**	**< 500**
SWID Raw	36.6	32.8	29.9	11.2	6.5	3.1
Alum 3	35.3	31.8	29.4	11.4	6.8	3.3
Alum 10	30.9	28.2	26.2	10.9	6.5	3.1
Alum 30	22.9	21.1	20.0	10.2	5.8	2.6
Alum 50	17.0	15.7	14.9	9.1	5.5	2.4

Table 5.33 – Chlorine dose for THM-FP tests based on 3:1 Cl2 to DOC ratio (mmol Cl_2/mmol C) for ferric sulfate treated SWID raw composite water

	Cl_2 Dose (mg/L)					
	Composite	<30,000	< 10,000	< 3,000	< 1,000	< 500
SWID Raw	36.6	32.8	29.9	11.2	6.5	3.1
Ferric 3	35.3	32.5	29.9	11.5	7.0	3.3
Ferric 10	30.9	27.0	25.2	11.2	6.6	3.1
Ferric 30	22.9	18.1	17.0	10.4	5.9	2.7
Ferric 50	17.0	12.7	12.4	9.2	6.0	2.7

Table 5.34 – Average specific THM-FP for SWID raw water and alum treated MW fractions at various coagulant doses (pH=5.5)

	THM-FP (µg/mg C)					
Water	Composite	<30 kDa	<10 kDa	<3 kDa	<1 kDa	<0.5 kDa
Raw SWID	24.16	24.63	21.12	23.05	32.41	34.69
Alum 50	20.12	21.88	20.12	23.46	33.11	38.26
Alum 30	23.75	23.46	20.83	20.71	30.50	32.99
Alum 10	23.17	24.34	21.76	25.56	31.77	29.31
Alum 3	22.93	24.57	20.71	29.02	29.90	27.96

Table 5.35 – Average specific THM-FP for SWID raw water and alum treated MW fractions at various coagulant doses (pH=5.5)

	THM-FP (µg/mg C)					
Water	Composite	<30 kDa	<10 kDa	<3 kDa	<1 kDa	<0.5 kDa
Raw SWID	24.16	24.63	21.12	23.05	32.41	34.69
Ferric 50	12.93	16.03	14.86	18.54	36.45	44.87
Ferric 30	19.83	20.36	13.34	17.96	35.16	41.01
Ferric 10	21.47	20.83	15.44	21.35	38.20	37.15
Ferric 3	20.71	23.46	21.29	20.18	34.34	35.16

Within SWID raw water, larger composite size fractions of NOM produced the fewest THMs per mg C. As the "relative size" of the fractions decreased, the amount of THMs formed per mg C increased with the exception of the < 10 kDa fraction. This may have been caused due to the change in chlorine dosing levels or reaction kinetics between

the different size classes. This observation remained relatively consistent over all measured coagulant doses for both alum and ferric sulfate.

Elevated coagulant doses demonstrated increased TTHM formation in the small MW fractions (< 3 kDa, < 1 kDa, and < 0.5 kDa). This observation was particularly true for ferric sulfate treated water and may be seen in Figure 5.58. These data oppose the relationship found by (Chadik and Amy 1983) who reported that high MW fractions produced more THMs per mg C. However, another study by (Collins et al. 1986) observed similar trends in specific THM formation with respect to apparent MW size fractions. Both studies further support the evidence that THM formation is specific to NOM character in addition to size fractions.

Although the smallest MW fractions accounted for the majority of THMs formed per unit carbon, the largest MW fractions accounted for the majority of total THMs formed. The smallest size fractions (R5 and F6) demonstrated the lowest percent reduction in THM formation after coagulation with both alum and ferric sulfate. These data are consistent with studies conducted by Fearing (2004) who demonstrated poor removal of NOM in the < 3 kDa size range as determined by GPC.

Figure 5.59 demonstrates the total THMs formed by each size fraction after treatment with various coagulant doses. It should be noted that the TTHM-FP of the individual fractions totaled more than the bulk water TTHM-FP for each water sampled (raw and treated). (Owen et al. 1993) observed similar trends in a study where the sum of THMs produced by fractionated substances had a combined reactivity of 100 μg THM/mg-C compared with a raw water reactivity of 38 μg THM/mg-C. The increased combined reactivity was attributed to the synergistic effects in chlorine substitution or

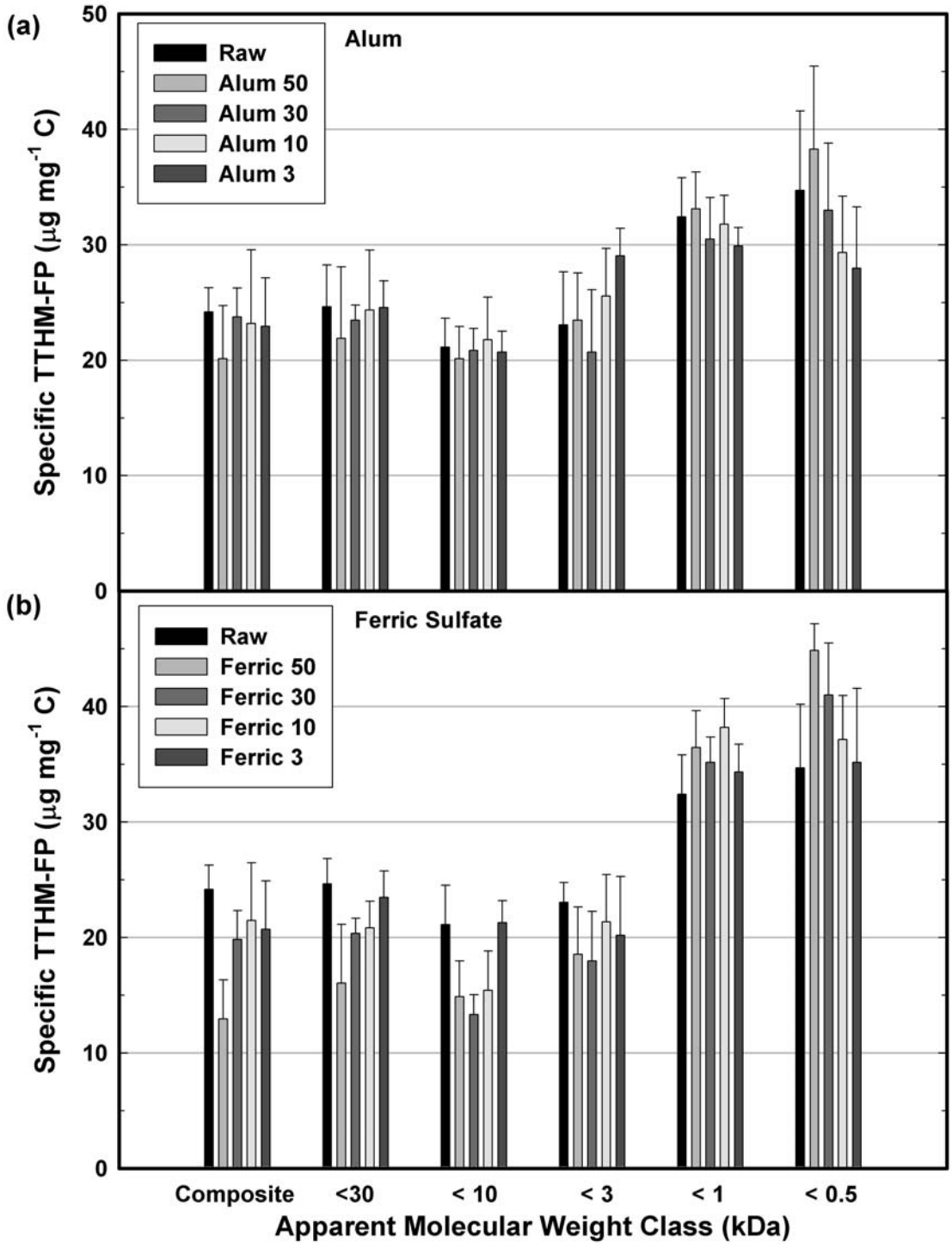

Figure 5.58 - Specific TTHM-FP for MW fractions and composite (unfractionated) water over various coagulant doses for (a) alum and (b) ferric sulfate

oxidation reactions in the presence of NOM fractions compared to bulk NOM. In addition, the heterogeneous nature of NOM may affect the reactivity of individual size classes when compared to combined size classes. Note, for example, that the isolated NOM < 30,000 Da size class includes all size classes smaller than 30 kDa (i.e., < 10 kDa, < 3 kDa, < 1 kDa, and < 0.5 kDa size classes) and all THM-FP data interpretation must consider the reactivity of the aggregate group.

The chlorination ratio may account for the variable specific THM formation between NOM size classes. (Luong et al. 1982) hypothesized that when chlorinating humic substances, some chlorine is initially expended in 'activiation' of the humic structure. The activation of humic substances occurs through oxidation reactions to produce active sites followed by substitution reactions with chlorine. Under this hypothesis, subjecting < 0.5 kDa NOM fraction to the same chlorination ratio as a < 30 kDa fraction may be providing a catalyst for organo-chlorine formation under the assumption that less chlorine is required for partial oxidation of the NOM molecules. This hypothesis may account for the high TTHM-FP values seen in the low MW fractions. Under this consideration, less chlorine is required for partial oxidation of the molecules so more chlorine is available to participate in reactions leading to the formation of THMs. Increased chlorine concentration leads to the formation of more THMs (Singer 1999), therefore under this consideration more THMs will be formed per unit carbon by the smaller molecules.

Figure 5.60 displays the THM-FP with respect to size class and coagulant dose. Both coagulants removed significant portions of THM precursors with MW > 1000 Da, However, a trivial amount of THM precursors with MW < 1000 Da were removed by

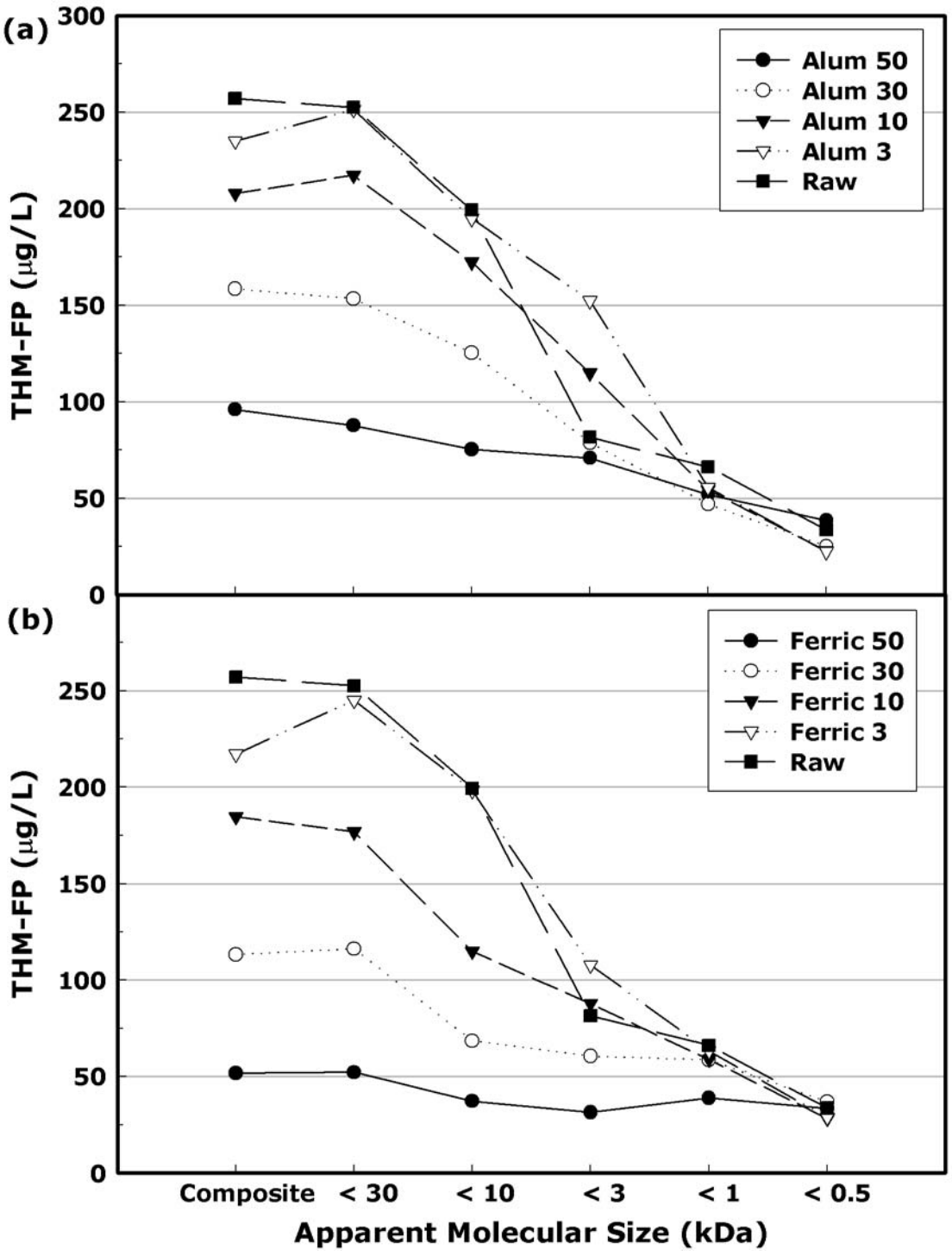

Figure 5.59 – Change in THM-FP of SWID raw composite water and MW size classes after treatment with alum and ferric sulfate at varying coagulant doses.

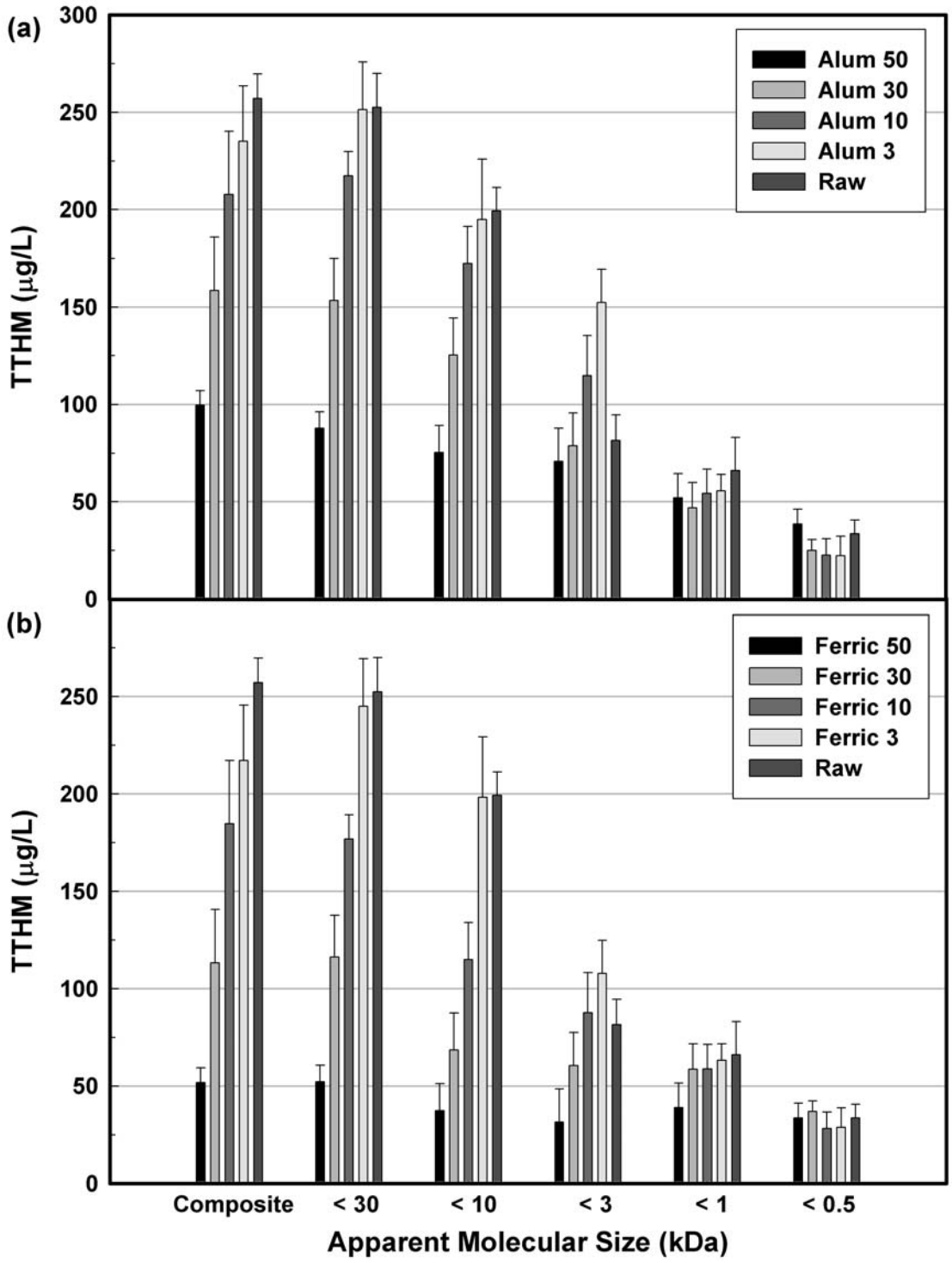

Figure 5.60 - Total TTHM-FP for MW fractions and composite (unfractionated) water over various coagulant doses for (a) alum and (b) ferric sulfate

either coagulant. This demonstrates that coagulation by alum and ferric sulfate was not effective at removing THM precursors with MW < 1000 Da, consequently, the majority of THMs formed at elevated coagulant doses are caused by this same size class.

It must be noted that specific TTHM-FP for the smallest MW fractions in both raw and treated water were proportionately higher than any other size fraction and accounted for a significant portion TTHM formation at elevated coagulant doses. This observation is illustrated in Figure 5.61 and Figure 5.62 for alum and ferric sulfate treated water, respectively. At the 50 mg/L coagulant dose the < 500 Da MW size class composes the majority of THMs formed. These data support the idea that the majority of THMs formed at coagulant doses in the optimal range are produced by the smallest size fraction (F6).

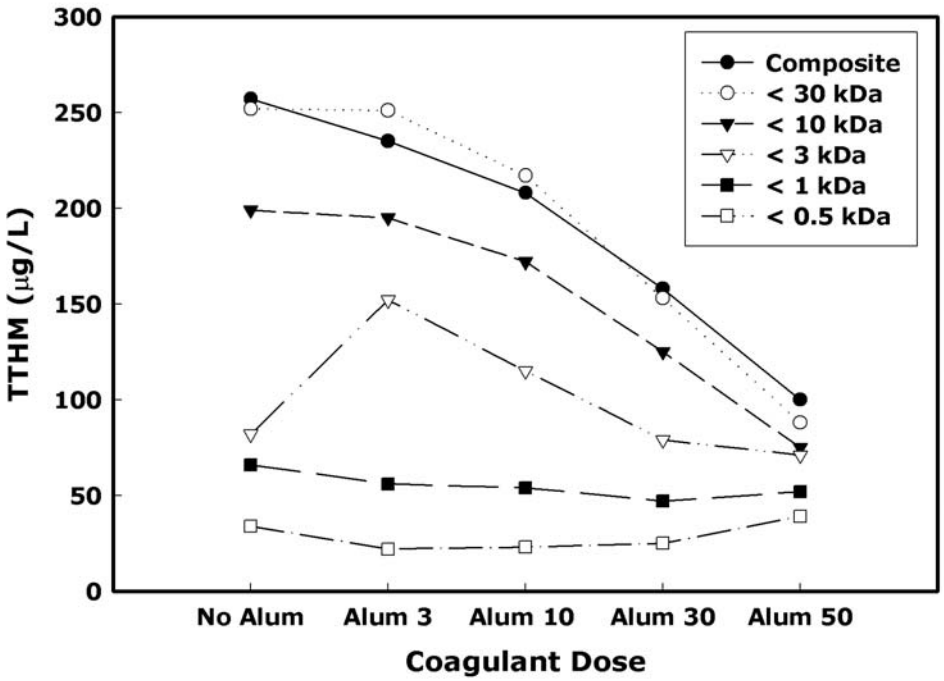

Figure 5.61 – Change in THM-FP of SWID raw composite water and MW size classes after treatment with alum

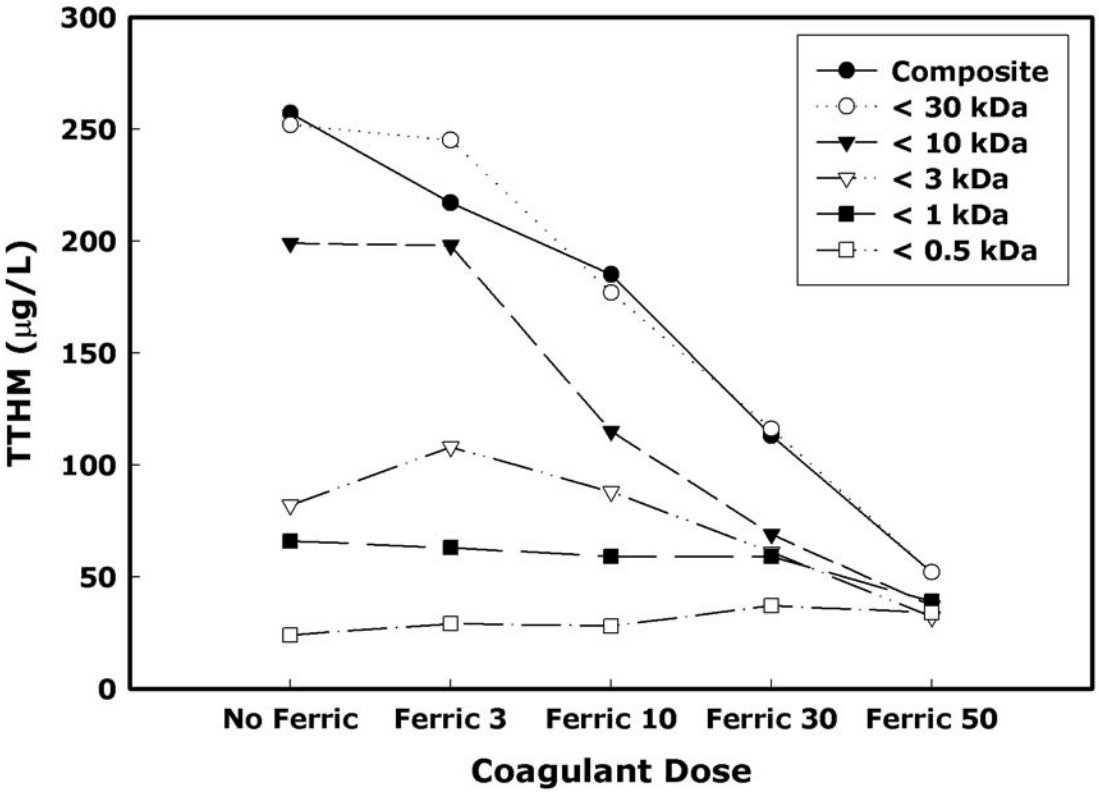

Figure 5.62 – Change in THM-FP of SWID raw composite water and MW size classes after treatment with alum

5.5.1 – THM-FP and MW distribution summary

The results herein are based on a SWID raw composite water and the subsequent treatment of the water by coagulation. TTHM yield coefficients ranged from 20 μg/mg C to 38 μg/mg C for alum treated water and 13 μg/mg C to 45 μg/mg C for ferric sulfate. As the molecular weight of the fractions decreased, TTHM yield coefficients increased. The smallest molecular weight fraction (MW < 500 Da) had the highest yield coefficient for alum treated water, ferric sulfate treated water, and SWID bulk raw composite water (38.3 μg/mg C, 44.9 μg/mg C, and 34.7 μg/mg C, respectively). Conversely, the largest size fractions displayed the lowest THM yield coefficient. A possible reason is that

halogenated intermediates formed as the smaller molecular weight DOC decomposes could favor the increased formation of THMs.

Ferric sulfate provided increased removal of DBP precursors in the 30000 Da < MW < 1000 Da size fraction. However DBP precursors present in the 1000 Da > MW and 500 Da > MW size fractions demonstrated similar TTHM formation after treatment with either coagulant. As coagulant dose increased TTHM formation decreased precipitously in all size fractions with the exception of the 1000 Da > MW and 500 Da > MW sizes fractions. Additionally, as coagulant dose increased there was no significant change in the amount of THMs formed in the 500 Da > MW size fraction. This same size fraction comprises the majority of the THMs formed after coagulation with 50 mg/L of alum and ferric sulfate. Considering only the THMs formed in the smallest size fraction after coagulation at Alum 50 and Ferric 50, proposed Stage II DPBR limits of 40 mg/L of THM formation may not be met under the specified chlorination ratio and incubation time period. This observation indicates that coagulation itself may not provide adequate DBP precursor removal to meet future Stage II DPBR criteria.

5.6 – SUVA and TTHM formation

Studies have demonstrated that SUVA can provide a good indication of THM-FP for a single water sample and its corresponding DOM size fractions (Edzwald et al. 1985; Kitis et al. 2001; Reckhow and Singer 1990; Tadanier et al. 2003). Investigation of the THM-FP of fractions within a raw water sample can give some indication of the type of NOM that is forming the largest amount of THMs. In this study, the relation between

TTHM-FP, UV absorbance, and SUVA in SWID bulk raw composite water was assessed to better understand the composition of THM precursor material.

5.6.1 – Bulk NOM

Whole-water samples for SWID show well-defined linear relations between DOC and UV (see section 5.1.2). The utility of a linear regression between two water quality variables (i.e, DOC and UVA) in development of water treatment strategies depends on the accuracy of the prediction defined by the regression equation for the independent variable.

Raw water samples were fractionated using the procedure described in section 5.3. The relation of UVA and DOC within SWID bulk water fractions is displayed in Figure 5.63. The linear relation shown here is consistent with the relationship demonstrated by SWID bulk NOM. Figure 5.64 displays SUVA plotted against specific THM formation potential (STHMFP). A positive linear relation is observed between SUVA and STHMFP in UF separated NOM fractions. This behavior is similar of that reported in literature (Collins et al. 1985). With UF separated fractions, THM-FP increased with increasing SUVA. This may be attributed to the high THM-FP values seen for low MW fractions (Luong et al. 1982).

SWID samples consist of composite DOC from sample sites within the watershed. Therefore, a linear relation between STHMFP and SUVA may be an accurate method for predicting STHMFP for some water systems, however this situation only applies for systems in which the temporal and spatial variation in DOC composition is very small because of extensive mixing of large amounts of water. However, there is no reason to expect that all such systems will show the same relation between STHMFP and SUVA.

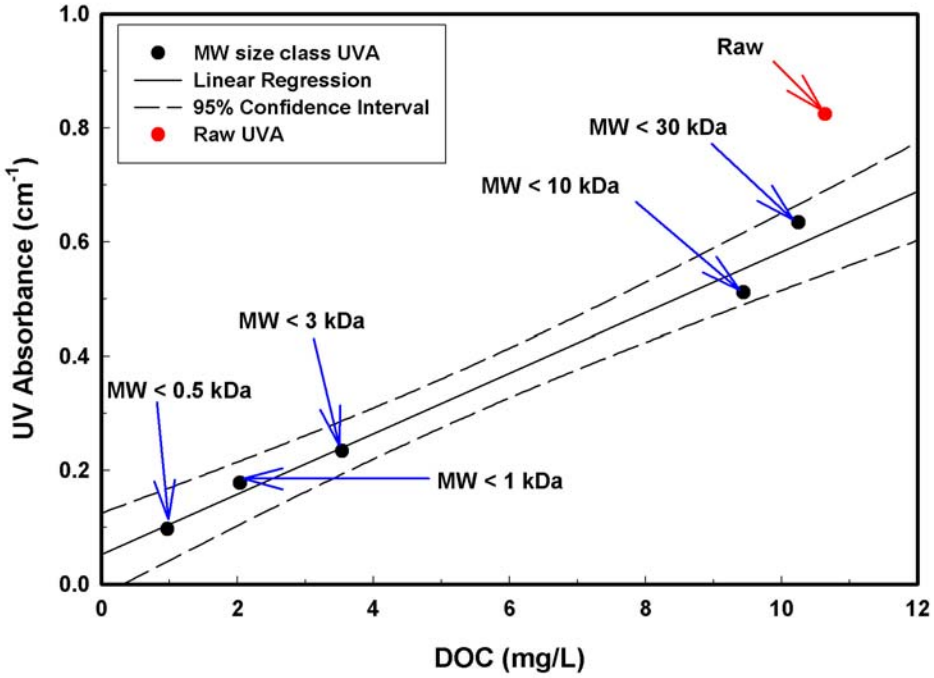

Figure 5.63 – UV_{254} absorbance versus DOC concentration for SWID composite bulk NOM and MW fractions.

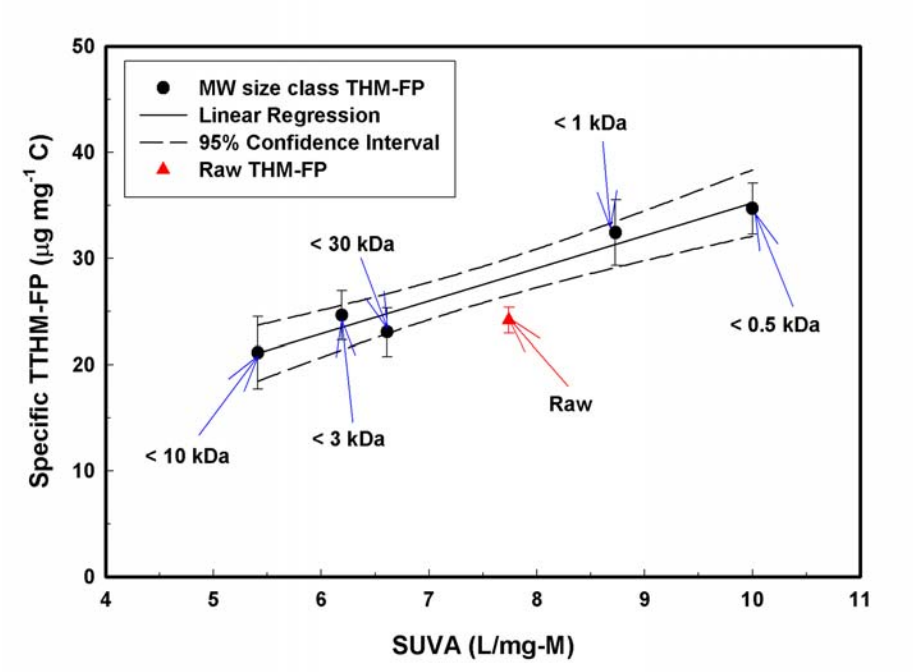

Figure 5.64 – Specific UV_{254} absorbance (SUVA) versus specific TTHM formation potential (STTHMFP) concentration for SWID composite bulk NOM and MW fractions.

Several types of organic structures that are generally present in the DOC pool are capable of absorbing UV light, including aromatic rings and conjugated dienes and carbonyls (Rao, 1975). Experiments on model compounds indicate high yields of THM can be produced by chlorination of aromatic structures, such as phenolic compounds, as well as nonaromatic structures, such as enolizable β-di-ketones (Larson and Weber 1994). No two water systems have exactly the same sources of DOC, therefore, one would expect DOC from every water system to contain a unique combination of molecular structures, yielding a different relation between STHMFP and SUVA. The linear relation shown here is considered unique to SWID bulk NOM and any significant deviation from this relation in SWID samples may result from the change in NOM chemical and/or physical character.

5.6.2 – UF fractions and SUVA

SWID raw water samples were treated with alum and ferric sulfate at concentrations of 3, 10, 30, and 50 mg/L and fixed optimum coagulation pH (5.5 for alum and 4.5 for ferric sulfate). Aliquot settled water was fractionated using the UF procedure outlined in section 5.3. UF fractions were monitored for DOC, UVA, and THM-FP. The relation between UVA and DOC for each UF fraction is displayed for both alum and ferric sulfate treated water in Figures 5.65 thru 5.68. Overall, the linear relation between UV_{254} absorbance and DOC concentration observed with bulk NOM was maintained after treatment with alum and ferric sulfate over all coagulant concentrations. These data suggest that UV absorbing compounds were removed in proportionate quantities to those of non-UV absorbing compounds. Slope, coefficient of

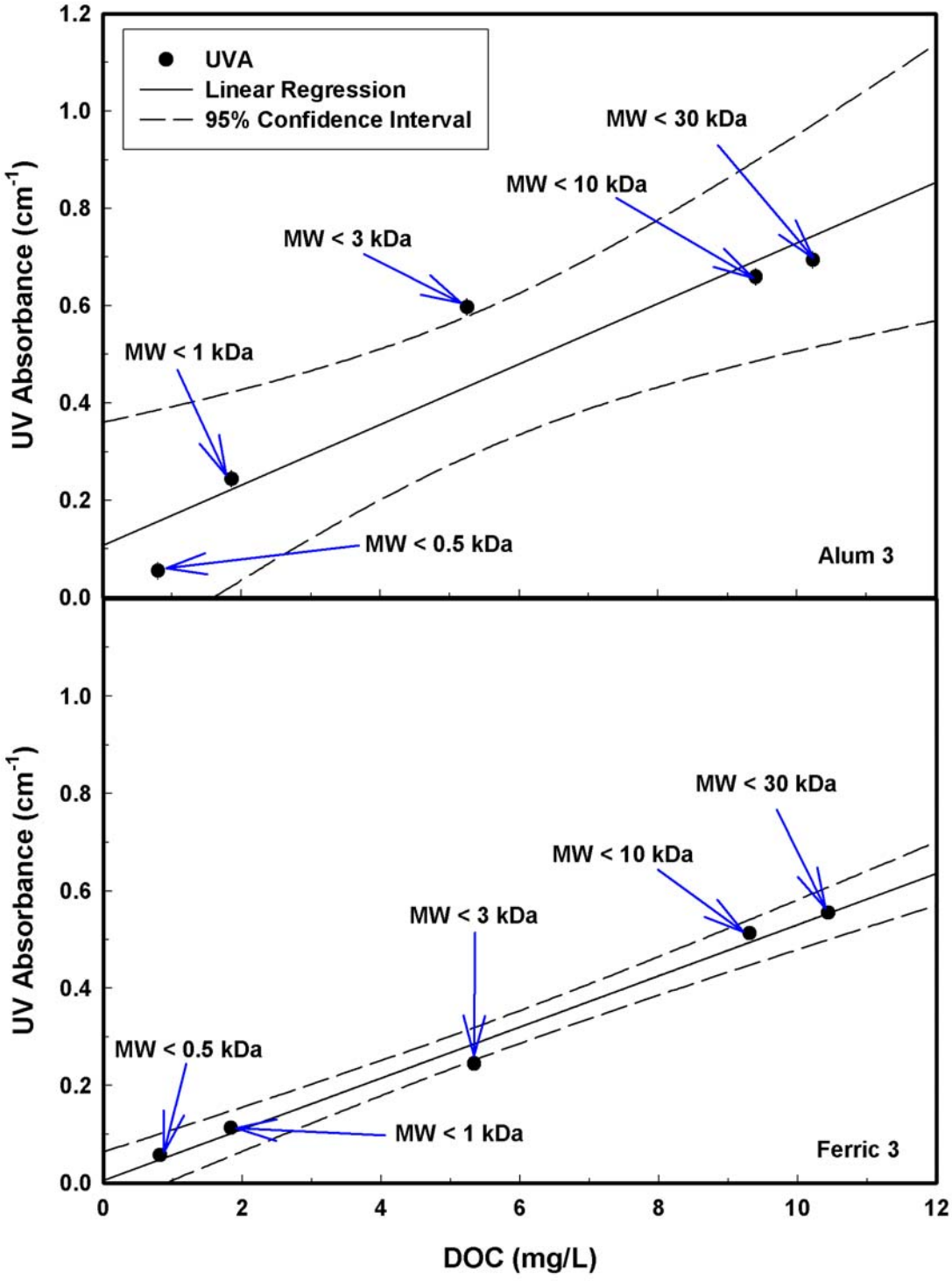

Figure 5.65 – UV_{254} absorbance versus DOC concentration for UF fractions treated with (a) 3 mg/L alum and (b) 3 mg/L ferric sulfate treated SWID water.

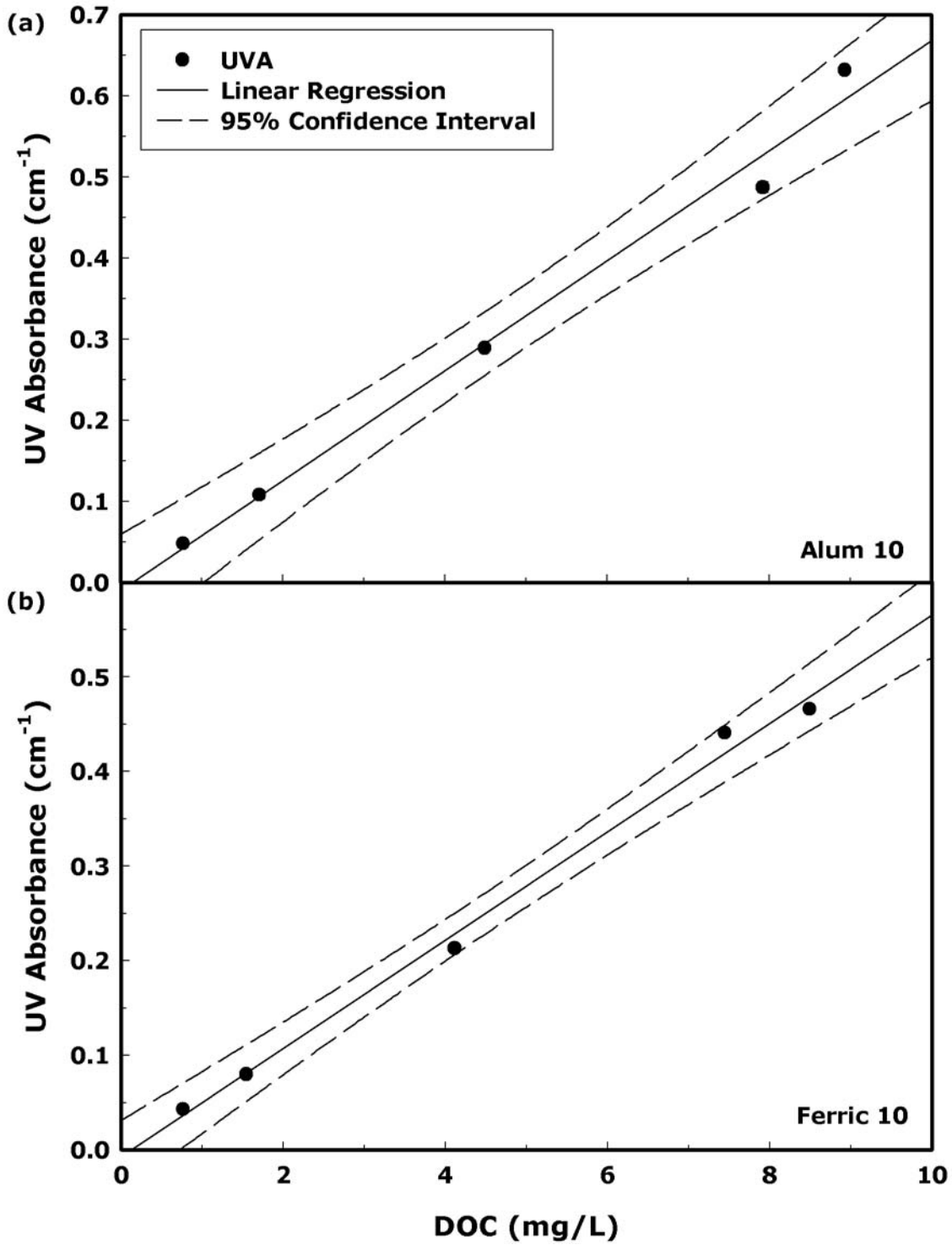

Figure 5.66 – UV_{254} absorbance versus DOC concentration for UF fractions treated with (a) 10 mg/L alum and (b)10 mg/L ferric sulfate treated SWID water.

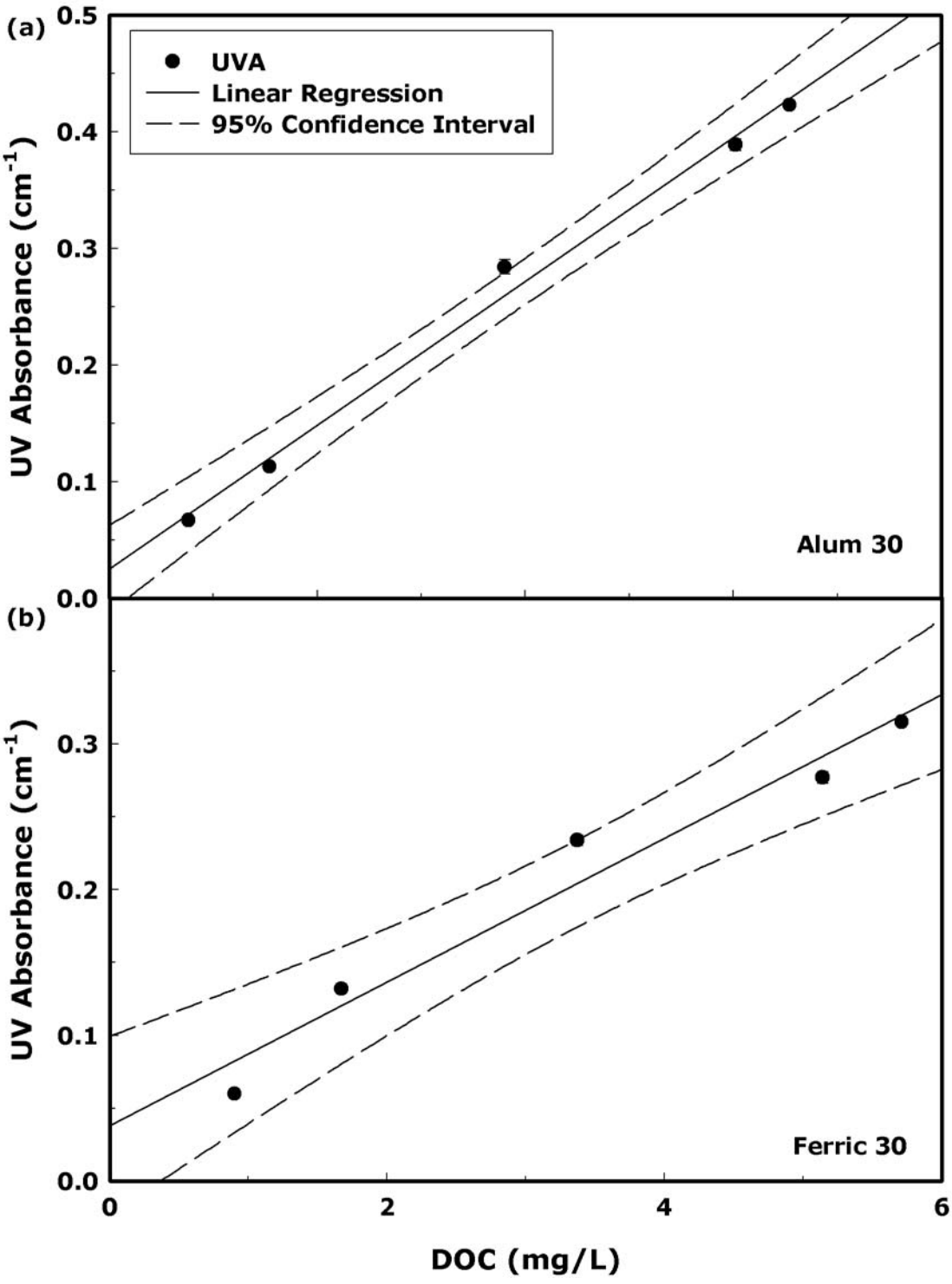

Figure 5.67 – UV_{254} absorbance versus DOC concentration for UF fractions treated with (a) 30 mg/L alum and (b)30 mg/L ferric sulfate treated SWID water.

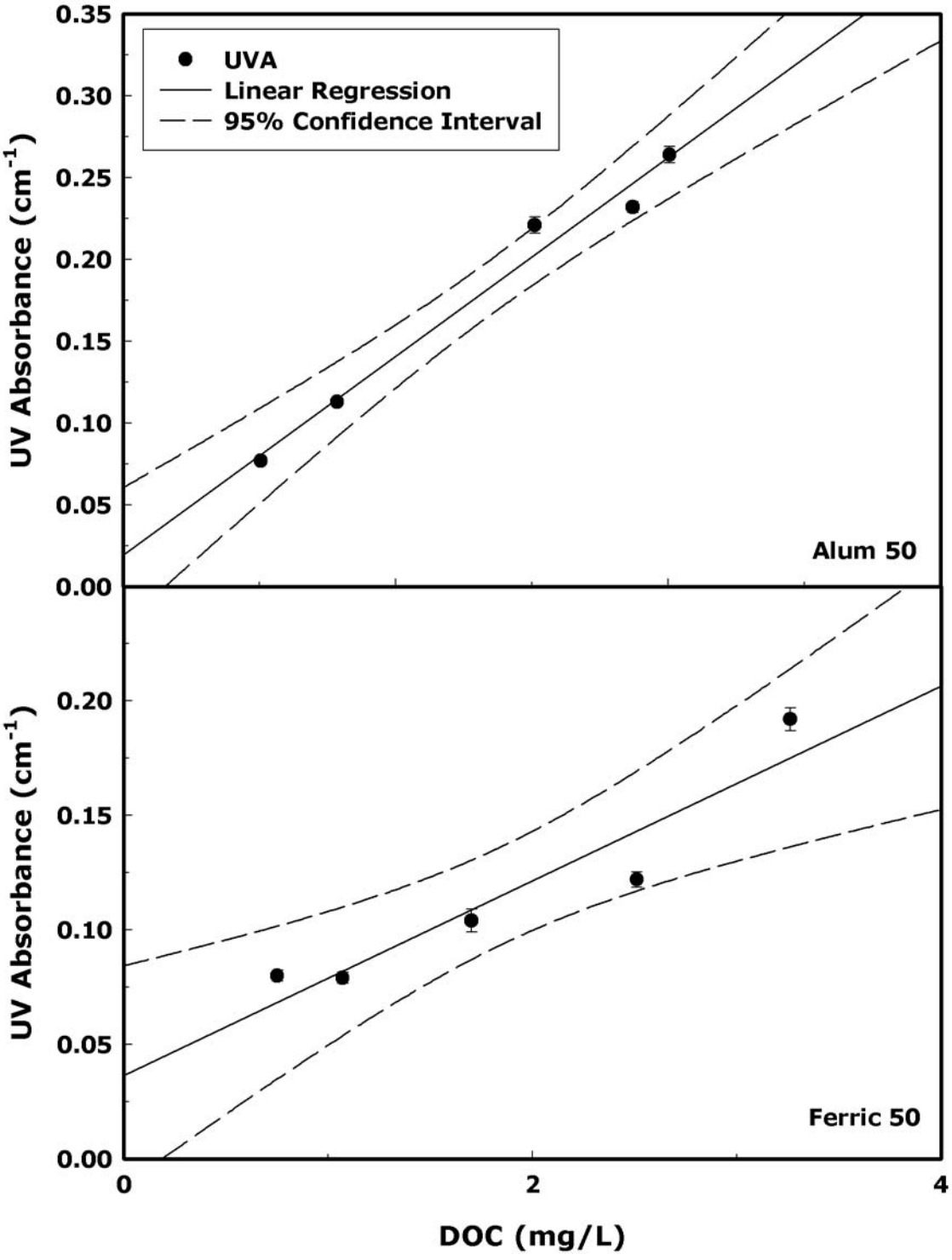

Figure 5.68 – UV_{254} absorbance versus DOC concentration for UF fractions treated with (a) 50 mg/L alum and (b) 50 mg/L ferric sulfate treated SWID water.

determination (r^2) values, and standard error are displayed in Table 5.36 for all linear regressions performed on the data. These data support the consistent linear relation observed between UV_{254} absorbance and DOC concentration in SWID bulk raw composite water.

Table 5.36 – R-squared and slope results from linear regression of UV_{254} absorbance versus DOC concentration for treated SWID water with alum and ferric sulfate at various coagulant doses.

Coagulant Dose	Coefficient of Determination (r^2)	Slope	Standard Error	UVA (L/mg-M)
Alum 3	0.82	0.0622	0.0137	6.22
Alum 10	0.9	0.0678	0.0044	6.78
Alum 30	0.93	0.0617	0.0031	6.17
Alum 50	0.92	0.0608	0.0052	6.08
Ferric 3	0.92	0.0526	0.0032	5.26
Ferric 10	0.93	0.0572	0.0026	5.72
Ferric 30	0.9	0.0505	0.009	5.05
Ferric 50	0.83	0.0425	0.0084	4.25

5.6.3 – Specific UV_{254} absorbance (SUVA) and specific THM formation potential (STHMFP)

An investigation into the relationship between SUVA and STHMFP is illustrated in Figures 5.69 thru 5.72. The linear relationship observed between these two parameters in SWID composite bulk NOM was not maintained over all UF treated fractions. Treated UF fractions after the lowest tested coagulant dose (3 mg/L) displayed a similar relation to that observed for bulk NOM. As coagulant dose (both alum and ferric sulfate) increased (10 mg/L and 30 mg/L), the linear relation between SUVA and STHMFP for treated UF fractions was not apparent. At the optimum coagulant dose for both ferric

sulfate and alum (50 mg/L), the linear relation initially observed between SUVA and STHMFP for bulk NOM was again observed, however the correlation was not as strong. These data suggest that intermediate coagulant doses remove disproportionate amounts of UV absorbing and non-UV absorbing material relative to low and optimized coagulant doses.

The relationship between UVA and DOC in alum and ferric treated water was very consistent. This indicates that UVA is a reliable estimation of DOC concentration at SWID. Observed regression slopes, equivalent to average SUVA, for alum and ferric sulfate treated water ranged between 6.06 –6.78 L/cm-m and 4.25 – 5.72 L/cm-m, respectively. Slightly lower SUVA values observed for ferric sulfate treated fractions indicates that lower MW constituents may exist in these fractions compared to alum treated water (Edzwald and Tobiason 1999). These data are consistent with previous studies (section 5.4 and 5.5) indicating that alum removes a larger percentage of low MW (< 1000 kDa) constituents compared to ferric sulfate.

Table 5.37 summarizes the change in linearity observed with respect to coagulant concentration expressed as a change in the coefficient of determination (r^2) value. It is clear that coagulant addition alters the relationship between SUVA and STHMFP. These data support the assumption that the balance between UV absorbing and non-UV absorbing species observed in SWID bulk raw composite water is altered after coagulant addition.

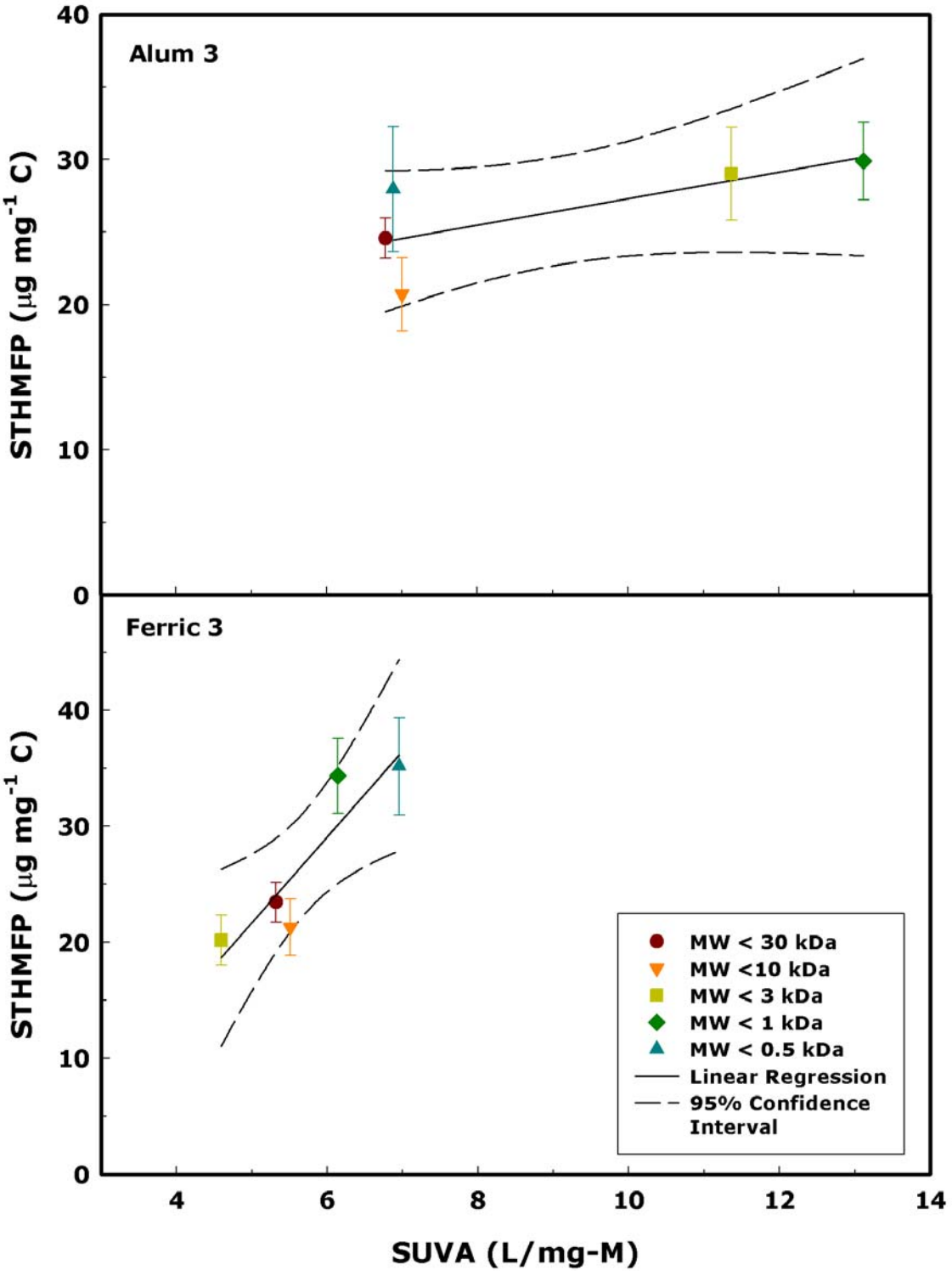

Figure 5.69 – Specific UV_{254} absorbance (SUVA) versus specific TTHM formation potential (STTHMFP) concentration for UF fractions treated with 3 mg/L alum (a) and 3 mg/L ferric sulfate (b) treated SWID water.

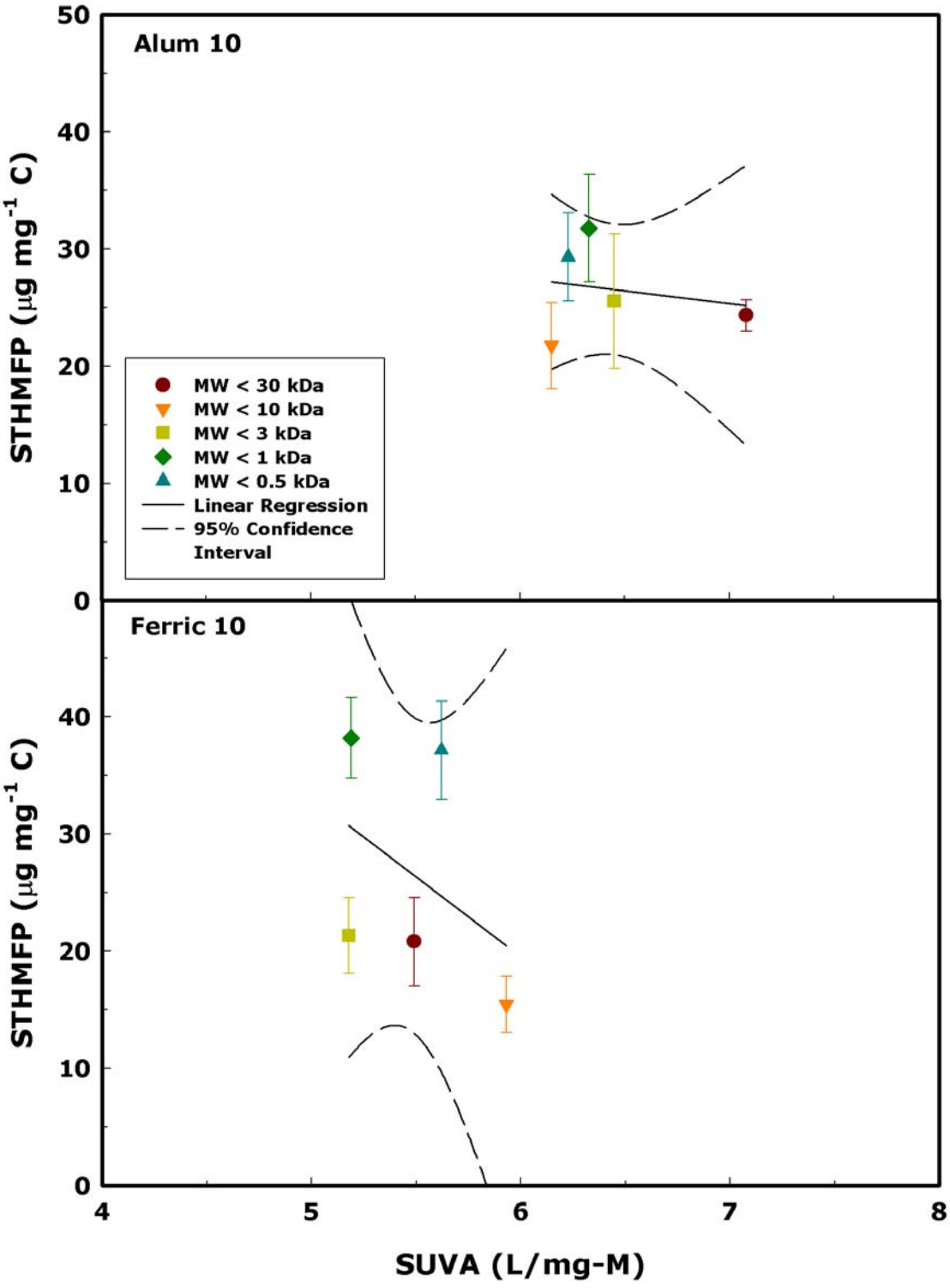

Figure 5.70 – Specific UV_{254} absorbance (SUVA) versus specific TTHM formation potential (STTHMFP) concentration for UF fractions treated with 10 mg/L alum (a) and 10 mg/L ferric sulfate (b) treated SWID water.

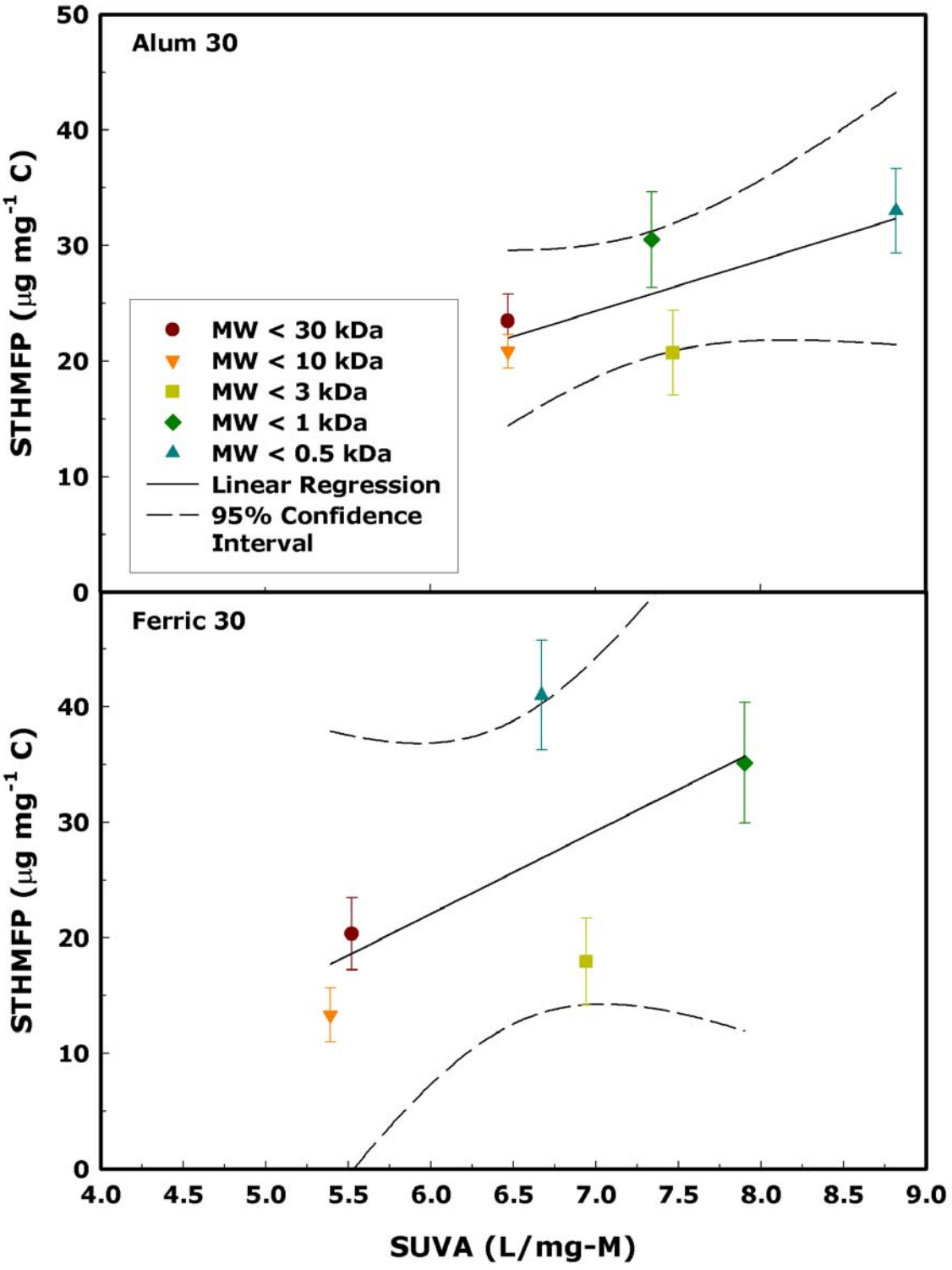

Figure 5.71 – Specific UV_{254} absorbance (SUVA) versus specific TTHM formation potential (STTHMFP) concentration for UF fractions treated with 30 mg/L alum (a) and 30 mg/L ferric sulfate (b) treated SWID water.

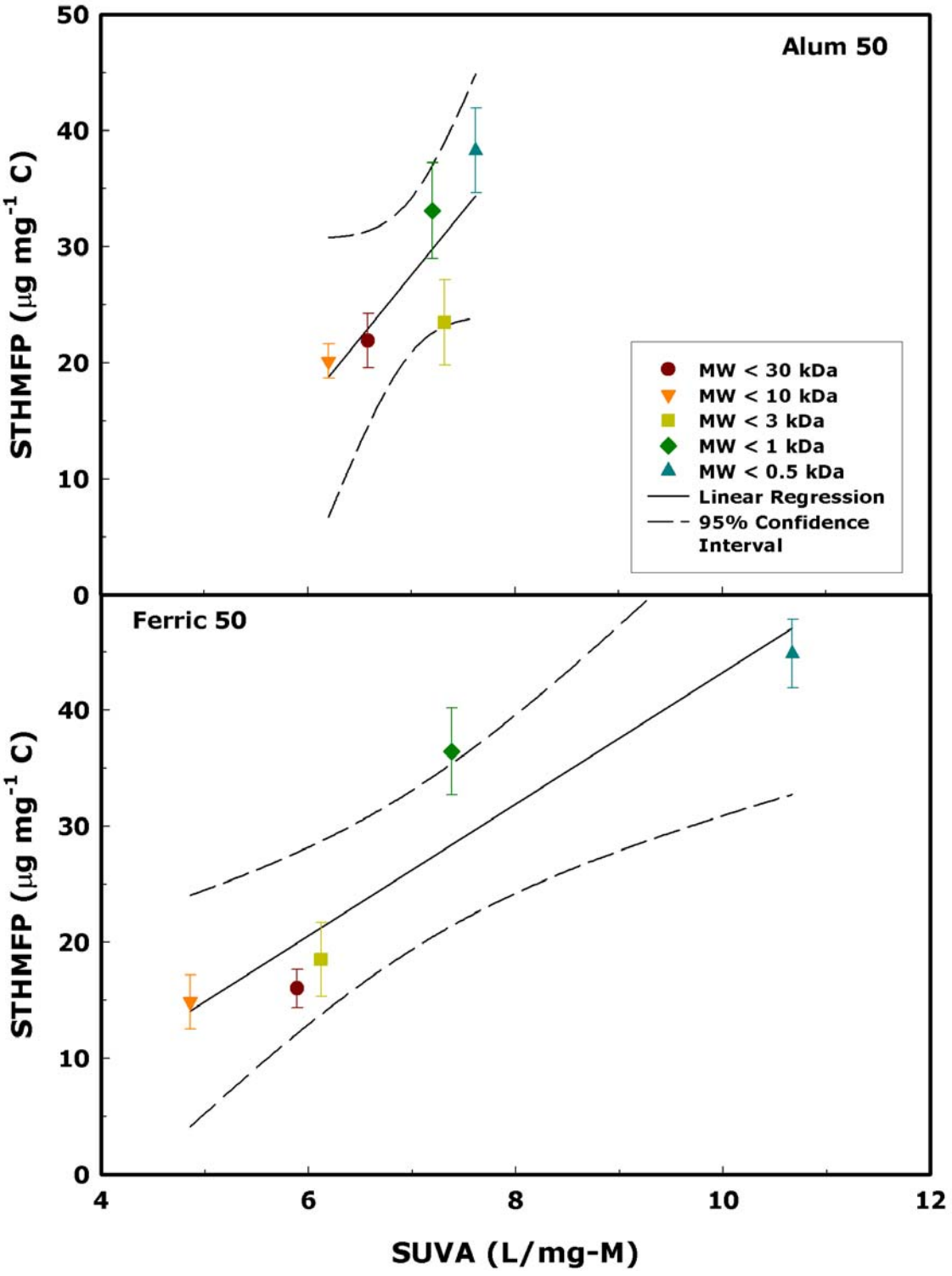

Figure 5.72 – Specific UV_{254} absorbance (SUVA) versus specific TTHM formation potential (STTHMFP) concentration for UF fractions treated with 50 mg/L alum (a) and 50 mg/L ferric sulfate (b) treated SWID water.

Table 5.37 – Coefficient of determination and slope for linear regression of SUVA versus STHMFP for alum and ferric sulfate treated SWID water at various coagulant doses.

Coagulant Dose	Coefficient of Determination (r^2)	Slope	Standard Error
Alum 3	0.41	0.908	0.504
Alum 10	0.04	2.16	6.09
Alum 30	0.45	4.39	2.28
Alum 50	0.55	10.99	4.66
Ferric 3	0.71	7.39	2.02
Ferric 10	0.06	13.6	17.35
Ferric 30	0.29	7.17	5.08
Ferric 50	0.77	5.68	1.24

SUVA values for individual size classes after treatment with alum and ferric sulfate treated water are displayed in Tables 5.38 and 5.39, respectively. The predominate trend in the data set shows increasing SUVA with decreasing MW suggesting that a larger portion of UV absorbing material is present in low MW NOM size classes. Additionally, SUVA generally decreased with increasing coagulant concentration over all MW fractions with the exception of the lowest coagulant dose (3 mg/L). However, based on the high standard error associated with STHMFP versus SUVA regression slope, it appears that SUVA is not a good indicator of THMFP in SWID raw composite water.

Table 5.38 – Specific UV_{254} absorbance (SUVA) for UF fractions and raw SWID water following alum coagulation

Alum Dose	SUVA					
	Raw	< 30	< 10	<3	<1	< 0.5
No alum	7.74	6.19	5.41	6.61	8.73	10.00
Alum 50	6.55	6.58	6.20	7.32	7.20	7.62
Alum 30	6.18	6.47	6.47	7.47	7.34	8.82
Alum 10	7.18	7.08	6.15	6.45	6.33	6.23
Alum 3	7.11	6.78	7.00	11.37	13.12	6.88

Table 5.39 – Specific UV_{254} absorbance (SUVA) for UF fractions and raw SWID water following ferric sulfate coagulation

Ferric Sulfate Dose	SUVA					
	Raw	< 30	< 10	<3	<1	< 0.5
No Ferric	7.74	6.19	5.41	6.61	8.73	10.00
Ferric 50	5.66	5.89	4.86	6.12	7.38	10.67
Ferric 30	6.16	5.52	5.39	6.94	7.90	6.67
Ferric 10	6.79	5.49	5.93	5.18	5.19	5.62
Ferric 3	6.53	5.32	5.51	4.59	6.14	6.95

5.6.4 – SUVA and THM formation summary

The relationship between SUVA and STHMFP has been investigated for SWID bulk raw composite water and MW size fractions. The smallest DOM size fraction (MW < 500 Da) displayed the highest SUVA and STHMFP. These data suggest that the highly reactive UV_{254} absorbing material present in this size class is not effectively removed by coagulation.

A positive linear relation exists between SUVA and STHMFP in untreated raw water. This relationship may be beneficial in predicting THM formation after chlorination based on monitoring UVA in the plant influent raw water. Coagulation affects this relationship such that the linear relation between SUVA and STHMFP is no longer observed suggesting that post-coagulation monitoring may not be as effective in predicting THM formation.

CHAPTER 6 - CONCLUSIONS

6.1 – Introduction

Natural organic matter (NOM) is an intricate mixture of organic compounds of variable chemical composition and size produced in the natural environment. Determining the removal of NOM from humic-rich waters for potable water treatment has historically relied on measurement of bulk parameters as an indicator of the efficacy of the treatment process employed to remove NOM. This holistic approach has led to many municipalities failing to meet regulations for the concentration of THMs in the final water, regardless of the level of color or TOC reduction achieved. Bulk analysis of NOM lends limited insight into the character of NOM, while fractionation of NOM yields a better understanding of its fate through treatment processes and variability in source material. The complete analysis of NOM must consider the effects of both bulk analysis where the NOM is unaltered from its natural state and separation of NOM where the organic constituents are altered and synergistic effects are lost. A review of current literature demonstrated that many researchers have optimized treatment processes based on bulk NOM parameters; however little information exists on the use of separation techniques to monitor treatment effectiveness.

An investigation was conducted to determine how NOM size composition varies throughout the Savannah water I&D (SWID) watershed, current and proposed treatment processes effectiveness in NOM removal and the reactivity of each NOM size fraction with chlorine. Ultrafiltration membrane separation has been used here to

demonstrate the effects of conventional water treatment on the removal of bulk and individual size fractions of SWID raw composite NOM.

6.2 – SWID watershed

The raw water pump station for SWID is located on Abercorn creek branching off of the Savannah River. The natural organic concentration (as measured by DOC and UVA) fluctuates with respect to tidal cycle, rain, and season. An investigation into the character of natural organics at several critical points surrounding and interior to the SWID watershed demonstrated that organic concentration changed significantly. During periods of heavy rainfall, SWID raw water samples exhibited relatively high levels of DOC and UVA compared to time periods of no rainfall. However, the overall character of SWID NOM was consistent throughout with respect to SUVA. This suggests that the overall character of NOM in the SWID watershed is consistent, irrespective of prevailing rainfall and tide conditions.

6.3 – Bulk NOM analysis

The removal of DOC, UV_{254} absorbing material, and THM precursor material from SWID raw bulk composite water showed that alum and ferric sulfate used as coagulants worked best at dissimilar pH values. Ferric sulfate generally removed 5% to 25% more DOC at equivalent doses (based on electron equivalents) at an optimum performance pH of 4.5. A pH reduction from current SWID practice resulted in a significantly reduced demand for the coagulant (both alum and ferric sulfate), leading to a reduction in overall coagulant required. This was coupled with a significant reduction in the amount of THMs formed upon chlorination. For bulk NOM, UVA appears to be a

good predictor of THM formation in SWID raw water and may be able to be used as an indicator of impending water quality or process failure.

6.4 – Fractional NOM analysis

The removal of NOM size fractions, > 30,000 Da (F1), 10,000 – 30,000 Da (R2), 3000 – 10,000 Da (R3), 1000 – 3000 Da (R4), 500 – 1000 Da (R5), and < 500 Da (F6), was assessed using alum and ferric sulfate as coagulants. DOC in the R5 and F6 size fractions demonstrated the smallest percent removal after coagulation. Ferric sulfate exhibited superior removal of DOC in all size fractions with the exception of the R5 and F6 size fractions. Although ferric sulfate removed more DOC overall, a larger percentage of the R5 and F6 fractions were removed using alum. Interestingly, the F6 size fraction contributed to the largest amount of specific THMs formed after coagulation at high coagulant doses. Therefore, at elevated coagulant doses any incremental DOC removal associated with the use of ferric sulfate may not translate to a significant reduction in THM formation.

6.5 – THM formation and DOC remvoal

THMFP studies conducted using SWID raw composite water and UF separated MW size classes illustrated that the < 1000 Da, R5 and F6, size fractions were responsible for the majority of THMs formed at high coagulant doses. The largest reduction in THMs by coagulation was observed in the < 30,000 Da and < 10,000 Da size classes. Ferric sulfate preformed better at reducing THMs formed in all size classes at optimum coagulant dose. However, neither coagulant was effective in removing DBP

precursor material with MW < 1000 Da. Furthermore, the amount of THMs formed from this size class alone were at values in excess of proposed Stage II DBPR limitations.

6.6 – UVA and SUVA

SWID raw composite water and UF separated MW size classes demonstrated a strong linear relationship between UVA and DOC concentration, indicating that UVA is a good indicator of DOC concentration at SWID in both raw and treated water. The linear relationship between SUVA and THM-FP in SWID raw composite water was not as strong as the trend observed between UVA and DOC. Additionally, no statistically significant relationship was observed between treated water SUVA and THM-FP.

6.7 – Engineering significance

Studies conducted at SWID suggest that current coagulation practice is optimized for turbidity removal and that there is additional potential for increased removal of DOC and DBP precursors. Significant improvement in DOC removal may be achieved by lowering coagulation pH to the optimum pH for DOC removal using alum (pH = 5.5). Although additional DOC removal was observed using ferric sulfate, the low pH required to achieve beneficial results may require significant alterations to the current treatment facilities. Additionally, the F6 size fraction exhibited the highest level of specific THM formation and any benefits observed with respect to an increase in overall DOC removed may not necessarily translate to a significant reduction in THMs, albeit a higher percentage of initial DOC removal.

Measurement of treated water UV_{254} may be used to assess the performance of SWID treatment and can be an early indicator upsets in the treatment process. Although

SUVA provides limited insight into the composition of NOM due to the complexity of NOM molecules, it may be used to measure the effectiveness of any alterations in the treatment process. It is evident that SUVA increases with decreasing MW; therefore this parameter may be used as an early indicator of changes in the proportions of NOM size fractions entering or exiting SWID water treatment plant.

The proposed processes demonstrate potential improvements in the treatment of NOM in humic rich waters. The cost implications and facility adjustments vary; however the likely reduction in current THM limits in the future will require all municipalities to examine new processes and optimize current treatment operations if they are to meet upcoming standards.

6.8 – Future studies

The work conducted here provides valuable insight into the character and coagulation behavior of NOM within a south eastern United States coastal surface water. Groundwater repositories along the coast are quickly diminishing and the need to understand treatment characteristics of coastal surface waters more important now than ever before. Based on the findings from this study, future studies investigating the removal of low MW NOM in coastal surface waters would be of great value in determining the best method of removal for this particular group of NOM. Suggested areas of research in the region include:

- An investigation into the use of GAC, or possibly naturally occuring bentonite or kaolin, during the rapid mix phase of the water treatment process to enhance removal of low MW NOM.

- The use of powder activated carbon (PAC) as an additional media layer to selectively remove low MW NOM in conventional rapid sand mixed-media filters.
- Laboratory procedures used in this study must be used to examine the effects of downstream processes (i.e., clarification and filtration) on the size distribution on NOM to determine the best treatment approach

REFERENCES

Aiken, G. R. (1985). "Isolation and Concentration Techniques for Aquatic Humic Substances." Humic Substances in Soil, Sediment adnn Water - Geochemistry, Isolation and Characterization, G. R. Aiken, D. M. Mcknight, R. L. Wershaw, and P. MacCarthy, eds., John Wiley and Sons Limited, New York, 363-384.

Aiken, G. R. (1988). "A Critical Evaluation for the Use of Macroporous Resins for the Isolation of Aquatic Humic Substances." Humic Substances and their Role in the Environment, F. H. Frimmel, Christman, R.F., ed., John Wiley and Sons Limited, New York, 15-28.

Aiken, G. R., McKnight, D. M., Thorn, K. A., and Thurman, E. M. (1992). "Isolation of hydrophilic organic acids from water using nonionic macroporous resin." *Organic Chemistry*, 18(4), 567-73.

Aiken, G. R., Mcknight, D. M., Wershaw, R. L., and MacCarthy, P. (1985). *An Introduction to Humic Substances in Soil, Sediment, and Water*, John Wiley & Sons, New York.

Allgeier, S. C., and Summers, R. S. (1995). "Evaluating NF for DBP control with the RBSMT." *American Water Works Association*, 87(3), 87-99.

Amicon. (1995). *Membrane Filtration and Chromatography Catalog, Publication 387*, Beverly, MA.

Amirtharajah, A., and Mills, K. M. *Annual Conference Proc., Water for the World Challenge of the 80's, Part 1 Session 1-20*.

Amirtharajah, A., and Mills, K. M. (1982). "Rapid mix design for mechanisms of alum coagulation." *American Water Works Association*, 74(4), 210.

Amirtharajah, A., and O'Melia, C. R. (1990). "Coagulation Processes: Destabilization, Mixing, and Flocculation." Water Quality and Treatment: A Handbook of Community Water Supplies, F. W. Pontius, ed., McGraw-Hill, New York, 269-335.

Amy, G. L., Collins, M. R., Kuo, C. J., and King, P. H. (1987). "Comparing Gel Permeation Chromatography and Ultrafiltration for the Molecular Weight Characterization of Aquatic Organic Matter." *American Water Works Association*, 79(2), 117-122.

Amy, G. L., Sierka, R. A., Bedessm, J., Price, D., and Tan, L. (1992). "Molecular Size Distribution of Dissolved Organic Matter." *American Water Works Association*, 84, 67-70.

Andrews, S. A., and Huck, P. M. "Identification of Disinfection By-Product Precursors using Fractionated Natural Organic Matter." *American Water Works Association Water Quality Technology Conference*, Miami, Fl, 177-189.

Assemi, S., Newcombe, G., Hepplewhite, C., and Beckett, R. (2004). "Characterization of natural organic matter fractions separated by ultrafiltration using flow field-flow fractionation." *Water Research*, 38(6), 1467-1476.

Baltpurvins, K. A., Burns, R. C., and Lawrance, G. A. (1996). "Effect of pH and anion type on the aging of freshly precipitated Iron (III) hydroxide sludges." *Environmental Science and Technology*, 30(3), 939-946.

Becher, G., Carlberg, G. E., Gjessing, E., Hongslo, J. K., and Monarca, S. (1985). "High-Performance Size Exclusion Chromatography of Chlorinated Natural Humic Water and Mutagenicity Studies Using the Microscale Fluctuation Assay." *Environmental Science and Technology* (19), 422-426.

Beckett, R., Wood, J., and Dixon, D. R. (1992). "Size and Chemical Characterization of Pulp and Paper Mill Effluents by Flow-Field-Flow Fractionation." *Environmental Technology*, 13, 1129-1140.

Benjamin, M. M. (2002). *Water Chemistry*, McGraw-Hill, Boston.

Bennion, D. N., and Rhee, B. W. (1969). "Mass Transport of Binary Electrolytes in Membranes." *Industrial Engineering and Chemistry Fund.*(8), 36-49.

Berliner, J. F. T. (1931). "Chemistry of chloramines." *American Water Works Association*, 23(9), 1320-1333.

Bernhardt, H., and Schell, H. (1995). "Experience with an on-line determination of the flocculant dosage using the LADUNGSTITRAMAT." *Water Supply*, 13(3-4), 279-284.

Beyer, G. L. (1991). Physical Methods of Chemistry, B. W. Rossiter and J. F. Hamilton, eds., John Wiley and Sons, New York, 415-513.

Bian, R., Watanabe, Y., Tambo, N., and Ozawa, G. (1999). "Removal of Humic Substances by UF and NF Membrane Systems." *Water Science and Technology*, 40(9), 121-129.

Bishop, K., Seibert, J., Kohler, S., Hruska, J., Cory, N., and Laudon, H. (2003). "Riparian Zone Controls on the Chemical Dynamics of DOC-Rich Runoff from a Boreal Hillslope with Transmissivity-Feedback Flow Paths." *Journal of the American Water Works Association*, 12(1), 132-136.

Buffle, J., and Deladoey, P. (1978). "The Use of Ultrafiltration for the Separation and Fractionation of Organic Ligands in Freshwaters." *Analytical Chemistry*, 109, 339-345

Carlson, D. A., and Lin, S. S. (1975). "Phosphorus removal by the addition of aluminum (III) to the activated sludge process." *Journal Water Pollution Control Federation*, 47(7), 1978-1986.

Chadik, P. A., and Amy, G. L. (1983). "Removing Trihalomethane Precursors from Various Natural Waters by Metal Coagulants." *Journal of the American Water Works Association*, 75(10), 532-536.

Chandrakanth, M. S., Krishnan, S., and Amy, G. L. (1996). "Interactions between ozone, AOM, and particles in water treatment." *Journal of Environmental Engineering*, 122(6), 459-468.

Cheng, K. L. (1977). "Separation of Humic Acid with XAD Resins." *Mikrochimica Acta*, 2, 389-396.

Cheryan, M. (1998). *Ultrafiltration and microfiltration handbook*, Technomic Publishing Company, Lancaster, Pa.

Cho, J., Amy, G. L., and Pellegrino, J. (1999). "Membrane Filtration of Natural Organic Matter: Initial Comparison of Rejection and Flux Decline Characteristics with Ultrafiltration and Nanofiltration Membranes." *Water Research*, 33(11), 2517-2526.

Cho, J., Amy, G. L., and Pellegrino, J. (2000). "membrane Filtration of Natural Organic Matter: Comparison of Flux Decline, NOM Rejection, and Foulants During Filtration with Three UF Membranes." *Desalination*, 127(283-298).

Chow, C., van Leeuwen, J., Fabris, R., King, S., Withers, N., Spark, K., and Drikas, M. (2000). "Enhanced Coagulation for Removal of Dissolved Organic Carbon with Alum - A Fractionation Approach." *Watertech, Australian Water and Wastewater Association*.

Clark, R. M., Adams, J. Q., Sethi, V., and Sivaganesan, M. (1998). "Control of Microbial Contaminants and Disinfection by-products for drinking water in the US: cost and performance." *Aqua*, 47(6), 255-265.

Collins, M. R., Amy, G. L., and King, P. H. (1985). "Removal of Organic Matter in Water Treatment." *Journal of Environmental Engineering*, ASCE 111(6), 850-864.

Collins, M. R., Amy, G. L., and Steelink, C. (1986). "Molecular Weight Distribution, Carboxylic Acidity, and Humic Substances Content of Aquatic Organic matter:

Implications for the Removal during Water Treatment." *Environmental Science and Technology*, 20, 1028-1032.

Croue, J. P. (2004). "Isolation of humic and non-humic NOM fractions: Structural characterizations." *Environmental Monitoring and Assessment*, 92(1-3), 193-207.

Croue, J.-P., Lefebvre, E., Martin, B., and Legube, B. (1993). "Removal of dissolved hydrophobic and hydrophilic organic substances during coagulation/flocculation of surface waters." *Water Science and Technology*, 27(11), 143-152.

Croue, J.-P., Violleau, D., Labouyrie-Rouillier, L., Leenheer, J. A., and Aiken, G. R. (1999). "DBP Formation Potentials of Hydrophobic and Hydrophilic NOM Fractions: A Comparison Between a Low and High Humic Water." *Division of Environmental Chemistry Preprints of Extended Abstracts*, 39(1), 218-219.

Crozes, G., White, P., and Marshall, M. (1995). "Enhanced Coagulation: its Effect on NOM Removal and Chemical Costs." *Journal of the American Water Works Association*, 87(1), 78-89.

De Nobili, M., and Chen, Y. (1999). "Size exclusion chromatography of humic substances: limits, perspectives and prospects." *Soil Science*, 164(11), 825-33.

Deen, W. M. (1987). "Hindered Transport of Large Molecules in Liquid-Filled Pores." *American Industrial Chemical Engineering*, 33(9), 1409-1425.

Dempsey, B. A. (1984). "Removal of Naturally Occurring Compounds by Coagulation and Sedimentation." *CRC Critical Reviews in Environmental Control*, 14(4), 311-331.

Dryfuse, M. J. (1995). "An evaluation of conventional and optimized coagulation for TOC removal and DBP control in bulk and fractionated waters," University of Cincinnati, Cincinnati, OH.

Dryfuse, M. J., Miltner, R. J., and Summers, R. S. "The removal of molecular size and humic/non-humic fractions of DBP precursors by optimized coagulation." *American Water Works Association, Annual Conference*, Anaheim, CA.

Dzombak, D. A., and Morel, F. M. M. (1990). *Surface Complexation Modelling: Hydrous Ferric Oxide*, John Wiley and Sons, New York.

Edwards, M. (1997). "Predicting DOC removal during enhanced coagulation." *Journal of the American Water Works Association*, 89(5), 78-79.

Edzwald, J. K., Becker, W. C., William, C., and Wattier, K. L. (1985). "Surrogate Parameters for Monitoring Organic Matter and THM Precursors." *Journal of the American Water Works Association*, 77(4), 122-132.

Edzwald, J. K., and Glaser, H. T. (1979). "Coagulation and Direct Filtration of Humic Substances with Polyethylenimine." *Environmental Science and Technology*, 13(3), 299-305.

Edzwald, J. K., and Tobiason, J. E. (1999). "Enhanced Coagulation: USA Requirements and a Broader View." *Water Science and Technology*, 40(9), 63-70.

Evanko, C. R., and Dzombak, D. A. (1998). "Influence of structural features on sorption of NOM-analogue organic acids to goethite." *Environmental Science and Technology*, 32(19), 2846-2855.

Fane, A. G. (1986). "Ultrafiltration: Factors influencing flux and rejection." *Prog. Filtration Separation*, 4, 101-179.

Fane, A. G., Kim, K. J., Fell, C. J. D., Suzuki, T., and Dickson, M. R. (1990). "Quantitative microscopic study of surface characteristics of ultrafiltration membranes." *Journal of Membrane Science*, 54(1-2), 89-102.

Fearing, D. A. (2004). "Process Options for the Treatment of Humic Rich Waters," Dissertation, Cranfield University. School of Water Sciences, England.

Finch, C. A. (1996). "Industrial Water Soluble Polymers." Royal Society of Chemistry, London.

Fu, P. L. K., Ruiz, H., Thmopson, K., and Spangenberg, C. (1994). "Selecting membranes for Removing NOM and DBP Precursors." *American Water Works Association*, 86(12), 55-72.

Gaffney, J. S., Marley, N. A., and Clark, S. B. (1996). "Humic and Fulvis Acids and Organic Materials in the Environment." Humic and Fulvic Acids: Isolation, Structure, and Environmental Role, J. S. Gaffney, Marley, N.A., Clark, S.B., ed., American Chemical Society, Chicago, 2-15.

Geoffrey, D., and Elham, G. A. "Understanding humic substances: Advanced methods, properties and applications." *Humic Substances Seminar*, Cambridge.

Gjessing, E. (2003). "Short Term And Long Term Changes And Variation In Quality." Atna.

Goslan, E. H. (2004). "Natural Organic Matter Character and Reactivity: Assessing Seasonal Variation in a Moorland Water," Dissertation, Cranfield University.

Gregory, J., and Jinming, D. (2001). "Hydrolyzing metal salts as coagulants." *Pure Applied Chemistry*, 73(12), 2017-2026.

Hall, E. S., and Packham, R. F. (1965). "Coagulation of organic color with hydrolyzing coauglants." *American Water Works Association*, 57(9), 1149-1166.

Hayes, M. H. B., Gjessing, E., and Sequi, P. (1989). *Humic Substances II*, John Wiley and Sons, New York.

Hazlett, J. D., Kutowy, O., and Tweddle, T. A. "Commercial ultrafiltration membrane performance evaluation." *2nd International Conference on Separations*, Canada, 65.

Helfrich, G., Haas, D., Fox, K., and Studstill, A. (1992). "Ferric chloride as an alternative coagulant." *Water Supply*, 10(4), 155-158.

Hongve, D., Baann, J., Becher, G., and Lomo, S. (1996). "Characterization of Humic Substances by Means of High-Performance Size Exclusion Chromatography." *Environment International*, 22(5), 489-494.

Huang, C., and Shiu, H. (1996). "Colloids and Surfaces." *Physicochemical and Engineering Aspects*, 113(1-2), 155-163.

Hundt, T. R., and O'Melia, C. R. (1988). "Aluminum-Fulvic Interactions: Mechanisms and Applications." *Journal of the American Water Works Association*, 80(4), 176-186.

Hwang, C. J., Sclimenti, M. J., Bruchet, A., Croue, J.-P., and Amy, G. L. "DBP Yields of Polar NOM Fractions from Low Humic Waters." *American Water Works Association Water Quality Technology Conference*, Nashville, TN, USA.

Jiang, Q., and Graham, N. J. D. (1998). "Preliminary Evaluation of the Performance of New Pre-Polymerised Inorganic Coagulants for Lowland Surface Water Treatment." *Water Science and Technology*, 37(2), 121-128.

Jodellah, A. M., and Weber, W. J. (1985). "Controlling Trihalomethane Formation Potential by Chemical Treatment and Adsorption." *Journal of the American Water Works Association*, 77(10), 95-100.

Johnson, P. N., and Amirtharajah, A. (1983). "Ferric Chloride and Alum as Single and Dual Coagulants." *Journal of the American Water Works Association*, 75(5), 232-239.

Kim, J. I., Buckau, G., Li, G. H., Duschner, H., and Psarros, N. (1990). "Characterisation of Humic and Fulvic Acids from Gorleben Groundwater." *Fresnius Journal of Analytical Chemistry* (338), 245-252.

Kitis, M., Karanfil, T., Kilduff, J. E., and Wigton, A. (2001). "The Reactivity of Natural Organic Matter to Disinfection By-Products Formation and its Relation to Specific Ultraviolet Absorbance." *Water Science and Technology*, 43(2), 9-16.

Knocke, W. R., Conley, L., and Van Benschoten, J. E. (1992). "Impact of dissolved organic carbon on the removal of iron during water treatment." *Water Research*, 26(11), 1515-1522.

Knocke, W. R., West, S., and Hoehn, R. C. (1986). "Effects of Low Temperature on the Removal of Trihalomethane Precursors by Coagulation." *Journal of the American Water Works Association*, 78(4), 189-195.

Kottegoda, N. T., and Rosso, R. (1997). *Statistics, Probability, and Reliability for Civil and Environmental Engineers*, McGraw-Hill, New York.

Koukouraki, E., and Diamadopoulos, E. (2003). "Modelling the formation of THM (trihalomethanes) during chlorination of treated municipal wastewater." *Water Science and Technology*, 3(4), 277-284.

Krasner, S. W., Croue, J.-P., Buffle, J., and Perdue, E. M. (1996). "Three Approaches for Characterizing NOM." *Journal of the American Water Works Association*, 88(6), 66-79.

Krasner, S. W., McGuire, M. J., Jacangelo, J. G., Patania, N. L., Regan, K. M., and Aieta, E. M. (1989). "The Occurrence of Disinfection By-Products in US Drinking Water." *Journal of the American Water Works Association*, 81(8), 41-53.

Kubicki, J. D., and Apitz, S. E. (1999). "Models of natural organic matter and interactions with organic contaminants." *Organic Chemistry*, 30(8), 911-927.

Laine, J.-M., Hagstrom, J. P., Clark, M. M., and Mallevaille, J. (1989). "Effects of Ultrafiltration Membrane Composition." *Journal of the American Water Works Association*, 81(11), 61-67.

Larson, R. A., and Weber, E. J. (1994). *Reaction Mechanisms in Environmental Organic Chemistry*, CRC Press, Boca Raton, FL.

Lee, S., Cho, J., Shin, H., Son, B., and Chae, S. (2003). "Investigation of NOM size, structure and functionality (SSF): Impact on water treatment with respect to disinfection by-products formation." *Journal of Water Supply: Research and Technology - AQUA*, 52(8), 555-564.

Leenheer, J. A. (1981). "Comprehensive Approach to Preparative Isolation and Fractionation of Dissolved Organic Carbon From Natural Waters and Wastewaters." *Environmental Science and Technology*, 15(5), 578-584.

Leenheer, J. A. (1985). "Fractionation Techniques for Aquatic Humic Substances." Humic Substances in Soil, Sediment, and Water: Geochemistry, Isolation and Characterization, G. A. Aiken, D. M. Mcknight, R. L. Wershaw, and P. MacCarthy, eds., John Wiley and Sons, New York.

Leenheer, J. A., Brown, P. A., and Noyes, T. I. (1989). "Implications of Mixture Characteristics on Humic Substance Chemistry." Humic Substances in Soil, Sediment and water. Geochemistry, Isolation and Characterization, I. H. Suffet and P. MacCarthy, eds., John Wiley and Sons, New York.

Leenheer, J. A., Croue, J. P., Benjamin, M., Korshin, G. V., Hwang, C. J., Bruchet, A., and Aiken, G. R. (2000). "Comprehensive isolation of natural organic matter from water for spectral characterizations and reactivity testing." Natural organic matter and disinfection by-products, S. E. Barrett, Krasner, S.W., Amy, G.L., ed., ACS, Washington, DC, 68-83.

Lind, C. B. (1998) "Experiments in TOC Removal by Polyaluminum Hydroxychloride and Enhanced Coagulants." *American Water Works Association*, Anaheim, CA, 351-362.

Logan, B. E., and Jiang, Q. (1990). "Molecular Size Distributions of Dissolved Organic Matter." *Journal of Environmental Engineering*, 116(6), 1046-1062.

Lovins III, W. A., Duranceau, S. J., Gonzalez, R. M., and Taylor, J. S. (2003). "Optimized coagulation assessment for a highly organic surface water supply." *Journal of the American Water Works Association*, 95(10), 94-108.

Luong, T. V., Peters, C. J., and Perry, R. (1982). "Influence of Bromide and Ammonia upon the formation of Trihalomethanes under Water-Treatment Conditions." *Environmental Science and Technology*, 16(8), 473-479.

Malcolm, R. L., and MacCarthy, P. (1992). "Quantitative Evaluation of XAD-8 and XAD-4 Resins used in Tandem for Removing Organic Solutes from Water." *Environment International*, 18, 597-607.

Matilainen, A., Lindgvist, N., Korhonen, S., and Tuhkanen, T. (2002). "Environment International." *28*, 6(457-465).

McKnight, D. M., Boyer, E. W., Westerhoff, P., Doran, P. T., Kulbe, T., and Andersen, D. T. (2001). "Spectrofluorometric Characterization of Dissolved Organic Matter for Indication of Precursor Organic Material and Aromaticity." *Limnology and Oceanography*, 46(1), 38-48.

Meier, M., Namjesnik-Dejanovic, K., Maurice, P. A., Chin, Y.-P., and Aiken, G. R. (1999). "Fractionation of Aquatic Natural Organic Matter upon Sorption to Goethite and Kaolinite." *Chemical Geology*, 157, 275-284.

Milton, J. S., and Arnold, J. C. (1995). *Introduction to Probability and Statistics: Principles and Applications for Engineering and the Computing Sciences*, McGraw-Hill, New York.

Munster, U. (1999). "Amino Acid Profiling in Natural Organic Matter Isolated by Reverse Osmosis from Eight Different Boreal Freshwaters." *Environment International*, 25((2/3)), 209-224.

Murphy, E. M., Zachara, J. M., and Smith, S. C. (1990). "Influence of mineral-bound humic substances on the sorption of hydrophobic organic compounds." *Environmental Science and Technology*, 24(10), 1507-1516.

Narkis, N., and Rebhum, M. (1977). "Stoichiometric relationship between humic and fulvic acids and flocculants." *Journal of the American Water Works Association*, 69(6), 325-328.

Newcombe, G., and Drikas, M. *WaterTECH*, Sydney, Australia, 442-447.

Newcombe, G., Drikas, M., Assemi, S., and Beckett, R. (1997). "Influence of Characterised Natural Organic Matter on Activated Carbon Adsorption: I. Characterisation of Concentrated Reservoir Water." *Water Research*, 31(5), 965-972.

Nilson, J. A., and DiGiano, F. A. (1996). "Influence of NOM Composition on Nanofiltration." *Journal of the American Water Works Association*, 88(5), 53-66.

Nokes, C. J., Fenton, E., and Randall, C. J. (1999). "Modelling the Formation of Brominated Trihalomethanes in Chlorinated Drinking Waters." *Water Research*, 33(17), 3557-3568.

Nordstrum, D. K. (1996). "Trace metal speciation in natural waters: computational vs. analytical." *Water, Air, and Soil Pollution*, 90(1-2), 257-267.

Norwood, D. L., Johnson, J. D., Christman, R. F., Haas, J. R., and Bobenrieth, M. J. (1980). "Reactions of Chlorine with Selected Aromatic Models of Aquatic Humic Material." *Environmental Science and Technology*, 14(2), 187-190.

Oliver, B. G., and Lawrence, J. (1979). "Haloforms in drinking water: A study of precursors and precursor removal." *Journal of the American Water Works Association*, 71(3), 161-163.

O'Melia, C. R. (1972). "Coagulation and Flocculation." Physicochemical Processes for Water Quality Control, J. Walter, ed., John Wiley and Sons, New York, 61-109.

O'Melia, C. R., Becker, W. C., and Au, K.-K. (1999). "Removal of Humic Substances by Coagulation." *Water Science and Technology*, 40(9), 47-54.

Onsager, L. (1931). "Reciprocal Relations in Irreversible Processes - Part. I." *Physics Review*, 37, 405-425.

Owen, D. M., Amy, G. L., and Chowdbury, Z. K. (1993). "Characterization of NOM and its Relationship to Treatability." *90631*, AWWA Research Foundation (AWWARF), CO, USA.

Owen, D. M., Amy, G. L., Chowdbury, Z. K., Paode, R., McCoy, G., and Viscosil, K. (1995). "NOM Treatability." *American Water Works Association*, 87, 46-63.

Parthasarathy, N., and Buffle, J. (1985). "Study of Polymeric Aluminum (III) Hydroxide Solutions for Application in Waste Water Treatment. Properties of the Polymer and optimal Conditions of Preparation." *Water Research*, 19(1), 25-36.

Perminova, I. V., Frimmel, F. H., Kovalevskii, D. V., Abbt-Braun, G., Kudryavtsev, A. V., and Hesse, S. (1998). "Development of predictive model for calculation of molecular weight of humic substances." *Water Research*, 32, 872-881.

Pomes, M. L., Larive, C. K., Thurman, E. M., Green, W. R., Orem, W. H., Rostad, C. E., Coplen, T. B., Curak, B. J., and Dixon, A. M. (2000). "Sources and Haloacetic Acid/Trihalomethane Formation Potentials of Aquatic Humic Substances in the Wakarusa River and Clinton Lake near Lawrence, Kansas." *Environmental Science and Technology*, 34, 4278-4286.

Porter, M. C. (1972). "Concentration polarization with membrane ultrafiltration." *Industrial Engineering and Chemistry Fund.*, 11(3), 234-248.

Probstein, R. F., Shen, J. S., and Leung, W. F. (1978). "Ultrafiltration of Macromolecular Solutions at High Polarization in Laminar Channel Flow." *Desalination*, 24(1-2-3), 1-16.

Rebenne, L. M., Gonzalez, A. C., and Olson, T. M. (1996). "Aqueous chlorination kinetics and mechanism of substituted dihydroxybenzenes." *Environmental Science and Technology*, 30(7), 2235-2242.

Reckhow, D. A., and Singer, P. C. (1990). "Chlorination of Humic Materials: Byproduct Formation and Chemical Interpretations." *American Water Works Association*, 82(4), 173-180.

Rook, J. J. (1974). "Formation of Haloforms During the Chlorination of Natural Water." *Water Treatment and Examination*(23), 234-243.

Rook, J. J. (1977). "Chlorination Reactions of Fulvic Acids in Natural Waters." *Environmental Science and Technology*, 11(5), 478-482.

Saito, T., Koopal, L. K., Riemsdijk, V., Willem, H., Nagasaki, S., and Tanaka, S. (2004). "Adsorption of humic acid on goethite: Isotherms, charge adjustments, and potential profiles." *Langmuir*, 20(3), 689-700.

Schaefer, A. I., Mauch, R., Waite, T. D., and Fane, A. G. (2002). "Charge Effects in the Fractionation of Natural Organics Using Ultrafiltration." *Environmental Science and Technology*, 36, 2572-2580.

Schaefer, A. I., Schwicker, U., Fischer, M. M., Fane, A. G., and Waite, T. D. (2000). "Microfiltration of Colloids and Natural Organic Matter." *Journal of Membrane Science*, 171(2), 151-172.

Schmitt, D., Saravia, F., Frimmel, F. H., and Schuessler, W. (2003). "NOM-facilitated transport of metal ions in aquifers: Importance of complex-dissociation kinetics and colloid formation." *Water Research*, 37(15), 3541-3550.

Sharp, E. L., Parsons, S. A., and Jefferson, B. (2004). "Seasonal Effects on NOM Coagulant Interactions." *Environmental Science and Technology*.5(8), 118-122

Siddiqui, M., Amy, G. L., Ryan, J., and Odem, W. (2000). "Membrances for the Control of Natural Organic Matter from Surface Waters." *Water Research*, 34(13), 3355-3370.

Simon, A. M., Doran, P. T., and Paterson, R. (1996). "Assessment of Diffusion Coupling Effects in Membrane Separation. Part I. Network Thermodynamics Modelling." *Journal of Membrane Science*, 109, 231-246.

Singer, P. C. (1999). "Humic Substances as Precursors for Potentially Harmful Disinfection By-Products." *Water Science and Technology*, 40(9), 25-30.

Singer, P. C., Obolensky, A., and Greiner, A. (1995). "DBPs in Chlorinated North Carolina Drinking Waters." *Journal of the American Water Works Association*, 87(10), 83-92.

Skjelkvale, B. L., Mannio, J., Wiklander, A., and Anderson, T. (2001). "Recovery From Acidification of Lakes in Finland, Norway, and Sweden 1990-1999." *Hydrology and Earth System Sciences 5*, 327-337.

Slavinskaya, G. V. (1991). "Chlorination effect on quality of drinking water." *Khimiya i Tekhnologiya Vody*, 13(11), 1013-1022.

Spengler, S., Benefield, L., and Jenkins, S. R. (1983). "Coagulation for Removal of Humic Materials from Groundwater." *Separation Science and Technology*, 18(2), 135-163.

Staub, C., Buffle, J., and Haerdi, W. (1984). "Measurement of Complexation Properties of Metal Ions in Natural Conditions By Ultrafiltration: Influence of Various Factors on the Retention of Metals and Ligands by Neutral and Negatively Charged Membranes." *Analytical Chemistry*, 56(14), 2843-2849.

Stumm, W., and O'Melia, C. R. (1968). "Stoichiometry of coagulation." *Journal of the American Water Works Association*, 60(5), 514-539.

Suzuki, T., Watanabe, Y., Ozawa, G., and Ikeda, S. (1998). "Removal of Soluble Organics and Manganese by a Hybrid MF Hollow Fibre Membrane System." *Desalination*, 117, 119-130.

Symons, J. M., Bellar, T. A., Carswell, J., Keith, J., Demarco, J., Kropp, K. L., Robeck, G. G., Seeger, D. R., Slocum, C. J., Smith, B. L., and Stevens, A. A. (1975). "National Organics Reconnaissance Survey for Halogenated Organics." *American Water Works Association*, 67(11), 634-648.

Tadanier, C. J. (1998). "Influence of Operational Characterization Methods on Observed DOM Physicochemical Properties and Reactivity with Aqueous Chlorine," Dissertation, Virginia Polytechnic Institute and State University.

Tadanier, C. J., Berry, D. F., and Knocke, W. R. (2000). "Dissolved Organic Matter Apparent Molecular Weight Distribution and Number-Average Apparent Molecular Weight by Batch Ultrafiltration." *Environmental Science and Technology*, 32, 2348-2353.

Tadanier, C. J., Berry, D. F., and Knocke, W. R. (2003). "Modeling Uncoupled Solute Transport in Natural Organic Matter Size Fractionation by Ultrafiltration." *Journal of Environmental Engineering*, 129(1), 33-42.

Thang, N. M., Geckeis, H., Kim, J. I., and Beck, H. P. (2001). "Application of the Flow Field Flow Fractionation (FFFF) to the Characterization of Aquatic Humic Colloids: Evaluation and Optimization of the Method." *Colloids and Surfaces A: Physicochemical and Engineering Aspects*(181), 289-301.

Thurman, E. M. (1985). *Organic Geochemistry of Natural Waters*, Nijhoff, Boston.

Thurman, E. M., and Malcolm, R. L. (1981). "Preparative Isolation of Aquatic Humic Substances." *Environmental Science and Technology*, 33(17), 3027-3032.

Van Benschoten, J. E., and Edzwald, J. K. (1990). "Chemical aspects of coagulation using aluminum salts. II Coagulation of fulvic acid using alum and polyaluminum chloride." *Water Research*, 24(12), 1527-1535.

Vilge-Ritter, A., Maison, A., Boulange, T., Rybacki, D., and Bottero, J.-Y. (1999). "Removal of Natural Organic Matter by Coagulation-Flocculation: A Pyrolysis-GC-MS Study." *Environmental Science and Technology*, 15(4), 463-466.

Volk, C., Bell, K., Ibrahim, E., Verges, D., Amy, G. L., and Lechevallier, M. (2000). "Impact of Enhanced and Optimised Coagulation on Removal of Organic Matter

and its Biodegradable Fraction in Drinking Water." *Water Research*, 34(12), 3247-3257.

Wershaw, R. L., McKnight, D. M., and Aiken, G. R. (1985). *Humic Substances in Soil, Sediment, and Water: Geochemistry, Isolation, and Characterization*, Wiler Interscience, New York City.

White, M. C., Thompson, J. D., Harrington, G. W., and Singer, P. C. (1997). "Evaluating Criteria for Enhanced Coagulation Compliance." *American Water Works Association*, 89, 64-67.

Zanardi-Lamardo, E., Clark, C. D., and Zika, R. G. (2001). "Frit Inlet/Frit Outlet Flow Field-Flow Fractionation: Methodology for coloured Dissolved Organic Material in Natural Waters." *Analytica Chimica Acta*, 443, 171-181.25

Zhou, Q., Maurice, P. A., and Cabaniss, S. E. (2001). "Size Fractionation upon Adsorption of Fulvic Acid on Goethite: Equilibrium and Kinetic Studies." *Geochimica et Cosmochimica Acta*, 65(5), 803-812.